

THE BASIS OF VARIATION IN THE SIZE AND COMPOSITION OF GRAPE BERRIES

John D. Gray, B.Sc. (Hons)

A thesis submitted in fulfilment of the requirement for the
degree of Doctor of Philosophy

Department of Horticulture, Viticulture and Oenology
Faculty of Agriculture and Natural Resource Sciences

The University of Adelaide

Waite Campus

Glen Osmond S.A. 5064

Australia

May 2002

TABLE OF CONTENTS

Table of Contents	ii
Statement of Authorship.....	iv
Acknowledgements.....	v
Abstract	vi
Abbreviations.....	ix
Chapter 1 – General Introduction.....	1
1.1 Introduction	1
1.2 Berry Development	1
1.2.1 Berry Set	2
1.2.2 Berry Growth	3
1.2.3 Ovule and Seed Development.....	10
1.3 Berry Composition	16
1.3.1 Sugars.....	17
1.3.2 Acids	19
1.3.3 Phenolic Compounds	21
1.3.4 Flavour Compounds.....	23
1.4 Variation.....	24
1.4.1 Levels and Components of Variation.....	27
1.4.2 When Does Variation Begin?.....	28
1.4.3 Measuring Variation	29
1.5 Conclusion.....	30
Chapter 2 – Variation in Shiraz Berry Size and Composition	32
2.1 Summary	32
2.2 Introduction	33
2.3 Experimental Procedures	34
2.3.1 Biological Materials.....	34
2.3.2 Berry Processing.....	34
2.3.3 Calculating the Amount of Malvidin, Quercetin and Catechin.....	35
2.3.5 Statistical Techniques.....	37
2.4 Results.....	37
2.4.1 Developmental Changes in Berry Physical Characteristics.....	37
2.4.2 Developmental Changes in Berry Compositional Characteristics.....	47
2.5 Discussion	54
Chapter 3 – Variation in Chardonnay Berry Size.....	58
3.1 Summary	58
3.2 Introduction	58
3.3 Experimental Procedures	59
3.3.1 Biological Materials.....	59
3.3.2 Ovary and Berry Mass	60
3.3.3 Berry Growth Rates	62
3.3.4 Combined Seed Mass.....	62
3.4 Results.....	62
3.4.1 Clonal Variation and Girdling Treatments.....	62
3.4.2 Berry Age Classes.....	66
3.4.3 Variation between Bunches.....	72

3.4.4	Ovary and Berry Growth Rates.....	85
3.4.5	The Relationship between Ovary/Berry Mass and Ovule/Seed Mass	90
3.5	Discussion	93
Chapter 4	– Confocal Measurement of 3D Cell Size and Shape	96
4.1	Summary	96
4.2	Introduction	96
4.3	Experimental Procedures	98
4.3.1	Tissue Preparation.....	98
4.3.2	Confocal Laser Scanning Microscopy (CLSM).....	100
4.3.3	Transmission Electron Microscopy (TEM) of Cell Walls	101
4.3.4	Calibration of Intensity Attenuation with Depth.....	101
4.3.5	Calibration of Axial Distortion	102
4.3.6	Three-Dimensional (3D) Reconstruction.....	102
4.4	Results.....	103
4.4.1	Staining and Mounting the Tissue Block.....	103
4.4.2	Visualising Cell Walls	103
4.4.3	Comparison of Cell Wall Thickness (TEM vs CLSM).....	105
4.4.4	Correcting the Confocal Z-Series for Signal Attenuation and Axial Distortion...	105
4.4.5	Reconstructed Three-Dimensional (3D) Models of Cells and Cell Walls.....	107
4.5	Discussion	109
4.5.1	Comments on Techniques Used.....	109
4.5.2	Shapes and Sizes of Parenchyma Cells.....	110
Chapter 5	– Berry Size and Cell Size in Chardonnay	113
5.1	Summary	113
5.2	Introduction	114
5.3	Experimental Procedures	114
5.3.1	Biological Materials.....	114
5.3.2	Calculating Berry Volume	115
5.3.3	Confocal Laser Scanning Microscopy (CLSM).....	116
5.3.4	Calculating Cell Volume.....	116
5.3.3	Statistical Techniques.....	117
5.4	Results.....	118
5.4.1	Ovary Cell Volumes (1-15 days)	118
5.4.2	Berry Cell Volumes (29-43 days)	122
5.5	Discussion	128
Chapter 6	– General Discussion.....	132
6.1	Summary	132
6.2	Future Directions.....	134
Bibliography	136
Publications	150

STATEMENT OF AUTHORSHIP

This work contains no material which has been accepted for the award of any other degree or diploma in any university or other tertiary institution and, to the best of my knowledge and belief, contains no material previously published or written by another person, except where due reference has been made in the text.

I give consent to this copy of my thesis, when deposited in the University Library, being available for loan and photocopying.

John D. Gray.

May, 2002.

ACKNOWLEDGEMENTS

The Australian Research Council, the Grape and Wine Research and Development Corporation and Southcorp Wines Pty Ltd are gratefully acknowledged for their financial support. I thank the following: Dr Peter Kolesik for sharing his microscopy skills; Prof. Ian Gibbins and Dr Grant Hennig from the Department of Anatomy and Histology, the Flinders University of South Australia, for access to the SGI Indigo 2 computer and 3D software; Dr Marilyn Henderson from the Centre for Electron Microscopy and Microstructural Analysis, the University of Adelaide, for assistance with the TEM analysis; Prue Henschke (C.A. Henschke and Co.) and John Harvey (Willunga), for providing the grape material; Dr Nick White from the Department of Plant Sciences, the University of Oxford, for commenting on a draft of part of the manuscript (Chapter 4); the Department of Horticulture, Viticulture and Oenology, its administration, staff and students, for providing a studentship, laboratory resources, and a stimulating work environment; Dr Bryan Coombe, Dr Peter Dry, and Prof. Peter Høj for their skilled supervision. I would like to make special mention of Dr Bryan Coombe for his enthusiasm, insight, and tutelage. Lastly, I thank my family. Without their patience, encouragement, and support this task would have been insurmountable.

ABSTRACT

The objective of this study was to explore the basis of variation in the size and composition of grape berries. The investigation focussed on selected aspects of berry development and ripening that were subject to variation. Shiraz and Chardonnay were chosen as experimental varieties because these cultivars presented a large range of variability in the field – Shiraz is susceptible to variation in colour development at veraison, whereas Chardonnay often displays variation in berry size at harvest. The extent of variation within each of the recorded berry parameters was assessed using the coefficient of variation (CV), a unitless measure of sample variability relative to the sample mean, ideally suited to comparative studies.

Chapter 1 is a literature review that documents research on selected aspects of grape berry development and ripening which are subject to variation. Berry development is explained in terms of berry set, berry growth and ovule/seed development. Berry composition is described by the relative concentration of sugars, acids, phenolics and flavour compounds in the berry tissues. Variation is discussed with respect to the Australian wine industry and the problem of supply and demand. Techniques for identifying and measuring components of variation are recommended. Experimental hypotheses are developed.

Chapter 2 describes an experiment designed to identify when variation in berry size and composition was initiated. The hypothesis was that relative levels of variation in size and composition would remain constant throughout the postflowering period of berry development. The physical properties of individual Shiraz berries were described in terms of their deformability, mass, volume, surface area and seed mass. The phenolic composition of these same individual berries was assessed. A comparison of CVs between sequential developmental stages indicated when variation in a particular physicochemical parameter was initiated. The CV in berry deformability reached a maximum at softening. The CV for berry mass was above 50% at berry set, but declined as the berries approached harvest maturity. The CVs for berry volume and berry surface area followed a similar trend. Interactions among these parameters were described by linear regressions, multiple regressions and correlation matrices. Seed mass and berry phenolics were analysed for individual berries during the growing, softening and preharvest stages. Both of these parameters were significantly correlated with berry mass, but the relationships were peculiar to each developmental stage. The CV for seed mass increased with maturity. The CV for berry phenolics was lowest during the softening stage. For most parameters, CVs had already attained high levels during the earliest growth stage (setting). The implication is that variation must have arisen at an even earlier time. This places considerable importance on the impact

that preflowering events may have on cell division in the floral primordia at budburst.

Chapter 3 describes an experiment that sought to identify the extent of variation present during the early developmental stages of berry growth. The hypothesis was that variation in berry size was already significant in the early postflowering period of berry development. Individual Chardonnay berries on two bunches from both ungirdled and girdled vines were assessed on four occasions throughout the flowering period. Individual flowers that had opened during the intervening time period were tagged. One bunch from each vine was sampled at 15 days and another at 43 days after the first flower had opened, giving a range of berry ages: bunch at 15 days comprised berry ages of 1-4, 5-7, 8-11 and 12-15 days; bunch at 43 days comprised berry ages of 29-32, 33-35, 36-39 and 40-43 days. Frequency distributions of berry mass were plotted for each age class for ungirdled and girdled vines. Distributions were negatively skewed for ungirdled vines and positively skewed for girdled vines. No “shot” berries were observed among bunches sampled from girdled vines at 43 days after flowering. Absolute and relative growth rates were typically higher for berries from girdled vines. The relationship between berry mass and seed mass was unaffected by trunk girdling. CVs for berry mass at all ages in the early bunch sample (15 days) were below 44%, and were generally lower for the girdled vines. In the later bunch sample (43 days), CVs in berry mass were all higher than those associated with the early bunch sample, and two- to three-fold lower for the girdled vines. This reduction is most likely the result of increased organic nutrition to the bunch counteracting the variation that arises from differences in hormonal stimulus to growth by the developing seed.

Chapter 4 describes a novel technique that was developed for the *in situ* measurement of cell shape and cell size using confocal laser scanning microscopy (CLSM). The technique encompassed the preparation, clearing, staining and whole mounting of large sections of berry tissue. Optical slices were collected at 1 μm intervals to a depth of 150 μm . The digital images were empirically corrected for attenuation of fluorescence intensity and axial distortion due to refractive index mismatch. Cell size and shape were determined from digital 3D reconstructions of the collected image stack. Cell volumes exhibited a 15-fold range with polysigmoidal distribution and groupings around specific size classes. The volume of individual, whole parenchyma cells within a block of grape berry mesocarp tissue could be measured *in situ* to a precision of 2 μm^3 .

Chapter 5 describes an experiment that sought to resolve the relationship between fruit size and cell size in a developing grape berry. The hypothesis was that variation in cell size occurs early in the postflowering period of berry development and that this variation was responsible for the subsequent macroscopic size differences observed between berries.

Chardonnay berries belonging to the eight age classes derived in Chapter 3 were sampled from ungirdled and girdled vines. Three berries from each age class were analysed under the CLSM – one “shot”, one “chick” and one “hen”. Volumes were calculated for ten cells from the inner mesocarp tissue of each berry. Differences in cell volume were observed between berry types. Larger berries often had a larger range of cell sizes, indicating they had undergone more cell expansion during the course of their development, but the distribution of cell sizes in “shot” and “chick” berries was similar. Girdling did not affect the berry cell size distribution, but the CVs of girdled vines were ~50% higher. Cell volume for “chicks and “hens” increased between day 15 and day 43, although the increase was proportionally greater for “hens”. Variation in cell size remains relatively constant during the early postflowering development, but variation in berry mass increase regardless. This indicates the operation of different metabolic controls over these two facets of berry growth.

Chapter 6 is a general discussion and an attempt to synthesise the salient points from the preceding experimental chapters. In light of the experimental results, it addresses the validity of each of the original hypotheses on variation in berry size and composition. Concepts of developmental synchronisation among berries are viewed from the perspective of changing levels of variation between developmental stages. Increases in CVs signify a loss of synchronisation (asynchronisation) among berries. Reductions in CVs signify a gain in synchronisation (resynchronisation) among berries. The general conclusion is that averages of measurements of the population reveal nothing about the variation within that population. Calculation of variance permits this, but requires that all individuals be measured. Cell size is only one component of the berry size equation. Cell number is the other. While cell size is determined by cell expansion, cell number is linked to cell division. Future applications of techniques developed in this thesis could resolve the interplay between cell division versus cell expansion. A better understanding of these processes might ultimately minimise the impact of variability on the quantity and quality of the Australian winegrape crop.

ABBREVIATIONS

3D	three-dimensional
ABA	abscisic acid
ACC	1-amino-2-ethylaminocyclopropanol carboxylic acid
AGR	absolute growth rate
ANOVA	analysis of variance
CCD	charge-coupled device
CLSM	confocal laser scanning microscopy
CV	coefficient of variation
E-L	Eichhorn-Lorenz
FPA₅₀	formalin:propionic acid:50% ethanol 1:1:18
GA	gibberellin
GMA	glycol methacrylate
IAA	indole-3-acetic acid
MW	molecular weight
n	sample number
r²	coefficient of determination
REML	residual mean likelihood
RGR	relative growth rate
RI	refractive index
s	standard deviation
SE	standard error
TCA	tricarboxylic acid
TEM	transmission electron microscopy
V	volume
\bar{x}	sample mean
ϵ	molar extinction coefficient
λ	wavelength
σ	sample variance

CHAPTER 1 – GENERAL INTRODUCTION

1.1 Introduction

The purpose of this review is to document research on selected aspects of grape berry development and ripening which are subject to variation. Our current understanding of the factors that regulate berry size and composition within the bunch will be outlined, and its shortcomings highlighted.

The first section deals with the biology of grape berry development. The importance of berry set and its modification by trunk girdling are discussed. Classical berry growth curves are presented and varietal differences noted. Berry morphology is related to tissue types, cell division and cell expansion. The sequential development of the ovule/seed, its relationship to the growth of the pericarp, and its regulation by the phytohormones contained in the developing seed are detailed.

The second section deals with berry composition, in particular the sugars, acids, phenolic compounds, and flavour compounds found in wine grapes. Their synthesis, translocation and storage are outlined from a developmental perspective. Typical concentration ranges are given. Environmental factors that modify their accumulation are listed.

The third part of the review is dedicated to variation, the problems it creates for the Australian wine industry, the levels that exist and their interdependence, when it arises developmentally, and how it can be measured. Examples of protocols for the prediction of maturity are given and special reference is made to those studies that have endeavoured to measure variation at different levels within the vineyard.

In conclusion, hypotheses on the possible causes of variation between berries within the bunch are developed. Questions are formulated to resolve these hypotheses. Experimental procedures are given in the research proposal that follows.

An understanding of the sequence of events in the processes of development and ripening at the berry level is critical to the experimental approach. The separate discussion of berry development, berry composition and variation is employed to simplify the following explanation. However, it is recognised that separation in this way is artificial; all three components are fundamentally inter-related.

1.2 Berry Development

The biology of grape berry development is explained in terms of berry set, berry growth and

ovule/seed development. All three phenomena are essential for a grape berry to achieve its maximum potential size on the vine. Limitations to any, or all, of these lead to variation between berries in the bunch.

1.2.1 Berry Set

Fruit set is a developmental stage common to many plant families occurring after fertilisation of the ovule but prior to significant fruit enlargement (see Monselise 1986). In *Vitis vinifera* fruit set occurs within 2 weeks of capfall (**Figure 1.1(a)**). At this time up to 95% of potential berries can abscise from the bunch. Below normal setting is called ‘poor set’ or *coulure*. Huglin (1986) cites an example from the Midi in France (Ravaz 1903) where a bunch of Aramon with 1830 flowers set only 80 berries. The percentage of berries that set in a bunch is a genetic characteristic of the variety, subject to phenotypic modification (Coombe 1962, 1989a, Ebadi *et al.* 1995a, 1995b). Seasonal variation in berry set is a clear indication of plant-environment interactions and low temperatures are often associated with poor set (May 1970, 1987). The organic nutrition of the bunch is regarded as being of primary importance in berry set; Coombe (1959, 1962) and Koblet (1966) established correlations between the supply of photosynthate to the bunch and percent berry set using leaf removal and trunk girdling treatments.

Girdling

The practice of girdling grapevines predates modern viticulture. An early record of the application of this technique is from Lambry 1817 (as cited by Winkler *et al.* 1974). Considerable improvements in fruit set and subsequent berry development were recognised. Girdling is achieved by an encircling cut of the bark of trunk or canes, down to the cambium. The objectives of girdling are to improve berry set, to increase berry size, and to advance maturation. The stage at which the operation is performed determines the nature and magnitude of the effect obtained (Winkler *et al.* 1974). Berries that might not have set due to ovule abortion are retained on the bunch and grow at the usual rate if girdling is done at the beginning of flowering. Normal berries exhibit an increase in size if vines are girdled immediately after set during the period of active cell division. Fruit ripening is advanced by girdling immediately prior to berry ripening and veraison.

Girdling at flowering is known to increase set and seedlessness in Muscat Gordo Blanco berries (Coombe 1959). The mechanism of this response is thought to be the physical modification of phloem translocation altering the source-sink balance by eliminating the roots as a competing sink for photosynthate (Kliwer 1981, Coombe 1989b). The developing

berries access these additional metabolites enhancing their growth potential (Weaver and McCune 1959a). Growth substances may also increase in tissues above the wound (Winkler *et al.* 1974, Huglin 1986). Weaver and Pool (1965) showed that girdling increased levels of endogenous gibberellin in berries of seedless varieties.

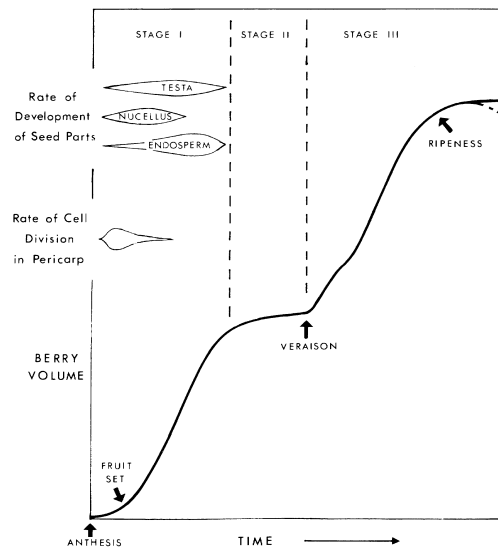
1.2.2 Berry Growth

The typical curve of cumulative grape berry growth is double sigmoidal (**Figure 1.1(a)**) (Coombe 1960). Similar patterns occur in other fruit (stone fruits, blueberry, raspberry, olive, fig) but single sigmoidal variants are not uncommon (see Bollard 1970), while triple sigmoid curves are rare (Pratt and Reid 1974). The curve is segmented into three phases: Stage I, the growing phase, Stage II, the lag phase, and Stage III, the ripening phase. Beginning at flowering, growth is initially rapid during Stage I, essentially static during Stage II, until softening of the berry signals renewed growth during Stage III, reaching a plateau at ripeness; berry weight may decline at the end of this stage in some varieties (McCarthy 1997, McCarthy and Coombe 1999). The same curve can be plotted on a log-linear scale (**Figure 1.1(b)**), giving the appearance of adjoining straight lines of different slope (Considine and Knox 1979b, Staudt *et al.* 1986), or as a rate curve (1st and 2nd derivatives of cumulative growth – **Figure 1.1(c)**) where peaks and troughs represent points of inflexion (Coombe 1960, 1976, Salisbury and Ross 1992) [see Zuconi (1986) for a comparison of the relative merits of these curves].

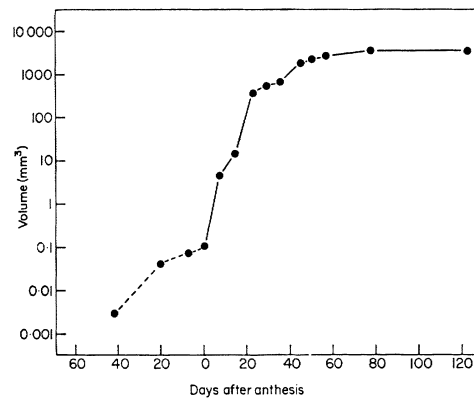
Grape varieties differ in the rate and duration of growth within each stage. Nakagawa and Nanjo (1966) identified differences in the duration of Stages I, II and III among three table grape cultivars Campbell Early, Muscat Bailey and Koshu. The total duration of the three growth periods for these varieties was 71 days (32 + 5 + 34), 95 days (35 + 32 + 28) and 120 days (38 + 31 + 51), respectively. Additional data is provided by Bollard (1970). In stenospermocarpic and parthenocarpic varieties the lag phase (Stage II) is so short as to be virtually non-existent (Harris *et al.* 1968). Seasonal differences within varieties have also been noted, implicating environmental factors as modifiers of developmental characteristics. Coombe (1973) showed that the lag phase in Muscat Gordo Blanco varied from 8-48 days depending on the time of flowering, competition between bunches and the vine's environment.

Millerandage, or "Hen and Chicken", is an extreme case of variation among berries within the bunch, prevalent in certain wine grape varieties grown in cooler districts (e.g., Chardonnay in the Adelaide Hills) (Jaquinet *et al.* 1982). At harvest, the smaller "chicks" typically weigh 75% less than the larger "hens" although they may contain 25% more sugar

(a)



(b)



(c)

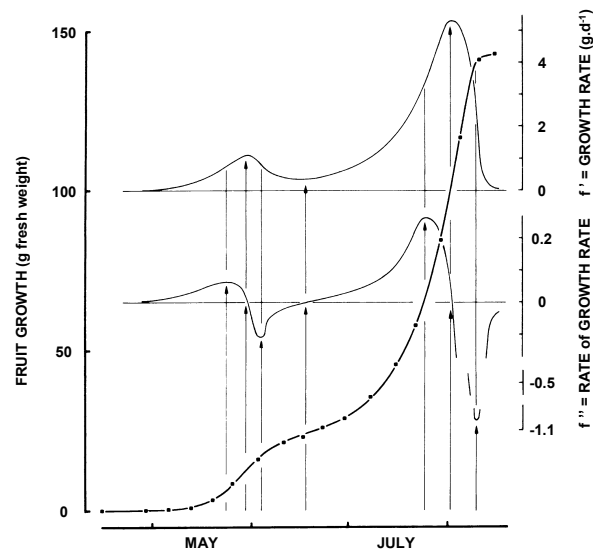


Figure 1.1 Representations of fruit growth. Three alternative representations of fruit growth: (a) double sigmoidal curve of cumulative berry growth showing Stages I, II and III (Coombe 1960); (b) log-linear growth of pistil and fruit of Muscat Gordo Blanco (Considine and Knox 1979b); (c) peach growth expressed by cumulative fresh weight and its first- and second-order derivatives (f' and f'') (Zucconi 1986).

per gram fresh weight. The "chicks" always exhibit incomplete seed development, whereas the hens do not (Stout 1936). Crop losses are significant and making balanced wines is more difficult in years when the incidence of *millerandage* is high (B.C. Croser personal communication).

It is important to note that the flower itself commences growth at bud burst, some nine weeks prior to flowering. At this time the floral primordium is composed of undifferentiated meristematic tissue that forms on the branch primordium (Pratt 1971, Srinivasan and Mullins 1976, 1981). The four ovaries are well developed three weeks prior to flowering and the style and stigma begin to differentiate during these three remaining weeks (Considine and Knox 1979b).

Berry Morphology

The form and structure of the grape berry is determined by its tissues and the cells from which these tissues are constructed. Growth of the berry is discussed in terms of the changes that occur in these tissues as a result of differential cell division and cell expansion postflowering.

Tissues

In the grape berry at flowering, 8 regions of tissue are distinguishable based on their ontogeny, cell types and cellular constituents: septum; ovule; inner epidermis; inner mesocarp; vascular bundles; outer mesocarp; hypodermis; outer epidermis (**Figure 1.2**) (Harris *et al.* 1968, Coombe 1976, Bernard 1977, Considine and Knox 1979a, 1981, Gerrath 1991, Hardie 1992). All regions persist through to berry maturity but major morphological changes accompany their development. The inner and outer mesocarps, together with the septa, represent the majority of berry tissue at maturity: 54% and 25% of cross-sectional area, respectively (Nakagawa and Nanjo 1966). The sum of cell division and cell expansion in all eight regions constitutes the growth and development of a single berry.

In Muscat Gordo Blanco berries at flowering (**Figure 1.3**), the pericarp is typically composed of a uniseriate outer epidermis, a single hypodermal layer, four layers of outer mesocarp cells, five layers of inner mesocarp cells, and a single layered inner epidermis adjacent to the locule. A network of anastomosing vascular bundles separates the outer and inner mesocarps (Considine and Knox 1979a).

Differential cell division and cell expansion occur within these regions after flowering (Nakagawa and Nanjo 1965). The epidermal cells undergo a series of anticlinal and periclinal divisions forming a layer of regular suberised cells with an outer wax cuticle by day 16. The

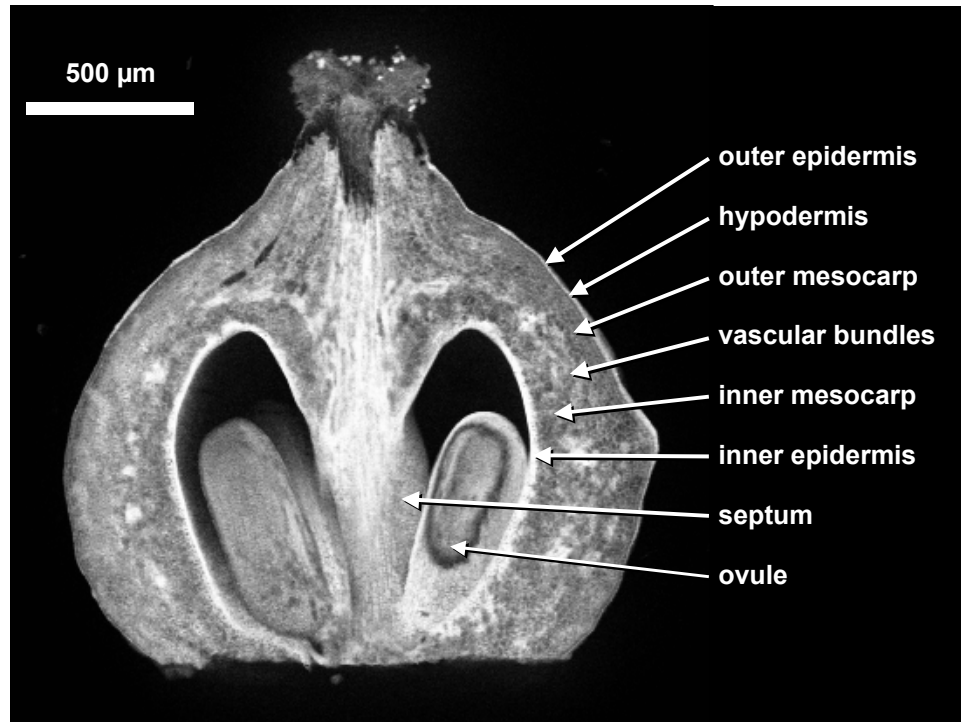


Figure 1.2 Tissue regions of grape ovary. Eight tissue regions in equatorial longitudinal section of Chardonnay at flowering: ovule, septum, inner epidermis, inner mesocarp, outer mesocarp, hypodermis, outer epidermis.

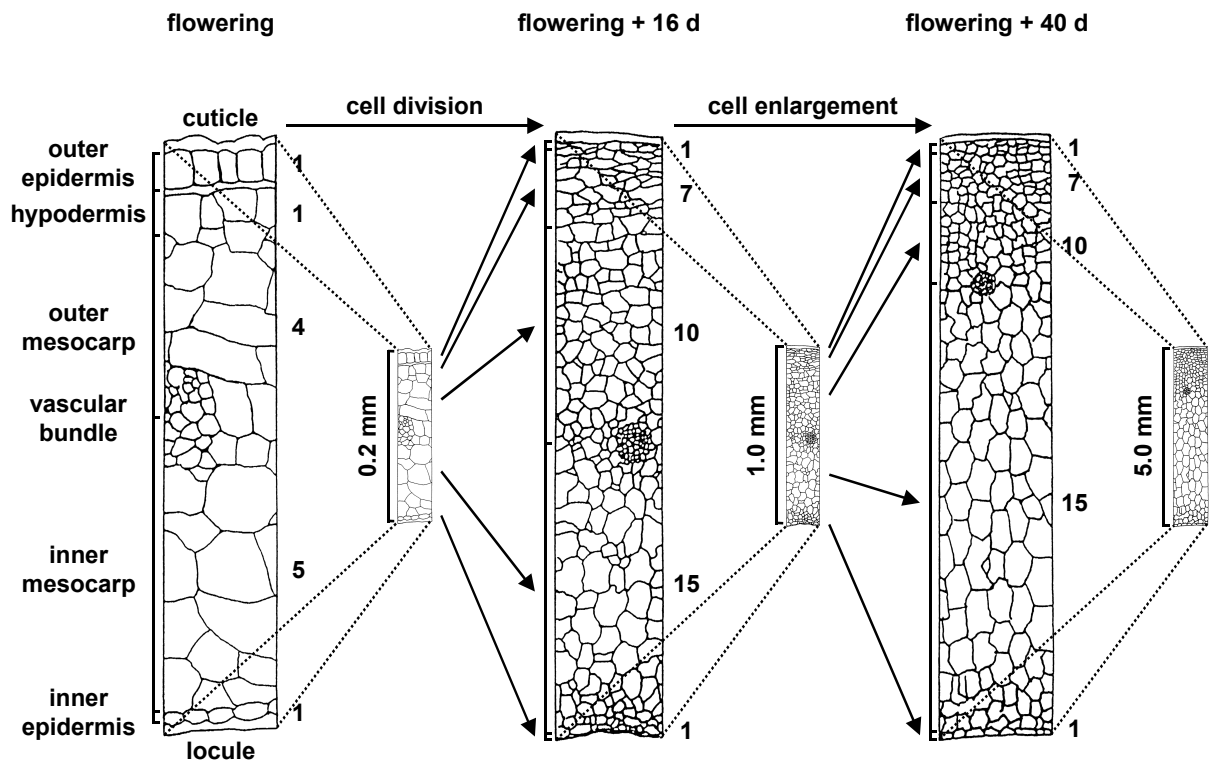


Figure 1.3 Cell division and cell expansion. Comparison of pericarp tissues of Muscat Gordo Blanco berries at flowering, at day 16 after flowering, and at day 40 after flowering (data from Considine and Knox 1979a and Coombe; drawing by Coombe and Gray).

hypodermal cells also divide within the first two weeks to create 7-8 cell layers of collenchymatous cells rich in phenolic compounds. The outer mesocarp cells differentiate into ten layers of large isodiametric cells, highly vacuolated, containing several distinctive types of phenolic deposits. The inner mesocarp cells form 15 layers of large, isodiametric cells devoid of polyphenols (Considine and Knox 1981).

After day 16, no further increase in cell layer number occurs in any of the pericarp tissues. Cell division stops first in the innermost, placental tissues and the remaining tissues follow in order of proximity to the berry centre (Nakagawa and Nanjo 1965). Increase in berry size beyond this time is due entirely to cell expansion. Differential cell expansion occurs within the tissues to such an extent that, by day 40, the inner mesocarp has radially enlarged 4-fold relative to the outer mesocarp and other berry tissues. At maturity these relative differences would be even greater. [The dimensions and timing mentioned above vary between varieties.]

Cell Division and Cell Expansion

Fruit growth is a combination of two independent processes, cell division and cell enlargement. Much of the early work in this field focused on separating these genetically distinct growth components in cultivars of various fruits (Sinnott 1958). Researchers adopted two mathematical models in the analysis of fruit growth, the allometric growth equation and the compound interest law.

The allometric growth equation:

$$y = bx^{\alpha}$$

Equation 1.1

measures the growth of a part relative to the growth of the whole: where y is the part, x is the whole, b is the initial growth-index constant ($=y$ when $x=1$), and α is the allometric growth constant (Huxley and Teissier 1936, Thompson 1942). Substituting cell size for y , fruit size for x , and plotting the data on a log-log scale (**Figure 1.4**), the slope of the line equals α : if $\alpha < 1$, cell division and cell expansion occur simultaneously; if $\alpha = 1$, only cell expansion occurs. The duration of cell division and cell expansion phases in fruit growth are readily determined (Sinnott 1939).

The compound interest law describes phenomena in which the rate of change of a quantity is proportional to the quantity itself. Blackmann (1919) applied this model to the growth of annual plants:

$$W_1 = W_0 e^{rt}$$

Equation 1.2

where, weight at any instant (W_1) is dependent upon the original weight (W_0), the rate (r) and duration (t) of growth, and the base of natural logarithms (e). Sinnott (1945) analysed fruit

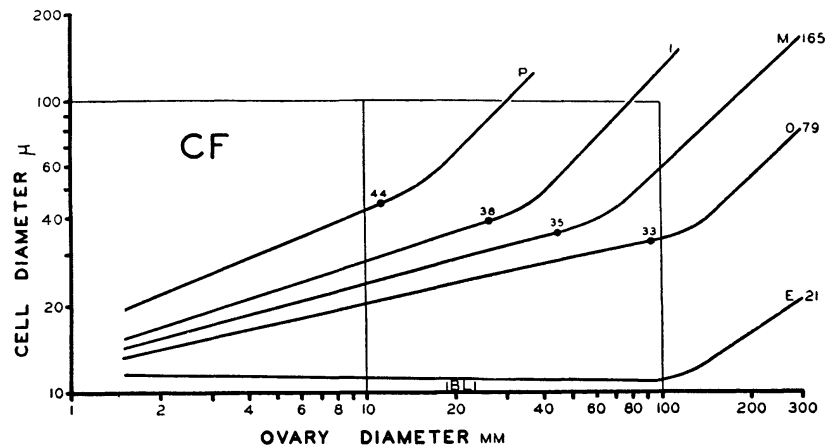


Figure 1.4 Cell versus ovary diameter in cucurbits. Relative growth of cell diameter to ovary diameter for all tissues in a cucurbit. Each line represents a different tissue region: P for placental, I for inner mesocarp, M for middle mesocarp, O for outer mesocarp, E for outer epidermis. Solid circles represent times of last cell division in each region: below these points the slope, $\alpha < 1$, so cell division and cell expansion occur simultaneously; above these points, $\alpha = 1$, so only cell expansion occurs (Sinnott 1939).

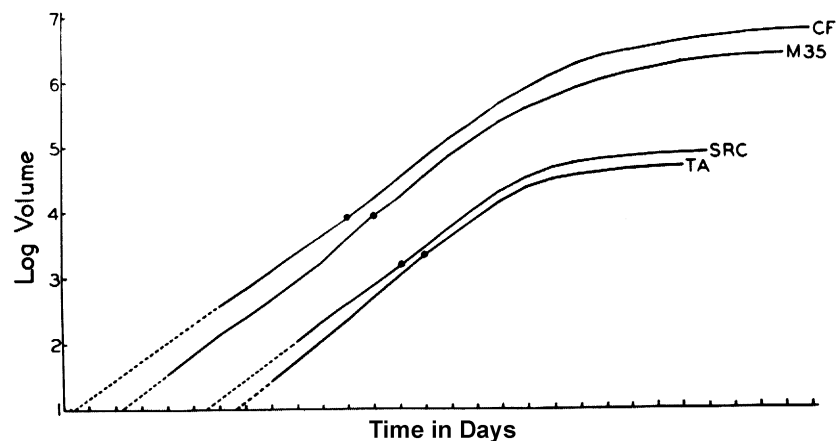


Figure 1.5 Ovary volume versus time in cucurbits. Plot of log ovary volume against time in days for four races of cucurbits, two with large fruits (CF and M35) and two with small fruits (SRC and TA). Solid circles represent time of flowering. Slope of lines indicate growth rates and subtended lengths indicate duration of growth (Sinnott 1945).

volume in a similar fashion. When fruit volume is plotted against time on a log-linear scale (**Figure 1.5**), changes in the rate (slope) and duration (subtended length) of growth become apparent (Sinnott 1945). Similarly, the rate and duration of cell division and cell expansion can be determined by making the appropriate substitutions into Equation 1.2.

Houghtaling (1935) was able to separate six varieties of tomato (*Lycopersicon esculentum*) on the basis of their relative growth using Equation 1.1. She concluded that fruit size at maturity derived from both cell number and cell size since neither had a dominant effect. Ultimate size differences were determined from the beginning of development in the floral primordia before differentiation of the ovary had even begun. MacArthur and Butler (1938) also analysed cell number and cell size in the developing tomato fruit. Growth followed a geometric progression characterised by differential cell division preflowering and differential cell expansion postflowering. As a result, cell number at flowering was proportional to fruit size increase due to later cell expansion. They postulated that unequal cell numbers and sizes established in the early anlage would account for the relatively enormous absolute differences in mature fruit size (1.1 g in *Lycopersicon pimpinellifolium* cv Red Currant cf 173 g in *L. esculentum* cv Tangerine). Sinnott (1939, 1945) sought differences between large-fruited and small-fruited races of cucurbits (*Cucurbita pepo*) through a developmental analysis of the growing fruit in terms of changes in size and number of cells. He found no relation between rates of cell division or cell expansion and final fruit size, but the *duration* of cell division and cell expansion was longer in races that bore larger fruit.

The scientific literature on whether cell division or cell expansion contributes most to berry size is inconclusive. Harris *et al.* (1968) showed that for Sultana vines grown in the field, cell volume rather than cell number was the primary determinant of final berry size, but the opposite was true for glasshouse-grown vines. Nakagawa and Nango (1965, 1966) found that berries grow largely by a process of cell expansion supplemented in the early stages of postflowering growth by cell division. In three table grape varieties, cell volume at maturity had increased by ~4000 times since flowering, whereas cell number had increased by only ~3 times. Using the epidermis as a reference, Considine and Knox (1981) discovered that the rate of cell division was most important to final fruit volume in the grape berry. They reiterated the findings of the earlier researchers, stating that the cell divisions which occur in the primordial ovary wall determine the "capital" of cells available for fruit development (Considine and Knox 1979b). Coombe (1976) suggested that differences in early cell division might contribute much to fruit size variation.

All of the above references attest to the importance of the cell cycle in the developing fruit (see Bryant 1976). The possibility that similar cells in separate fruits will enter and leave

the cell cycle at different times resulting in more or less rounds of cell division per fruit has received scant scientific attention despite its potential bearing on variation. MacArthur and Butler (1938) predicted that asynchronous mitosis in the Anlage would contribute to size variation in tomatoes. Korn and Spalding (1973) demonstrated that variation in cell cycle duration generated an unordered cell pattern in geometric models. Considine and Knox (1981) verified asynchronous and irregular distribution of cell division in grape epidermal cells.

1.2.3 Ovule and Seed Development

Ovule/seed development adheres to a precise sequence of events: integument and nucellus growth; endosperm development; embryo sac formation; and embryo growth (**Figure 1.6**) (Barritt 1970, Ebadi *et al.* 1995b, 1996a, b). Fertilisation distinguishes the ovule from the seed. The timing of these events varies among varieties and environments (Pratt 1971). Failure to successfully complete one part of the sequence will cause the seed to abort (Ledbetter and Ramming 1989, Ledbetter and Shonnard 1990, 1991). Seed abortion may occur at any time throughout its course of development, resulting in a continuum of partially developed seeds (Stout 1936, Ledbetter and Ramming 1989). Ebadi *et al.* (1996a, 1996b) described positive linear relationships between total seed weight and final pericarp weight. Although this relationship had been documented previously (Müller-Thurgau 1898, Winkler and Williams 1936, Olmo 1946, Coombe 1959), the impact of pre- and postflowering events on seed development and cell division in the pericarp were less well understood.

The normal ovary in *Vitis vinifera* has two carpels, each with two ovules (see **Figure 1.2**). The capacity of each of the four ovules to function in fertilisation and seed formation differs. Those ovules that do not abort and continue to develop determine the character of the fruit (Stout 1936). Grape varieties are commonly differentiated as "seedless" or "seeded", however, many of the "seedless" varieties contain fertilised ovules which subsequently abort (e.g., Sultana). The extent, degree, and time of abortion in ovules and in seeds and whether pollination or fertilisation is required for fruit development are significant factors in the classification of varieties. Stout (1936) recognised three classes of fruit: parthenocarpic, stenospermocarpic and seeded.

Parthenocarpic fruits are seedless and will develop without fertilisation of the ovules. Zante Currant, prized for its small size and drying capacity, is an important member of this category. Several sub-divisions exist within this group. Vegetative (autonomic) parthenocarpy is applicable to fruits which develop without pollination. This condition may be obligate, where all ovules are aborted, or facultative, where ovules abort if there is no

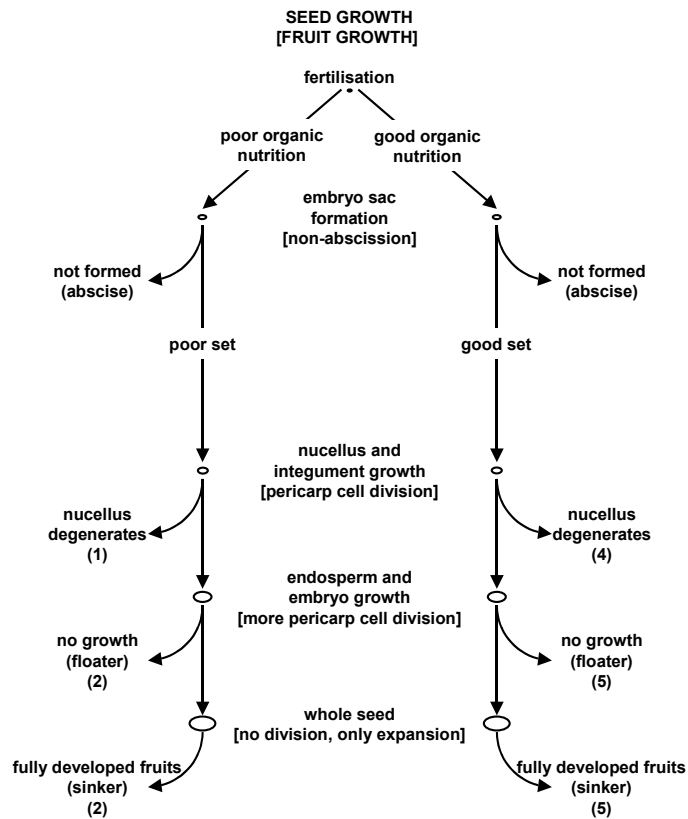


Figure 1.6 Seed development sequence. The sequence of events during seed development is dependent on organic nutrition. Each successive step will invoke a step-wise response in fruit growth. Numbers in parentheses correspond to columns of the histogram in **Figure 1.7**.

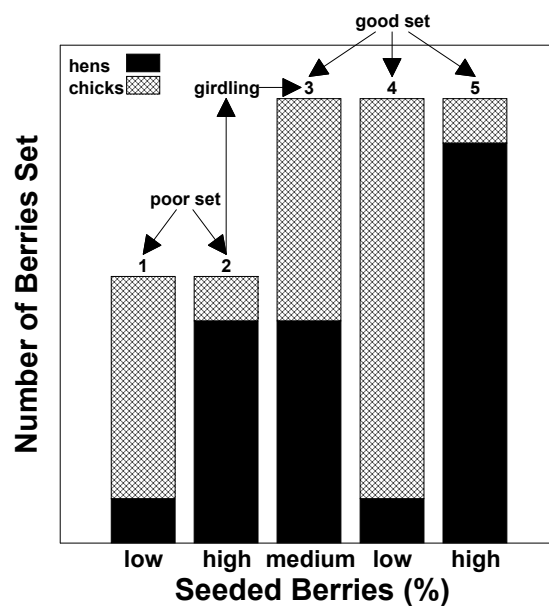


Figure 1.7 Set, growth, seed development and nutrition. Hypothetical representation of the interaction per bunch between berry set, berry growth, seed development and organic nutrition. Numbers 1, 2, 4 and 5 correspond to the levels of seed and fruit growth in **Figure 1.6**. Column 3 indicates the anticipated response of the vine to trunk girdling: an increase in the number of berries which set and an increase in the proportion of seedless berries.

pollination. Stimulative (aitionomic) parthenocarpy describes fruits that develop only after a stimulus such as the growth of pollen tubes or fungi in the pistil. Nitsch (1970) details the importance of the ovule at the time of flowering in the development of parthenocarpic fruits.

Stenospermocarpic fruits have one or more ovules that develop into stenospermic seeds without developed seeds. Many of the "seedless" tablegrape varieties fit into this category (eg, Sultana, Flame Seedless). Fertilisation is required, but abnormalities in embryo sac, nucellus or integument growth lead to seed abortion. Seed trace size is a function of the relative time of embryo/endosperm abortion (Barritt 1970).

Seeded fruits contain fertilised ovules that develop a normal integument, nucellus, endosperm, and embryo. If the embryo grows, the ovule will mature into a normal viable seed. If the embryo aborts, the ovule will become an empty seed characterised by degeneration of the endosperm (see Ebadi *et al.* 1996b). Normal seeds and empty seeds are often identical in outward appearance but may be differentiated by their respective capacity to sink ("sinkers") or float ("floaters") when immersed in water (Olmo 1934). Winegrapes are conventionally described as seeded.

Characterising the relationship between seed development and berry growth has proved problematic because variable development of each of the four ovules within individual berries leads to an infinite range of combinations and permutations for berry growth. Many previous attempts to quantify seed development are recorded in the literature, but most have been of a subjective nature. Objective chemical measures of seed trace size include total polyphenol content (Merin *et al.* 1983) and the inhibition of luciferase activity (Perl *et al.* 1985). Fougère-Rifot *et al.* (1993) noted the presence of vacuolar tannins in the outer integuments of normal ovules prior to flowering, but these were absent from abnormal ovules.

Hormone Production and Berry Growth

Regulation of seed and pericarp growth responses are believed to be hormonal (Weaver and McCune 1959b, Coombe 1960, 1973, Hale 1968, Considine 1969, Nitsch 1970, Coombe and Hale 1973, Rock and Quatrano 1995). Hormones are chemical regulators that act as messengers: they are synthesised in one location and often transported to another location at which they have specific effects at low concentrations (Matthysse and Scott 1984). Their function is to communicate between plant parts and to integrate the responses of one part of the plant with another. The cellular response is transduced by a secondary messenger. Changes in the concentration of free calcium ions in the cytosol has been implicated in almost every response of plant cells to hormones, with the exception of ethylene (Bethke *et al.* 1995).

Five major groups of phytohormones have been found in tissues of *Vitis* species: auxins, gibberellins, cytokinins, abscisins, and ethylene (Hale 1968, Nitsch 1970, Coombe and Hale 1973, Coombe 1976, Bearder 1980). These endogenous hormones are involved in all aspects of reproductive and vegetative growth of the grape vine (Considine 1983, Naylor 1984, Mullins *et al.* 1992).

Their role in fruit development has largely been inferred from studies of applied growth substances in experiments where normal pollination and seed development are prevented (see classical study by Gustafson 1936). The rationale for such experiments is that additional hormone should enhance or promote an effect, provided that the endogenous hormone is present at a sub-optimal concentration. Several problems allied to this approach are discussed by Zeroni and Hall (1980), most especially, the need to distinguish between direct and indirect effects. While hormones rarely determine the cellular processes by which a cell or tissue may respond, they will frequently induce predetermined ("programmed") cellular responses.

The cell cycle is traditionally described in terms of four distinct phases: postmitotic interphase (G1), DNA synthetic phase (S), postsynthetic interphase (G2) and mitosis phase (M). More recently, cytokinesis (C), a subdivision of mitosis, and a non-cycling G1-phase (G0) have been included for descriptive purposes (Francis and Sorrell 2001). Stages G1 and G2 are principal control periods of the cell cycle (Evans 1984). They are noticeably responsive to hormones and constitute the primary targets for hormonal regulation of mitosis. This control may be direct or indirect (permissive). Gibberellin and cytokinin are important for the progression from G1 to S and G2 to M, respectively. Auxin may play a permissive role in both transitions. Ethylene and ABA are usually inhibitory. The precise mode of action of hormones in fruit is unknown, but they function by regulating the movement and utilisation of nutrients, and by stimulating metabolism, cell division, cell enlargement and cell maturation (Nitsch 1970, Matthyse and Scott 1984, Davies 1995a, 1995b). A summary of these responses is presented in **Table 1.1**.

Varietal differences in responsiveness and sensitivity complicate the generalisations derived from the application of exogenous growth regulators (Coombe and Hale 1973, Considine 1983). The concentration and effectiveness of applied growth regulators also depend on the stage of berry development. To demonstrate this aspect, consider the idealised gibberellin response curves for grape cultivars varying in degree of embryo and seed development (**Figure 1.8**) (Coombe and Dry 1992 Chapter 12). The presence and degree of seed development regulates the timing rather than the responsiveness of fruit growth. Parthenocarpic cultivars show a peak response near full bloom, stenospermocarpic cultivars

Table 1.1 Hormone responses. Summary of typical responses to the application of exogenous hormones to developing fruit.

Hormone	Fruit Response
auxin	<ul style="list-style-type: none"> • set and produce fruit without pollination • enhance vascularisation of fruit (with gibberellin) • inhibit vegetative growth during active fruit development (with gibberellin) • promote cell division (with cytokinin) • promote cell enlargement (wall extensibility, water uptake, respiration) • increase respiration, water uptake, enzyme activity, CHO accumulation • delay fruit ripening
gibberellin	<ul style="list-style-type: none"> • increase fruit size in seedless varieties • enhance vascularisation of fruit (with auxin) • inhibit vegetative growth during active fruit development (with auxin) • promote/inhibit cell division • delay cell ripening
cytokinin	<ul style="list-style-type: none"> • promote cell division (with auxins) • delay cell ripening
abscisic acid	<ul style="list-style-type: none"> • induce and maintain seed dormancy
ethylene	<ul style="list-style-type: none"> • trigger ripening

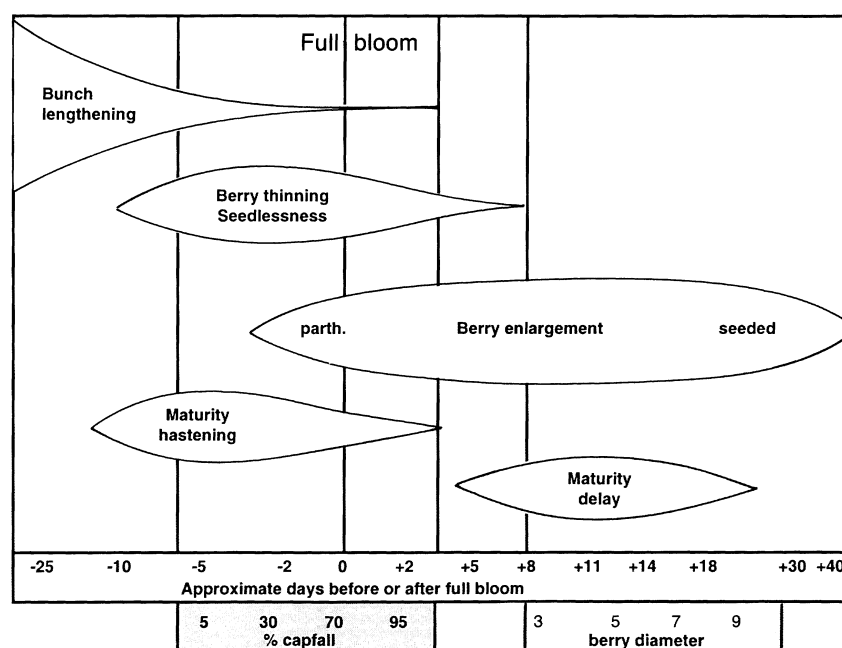


Figure 1.8 Response to GA₃ in grapes. Idealised response curve for exogenous application of gibberellic acid to grape cultivars with varying degree of embryo and seed development. Presence and degree of seed development regulates the timing of the response, but not the responsiveness of fruit growth (Coombe and Dry 1992.)

near fruit set, and seeded cultivars at the end of Stage I.

Despite the empirical difficulties that the *in vivo* study of plant hormones entail, studies on the developing grape berry and other fruit allow the following conclusions to be drawn about their structure, synthesis and localisation. [See reviews by Sembdner *et al.* 1980 and in Davies 1995a for details on biosynthesis and metabolism.]

Indole-3-acetic acid (IAA) is the principal auxin, ubiquitous in higher plants. All auxins that have been isolated and chemically identified in fruits are of the indole family. Biosynthesis from tryptophan occurs in the seeds of young fruits and in the flesh during later development (Nitsch 1970). Phenolic substances regulate IAA oxidation *in vivo*. Conjugates serve a storage function for rapid (im)mobilisation (also in gibberellins and cytokinins) (Kleczkowski and Schell 1995). Endogenous levels fluctuate over time. In the strawberry, peak concentration corresponds with cellularisation of the endosperm (Nitsch 1952).

All gibberellins possess the gibberellane skeleton with a carboxylic group at C₆ (Bearder 1980). Trivial nomenclature assigns each new naturally occurring gibberellin an A number (GA₁...GA_∞) as it is chemically characterised (MacMillan and Takahashi 1968). Gibberellins are synthesised from mevalonate in the nucellus of seedless fruit, and in the nucellus and endosperm of seeded ones (Nitsch 1970). Levels fluctuate throughout development. Typically a wave of gibberellins precedes that of endogenous auxins. Interconversions from one gibberellin to another are common (Bearder 1980).

The biosynthetic pathway of cytokinins is closely related to the metabolism of tRNA. Bound cytokinins are released by oxidation of the isoprenoid side chain of tRNA-bound N⁶-(Δ^2 -isopentenyl)adenine (i⁶Ade) to cis-zeatin. Free cytokinins are synthesised via an alternative pathway involving the trans-hydroxylation of free i⁶Ade and its nucleotide to trans-zeatin (Letham 1973). Cytokinins in fruits reach their maximum concentration in the endosperm (Nitsch 1970).

Abscisic acid (ABA) is a sesquiterpene and was proposed by Sembdner *et al.* (1980) to be synthesised from mevalonate like GA. A preferred pathway involves the photolytic splitting of a C₄₀-carotenoid (xanthoxin) and its subsequent oxidation to ABA (Seo and Koshiha 2002). Levels of abscisic acid vary during fruit development. Sites of production within fruit include the mesocarp and embryo (Nitsch 1970). It is metabolised by conjugation with glucose or oxidative degradation (Kleczkowski 1995).

A number of substances have been proposed as precursors of ethylene (for historical context see Sembdner *et al.* 1980). Recent evidence suggests that the immediate precursor is 1-amino-2-ethylaminocyclopropanol carboxylic acid (ACC) (Yang and Hoffman 1984). Rates of ethylene production vary in different organs and tissues, and are dependent on growth and

developmental stages. Correlations of ethylene production and physiological processes such as germination, vegetative growth, flower formation, fruit ripening, leaf senescence, and environmental stress are cited in Reid (1995), but regulatory mechanisms are poorly understood. The seed coat is the site of biosynthesis in fruits of peach and avocado, but in apple and tomato, the cell wall and cell membrane fulfil this role (Sembdner *et al.* 1980). Fruits are distinguished as climacteric or non-climacteric depending on whether or not they display an increase in respiration at maturity (Biale 1964). Respiration in climacteric fruit is stimulated by a burst ethylene production, but this phenomenon is not observed in grapes (Hawker 1969b).

No clear relationships have emerged from comparisons between the growth rates of fruit and the variations in endogenous hormones. Nitsch (1970) attributes this situation to the complexity of fruit development. Researchers must not only contend with interactions between seeds and fruits, but with competition which may arise between the competing sinks of vegetative growth and fruit growth (Weaver and Johnson 1985). The growing fruit is a very active metabolic centre that functions as a sink for nutrient attraction (Coombe 1989b). Competitive phenomena among the various sinks are modulated by hormones. Competition between fruits has been recognised in some species. Even when neighbouring fruits set at the same time, one may inhibit the growth of another (Nitsch 1970) and it is proposed that auxin is involved in this response. These factors change continuously throughout development of the fruit and plant. Interactions among hormones at the whole plant level magnify this complexity. Evans (1984) cites examples of independent, interdependent, synergistic promotive, synergistic inhibitory, opposite, and antagonistic responses in endogenous hormones following exogenous applications. In addition, environmental parameters that affect growth and development will modify the balance of endogenous hormones and may be a potential source of confusion in the literature (Evans 1984). Crane (1969) simplifies the diversity of hormonal effects by suggesting that they bring fruit development over a particular hurdle. Francis and Sorrell (2001) review the interactions of plant growth regulators with the cell cycle.

1.3 Berry Composition

The important chemical components of the grape berry are stated by Hulme (1970, 1971) to be sugars, acids, phenolics and flavour compounds. This selection is biased towards wine grapes since each group elicits a specific sensory response in the finished wine (Amerine and Roessler 1976). Tablegrapes and drying grapes have additional physical and chemical requirements (e.g., size, visual presentation, bloom, colour, soundness, storage capacity,

firmness, taste, texture, uniformity, early ripening, presence/absence of seeds, etc) [see reviews by Cirami *et al.* 1992 and Whiting 1992).

A schematic overview of changes in relative concentration of principal berry metabolites from flowering to senescence is displayed in **Figure 1.9**. The typical concentration range of these compounds in the mature berry and their distribution between the skin and flesh is given in **Table 1.2** (Peynaud and Ribéreau-Gayon 1971, Niketić-Aleksić and Hrazdina 1972, Coombe 1987a, Abbott *et al.* 1990, Park *et al.* 1991, Hamilton and Coombe 1992, Price 1994).

One aspect of berry composition, that is insufficiently emphasised, is its dependence on berry size. The interdependence is a result of the relative proportions of solutes and the solvent water, and the compartmentation of different compounds in the various berry tissues, especially the division between skin and flesh. Berry composition is a function of berry size and cell type. In turn, berry size is a function of cell number and cell size:

$$\begin{aligned} \text{berry composition} &= f(\text{berry size} \times \text{cell type}) \\ &= f(\text{cell size} \times \text{cell number} \times \text{cell type}) \end{aligned} \qquad \text{Equation 1.3}$$

A correlative study between berry composition and cell number, cell size, and cell type has not been undertaken although the idea has been mooted in the literature (see MacArthur and Butler 1938, Coombe 1960, 1973, Considine 1983).

1.3.1 Sugars

Glucose and fructose are the principal grape sugars (Kliwer 1965a). They are released in berry tissues by the action of invertase on sucrose translocated from the leaves as photosynthate or from storage tissues (Swanson and El-Shishiny 1958, Sepúlveda and Kliwer 1986, Motomura 1990a, 1990b). The invertase is presumed to be vacuolar in origin (Davies *et al.* 1997). The sugars are stored in the large vacuoles of pericarp cells (Possner and Kliwer 1985, Coombe 1987a, Gutiérrez-Granda and Morrison 1992). Compartmentation of reducing sugars was demonstrated in Sauvignon grapes by elevated concentration in the skin, relative to the pulp (see **Table 1.2**) (Peynaud and Ribéreau-Gayon 1971). Immature berries contain chlorophyll and are capable of photosynthesis, but their contribution to the carbohydrate pool is minor in comparison to that from the leaves (Ribéreau-Gayon 1966).

One model of carbohydrate translocation, metabolism and compartmentation in the grape berry envisaged the following sequence of events: sucrose synthesised in the leaves is unloaded from the phloem of the berry's vascular bundles via a proton-cotransport mechanism; sucrose diffuses via the apoplast where it is hydrolysed; the hexoses (glucose and fructose) are transported across the plasmalemma; these are metabolised in the cytoplasm;

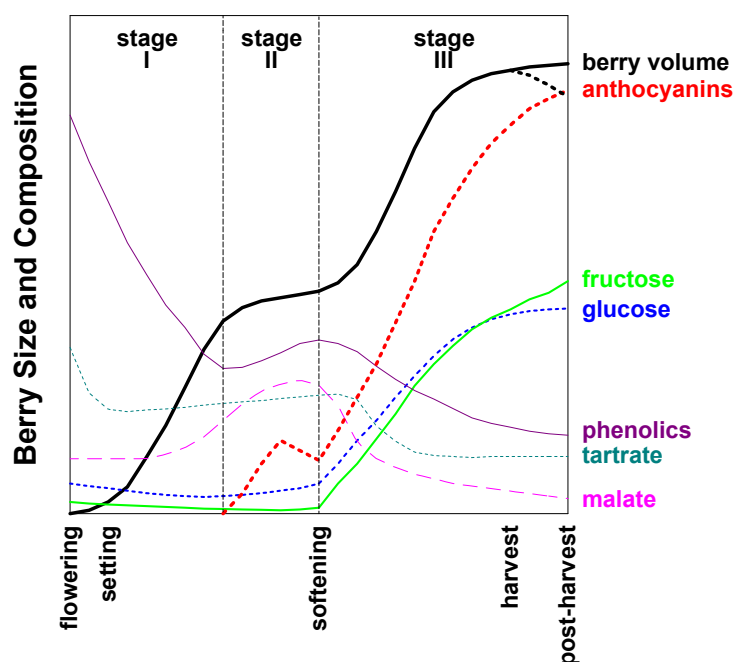


Figure 1.9 Developmental changes in grape metabolites. Changes in the relative concentration of principal berry metabolites from flowering to senescence (Singleton 1966, Coombe 1975, Crippen and Morrison 1986b).

Table 1.2 Grape metabolite concentration at maturity. Typical concentration range of sugars, acids, phenolic compounds and flavour compounds in the mature grape berry and their percentage distribution between the skin and the flesh (units are indicated by superscripts).

component	concentration at maturity	distribution	
	whole berry	skin (%)	flesh (%)
Sugars			
Glucose	80-150 ^a	7	93
Fructose	70-120 ^a	7	93
Sucrose	trace-5 ^a	100	trace
Acids			
Malate	1-9 ^a	72	28
Tartrate	2-10 ^a	64	36
Citrate	trace-0.5 ^a	86	14
Phenolic compounds			
Phenols	0.8-5 ^a	91	9
Anthocyanins	0.2-3 ^a	100	trace
Flavonols	8-97 ^b	100	trace
Flavour compounds			
Volatiles	3-7 ^c	35	65
Non-Volatiles	35-54 ^c	68 ^d	32 ^d

^a g/L free-run juice

^b µg/g fresh weight berry

^c µg/L berry homogenates

^d unpublished data

secondary metabolites are transported across the tonoplast into the vacuole (Coombe and Matile 1980). However, it should be said that the whole subject remains unclear at this stage.

The accumulation of glucose and fructose in berries is negligible prior to berry softening, but increases rapidly thereafter (see **Figure 1.9**) (Coombe 1960, Kliewer 1965a). This period of development is characterised by a major shift in the vine's translocation pattern when the berry replaces the shoot apex as the major sink (Mullins *et al.* 1992). The transition is accompanied by an increase in the activities of invertase, sucrose synthase, sucrose phosphate synthase, and sucrose phosphatase (Hawker 1969a). The trigger for this response is unknown, but may involve the phytohormone ABA (Hale and Coombe 1974). The accumulation of ABA in the flesh of grape berries increases as berries soften. The concentration of ABA in the seed is higher than in the flesh throughout development (Coombe and Hale 1973). Environmental factors such as temperature (Kliewer 1964, Coombe 1987b), light (Crippen and Morrison 1986a), water availability (Matthews and Anderson 1988) and vine canopy (Smart 1974) all impact on the rate and extent of accumulation of glucose and fructose in the berry.

Trace amounts of arabinose, xylose, stachyose, raffinose, melibiose, maltose, and galactose have been recovered from grape berries (Kliewer 1965c, Peynaud and Ribéreau-Gayon 1971). The synthesis of these minor grape sugars and the impact of environmental factors on their accumulation is less well understood, but developmental and varietal differences have been identified (Kliewer 1965c). Their contribution to the sensory perception of sweetness in the wine is limited in comparison with glucose and fructose. Their physiological significance in berry metabolism has not been widely researched.

1.3.2 Acids

The principal organic acids in the grape berry are malate and tartrate (Kliewer 1965b). Together these account for more than 90% of the total acidity at maturity (Peynaud and Ribéreau-Gayon 1971). Synthesis occurs via separate metabolic pathways (Peynaud and Ribéreau-Gayon 1971, Ruffner 1982a, 1982b). Sucrose is transported from the leaves and absorbed via the peripheral vascular bundles into the developing berry where malic acid is synthesised by the carboxylation of pyruvic acid according to the Wood-Werkman reaction (Ruffner 1982a). The synthesis of tartaric acid is less well documented but probably involves the metabolism of glucose in the pentose-phosphate cycle (Peynaud and Ribéreau-Gayon 1971). Both acids are sequestered in the vacuoles of pericarp cells (Possner and Kliewer 1985, Iland and Coombe 1988). Differential concentration of the acids in various berry tissues is a result of compartmentation (Iland 1984, Coombe 1987a, Iland and Coombe 1988).

Peynaud and Ribéreau-Gayon (1971) cite much higher concentrations of malate, tartrate and citrate in skin fractions of mature Sauvignon berries than in pulp fractions (see **Table 1.2**).

Malate is an energy-rich molecule that is respired during the course of berry ripening. Tartrate is not metabolised so the amount per berry changes little throughout development although the concentration gradually declines (Hale 1977). The course of acid concentration against time is plotted in **Figure 1.9** (Kliewer 1965b).

Minor acids include citric-, succinic-, fumaric-, pyruvic-, α -oxoglutaric-, glyceric-, glycolic-, dimethyl-succinic, shikimic-, quinic-, mandelic-, *cis*- and *trans*-aconitic-, maleic-, and isocitric-acid (Peynaud and Ribéreau-Gayon 1971). A number of these are intermediates in the tricarboxylic acid (TCA) cycle.

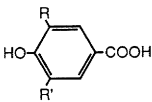
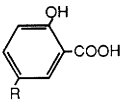
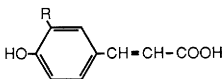
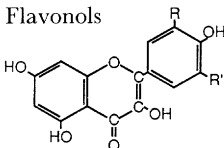
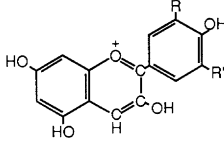
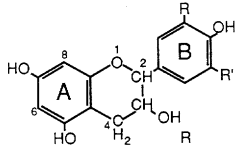
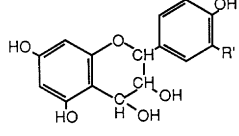
Three distinct terminologies are required to define grape berry acidity: pH, titratable acidity and total acidity. pH is the log concentration of free hydrogen ions in solution. Titratable acidity measures the amount of total available hydrogen ions in solution by base titration. Total acidity measures the amount of the total available organic acid anions in the solution (Iland 1987). The inter-relationship among these parameters is modified by the ionic concentrations of sodium and potassium (Hale 1968, 1977). Boulton described this relationship in terms of the extent of exchange (Equation 1.4: all concentrations are expressed on a molar basis) and used it to predict juice and wine pH (1980a, 1980b):

$$\text{Extent of Exchange} = \frac{[\text{K}^+] + [\text{Na}^+]}{[\text{Tartaric acid}] + [\text{Malic acid}]} \quad \text{Equation 1.4}$$

Malic acid predominantly remains in an undissociated form throughout berry development, whereas tartaric acid undergoes ion exchange with potassium and is converted to potassium bitartrate (less soluble) and di-potassium tartrate (most soluble) salts. These exchanges are postulated to occur across cellular membranes via a membrane-bound enzyme with a strong preference for potassium over other monovalent cations (Boulton 1980a). The leaching of K^+ ions from skins during fermentation will raise wine pH and may require acid addition (Iland 1987). Winemaking techniques that macerate skins to a greater or lesser extent will significantly alter the balance of H^+ ions in solution.

Environmental factors modify the acid balance by altering membrane permeability, which in turn modifies the availability of acids for metabolic conversion into carbohydrates (Peynaud and Ribéreau-Gayon 1971). Ripening has a similar effect. Kliewer (1971) showed that the rate of decrease in tartrate and malate concentration in fruits from the cultivars Cardinal and Pinot Noir was dependent on temperature but relatively independent of light intensity.

Table 1.3 Phenolic compounds of grapes. Structure of phenolic compounds that have been isolated from grape berries (Mullins *et al.* 1992).

General formula	Nature of specific compounds	Type of combination
Benzoic acids  	$R=R'=H$ gives <i>p</i> -hydroxybenzoic acid $R=OH, R'=H$ gives protocatechuic acid $R=OCH_3, R'=H$ gives vanillic acid $R=R'=OCH_3$ gives syringic acid $R=H$ gives salicylic acid $R=OH$ gives gentisic acid	Combinations labile to alkali (esters and other compounds)
Cinnamic acids 	$R=H$ gives <i>p</i> -coumaric acid $R=OH$ gives caffeic acid $R=OCH_3$ gives ferulic acid	Acyl combinations on anthocyanins' sugar on tartaric acid and caftaric, coutaric, fertaric acids
Flavonols 	$R=R'=H$ gives kaempferol $R=OH, R'=H$ gives quercetin $R=R'=OH$ gives myricetin	Two or three glycosides are present, and one glucuronoside
Anthocyanidins 	$R=OH, R'=H$ gives cyanidin $R=OCH_3, R'=H$ gives peonidin $R=R'=OH$ gives delphinidin $R=OCH_3, R'=OH$ gives petunidin $R=R'=OCH_3$ gives malvidin	3-Glucosides and acylated glucosides and additional forms depending on the species of <i>Vitis</i>
Tannin 'precursors'  	$R=OH, R'=H$ gives catechin $R=R'=OH$ gives gallocatechin $R=OH, R'=H$ gives leucocyanidin $R=R'=OH$ gives leucodelphinidin	Tannins present are polymers of flavans, chiefly flavan-3,4-diols. These flavans are present in small amounts as monomers

1.3.3 Phenolic Compounds

Phenolics are a general title for all organic compounds with an aryl hydroxide group present in their structural formula. In the grape berry, these include benzoic acids, cinnamic acids, flavonols and tannin "precursors", with the addition of anthocyanidins in black grape varieties (**Table 1.3**) (Peynaud and Ribéreau-Gayon 1971). *Vitis* species differ in their capacity to glycosidate the anthocyanidin pigments: *V. vinifera* can only synthesise mono-glucosides, but *V. riparia* and *V. rupestris* can synthesise both mono- and di-glucosides. Synthesis of

cinnimates and anthocyanins is via the shikimic acid pathway (Mullins *et al.* 1992). An alternative pathway present in higher plants involving condensation of three molecules of acetyl-coA may contribute to other phenols (Peynaud and Ribéreau-Gayon 1971). On the basis of $^{14}\text{CO}_2$ leaf feeding experiments, Peynaud and Ribéreau-Gayon (1971) proposed that the shikimic acid is synthesised in the leaves and transported to the berries for the active synthesis of anthocyanins during veraison. However, recent experiments support the view that berries are independent of leaves and roots for the synthesis of anthocyanins and other secondary metabolites (Gholami and Coombe 1995, Gholami *et al.* 1995). Carbohydrate metabolism is coincident with anthocyanin synthesis (Pirie and Mullins 1977). In suspension cultures of grape pericarp cells, the accumulation of anthocyanins in pigmented cells is enhanced by increasing the osmotic potential of the medium (Do and Cormier 1990). Anthocyanoplasts have been observed in pigmented and non-pigmented cells of these suspensions (Cormier *et al.* 1990). Studies on the synthesis and translocation of anthocyanins in berries and leaves (Darné 1993) suggest the seed may be indirectly involved. Berries on shoot-girdled bunches can produce anthocyanins from tannins accumulated prior to veraison in the seeds and pericarps.

Localisation of phenolic compounds is of particular importance to winemaking strategies. The C_{15} flavonoid components are localised in skins, seeds and vascular tissue, whereas the smaller non-flavonoid phenolics accumulate in vacuoles of the pericarp cells (Somers and Verette 1988, Mullins *et al.* 1992). The flavonoid phenolics present in white grape varieties are negatively associated with wine quality, so extraction of these during fermentation is minimised. The opposite is true of red wines, where extraction of the coloured anthocyanins is maximised (Somers and Verette 1988). Besides colour, phenolics contribute taste and body to finished wines. Polymeric phenolics (tannins) are complex esters of phenolic acids and sugars (Lavee and Nir 1986). Polymerisation and co-pigmentation phenomena are responsible for the change in colour of red wines during storage (Somers and Evans 1977), as well as astringency in both red and white wines (Singleton and Trousdale 1992). The grape seed is the primary source of detrimental phenolic compounds during wine processing (Oszmianski *et al.* 1986, Ricardo da Silva *et al.* 1991).

The accumulation of some groups of phenolic compounds during grape maturation has been documented (see **Figure 1.9**, and Pirie 1977). Singleton (1966) analysed total phenolics in a developmental series for 5 white and 7 black cultivars. He recorded considerable variation among varieties, unrelated to berry colour. Marked fluctuations between weekly sampling intervals were indicative of a metabolically active substance. Environmental conditions during maturation will modify the ultimate concentration at the berry level.

Differences in cluster exposure or even berry exposure can elicit profound responses. Crippen and Morrison (1986b) obtained conflicting results when assessing the effects of cluster exposure on the phenolic content of Cabernet Sauvignon berries during development. Sun-exposed berries had higher concentrations of total soluble phenols and anthocyanins throughout development, but at harvest, total soluble phenols were identical and anthocyanins were lower. Price (1994) identified quercetin as being responsible for extreme differences in flavonol content of berries within a bunch as a result of variable sun exposure. He suggested this substance might function to protect the developing berry from excessive uv-light. Different cultivars produce different phenolic profiles, particularly in regard to anthocyanins (Somers and Vérette 1988). Profiles within a cultivar are subject to change during berry maturation (Fernández-López *et al.* 1992).

The general role of phenolics in berry metabolism is believed to be anti-pathogenic, although many modifications could have been introduced under the selection pressures of human cultivation (Salisbury and Ross 1992). Hardie (1992) lists a range of other functions phenolics may have assumed in the course of grapevine evolution. Black grapes are thought to have arisen as genetic mutations along this path from ancestral white varieties. Gholami and Coombe (1995) even demonstrated the capacity of a white variety to produce black grape pigments (but see Winkler *et al.* 1974).

1.3.4 Flavour Compounds

The descriptive terminology of wine sensory analysis (Noble *et al.* 1984, 1987) is testimony to the array of aromas and flavours found in wine (Amerine and Roessler 1976, Rankine 1990). Many hundreds of recognised flavour compounds have been isolated from grapes and wines and their number continually increases [see reviews of Schreier 1979, 1982, Marais 1983, Williams *et al.* 1987, Rapp 1988, and Etiévant 1991]. These compounds occur widely throughout the plant kingdom, particularly among developing fruit (Nursten 1970, Coombe 1976). Perception thresholds in sugar-water model solutions range from parts-per-trillion to parts-per-thousand (Stahl 1973, Ewart and Brien 1986, Park *et al.* 1991). Since wines are complex media, synergism, masking, additivity or blending may occur between the individual flavour components (Ewart and Brien 1986).

Flavour compounds can be subdivided into volatile and non-volatile fractions. Some of the volatile flavour compounds that have been isolated from grapes include: monoterpenes in Muscat varieties (Williams *et al.* 1980), methoxypyrazines in Cabernet Sauvignon, Sauvignon Blanc and Semillon (Allen and Lacey 1992), and methyl anthranilate in *Vitis labrusca*. (Power and Chesnut 1921). Many non-volatile flavour "precursors" are present in

grapes as glycosides, with low sensory impact (see reviews by Stahl-Biskup *et al.* 1993, Williams 1993), and often at higher concentrations than the volatile compounds.

Glycosylation is catalysed by membrane-bound cytochrome P-450, producing stable hydroxylated metabolites that are rapidly conjugated to sugars (Rivière and Cabanne 1987). Ford and Høj (1998) have demonstrated the existence of multiple glycosyltransferases in berries and leaves of the grapevine cvs Muscat of Alexandria and Shiraz. These more soluble glucose conjugates are stored in cell vacuoles (Hassall 1990). This function is believed to be part of the grapevine's mechanism for isolating excess or undesirable organic compounds (Frear 1976). Differential compartmentation of volatile and non-volatile monoterpenes occurs in the skin and mesocarp of Muscat Gordo Blanco berries throughout development (Park *et al.* 1991). Prior to veraison, 90% of the total monoterpenes (~280 µg/kg pericarp) were in the volatile form: skin 74%; mesocarp 16%. After harvest, 90% of the total monoterpenes (~2100 µg/kg pericarp) were in the bound form: skin 42.2%; mesocarp 47.9%. Levels of monoterpenes in the berry continued to increase after conventional harvest maturity had been reached and sugar accumulation had levelled out.

Variable amounts of these non-volatile secondary metabolites will be released during fermentation, depending on the degree of skin contact and extraction. During storage, the glycosidic bonds of these secondary metabolites are gradually hydrolysed in the acid wine medium and they are transformed into "flavour-active" compounds (Francis 1994). It has been suggested that the total amount of glycosylated secondary metabolites in the grape berry may be proportional to its total potential flavour as a wine (Abbott *et al.* 1990, Abbott *et al.* 1991, Williams *et al.* 1995).

Flavour compounds are subject to dynamic variation. Replicate determinations of monoterpenes in 10 berry samples of Muscat Gordo Blanco displayed significant standard deviations (Park *et al.* 1991). Large, unpredictable fluctuations between consecutive sampling dates have been recorded in other white varieties (Wilson *et al.* 1986). Environmental factors and cultural practices also modify fruit flavour (McCarthy and Coombe 1985, McCarthy 1986, Eschenbruch *et al.* 1987, Williams *et al.* 1987). These effects have a physiological and morphological basis: they may operate by stimulating the production of phytohormones that modify the internal environment of the cell altering its rate of growth and development.

1.4 Variation

Variation poses significant problems to the wine industry in Australia with regard to the quantity and quality of wine produced. Variation in berry size will affect vineyard yield, wine quantity, and berry composition. Variation in berry composition will affect fruit flavour and

wine quality. Related problems include inaccurate crop forecasting and maturity assessment techniques that affect planning and operational decisions for both grape growers and winemakers on an annual basis.

The Australian winegrape crop shows season-to-season variation of $\pm 40\%$ (**Figure 1.10**). Fluctuations of this magnitude destabilise the industry, as supply and demand are frequently out-of-phase. Annual statistical surveys are undertaken to predict these episodes and minimise their impact (e.g., Anon. 1994a, 1994b, Strachan *et al.* 1994). Vine yield fluctuations (**Figure 1.11**) are the culmination of a complex sequence of events over a 2 year cycle which have been documented by May (1972) (**Figure 1.12**). Yield derives ultimately from average number of berries per hectare and berry size. An understanding of the contribution and cause of variation in both the size and number of berries is crucial to understanding this annual yield fluctuation.

The potential for compositional variation to reduce wine quality is recognised throughout the industry, but empirical evidence of its occurrence is rare. However, it is logical that the quality of wine from a 20 tonne crush will be lessened if poor quality grapes are part of the mixture. A lack of efficient, reliable vineyard sampling protocols is partially responsible for this shortcoming (Gray *et al.* 1994, 1997). Compounding this is the prevailing absence of objective analytical measurements of grapes and wine that correlate with subjectively assessed wine quality. In addition, the measurement of variation has rarely been the purpose of a detailed investigation, but merely an incidental outcome. Exceptions to this statement include studies by Strickland *et al.* 1932, Rankine *et al.* 1962, Nelson *et al.* 1963, Singleton *et al.* 1966, Kasimatis *et al.* 1975, Coombe 1984, Coombe and Iland 1987, Trought and Tannock 1994, Trought 1995.

A considerable literature exists on predicting the optimum maturity for harvesting winegrapes (e.g., Amerine 1956, and Roessler 1958a, 1958b, Roessler and Amerine 1958, 1963, Baker *et al.* 1965, Du Plessis 1984, and Van Rooyen 1982, Wolpert and Howell 1984, Kasimatis and Vilas 1985). These studies have been method oriented, concerned with developing protocols for accurately sampling vineyard composition to optimise the timing of the harvest. All researchers were aware of variation and some of the factors that contributed to it (e.g., position of fruit on the bunch, of the bunch on the vine and of the vine in the vineyard: Roessler and Amerine 1958). Stratified bunch and berry sampling programs were devised to overcome some of these problems (Roessler and Amerine 1963) but it soon became apparent that seasonal, varietal and site-specific considerations would confound any general sampling protocol (Wolpert and Howell 1984, Kasimatis and Vilas 1985).

Several studies have identified problems induced by variation and suggested cultural

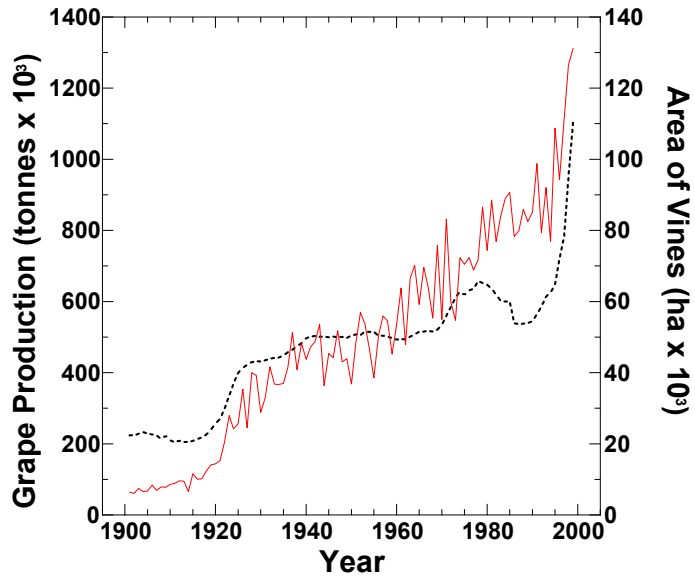


Figure 1.10 Grape production and area of vines in Australia (1902-1999). Annual fluctuations in grape production (—), of $\pm 40\%$ are not uncommon, despite the relative stability of planting area (----)

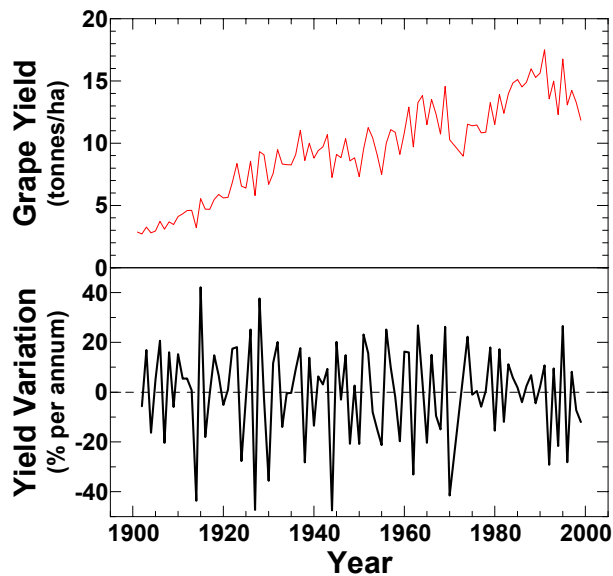


Figure 1.11 Grape yield and yield variation in Australia (1902-1999). Grapevine yield has increased steadily with time from less than 3 tonnes/ha in the early 1900s to more than 15 tonnes/ha in the early 1990s. Variation in yield between one year and the next has been as high as 87%.

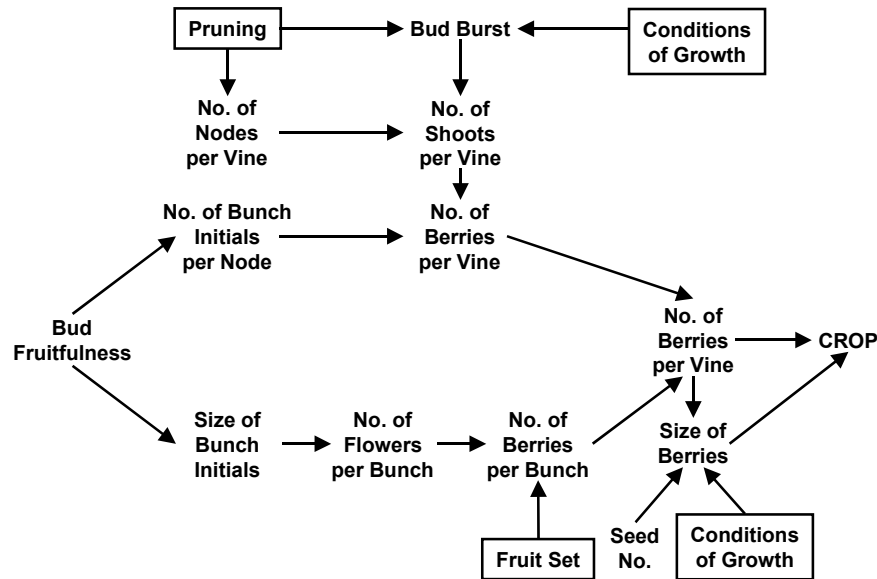


Figure 1.12 Yield components. The components of vine yield from bud initiation in late spring of one season until harvest of the next season (May 1972).

and statistical techniques to overcome them. Strickland *et al.* (1932) investigated variation in vine yield among unirrigated Shiraz vines on *rupestris* rootstock. The inherent variation among individual vines proved more significant to yield than external influences such as soil gradients and drainage or fertility irregularities. Rankine *et al.* (1962) analysed between vine and within vine variation of sugar, titratable acid and bunch weight for the varieties Pedro Ximines, Riesling, Shiraz and Semillon. They concluded that variation between vines was much greater than within vines. Kasimatis *et al.* (1975) measured weight and °Brix of 300 Sultana berries from seven Californian vineyards on two separate occasions: 100 berries each were taken from the shoulder, central and tip regions within the bunch during the latter stages of ripening. Berries from the tip were significantly more mature (higher °Brix), smaller (lower weight) and more variable (larger standard deviation) than berries from the shoulder or centre of the bunch.

1.4.1 Levels and Components of Variation

Variation in the size and composition of grape berries is multi-levelled. It occurs between berries within the bunch, between bunches within the vine, between vines within the vineyard, and between vineyards (Amerine and Roessler 1958b). The variation at each successive level is dependent on the variation in the preceding one. In accordance with the method of residual maximum likelihood (REML), variance components can be calculated by equating the residual mean squares to their expectations (Rankine *et al.* 1962, Robinson 1987, Genstat 5 Committee 1987b). The sources of variation, degrees of freedom, and estimated

Table 1.4 Variance components in the vineyard. Sources of variation, degrees of freedom and estimated mean square for variance components in a vineyard using method of residual mean likelihood (REML) (where, v = number of vines, c = number of bunches, b = number of berries).

source of variation	degrees of freedom	estimated mean square
between vines	$v-1$	$\sigma_b^2 + b\sigma_c^2 + bc\sigma_v^2$
between bunches within vines	$v(c-1)$	$\sigma_b^2 + b\sigma_c^2$
between berries within bunches within vines	$vc(v-1)$	σ_b^2

mean square for the variance components within a vineyard are listed in *Table 1.4*. The prerequisite calculations are detailed in Equations 1.5, 1.6, and 1.7:

$$\sigma_b^2 = \sigma_b^2 \quad \text{Equation 1.5}$$

$$\sigma_c^2 = \frac{\sigma_b^2 + b\sigma_c^2 - \sigma_b^2}{b} \quad \text{Equation 1.6}$$

$$\sigma_v^2 = \frac{\sigma_b^2 + b\sigma_c^2 + bc\sigma_v^2 - (\sigma_b^2 + b\sigma_c^2)}{bc} \quad \text{Equation 1.7}$$

where, σ is the variance, and the subscripts b , c , and v denote the variance attributed to the berry, bunch and vine stratum, respectively. The following discussion will focus on variation at its most basic level, between berries within a bunch.

Asynchronous development is one source of this variation. The extent and impact of asynchronous development at the berry level is largely undocumented. Stout (1936) noted that mixtures of berry types within a bunch, in respect of seededness and size, were a frequent occurrence. He named the phenomenon "partial variation". Coombe (1984) pointed out that asynchrony between berries at the onset of Stage III would be missed in samples from mixed populations. To ensure synchronous populations he advocated the use of individual berries in developmental studies (Coombe and Iland 1987). Two recent studies from New Zealand (Trought and Tannock 1994, Trought 1995) have determined the extent of variation in the size (weight and volume) and composition ($^{\circ}$ Brix) of berries within bunches of the varieties Chardonnay, Pinot Noir and Chardonnay. Seed weight, berry volume and vascular development of the pedicel were all inter-correlated.

1.4.2 When Does Variation Begin?

Variation could arise at any time during the development of the ovary/berry, from initiation of the floral primordia before budburst to berry senescence. Harris *et al.* (1968) recorded 0.2 million pericarp cells in a Sultana berry at flowering, and 0.6 million pericarp cells 40 days

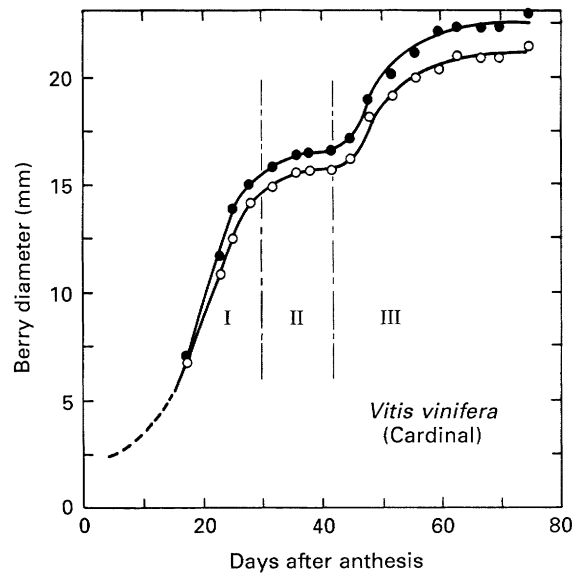


Figure 1.13 Diverging growth curves. Serial measurements of berry diameter on two berries from the same bunch of Cardinal grapes. Note the separate double sigmoid curves of cumulative growth diverging early in Stage I (Mullins *et al.* 1992).

later. This suggests 17 doublings before flowering and 1.5 doublings thereafter (Coombe 1973). Ample opportunity exists both before and after flowering for differences to arise in the overall number of cells in the pericarp.

While **Figure 1.1(a)** represents the growth of an average berry, individual berries may follow quite different courses (**Figure 1.13**) (Mullins *et al.* 1992). Within the population of berries on a bunch, such differences in growth, apparent shortly after flowering, are the most obvious display of berry-berry variation. Within a bunch, flowering itself may span many days (Staudt 1986, 1999). Metabolic variation between berries, for instance differential rates of enzyme synthesis due to slight changes in microclimate across the bunch, is less obvious.

1.4.3 Measuring Variation

Statistical science was created to analyse natural variation. Several techniques were developed to quantify the level of dispersion around a population mean. These included range, mean deviation, sum of squares, variance, standard deviation, and the coefficient of variation. Additionally, standard error and probability tests were developed using the central limit theorem to measure departures from normality (Zar 1974). Comparative studies have frequently assessed relative variation using the coefficient of variation:

$$\text{coefficient of variation (CV)} = \frac{\text{standard deviation (s)}}{\text{mean } (\bar{x})} \times \frac{100}{1} \quad \text{Equation 1.8}$$

This is a unitless measure of the sample variability relative to the sample mean as a percentage.

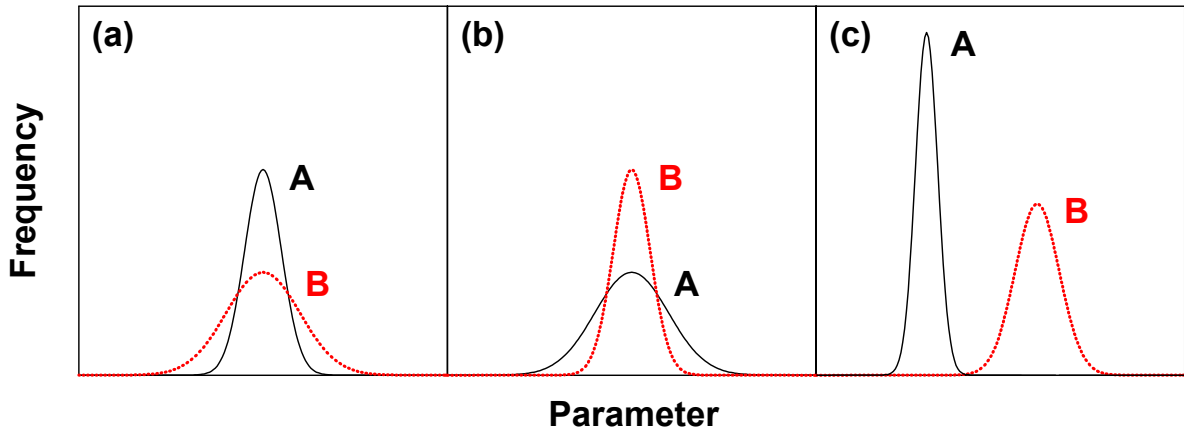


Figure 1.14 Comparative frequency distributions. Theoretical frequency distributions are plotted for samples A and B (denoted by subscripts). Modifying the relationship between the mean (\bar{x}) and the standard deviation (s) results in different levels of variation, indicated by the coefficient of variation (CV). In (a), where $\bar{x}_A = \bar{x}_B$ and $s_A = s_B/2$, there is a doubling in variation between samples A and B ($CV_B = 2CV_A$). In (b), where $\bar{x}_A = \bar{x}_B$ and $s_A = 2s_B$, there is a halving in variation between samples A and B ($CV_B = CV_A/2$). However, in (c), where $\bar{x}_A = 2\bar{x}_B$ and $s_A = 2s_B$, there is no change in variation between samples A and B ($CV_A = CV_B$).

The value of comparing coefficients of variation is illustrated in **Figure 1.14**. The following function was used to generate theoretical frequency distributions for samples with different relationships between the mean and the standard deviation:

$$y = \frac{1}{s\sqrt{2\pi}} e^{-\frac{(x-\bar{x})^2}{2s^2}} \quad \text{Equation 1.9}$$

The three possible outcomes are:

- (i) increasing population variation between sample A and sample B (**Figure 1.14(a)**)
- (ii) decreasing population variation between sample A and sample B (**Figure 1.14(b)**)
- (iii) no difference in population variation between the 2 samples (**Figure 1.14(c)**)

1.5 Conclusion

This review of some aspects of berry development and berry composition that exhibit variation at the individual berry level enables the development of hypotheses on the possible causes of this variability.

The rate and duration of cell division and cell expansion in berry tissues are modulated by the balance of hormones from the developing seed. The cell cycle is an important control point of hormonal action. Asynchronous mitosis and variation in the rate and duration of cell division will lead to variable cell number, cell size and, ultimately, fruit size. The reasons for

differential seed development are unknown, but may involve such diverse aspects as inflorescence structure, flower position, vasculature, environment, physiological age, and phenotype. Whether these effects are direct or indirect remains to be seen.

To resolve the basis of variation in the composition and size of grape berries, three questions must be addressed:

- (i) what levels of variation in size and composition exist between berries?
- (ii) when does this variation begin?
- (iii) how does seed development affect the rate and duration of pericarp cell division?

The following chapters detail testable hypotheses and experimental procedures designed to help resolve these questions.

CHAPTER 2 – VARIATION IN SHIRAZ BERRY SIZE AND COMPOSITION

2.1 Summary

This chapter describes an experiment that sought to determine the existing levels of variation in size and composition between berries. The hypothesis was that relative levels of variation in size and composition would remain constant throughout the postflowering period of berry development. Four Shiraz bunches from separate vines were harvested at seven developmental stages during the course of berry development. Individual berries were weighed, measured, and deformability assessed. Seeds were excised from a subsample of these berries (two bunches x three stages), and the remaining flesh and pulp were homogenised to determine flavonoid amount and concentration. Frequency distributions, means, standard errors, correlations, and coefficients of variation were used to analyse the physical and chemical data collected. Frequency distributions of berry mass, volume, and surface area displayed similarities throughout development, but berry deformability differed markedly. Developmental curves for berry mass, volume, and surface area all followed double sigmoid patterns that peak during the coloured stage at day 91 then decline with berry shrinkage. Berry deformability peaked during the preharvest stage. Berry mass and berry volume were significantly correlated, and berry density remained constant throughout development at 1.202 kg/dm³. Seed mass attained a maximum value during the softening stage and was correlated with berry mass. The curvilinear relationships were unique to each stage of berry development. The amount of malvidin-3-glucoside increased markedly after softening, quercetin-3-glucoside decreased slightly after softening, and catechin increased steadily throughout development. The concentration of malvidin-3-glucoside increased markedly after softening, quercetin-3-glucoside increased marginally at softening, and catechin increased throughout development, especially during the preharvest stage. Bunch-to-bunch differences in the amounts and concentrations of berry flavonoids were evident during the growing stage for all three compounds. The softening stage was characterised by a lack of bunch-to-bunch differences among any of the compounds. During the preharvest stage, bunch-to-bunch differences were confined to malvidin-3-glucoside and catechin, but quercetin-3-glucoside was excluded.

Variation (CV) in berry mass, berry volume, and berry surface area was consistently high throughout the postflowering period, but declined marginally as the berries approached

harvest maturity. Variation in berry deformability was greatest at softening. Variation in seed mass was high throughout development. Variation in the amount per berry of flavonoids was initially high during the growing stage, was reduced during softening stage, and had increased again by the preharvest stage. Variation in concentration of flavonoids was initially high during the growing stage, but it decreased marginally during the softening stage. The CV for malvidin-3-glucoside was lowest during preharvest, but highest for quercetin-3-glucoside and catechin during the same developmental stage. Berry softening and berry shrivel appear to have a major impact on variation in berry size and composition. Both events seem to synchronise physiological changes that occur within the berry, bunch and vine. For most parameters, CVs had already attained high levels during the earliest growth stage (setting). The implication is that variation must have arisen at an even earlier time. This places considerable importance on the impact that preflowering events (e.g. temperature, nutrition, irrigation) may have on cell division in the floral primordia at budburst.

2.2 Introduction

Variation is evidenced in all quantifiable aspects of berry development and ripening. It is so pervasive that it is frequently ignored, or at best tolerated, by viticultural researchers. The purpose of the present investigation is not just to measure this variation, but also to try and perceive its underlying cause. The three questions that were proposed at the end of the literature review are a starting point for the experimental investigation of variation in the developing grape berry. Each question is engendered by a simple, focused hypothesis but their combined answers will greatly advance our understanding of the regulation of growth processes within the grape berry, and between berries on the bunch.

The objective of the **first experiment** was to determine what levels of variation in size and composition exist between berries. The hypothesis was that relative levels of variation in size and composition would remain constant throughout the postflowering period of berry development.

The results of this initial experiment could reveal the extent of variation in size and composition that exists among berries within a bunch. Inter-correlations among these factors at the individual berry level throughout the course of development are presently unknown. The assessment of relative variability over time might indicate when changes begin in berry growth components and in some physico-chemical characteristics (see 1.4.3). This information should therefore enable hypotheses on the interdependence of berry composition and berry morphology, and on mechanisms that lead to variation.

2.3 Experimental Procedures

2.3.1 Biological Materials

A 1975 planting of own-rooted Shiraz vines (Clone 1127) on a hedged, single wire trellis at Willunga was selected as the experimental site (35°20'S, 138°37'E). Four adjacent vines were tagged at E-L stage 17 (12 leaves separated, Coombe 1995). Seven bunches from each vine were randomly selected at flowering (E-L stage 23) and tagged. One tagged bunch was removed at random from each vine on 7 occasions during the course of berry development (E-L stages 27, 31, 34, 36, 37, 38, 39) (setting, growing, softening, coloured, preharvest, harvest, postharvest), representing a total of 28 bunches which is less than 10% of the available crop. Each bunch was stored in a plastic bag on ice until returning to the lab where it was photographed and weighed.

2.3.2 Berry Processing

Berry Physical Characteristics

Berries from all seven developmental stages were used as the sample population. All four Shiraz bunches that had been sampled at each stage were included. Individual berries were removed and their position on the bunch identified separately by lateral, lateral branch, and order on the branch. Each berry was weighed, three diameters (x, y, z) measured and deformability assessed (Coombe and Bishop 1980). The 28 bunches (7 stages x 4 replicates) yielded a total sample population of 3210 individual berries. These berries were frozen in liquid nitrogen and stored at -80°C until ready for further processing.

Berry Compositional Characteristics

Only berries from three developmental stages were assessed for their compositional characteristics – growing, softening, and preharvest. It was anticipated that these three stages would provide sufficient variation in composition since they span Stages I, II and III of berry growth. Only two of the four Shiraz bunches that had been sampled at each stage were included because of time constraints. This still represented a sample population of 693 berries, the composition of each being determined individually.

Single berries were thawed in a mortar and pestle at room temperature. Seeds and seed traces were excised, counted and weighed individually. Flesh and pulp were homogenised, taken up in water, and made up to a volume of 25 mL with water. A 2.5 mL aliquot of the solution was drawn off for determination of phenolics, flavonols and anthocyanins. The

remaining 22.5 mL was retained and frozen for replicate determinations if required.

2.3.3 Calculating the Amount of Malvidin, Quercetin and Catechin

The phenolics, flavonols and anthocyanins aliquot was volumetrically transferred to a 10 mL polyurethane centrifuge tube with 2.5 mL 100% ethanol and extracted for 1 hour on a rotary suspension mixer (Iland *et al.* 1993). The tubes were centrifuged at 3500 rpm for 5 minutes and the centrifugate decanted off and refrigerated prior to analysis. Spectrophotometric techniques were employed to determine the levels of phenolics (Singleton 1966, Somers and Verette 1988), flavonols (Price 1994) and anthocyanins (Niketić-Aleksić and Hrazdina 1972). Subsamples (3.0 mL) of the centrifugate were acidified with 1 M HCl (1:1 v/v) 3 hours prior to spectral scanning in the ultraviolet to visible wavelength range (250-720 nm) using a Cary 100 spectrophotometer (Varian, Palo Alto, CA). Spectral data were imported into Grams/32 Spectral Notebook (Version 4.01, Galactic Industries Corporation), converted to absorbance values, zeroed at 720 nm, smoothed (binomial 50 point) and peak absorbance values determined at 275 nm, 364 nm and 528 nm. These values were recorded and substituted into the equations below. Dilutions were undertaken as required and dilution factors (df) incorporated into these equations. Reported molar extinction coefficients (ϵ) for these compounds vary widely in the literature, but the selected values are derived from reliable sources (*Table 2.1*).

Table 2.1 Constants used to estimate amounts of Shiraz flavonoids. Formulae, molecular weights, peak wavelengths and molar extinction coefficients used to estimate the amounts of individual Shiraz flavonoids from Uv-Vis spectrophotometric scans.

compound	formula	MW	λ (nm)	ϵ
malvidin-3-glucoside ^a	C ₂₃ H ₂₄ O ₁₂	492.4	528	30000
			364	6500
			275	26000
quercetin-3-glucoside ^b	C ₂₁ H ₂₀ O ₁₂	464.4	364	24500
			275	10500
catechin ^c	C ₁₅ H ₁₄ O ₆	290.3	275	4500

^a Asenstorfer 2001

^b Falco and de Vries 1964

^c Whiting and Coggins 1975

Malvidin

The λ_{\max} for malvidin-3-glucoside is 528 nm, and only malvidin-3-glucoside contributes to the absorbance peak at this wavelength. The concentration (g/L) of malvidin-3-glucoside in the extraction mixture is given by the Beer-Lambert equation:

$$c = \frac{A}{\varepsilon} \cdot MW \cdot df \cdot \frac{1}{pl} \quad \text{Equation 2.1}$$

where

A	=	absorbance at λ_{\max}
ε	=	molar extinction coefficient
MW	=	molecular weight
df	=	dilution factor
pl	=	path length

The mass (mg) of malvidin-3-glucoside in the total volume of extraction mixture (mL) is given by:

$$m = \frac{A_{528(M-3-G)}}{\varepsilon_{528(M-3-G)}} \cdot MW \cdot df \cdot \frac{1}{pl} \cdot \frac{\text{volume extract}}{1000} \cdot \frac{1000}{1} \quad \text{Equation 2.2}$$

This mass derives from a single berry and hence the units equate to mg/berry. To convert to mg/g berry fresh weight, the mass is simply divided by berry fresh weight.

Quercetin

The λ_{\max} for quercetin-3-glucoside is 364 nm, but malvidin-3-glucoside also contributes to the absorbance peak at this wavelength. The absorbance attributed to quercetin-3-glucoside alone is given by:

$$A_{364(Q-3-G)} = A_{364(\text{total})} - A_{364(M-3-G)} \quad \text{Equation 2.3}$$

$$A_{364(Q-3-G)} = A_{364(\text{total})} - \left(\frac{m \cdot \varepsilon \cdot pl}{MW \cdot df} \cdot \frac{1000}{\text{volume extract}} \cdot \frac{1}{1000} \right)_{364(M-3-G)} \quad \text{Equation 2.4}$$

The equation is solved by substituting the mass of malvidin-3-glucoside calculated in Equation 2.2. The mass of quercetin-3-glucoside per berry (mg/berry) is derived from this absorbance value:

$$m = \frac{A_{364(Q-3-G)}}{\varepsilon_{364(Q-3-G)}} \cdot MW \cdot df \cdot \frac{1}{pl} \cdot \frac{\text{volume extract}}{1000} \cdot \frac{1000}{1} \quad \text{Equation 2.5}$$

Catechin

The λ_{\max} for catechin is 275 nm, but malvidin-3-glucoside and quercetin-3-glucoside both contribute to the absorbance peak at this wavelength. The absorbance attributed to catechin alone is given by:

$$A_{275(\text{Cat})} = A_{275(\text{total})} - A_{275(\text{M-3-G})} - A_{275(\text{Q-3-G})} \quad \text{Equation 2.6}$$

$$A_{275(\text{Cat})} = A_{275(\text{total})} - \left(\frac{m \cdot \epsilon \cdot \text{pl}}{\text{MW} \cdot \text{df}} \cdot \frac{1000}{\text{vol ext}} \cdot \frac{1}{1000} \right)_{275(\text{M-3-G})} - \left(\frac{m \cdot \epsilon \cdot \text{pl}}{\text{MW} \cdot \text{df}} \cdot \frac{1000}{\text{vol ext}} \cdot \frac{1}{1000} \right)_{275(\text{Q-3-G})} \quad \text{Equation 2.7}$$

The equation is solved by substituting the mass of malvidin-3-glucoside calculated in Equation 2.2 and the mass of quercetin-3-glucoside calculated in Equation 2.5. The mass of catechin per berry (mg/berry) is derived from this absorbance value:

$$m = \frac{A_{275(\text{Cat})}}{\epsilon_{275(\text{Cat})}} \cdot \text{MW} \cdot \text{df} \cdot \frac{1}{\text{pl}} \cdot \frac{\text{volume extract}}{1000} \cdot \frac{1000}{1} \quad \text{Equation 2.8}$$

2.3.5 Statistical Techniques

Frequency distributions were plotted for berry mass, berry volume, berry surface area, and berry deformability at each of the 7 developmental stages sampled. Means and standard errors were calculated and these data were plotted against berry age (days after flowering). A linear regression between berry mass and berry volume was fitted and the slope calculated to investigate changes in berry density during development. Correlations between individual berry mass and total seed mass per berry were plotted at 3 of the 7 developmental stages. Means and standard errors of the amount and concentration of flavonoids were determined for the same 3 developmental stages.

Coefficients of variation (CVs) for each physico-chemical berry characteristic were calculated at each developmental stage using the general formula:

$$\text{coefficient of variation (CV)} = \frac{\text{standard deviation (s)}}{\text{mean}(\bar{x})} \times \frac{100}{1} \quad \text{Equation 2.9.}$$

These were compared over time to determine at what stage of berry development variability for a specific characteristic arose. The potential theoretical outcomes for comparisons of relative variability between any two stages are described in **Figure 1.4**.

2.4 Results

2.4.1 Developmental Changes in Berry Physical Characteristics

Berry Growth Stages

Berry sampling covered seven developmental stages – setting, growing, softening, coloured, preharvest, harvest, and postharvest. According to the terminology introduced by Lorenz *et al.* (1994), and described in Coombe (1995), these represent E-L stages 27, 31, 34, 36, 37, 38,

Table 2.2 Berry growth stages. The relationship between developmental stage, Eichhorn-Lorenz stage, and berry age (days after flowering) for Shiraz bunch samples.

developmental stage	Eichhorn-Lorenz stage	berry age (days after flowering)
flowering	23	0
setting	27	23
growing	31	33
softening	34	72
coloured	36	91
preharvest	37	120
harvest	38	135
postharvest	39	149

39. Berry age (days after flowering) at each stage was 23, 33, 72, 91, 120, 135, and 149 days, respectively (**Table 2.2**). Individual berries from four Shiraz bunches from separate vines were analysed at each stage.

Variation Values

Several of the following graphs display the mean (\bar{x}), standard error (SE) and coefficient of variation (CV) for berry parameters at specified stages of development. Note that the values for SE are much smaller than those of CV. The reason for this apparent discrepancy is that the denominator term in SE calculations is given by the square root of the sample number (n). Where n is very large, as in the present case, SE can be very small.

Berry Mass

The frequency distribution of berry mass changed as the berries developed (**Figure 2.1**). Two peaks were evident at every developmental stage. The smaller peak to the left of berry mass represented the “shot” berries, those that remained on the bunch after set but did not increase in mass beyond ~200 mg. The larger peak indicated the “hens”, those berries that continued to grow and develop through to ripening. [“Chicks” were not a feature of Chapter 3.] Note that the distribution of “hens” appeared to remain normal as it shifted from a compact peak at setting, expanded to a maximum width during the coloured stage, then apparently contracted again as the berries approached harvest.

The relationship between mass per berry (g) and berry age (days after flowering) is shown in **Figure 2.2**. Mean berry mass at each developmental stage was as follows: 0.174 g (setting), 0.374 g (growing), 0.544 g (softening), 1.117 g (coloured), 1.043 g (preharvest),

0.941 g (harvest), and 0.893 g (postharvest). The graph followed a typical double sigmoid pattern except for berry shrinkage after day 91. The gain in berry mass was initially rapid between the setting and growing stages, but slowed as softening approached. At the end of the lag phase, between the softening and coloured stages, berry mass increased rapidly. Berry mass declined during the final three developmental stages.

The CVs of mean berry mass throughout this same period were as follows: 52.74% (setting), 43.50% (growing), 47.76% (softening), 48.45% (coloured), 53.03% (preharvest), 41.66% (harvest), 41.33% (postharvest). The consistently high CVs within each developmental stage indicate only minor changes in variation between the sequential stages. This would suggest that variation in berry mass must be initiated prior to setting. The slight

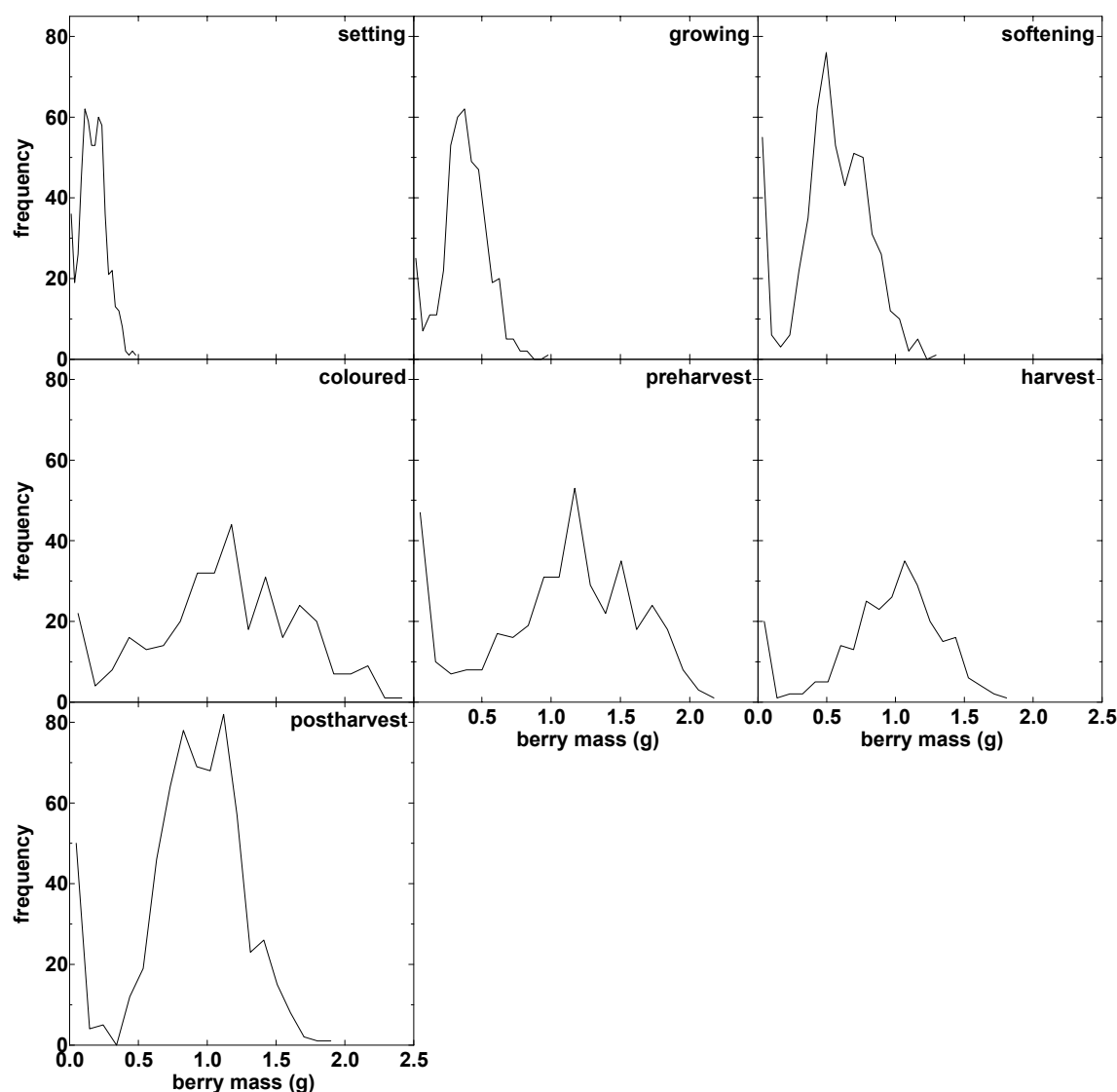


Figure 2.1 Frequency distribution of berry mass during development. Four Shiraz bunches were harvested at 7 stages of development: setting, growing, softening, coloured, preharvest, harvest, and postharvest. Frequency distributions of individual berry mass are plotted for each developmental stage using 20 equal divisions on the x-axis.

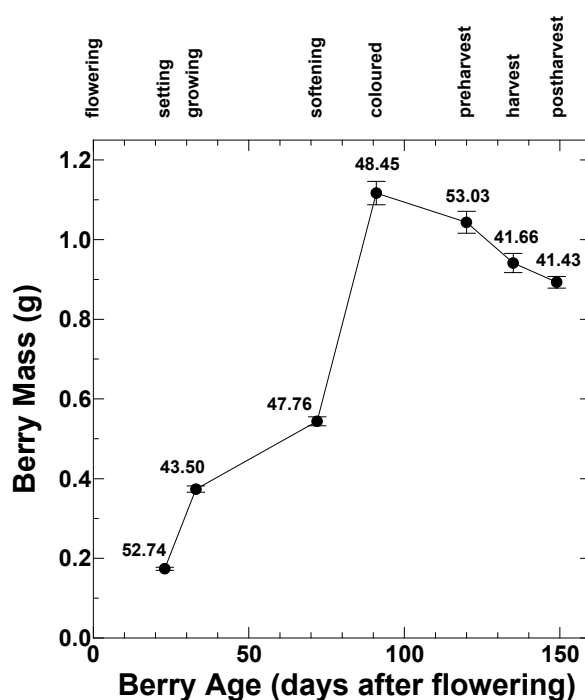


Figure 2.2 Changes in berry mass during development. Four Shiraz bunches were harvested at 7 stages of development: setting, growing, softening, coloured, preharvest, harvest, and postharvest. Mean mass of individual berries is plotted for each stage (\pm one standard error). Coefficients of variation (%) are indicated by the numbers adjacent to the means.

decline in CVs during the harvest and postharvest stages may indicate that berry mass will not decline below a certain minimum proportion of the maximum mass, and that eventually the majority of berries will approach this minimum.

Berry Volume

The frequency distributions of berry volume mirror those of berry mass within each developmental stage (**Figure 2.3**). Once again the “shot” berries (volume less than ~ 200 mm³) and “hens” were evident. The shift in distribution from setting (minimum peak width) to coloured (maximum peak width) to harvest (reduced peak width) was almost identical.

The relationship between berry volume (mm³) and berry age (days after flowering) is shown in **Figure 2.4**. Mean berry volume at each developmental stage was as follows: 163 mm³ (setting), 366 mm³ (growing), 514 mm³ (softening), 980 mm³ (coloured), 890 mm³ (preharvest), 748 mm³ (harvest), and 736 mm³ (postharvest). The graph mirrors the plot of berry mass in **Figure 2.2**. The gain in berry volume was initially rapid between the setting and growing stages, but slowed as softening approached. At the end of the lag phase, between the softening and coloured stages, berry volume increased rapidly. Berry volume declined

during the final three developmental stages.

The CVs of mean berry volume throughout this same period were as follows: 55.17% (setting), 43.84% (growing), 48.01% (softening), 47.60% (coloured), 51.10% (preharvest), 39.41% (harvest), 40.39% (postharvest). In similar circumstances to berry mass, the CVs in berry volume are consistently high within each developmental stage and indicate only minor changes in variation between the sequential stages. This would suggest that variation in berry volume is also initiated prior to setting. The same applies to the slight decline in CVs during the harvest and postharvest stages. This indicates that berry volume will not decline below a certain minimum proportion of the maximum volume and that eventually the majority of berries will attain this minimum if they remain on the vine.

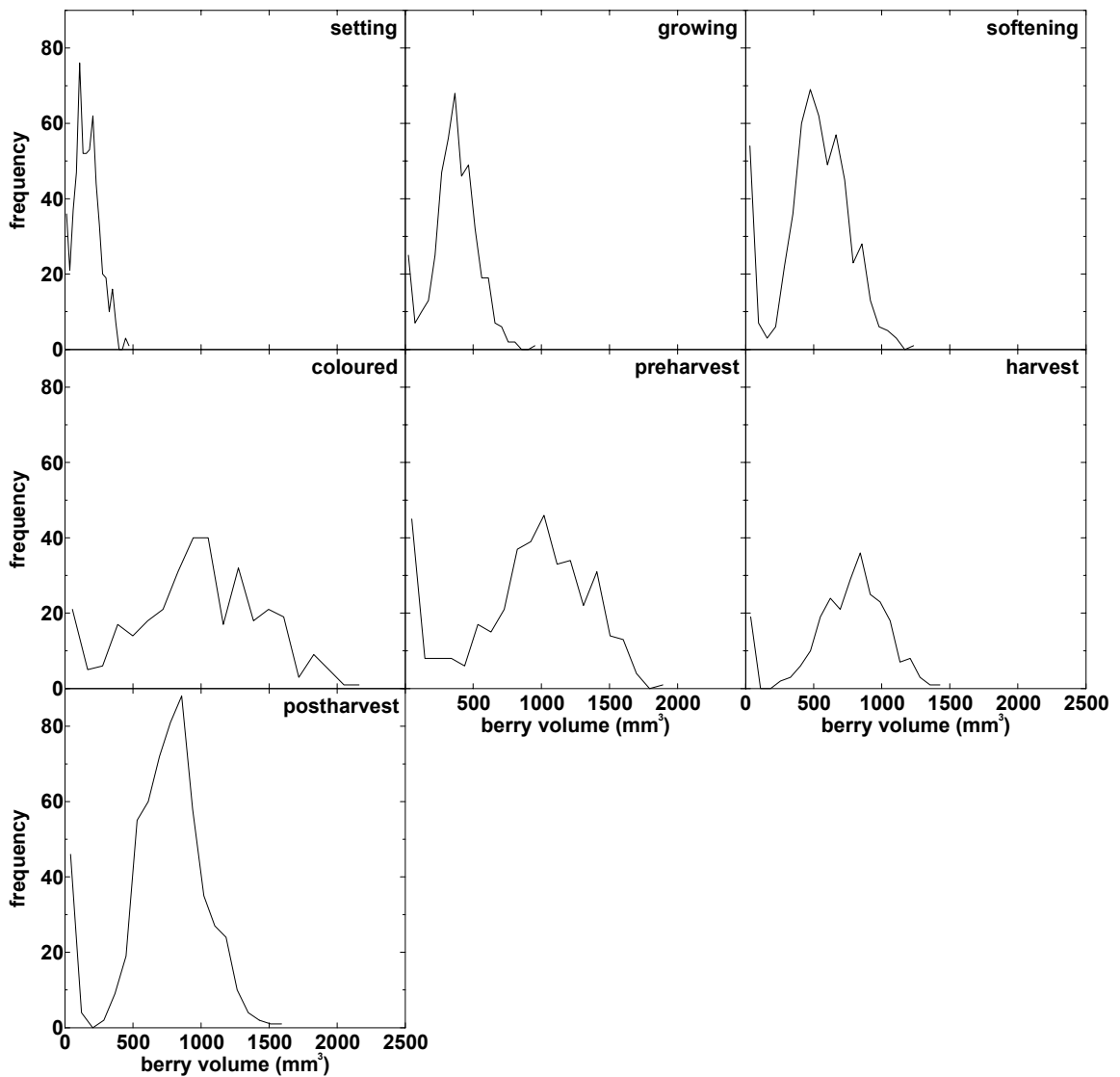


Figure 2.3 Frequency distribution of berry volume during development. Four Shiraz bunches were harvested at 7 stages of development: setting, growing, softening, coloured, preharvest, harvest, and postharvest. Frequency distributions of individual berry volume are plotted for each developmental stage using 20 equal divisions on the x-axis.

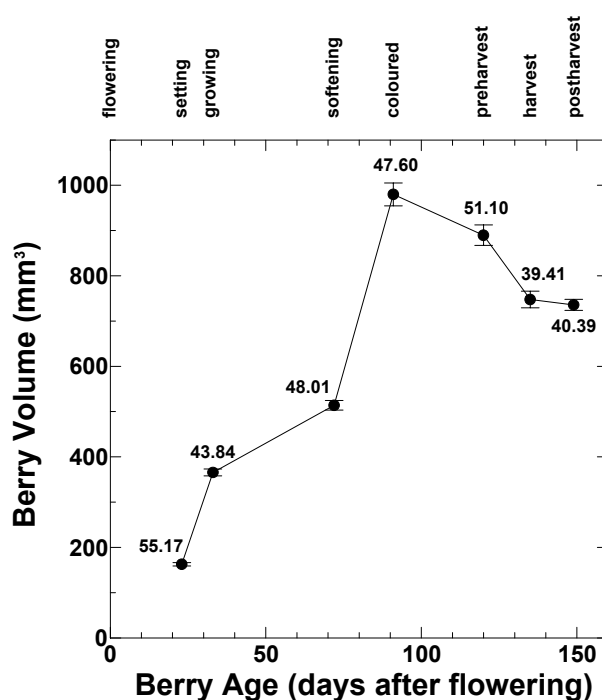


Figure 2.4 Changes in berry volume during development. Four Shiraz bunches were harvested at 7 stages of development: setting, growing, softening, coloured, preharvest, harvest, and postharvest. Mean volume of individual berries is plotted for each stage (\pm one standard error). Coefficients of variation (%) are indicated by the numbers adjacent to the means.

Berry Surface Area

Given that berry surface area and berry volume are calculated from the same set of diameter measurements, it is not surprising that the frequency distributions for both parameters were very similar (**Figure 2.5**). The two peaks for “shot” berries (surface area less than ~ 100 mm² at harvest) and “hens” were easily distinguished. Distributions shifted from a narrow peak width (setting) to a maximum peak width (coloured) to a reduced peak width (harvest).

The relationship between berry surface area (mm²) and berry age (days after flowering) is shown in **Figure 2.6**. Mean berry surface area at each developmental stage was as follows: 141 mm² (setting), 243 mm² (growing), 300 mm² (softening), 461 mm² (coloured), 427 mm² (preharvest), 390 mm² (harvest), and 387 mm² (postharvest). The graph mirrors the plot of berry mass in **Figure 2.2**. The gain in berry surface area was initially rapid between the setting and growing stages, but slowed as softening approached. At the end of the lag phase, between the softening and coloured stages, berry surface area increased rapidly. Berry surface area declined during the final three developmental stages.

The CVs of mean berry surface area throughout this same period were as follows:

39.82% (setting), 33.11% (growing), 38.25% (softening), 36.77% (coloured), 42.08% (preharvest), 32.12% (harvest), 32.34% (postharvest). In similar circumstances to berry mass and berry volume, the CVs in berry surface are consistently high within each developmental stage and indicate only minor changes in variation between the sequential stages. This would suggest that variation in berry surface area is also initiated prior to setting. The same applies to the slight decline in CVs during the harvest and postharvest stages. This indicates that berry surface area will not decline below a predetermined minimum and that some berries have already achieved this value.

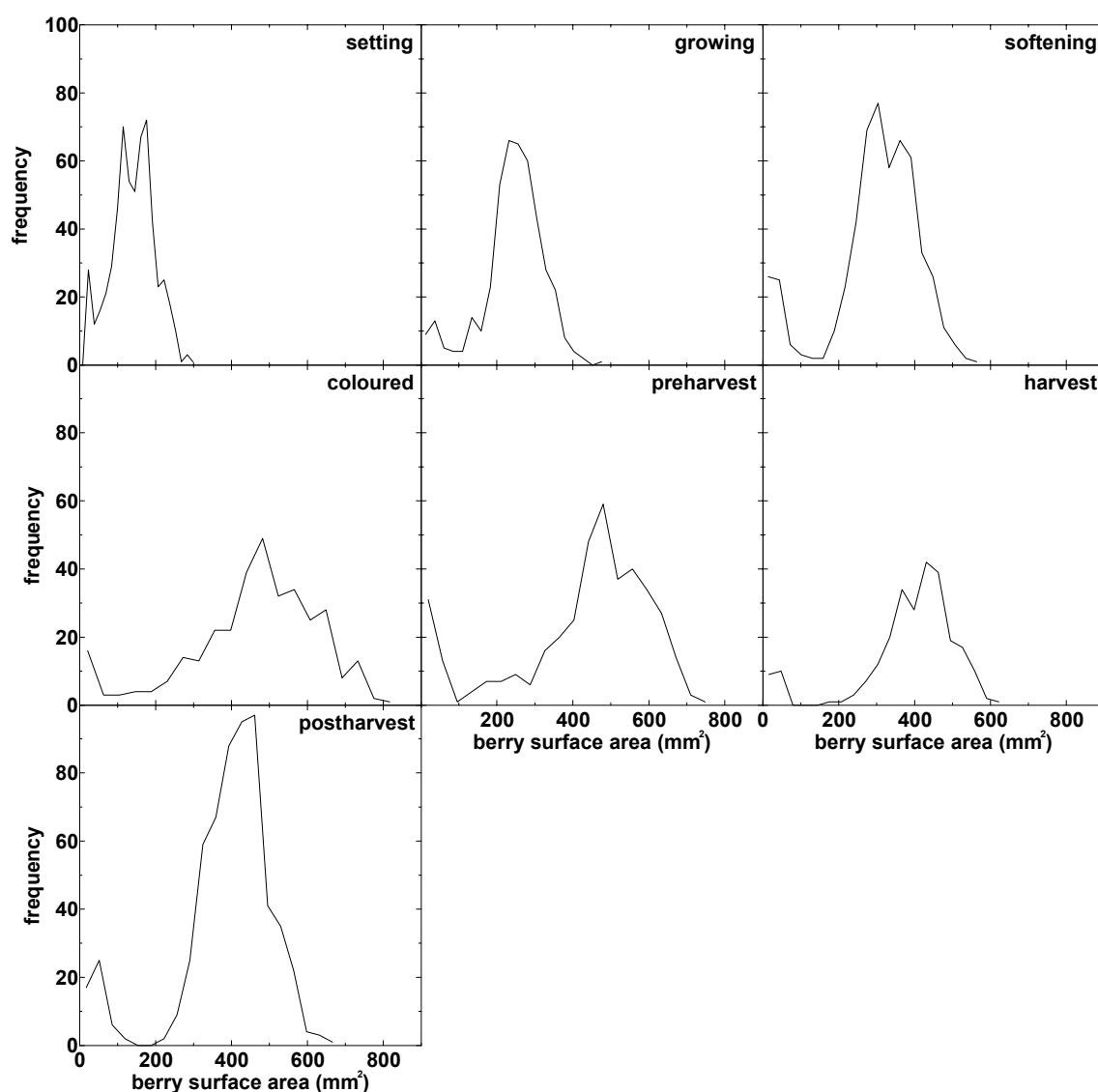


Figure 2.5 Frequency distribution of berry surface area during development. Four Shiraz bunches were harvested at 7 stages of development: setting, growing, softening, coloured, preharvest, harvest, and postharvest. Frequency distributions of individual berry surface area are plotted for each developmental stage using 20 equal divisions on the x-axis.

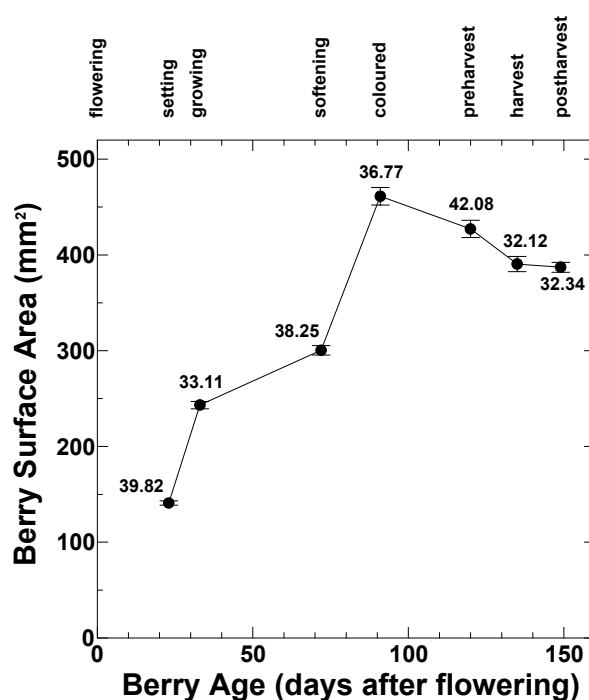


Figure 2.6 Changes in berry surface area during development. Four Shiraz bunches were harvested at 7 stages of development: setting, growing, softening, coloured, preharvest, harvest, and postharvest. Mean surface area of individual berries is plotted for each stage (\pm one standard error). Coefficients of variation (%) are indicated by the numbers adjacent to the means.

Berry Deformability

Although berry sampling covered seven developmental stages – setting, growing, softening, coloured, preharvest, harvest, and postharvest – deformability of berries in the latter two stages exceeded instrument capacity. The frequency distribution of berry deformability for the first five stages is shown in **Figure 2.7**. No obvious division between “shot” berries and “hens” was observed until the berries reached the coloured stage, when the distribution became bimodal. The “hens” deformed to a greater extent (~ 2.0 mm) than the “shot” berries (~ 0.6 mm). The minimum peak width was attained during the growing stage. Thereafter, the peak expanded during softening and attained a maximum width at preharvest.

The relationship between berry deformability (mm) and berry age (days after flowering) is shown in **Figure 2.8**. The course of mean berry deformability throughout development was as follows: 0.48 mm (setting), 0.31 mm (growing), 0.55 mm (softening), 1.87 mm (coloured), 2.38 mm (preharvest). The high level of deformability at set was unexpected, but the remaining values followed the pattern anticipated from the literature, with the maximum rate of change occurring between the softening and coloured stages.

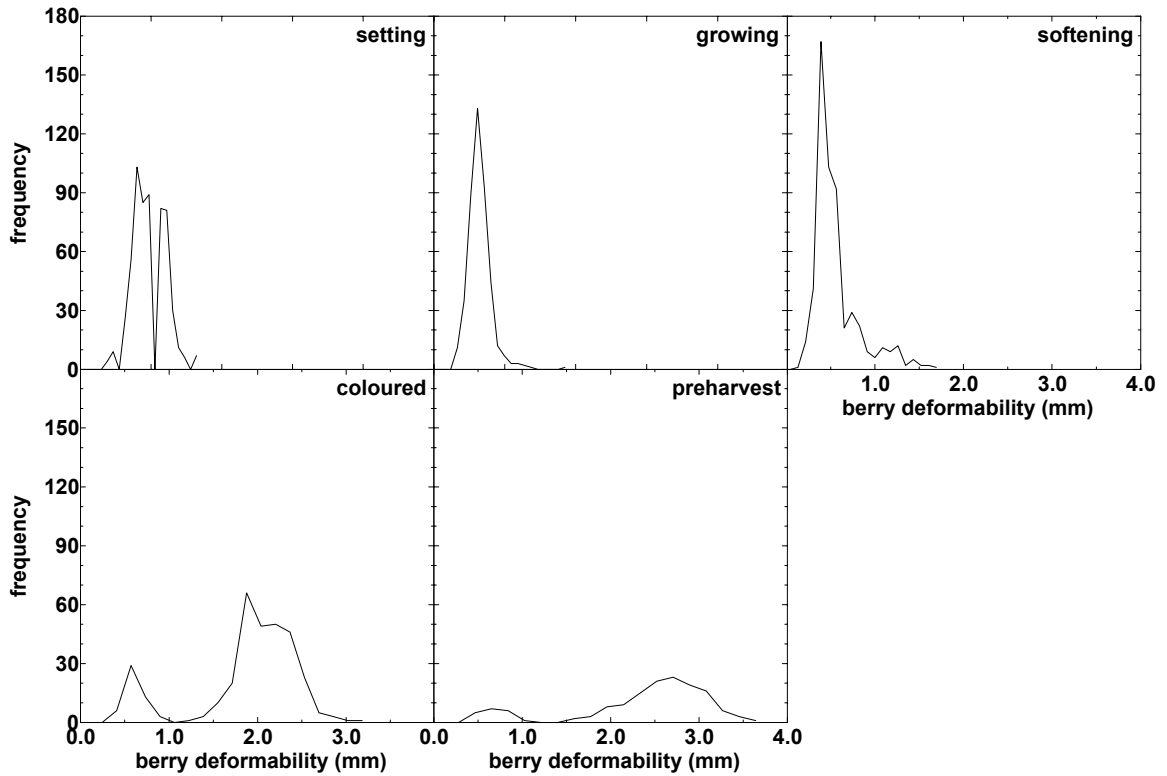


Figure 2.7 Frequency distribution of berry deformability during development. Four Shiraz bunches were harvested at 7 stages of development: setting, growing, softening, coloured, preharvest, harvest, and postharvest. Frequency distributions of individual berry deformability are plotted for the first 5 developmental stages using 20 equal divisions on the x-axis.

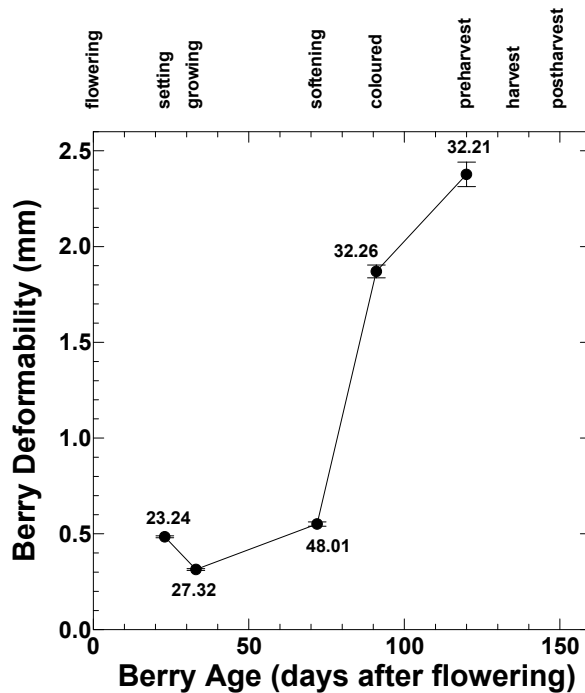


Figure 2.8 Changes in deformability during development. Four Shiraz bunches were harvested at 7 stages of development: setting, growing, softening, coloured, preharvest, harvest, and postharvest. Mean deformability of individual berries is plotted for the first five stages (\pm one standard error). Coefficients of variation (%) are indicated by the numbers adjacent to the means.

The CVs of mean berry deformability throughout this same period were as follows: 23.24% (setting), 27.32% (growing), 48.01% (softening), 32.26% (coloured), 32.21% (preharvest). It is reasonable that the maximum CV is associated with the softening stage because this is a time when berry deformability is in its greatest state of flux. Berries soften at slightly different ages hence the duration of Stage II of berry development is subject to considerable variation.

Berry Mass versus Berry Volume

The correlation between berry mass (g) and berry volume (mm^3) across all of the seven developmental stages sampled is shown in **Figure 2.9**. The correlation is linear and the fitted curve is described by the equation $y = 0.001202x - 0.02465$ ($r^2 = 0.984$). A berry density of 1.202 kg/dm^3 is given by the slope of the equation, using the appropriate conversion factors. The linearity of the relationship indicates that berry density is essentially constant throughout development. The curve only deviates from linearity as berry mass and berry volume approach their respective maxima. This would suggest that berries might decrease in density when they become large.

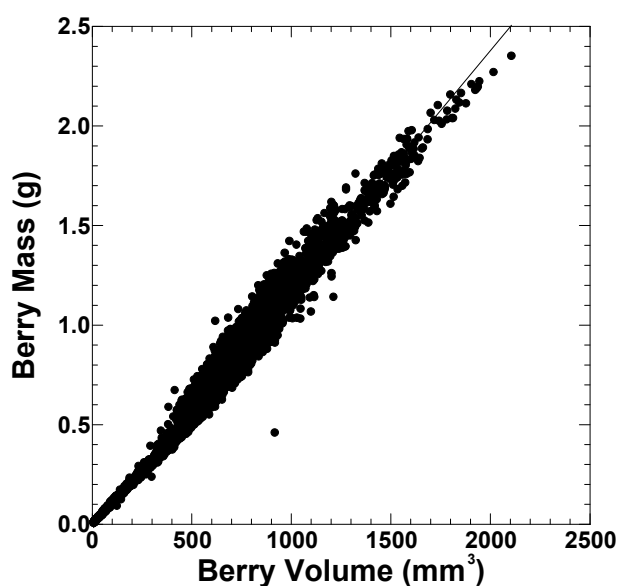


Figure 2.9 Berry mass and berry volume correlation throughout development. Four Shiraz bunches were harvested at 7 stages of development: setting, growing, softening, coloured, preharvest, harvest, and postharvest. Berry mass is plotted against berry volume for individual berries from all developmental stages. The fitted curve is a linear regression with the equation $y = 0.001202x - 0.02465$ ($r^2 = 0.984$).

2.4.2 Developmental Changes in Berry Compositional Characteristics

Berry Growth Stages

Although berry sampling covered seven developmental stages, only three stages were included in the compositional analyses – growing, softening, and preharvest. Individual berries from two Shiraz bunches from separate vines were analysed at each stage.

Combined Seed Mass

The relationship between combined seed mass per berry (g) and berry age (days after flowering) is shown in **Figure 2.10**. Mean combined seed mass at each developmental stage was as follows: 0.0460 g (growing), 0.0485 g (softening), and 0.0425 g (preharvest). The preharvest value was significantly less than both of the preceding developmental stages indicating that the seeds had begun to lose moisture with the onset of maturity.

The CVs of mean combined seed mass throughout this same period all exceeded 50%: 50.97% (growing), 59.32% (softening), 58.21% (preharvest). These consistently high values suggest that variation in seed mass had been initiated earlier in berry development.

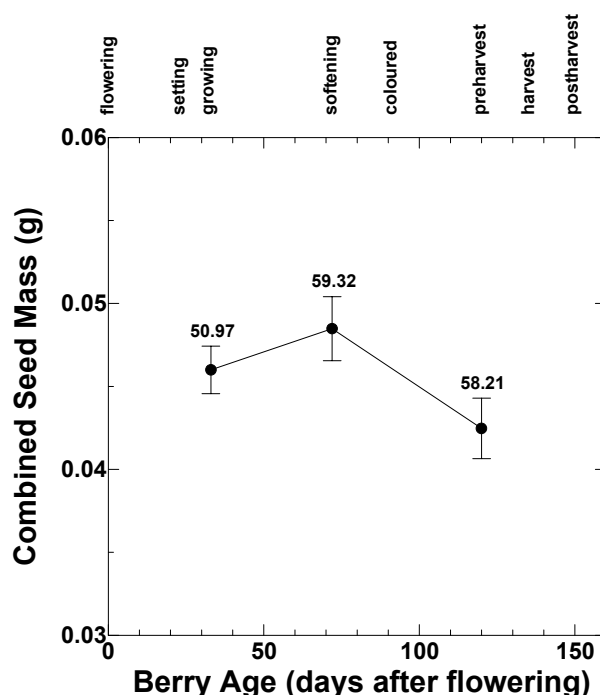


Figure 2.10 Changes in berry combined seed mass during development. Two Shiraz bunches were harvested at 3 stages of development: growing, softening, and preharvest. Mean combined seed mass of individual berries is plotted for each stage (\pm one standard error). Coefficients of variation are indicated by the numbers adjacent to the means.

Berry Mass versus Combined Seed Mass

Individual berry mass is plotted against combined seed mass for the two Shiraz bunches sampled during the growing, softening and preharvest stages (**Figure 2.11**). As indicated by the fitted polynomial curves, unique relationships exist between these parameters at each developmental stage, berry mass per unit seed mass being greater at higher berry mass values. Each of these curves tend to approach a plateau in berry mass. As berry maturity advances, so does the steepness of the relationship between berry mass and combined seed mass.

UV-Vis Spectrophotometric Scans

Examples of typical uv-visible spectrophotometric scans of individual berry extracts taken from Shiraz bunches sampled during the growing, softening, and preharvest stages of development are shown in **Figure 2.12**. The arrows on the figure indicate the wavelengths of maximum absorbance for catechin ($\lambda_{\max} = 275$ nm), quercetin-3-glucoside ($\lambda_{\max} = 364$ nm), and malvidin-3-glucoside ($\lambda_{\max} = 528$ nm). A preliminary observation of absorbance values would suggest that concentrations of catechin and quercetin-3-glucoside are highest during the softening stage and lowest during the preharvest stage, and that malvidin-3-glucoside is only present during the preharvest stage. Detailed analyses of the data reveal a much more complex scenario. The analyses that follow are presented first as “amounts per berry” then as “concentrations”.

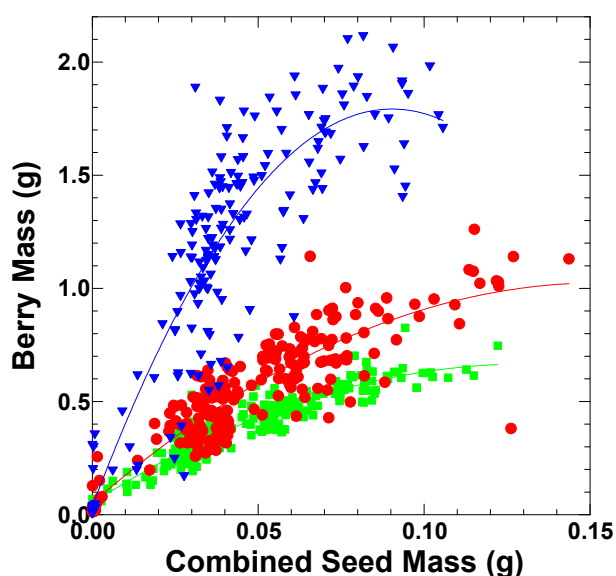


Figure 2.11 Berry and seed mass relationship during development. Individual berry weights and combined seed weights per berry are plotted for two Shiraz bunches sampled during the growing (■), softening (●), and preharvest (▼) stages. Polynomial curves are fitted for each developmental stage.

Variation in Flavonoids per Berry

The amount of malvidin-3-glucoside, quercetin-3-glucoside and catechin extracted from individual berries is plotted against berry mass for two Shiraz bunches sampled during the growing, softening and preharvest stages (**Figure 2.13**). Curves are fitted for each bunch.

During the growing stage, bunches differed markedly in the amount of flavonoids extracted from their berries. A comparison of the fitted curves indicated that one bunch consistently yielded a greater amount of malvidin-3-glucoside, quercetin-3-glucoside and catechin per berry. During the softening stage, the fitted curves for both bunches were markedly similar, as were the amounts of extracted flavonoids per berry. By the time the berries entered the preharvest stage, differences in flavonoids had become apparent once again. On this occasion, the vine that had originally displayed lower levels of malvidin-3-glucoside, now displayed higher levels. The rate of accumulation was similar for both bunches, but it was initiated at an earlier stage in the latter bunch. There was no apparent relationship between quercetin-3-glucoside and berry mass for either bunch. Catechin levels were higher in one bunch from the same vine that showed higher catechin levels during the growing stage. The rate of catechin accumulation was similar in both bunches, but it was initiated at an earlier stage in the former bunch.

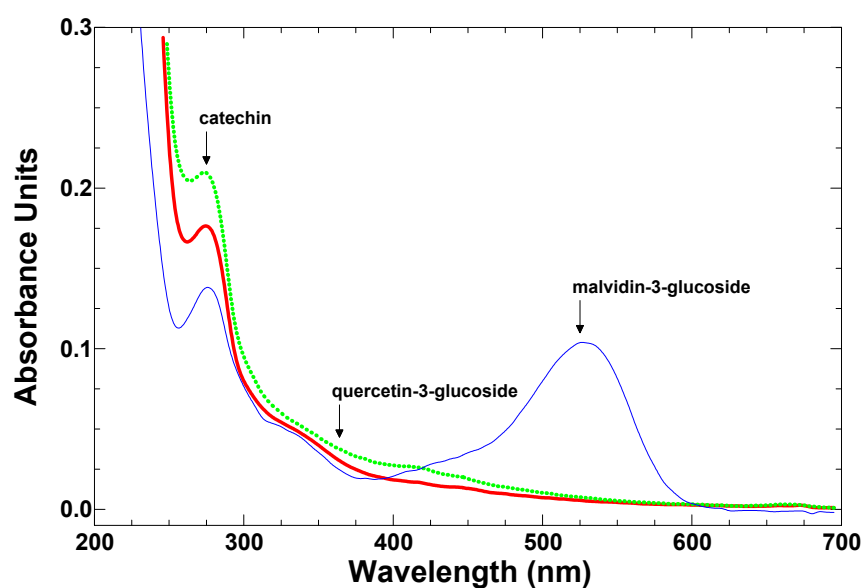


Figure 2.12 UV-visible spectrophotometric scans of berry flavonoids. Typical uv-visible spectrophotometric scans of individual berry extracts taken from Shiraz bunches sampled during the growing (—), softening (---) and preharvest (—) stages of development. Arrows indicate wavelengths of maximum absorbance for catechin, quercetin-3-glucoside and malvidin-3-glucoside.

The mean amount of malvidin-3-glucoside, quercetin-3-glucoside and catechin extracted from the individual berries of both Shiraz bunches is indicated for each growing stage in *Table 2.3*.

The mean amount of malvidin-3-glucoside per berry increased 100-fold between the growing and preharvest stages: viz., growing (0.0051 mg/berry), softening (0.0092 mg/berry,) and preharvest (0.5529 mg/berry). The major increase occurred between the softening and preharvest stages. The amount of quercetin-3-glucoside per berry increased between the growing (0.0386 mg/berry) and softening (0.0537 mg/berry) stages, but declined preharvest

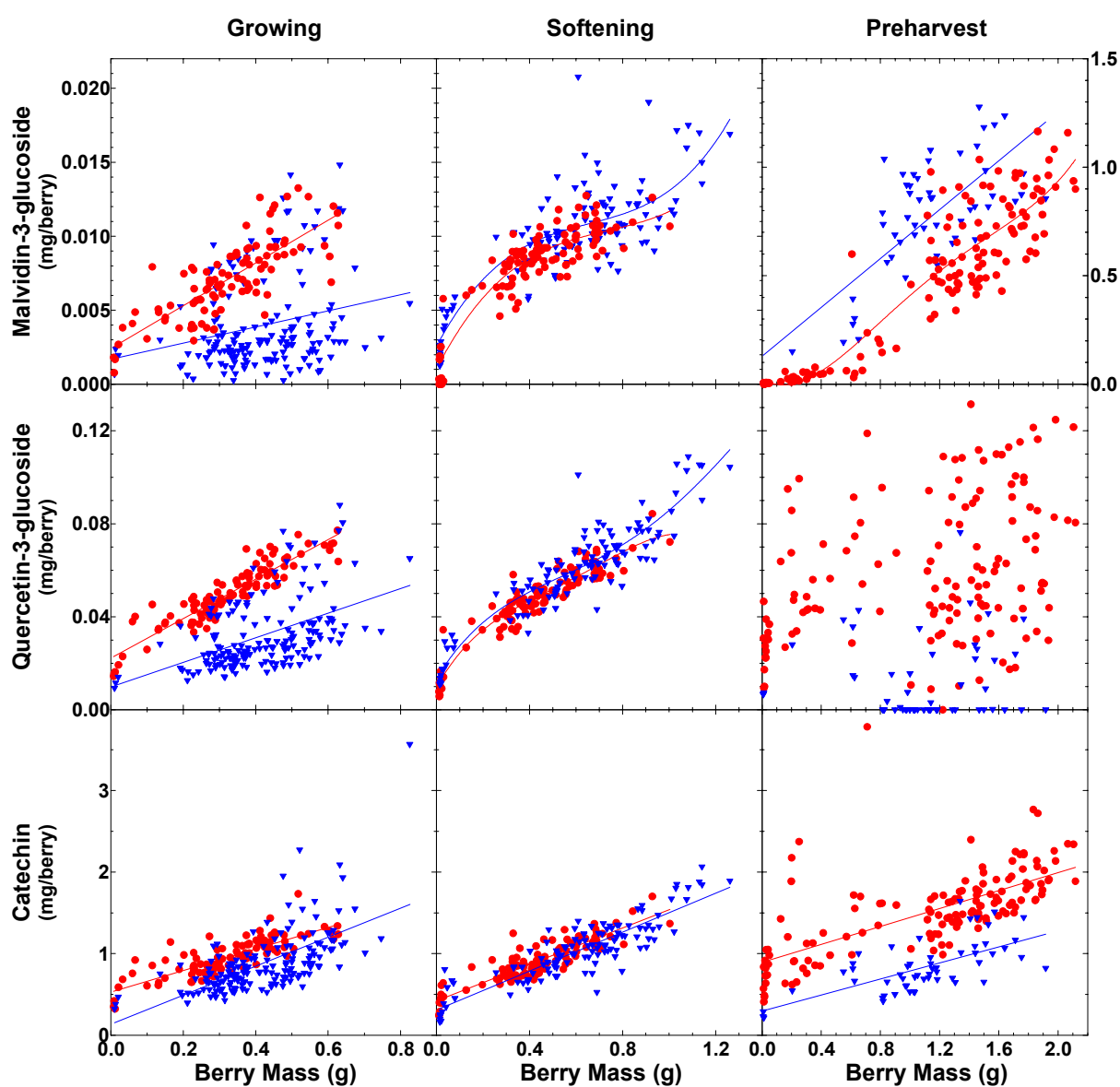


Figure 2.13 Flavonoids per berry versus berry mass during development. The amount of malvidin-3-glucoside, quercetin-3-glucoside and catechin extracted from individual berries is plotted against berry mass for two Shiraz bunches (● and ▼) sampled during the growing, softening and preharvest stages. Curves are fitted for each bunch. Note that the y-axis scale for malvidin-3-glucoside differs during the preharvest stage.

Table 2.3 Flavonoids per berry during development. The amount of malvidin-3-glucoside, quercetin-3-glucoside and catechin extracted from the individual berries of two Shiraz bunches harvested during the growing, softening and preharvest stages. Coefficients of variation are indicated for each flavonoid at each stage.

flavonoid	growing		softening		preharvest	
	Mean Amount (mg/berry)	Coefficient of Variation (%)	Mean Amount (mg/berry)	Coefficient of Variation (%)	Mean Amount (mg/berry)	Coefficient of Variation (%)
malvidin-3-glucoside	0.0051	64.43	0.0092	36.81	0.5529	64.27
quercetin-3-glucoside	0.0386	43.45	0.0537	37.07	0.0458	75.66
catechin	0.9062	37.22	0.9702	35.49	1.3175	42.52

(0.0458 mg/berry). Catechin levels per berry were relatively high throughout berry development, and increased slightly with each successive growth stage: viz., growing (0.9062 mg/berry), softening (0.9702 mg/berry), and preharvest (1.3175 mg/berry).

The CVs for all three compounds were lowest during the softening stage, indicating that variation in flavonoids per berry had achieved its minimum level during this period of development: malvidin-3-glucoside (36.81%), quercetin-3-glucoside (37.07%), and catechin (35.49%). Among the flavonoids, catechin was the least variable across all stages of development: CVs were 37.22% (growing), 35.49% (softening), and 42.52 (preharvest).

Variation in Flavonoid Concentration

The concentrations of malvidin-3-glucoside, quercetin-3-glucoside and catechin extracted from individual berries are plotted against berry mass for two Shiraz bunches sampled during the growing, softening and preharvest stages (**Figure 2.14**). Curves are fitted for each bunch.

Similarities exist between the amount of flavonoids per berry and their concentration. During the growing stage, the concentration of flavonoids within individual berries differed between bunches. One bunch displayed a higher concentration of malvidin-3-glucoside, quercetin-3-glucoside and catechin per unit berry mass. The fitted polynomials indicated an inverse relationship between the log of flavonoid concentration and berry mass. A comparison of the fitted curves during the softening stage indicated that both bunches were essentially identical with respect to the concentrations of extracted flavonoids per unit berry mass. Differences in flavonoid concentration reappeared when the berries entered the

preharvest stage. There was a weak positive relationship between malvidin-3-glucoside concentration and berry mass, but the shapes of the fitted curves differed for each bunch. The vine that had originally displayed a lower concentration of malvidin-3-glucoside during the growing stage, now displayed a higher concentration. One of the two bunches displayed an inverse relationship between the log concentration of quercetin-3-glucoside and berry mass. No such relationship existed for the other bunch. The log of catechin concentration was inversely related to berry mass for both bunches, but one bunch displayed a greater concentration than the other. This same vine displayed an elevated catechin concentration

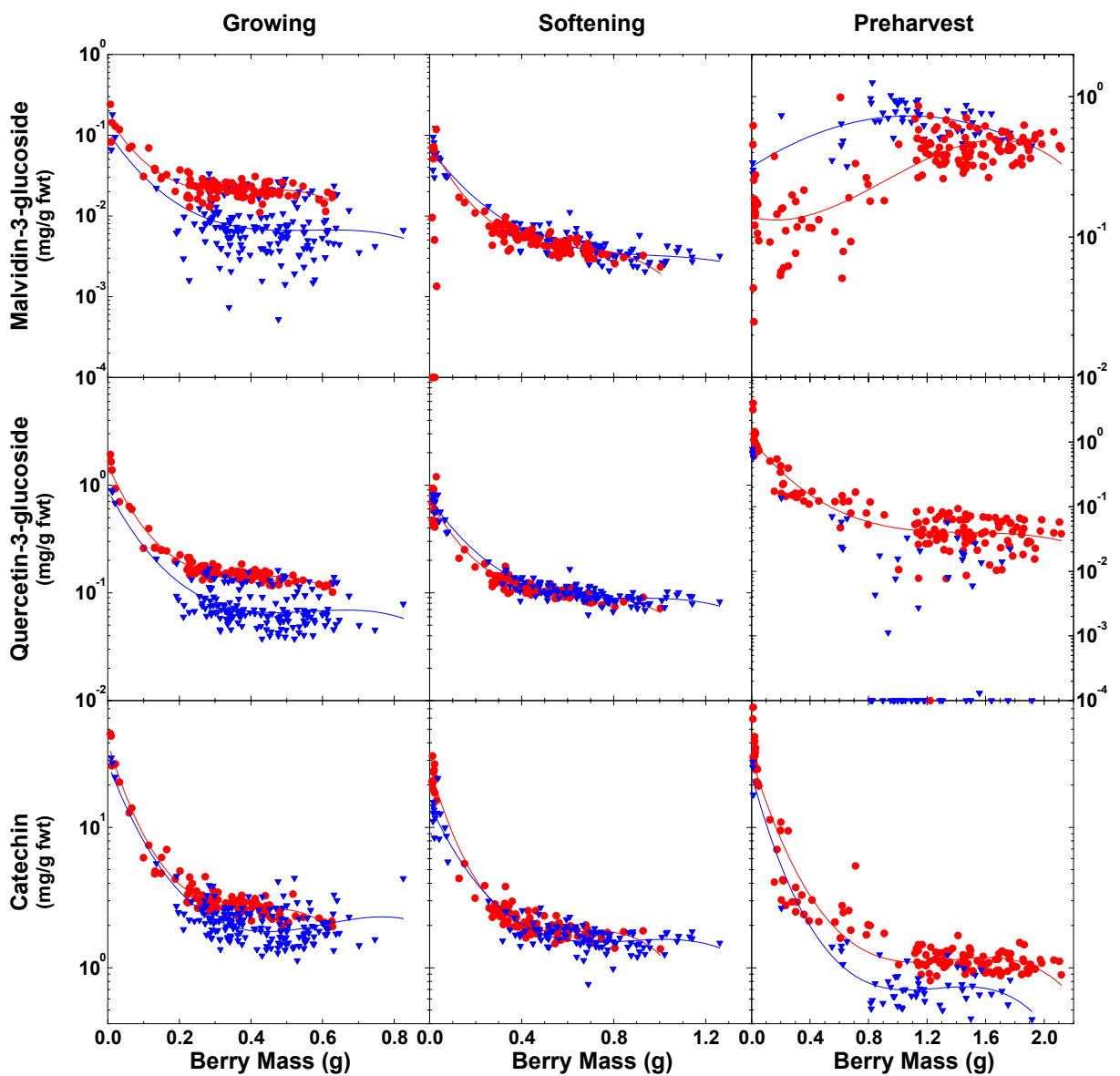


Figure 2.14 Flavonoid concentration versus berry mass during development. The concentration of malvidin-3-glucoside, quercetin-3-glucoside and catechin extracted from individual berries is plotted on a log scale against berry mass for two Shiraz bunches (● and ▼) sampled during the growing, softening and preharvest stages. Curves are fitted for each bunch. Note that the y-axis scales for malvidin-3-glucoside and quercetin-3-glucoside differ during the preharvest stage.

Table 2.4 Flavonoid concentration during development. The concentration of malvidin-3-glucoside, quercetin-3-glucoside and catechin extracted from the individual berries of two Shiraz bunches harvested during the growing, softening and preharvest stages. Coefficients of variation are indicated for each flavonoid at each stage.

flavonoid	growing		softening		preharvest	
	Mean Conc. (mg/g fwt)	Coefficient of Variation (%)	Mean Conc. (mg/g fwt)	Coefficient of Variation (%)	Mean Conc. (mg/g fwt)	Coefficient of Variation (%)
malvidin-3-glucoside	0.0183	132.38	0.0275	117.06	0.4492	52.30
quercetin-3-glucoside	0.1417	140.96	0.1682	110.53	0.1683	260.11
catechin	3.4045	154.70	3.6227	147.36	4.5537	226.06

during the growing stage.

The mean concentration of malvidin-3-glucoside, quercetin-3-glucoside and catechin extracted from the individual berries of both Shiraz bunches is indicated for each growing stage in **Table 2.4**. Malvidin-3-glucoside concentration increased 20-fold as the berries ripened: viz., growing (0.0183 mg/g fwt), softening (0.0275 mg/g fwt), and preharvest (0.4492 mg/g fwt). The majority of this change occurred between the softening and preharvest stages. Quercetin- 3-glucoside concentration increased between the growing (0.1417 mg/g fwt) and softening (0.1682 mg/g fwt) stages, but no significant increase was observed preharvest (0.1683 mg/g fwt) (even though there was a huge increase in variation). Catechin concentration increased marginally between the growing (3.4045 mg/g fwt) and softening (3.6227 mg/g fwt) stages, then increases by a further 20% preharvest (4.5537 mg/g fwt).

CVs for flavonoid concentrations at all stages of development were high, all but one being in excess of 100%. The CV for malvidin-3-glucoside concentration was lowest during the preharvest stage (52.30%). In contrast, CVs for both quercetin-3-glucoside and catechin concentrations attained their maxima during the preharvest stage (260.11% and 226.06%, respectively) and their minima during the softening stage (110.53% and 147.36%, respectively).

2.5 Discussion

The objective of Chapter 2 was to identify when variation in berry size and composition was initiated. The hypothesis was that relative levels of variation in size and composition would remain constant throughout the postflowering period of berry development.

Berries were sampled at setting, growing, softening, coloured, preharvest, harvest, and postharvest stages of development. The physical properties of individual Shiraz berries were described in terms of their mass, volume, surface area, deformability, and seed mass. The flavonoid composition of these same individual berries was assessed. A comparison of CVs between sequential developmental stages indicated when variation in a particular physicochemical parameter was initiated.

The frequency distributions of berry mass, volume and surface area are virtually identical throughout development. “Shot” berries and “hens” were evident from setting onwards, and distributions shifted from a narrow peak width (setting) to a maximum peak width (coloured) to a reduced peak width (harvest). The frequency distribution of berry deformability was markedly different. “Shot” berries and “hens” could not be distinguished until the coloured stage, minimum peak width occurred during the growing stage, and maximum peak width occurred at preharvest.

Berry mass, volume and surface area all follow a similar course of development with time. The relationships are described by double sigmoid curves with peak values during the coloured stage that decline with berry shrinkage through to the postharvest stage. Berry deformability differs from the other parameters in that the setting value exceeds the growing value, and a peak occurs during the preharvest stage. Later stages were beyond the instruments capacity. Seed mass was only measured during the growing, softening, and preharvest stages. It attained a maximum value at softening, and had declined by the preharvest stage. A linear relationship between berry mass and berry volume indicated that berry density remained constant throughout development, although a slight decline was noted after the coloured stage. The curvilinear relationships between berry mass and seed mass were unique for each developmental stage. Seed maturation proceeds independently of berry development (Petrie *et al.* 2000). The end of seed growth occurs during berry softening (Staudt *et al.* 1986, Hardie and Aggenbach 1996), although seed development continues until the berry attains its maximum weight (Kennedy *et al.* 2000, R. Ristic personal communication). However, the development of seed and berry are inter-related during the early postflowering period (Ebadi *et al.* 1996a, 1996b).

Flavonoids were only measured during the growing, coloured, and preharvest stages. Individual berry extracts were assessed for malvidin-3-glucoside, quercetin-3-glucoside and

catechin. These compositional parameters were determined both as amounts per berry and concentrations. Firstly, considering amounts per berry, malvidin-3-glucoside increases markedly after softening, quercetin-3-glucoside decreases slightly after softening, and catechin increases steadily throughout development. In terms of concentrations, malvidin-3-glucoside increases markedly after softening, quercetin-3-glucoside increases marginally at softening, and catechin increases throughout development, especially during the preharvest stage. Differences between bunches were apparent in the amounts per berry and concentrations of berry flavonoids, so the following statements apply equally to both. Bunch-to-bunch differences were evident during the growing stage for all three compounds. The softening stage was characterised by a lack of bunch-to-bunch differences among any of the compounds. During the preharvest stage, bunch-to-bunch differences were confined to malvidin-3-glucoside and catechin, but quercetin-3-glucoside was excluded. Note that the preharvest concentration of malvidin-3-glucoside is up to 10-fold greater in larger berries than in smaller berries. This casts some doubt on the current winemaking philosophy that assumes smaller berries have a greater concentration of colour and flavour compounds simply by virtue of their increased surface area to volume ratio (Freeman 1983, Matthews and Anderson 1988).

CVs indicate changing levels of variation between consecutive developmental stages. Variation in berry mass, berry volume, and berry surface area is consistently high throughout the postflowering period, but it declines marginally as the berries approach harvest maturity (**Table 2.5**). In contrast, variation in berry deformability is greatest at softening. Variation in seed mass was high throughout development, suggesting that their course of development and variability had been determined much earlier. Seeds reach their maximum size at berry softening (Staudt *et al.* 1986, Hardie and Aggenbach 1996).

Variation in the amount per berry of flavonoids was initially high during the growing stage, was reduced during softening stage, and had increased again by the preharvest stage. Variation in concentration of flavonoids was initially high during the growing stage, but it decreased marginally during the softening stage. The CV for malvidin-3-glucoside was lowest during preharvest, but the opposite was true for quercetin-3-glucoside and catechin where the preharvest stage saw these CVs skyrocket. It appears that some berries lose (metabolise) quercetin-3-glucoside and catechin at a faster rate than others leading to greater variability. In contrast, malvidin-3-glucoside is stored in the berry skin (up to a certain maximum level – saturation), thereby reducing variation. Notice that the magnitude and directional change of CVs do not necessarily match those of the measured values. Variation and developmental change are quite different things.

Table 2.5 Coefficients of variation in Shiraz berry parameters. The coefficients of variation (%) in the physical and chemical parameters of developing Shiraz berries that were sampled during the setting, growing, softening, coloured, preharvest, harvest, and postharvest stages. This table is a rearrangement of data presented in **Figures 2.2, 2.4, 2.6, and 2.8,** and **Tables 2.3 and 2.4.**

berry parameter	CV (%)						
	setting	growing	softening	coloured	pre-harvest	harvest	post-harvest
mass	53	44	48	50	53	42	41
volume	55	44	48	49	51	39	40
surface area	40	33	38	37	42	32	32
deformability	23	27	48	34	32	-	-
seed mass	-	51	59	-	58	-	-
flavonoid (amt)							
malvidin	-	64	37	-	64	-	-
quercetin	-	43	37	-	76	-	-
catechin	-	37	35	-	43	-	-
flavonoid (conc)							
malvidin	-	132	117	-	52	-	-
quercetin	-	141	110	-	260	-	-
catechin	-	155	147	-	226	-	-

The CV not only reflects a real or physical difference in variation, but it also embodies variation inherent in the rate of development. For example, berries will soften at different times according to their rate of development (Coombe 1975). The longer the softening period, the greater the variability it engenders. Variability is not just the result of physical factors, but is dependent upon time. The more synchronised the event, the lower the variation (Coombe 1992).

Two events in the course of berry development would appear to have the greatest impact on variation in berry size and composition – berry softening and berry shrivel. Both events seem to synchronise a number of physiological changes that occur within the berry, bunch and vine.

Berry softening signifies the end of Stage II of berry development, the lag phase. It is a period of major metabolic transformation within the berry, and described as the onset of ripening (Kliewer 1965a, 1965b, 1965c, Coombe 1975). Individual berries enter the lag phase at different times having attained different levels of development (Harris *et al.* 1968, Coombe 1980, 1992, Ollat and Gaudillere 1998). The berries remain in a virtual state of developmental inertia, with minimal change in size or composition. At this point the berries soften and ripening begins. The timing of softening is not synchronised between berries, but the rate of sugar accumulation is remarkably uniform once it is initiated (Coombe 1980).

Berry shrivel has been described in a number of grape varieties including Shiraz,

though its causes remain unknown (McCarthy 1997, McCarthy and Coombe 1999, Coombe and McCarthy 2000, Rogiers *et al.* 2001). The fact that it is associated with a decline in CVs in berry mass, volume, and surface area suggests that it too may be a point of resynchronisation during the latter stages of berry development.

In many instances, CVs were already at high levels during the earliest growth stage (setting). The implication is that variation must have arisen at an even earlier time. This places considerable importance on the impact that preflowering events may have on cell division in the floral primordia at budburst. Several researchers are investigating these phenomena with a view to incorporating climatic data into yield prediction models (Dunn and Martin 2000, Sommer *et al.* 2000).

CHAPTER 3 – VARIATION IN CHARDONNAY BERRY SIZE

3.1 Summary

This chapter describes an experiment that sought to identify the extent of variation present in the early stages of berry growth. The hypothesis was that variation in berry size was already significant in the early postflowering period of berry development. Individual Chardonnay berries on two bunches from both ungirdled and girdled vines were assessed on four occasions throughout the flowering period. Individual flowers that had opened during the intervening time period were tagged. One bunch from each vine was sampled at 15 days after the first flower had opened and another at 43 days, giving a range of berry ages: bunch at 15 days comprised berry ages of 1-4, 5-7, 8-11 and 12-15 days; bunch at 43 days comprised berry ages of 29-32, 33-35, 36-39 and 40-43 days. Coefficients of Variation (CVs) for berry mass on ungirdled vines at 15 days (all 3 clones and at all ages) were similar, ranging from 23 to 57%, and were unaffected by girdling. CVs for berry mass on ungirdled vines at 43 days were especially high (74 to 168%). Girdling reduced these high values by about half (45 to 75%). Frequency distributions of berry mass were plotted for each age class for ungirdled and girdled vines. Distributions were negatively skewed for ungirdled vines and positively skewed for girdled vines. No “shot” berries were observed among bunches sampled from girdled vines at 43 days after flowering. Absolute and relative growth rates were typically higher for berries from girdled vines. The relationship between berry mass and seed mass was unaffected by trunk girdling.

3.2 Introduction

The objective of the **second experiment** was to identify the extent of variation present during the early developmental stages of berry growth. The hypothesis was that variation in berry size was already significant in the early postflowering period of berry development.

Understanding the inter-relationship between ovary and seed growth in terms of rates and durations of cell division is essential to the study of variation in developing fruit. Selection of clonal material that display the phenomena of *coulure* and *millerandage* to varying extents, in conjunction with the modifying effect of girdling, generates a large array of experimental material. It is anticipated that the dependence of ovary growth on seed growth will be proven. Given a continuum of levels of seed development, the greatest

variation in berry size and composition will be associated with those factors that maximise variation in the developing seeds within berries on a bunch. An additional girdling treatment will permit testing whether organic nutrition is involved in the seed/pericarp interaction.

3.3 Experimental Procedures

3.3.1 Biological Materials

The experimental site consisted of a 1984 planting of own-rooted Chardonnay vines (clone I10V1) on Scott-Henry trellis at Lenswood, South Australia (34°55'S, 138°49'E). The poor performance of I10V1 in respect of yield initiated a clonal trial at this location in 1989 when 6 other clones (Antav 13, Antav 84, Bernard 76, Bernard 96, G9V7, I10V5) were grafted to the original I10V1 stock (P. Henschke personal communication). Ten vines were used for each treatment. Initial assessment of yield components over two vintages (1993/94 and 1994/95) suggests that Antav 13 and Antav 84 may provide useful experimental material for a developmental study of variation (**Table 3.1**). Both clones have a similar number of bunches per vine, but yield per vine varies: Antav 13 tends to have more berries per bunch than I10V1, but smaller berries; whereas Antav 84 tends to have more berries per bunch than I10V1, but larger berries.

These differences can be attributed to clonal variability with regard to the phenomena of *coulure* and *millerandage* under similar environmental conditions. Thus, I10V1, Antav 13 and Antav 84 appeared likely to provide an experimental system for unravelling the inter-relationship between seed development and cell division.

Thirty vines were selected, 10 each from I10V1, Antav 13, Antav 84. Inflorescence numbers were counted on each vine then four vines were selected from within each clonal group on the basis of a similar inflorescence number to the overall mean. Three similar shoots from each of these vines were selected and tagged, their length and node number were recorded, and the progress of flowering closely monitored. From these three shoots, two basal inflorescences that began flowering at the same time were selected and their potential flowers counted. Opened flowers (E-L stage 19) were tagged at 4 days after the first flower had opened by marking their pedicels with water-resistant acrylic ink (Opaque Magic Color, Royal Sovereign, UK) using a technical pen (Isograph, Rotring, Germany) (**Figure 3.1**). On the same day, half of the vines in each clonal group were trunk girdled with a 5 mm wide incision to the depth of the cambium severing the phloem vessels at 30 cm above ground level (Coombe and Dry 1992). Thereafter, bunches were checked at 3-4 day intervals. Individual flowers that had opened within this interval were also tagged (E-L stage 19).

Table 3.1 Chardonnay yield components. Assessment of Chardonnay yield components over two vintages for 6 clones grafted to I10V1 rootstock (P. Henschke unpublished). Clones I10V1, Antav 13 and Antav 84 were selected for an experimental analysis of variation. All three have a similar bunch numbers per vine but variable yield, primarily as a result of differences in berry size and berry number.

1993/94 means	Clones						I10V5
	I10V1	Antav 13	Antav 84	Bernard 76	Bernard 96	G9V7	
bunches/vine	14.80	16.10	20.50	14.00	12.90	8.78	17.20
yield/vine (kg)	0.54	0.54	1.28	0.71	0.72	0.84	0.60
bunch wt (g)	36.49	33.54	62.44	50.71	55.81	95.70	34.88
berry wt (g)	1.35	1.09	1.36	1.24	1.32	1.48	1.14
berries/bunch	27.03	30.77	45.91	40.90	42.28	64.66	30.60
pH	3.29	3.31	3.32	3.25	3.33	3.25	3.27
TA	9.15	9.08	9.23	10.95	8.18	10.95	8.95
°Brix	22.80	23.60	22.00	22.60	23.00	21.80	22.60

1994/95 means	Clones						I10V5
	I10V1	Antav 13	Antav 84	Bernard 76	Bernard 96	G9V7	
bunches/vine	26.00	27.44	28.40	20.33	24.70	12.00	25.80
yield/vine (kg)	1.02	1.34	1.86	1.41	1.78	1.50	1.22
bunch wt (g)	39.23	48.83	65.49	69.34	72.06	125.00	47.29
berry wt (g)	1.06	0.98	1.10	1.09	1.20	1.26	1.12
berries/bunch	37.01	49.82	59.54	63.62	60.05	99.21	42.22
pH	3.15	3.22	3.15	3.21	3.37	3.16	3.19
TA	10.65	9.75	10.28	9.83	9.60	11.85	10.28
°Brix	23.90	23.70	22.70	23.30	22.60	23.10	23.90

One of the two tagged bunches per vine was removed after 2 weeks when 100% of the flowers had opened (E-L stage 26). By this time, many of the flowers would have undergone nucellus and integument growth in the seed, and cell division in the pericarp would be well advanced (Barritt 1970, Ebadi *et al.* 1996b). The other bunch was sampled 4 weeks later (43 day sample) (E-L stage 30) after embryo formation and cell division in the pericarp would have finished (Barritt 1970, Ebadi *et al.* 1996b). Bunches were stored in plastic bags on ice until returning to the lab. Berries were removed from each bunch, sorted by flowering date, counted, fixed in FPA₅₀ for one week, and stored in 70% ethanol in the refrigerator until ready for analysis.

3.3.2 Ovary and Berry Mass

Pedicels and nectary structures were removed from individual ovaries/berries under a dissecting microscope in 70% ethanol. Berries were blotted dry and weighed to the nearest

0.01 mg on a digital balance (Sartorius, Model ME215S, Germany). Individual weights of all berries were recorded, and each berry was returned to 70% ethanol and stored in a separate vial for ease of recognition if required for further analysis.

Frequency distributions of ovary/berry mass were plotted for each clone to enable a comparison of ungirdled and girdled vines at each harvest time – E-L stage 26 (15 days after first capfall) and E-L stage 30 (43 days after first capfall). Another series of frequency distributions was plotted on the basis of age class.

Four age classes were represented within the 15 day sample (1-4 days, 5-7 days, 8-11 days, 12-15 days) and another four were represented in the 43 day sample (28-31, 32-35 days, 36-39 days, 40-43 days). Day 1 signifies the day on which capfall was initiated. Lastly, frequency distributions were plotted for each individual bunch. Significant differences in mean ovary/berry mass for each clonal selection, girdling treatment, age class, and bunch were checked using Genstat 5 Statistical Package (Genstat 5 Committee, 1987a). Significant differences between clones and age classes were determined by REML (LSD at $p < 0.05$). Significant differences between girdling treatment pairs and bunch pairs were determined by Student t-tests. The CVs associated with each mean were calculated using Equation 1.8.



Figure 3.1 Tagged flowers. Bunches were checked for opened flowers every three to four days. Pedicels of individual flowers that had opened in the intervening period were marked with water-resistant acrylic ink applied using a technical pen. A different coloured ink was used on each occasion so that flowering date could be determined at harvest.

3.3.3 Berry Growth Rates

Growth rates were calculated for individual berries from two bunch samples for each of the three clones using the formulae given in Hunt (1982). Absolute growth rate (AGR) has the units of mg/day and is described by the equation:

$$\text{AGR} = \frac{dW}{dt} \quad \text{Equation 3.1}$$

where dW = difference in weight between two time periods

dt = difference in time between two time periods

Relative growth rate (RGR) has the units of mg/day/day and is described by the equation:

$$\text{RGR} = \frac{d(eW)}{dt} \quad \text{Equation 3.2}$$

where dW = difference in weight between two time periods

dt = difference in time between two time periods

e = the base of natural logarithms

AGR and RGR were plotted for each of the three clones (I10V1, Antav 13, Antav 84), on both harvest dates (15 days, 43 days), for both girdling treatments (ungirdled, girdled). Differences are discussed qualitatively.

3.3.4 Combined Seed Mass

I10V1 was the only clone selected for analysis of combined seed mass. In short, it was because this clone was the most responsive to the girdling treatment. Twenty berries were randomly selected from each age class (where available). The seeds from each berry were excised under the dissecting microscope, and weighed collectively to the nearest 0.01 mg on a digital balance (Sartorius, Model ME215S, Germany). Ovary/berry mass versus ovule/seed mass was plotted for each bunch, girdling treatment, and berry age. Regressions were fitted to describe the relationships.

3.4 Results

3.4.1 Clonal Variation and Girdling Treatments

Two bunches were harvested at 15 days after first capfall, and two more at 43 days, from ungirdled and girdled vines belonging to the three clonal selections – I10V1, Antav 13 and Antav 84. The frequency distribution of ovary and berry mass is shown in **Figure 3.2**.

Clone I10V1

Ovary mass distribution at 15 days in the I10V1 sample exhibits a positive shift as a result of vine girdling. Ungirdled and girdled samples both exhibit bi-modal distributions. The peaks for ungirdled samples are at 1.75 mg and 2.75 mg. The peaks for girdled samples are at 2.25 mg and 4.25 mg. Mean ovary mass increases from 2.76 mg for ungirdled vines to 3.88 mg for girdled vines and the difference is significant at $p < 0.001$ (**Table 3.2**).

Berry mass distribution for the ungirdled sample is tri-modal, with peaks around 1.0, 3.0 and 30 mg. A high proportion of berries are associated with the 1.0 mg peak. These berries have essentially not grown since set and are referred to as “shot” berries. The 3.0 mg peak is relatively low and narrow, and represents the “chicks” – berries that do not attain full size. The 30 mg peak is relatively low but broad, and represents the “hens” – the larger berries within the bunch. The impact of girdling on berry mass distribution is much more obvious at 43 days. The distribution of the girdled sample indicates a single peak around 125 mg. The difference in mean berry mass between the ungirdled sample (30.09 mg) and the girdled sample (97.14 mg) is significant at $p < 0.001$ (**Table 3.2**).

Clone Antav 13

The distribution of ovary mass for Antav 13 appears to be similar between ungirdled and girdled samples at 15 days. Both distributions are bi-modal with peaks at 1.75 mg and 4.25 mg for the ungirdled sample, and 2.25 mg and 5.75 mg for the girdled sample. Nevertheless, mean ovary mass increases from 3.75 mg for ungirdled vines to 4.33 mg for girdled vines and the difference is significant at $p < 0.001$ (**Table 3.2**).

At 43 days, the differences between the girdling treatments are more apparent. The ungirdled vines display two major peaks – one at 1.0 mg, and another at 35 mg. There is no sign of the 3.0 mg peak that was present for I10V1. The height of both peaks is similar in Antav 13, which indicates that this clone has a lower proportion of “shot” berries and a higher proportion of “hens” relative to I10V1. The girdled vines have a minor peak around 1.0 mg, indicating that some “shot” berries still remain on the bunch at 43 days. The major peak around 125 mg indicates that most berries have developed into “hens”. The difference in mean berry mass between the ungirdled sample (43.06 mg) and the girdled sample (99.34 mg) is significant at $p < 0.001$ (**Table 3.2**).

Clone Antav 84

Ovary mass distribution for Antav 84 at 15 days is similar for both girdling treatments. Both distributions are bi-modal, with peaks at 1.75 mg and 4.25 mg. Mean ovary mass is

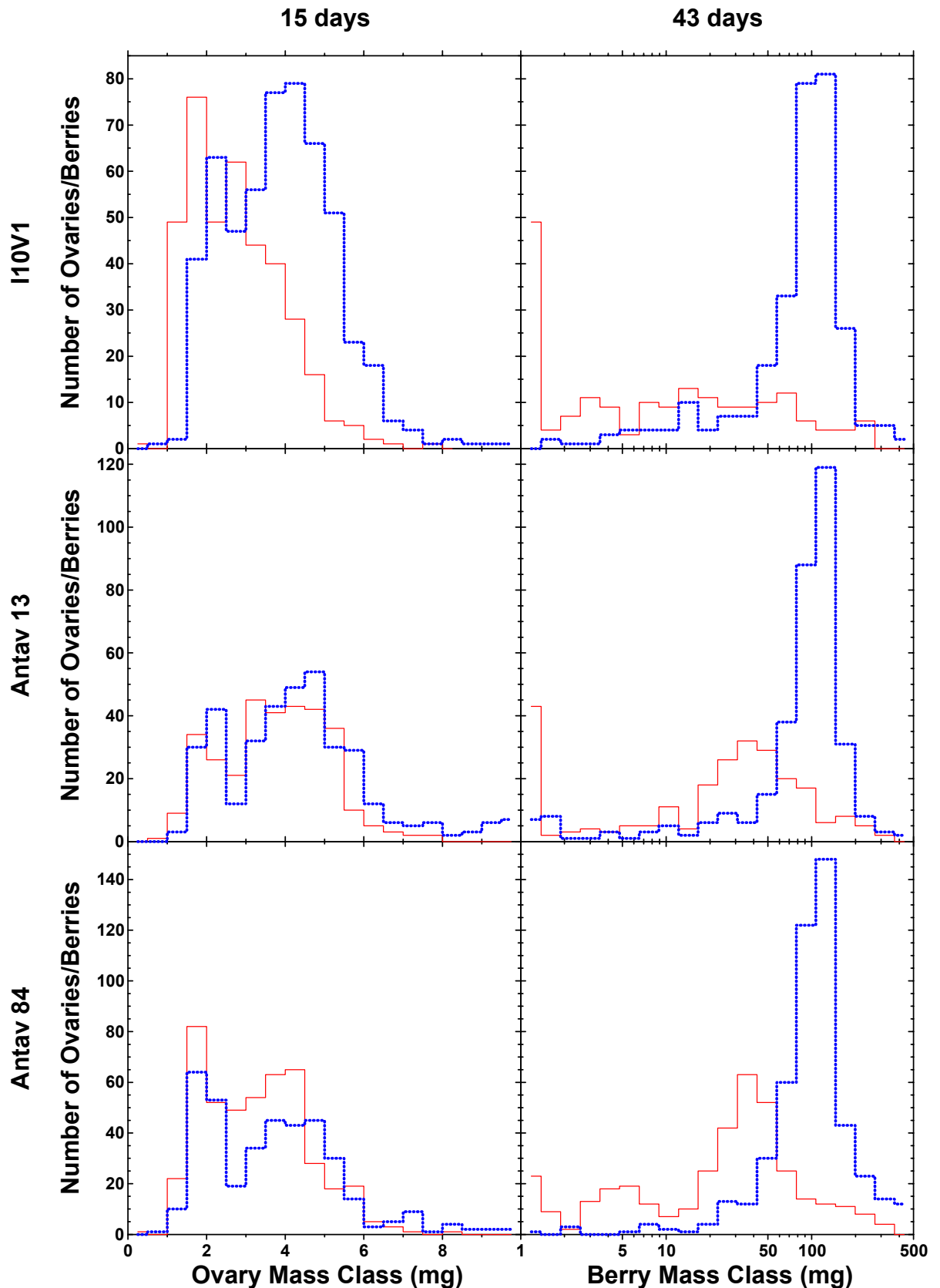


Figure 3.2 Frequency distribution of ovary and berry mass. Two bunches were harvested at 15 days (positioned on LHS) and 43 days (positioned on RHS) after first capfall from each of the three clones – I10V1, Antav 13 and Antav 84. Ovaries from ungirdled bunches are indicated by the thin, solid line (—). Ovaries from girdled bunches are indicated by the thick, broken line (---). Intervals of ovary mass class are 0.5 mg. Intervals of berry mass class are equal parts of log mg. Note that y-axis scales differ for each clone.

Table 3.2 Variation in ovary and berry mass with harvest date. The mean mass (mg) and coefficient of variation (%) for each harvest date of ovaries/berries from ungirdled and girdled vines for the three Chardonnay clones – I10V1, Antav 13, and Antav 84. Bunches were harvested at 15 days and at 43 days after first capfall. Each age class and girdling treatment is the mean of two bunches. Significant differences between clones were determined by REML and are indicated by the letters that follow the mean mass values (LSD at $p < 0.05$). Significant differences between ungirdled and girdled sample pairs were determined by Student t-tests and significance levels are indicated by the following symbols: “*” = $p < 0.05$, “**” = $p < 0.01$, “***” = $p < 0.001$, “ns” = not significant, “na” = not applicable (insufficient sample numbers).

harvest date (clone)	ungirdled		girdled	
	mean mass (mg)	CV (%)	mean mass (mg)	CV (%)
15 days				
I10V1	2.76 ^a	42.61	3.88 ^a ***	35.76
Antav 13	3.75 ^c	35.58	4.33 ^b ***	43.95
Antav 84	3.27 ^b	40.04	3.70 ^a ***	46.38
43 days				
I10V1	30.09 ^a	169.95	97.14 ^a ***	63.49
Antav 13	43.06 ^b	120.34	99.34 ^a ***	55.92
Antav 84	43.58 ^b	119.88	116.08 ^b ***	64.38

significantly different between the treatments at $p < 0.001$ – 3.27 mg (ungirdled) cf. 3.70 mg (girdled) (*Table 3.2*).

By 43 days after first capfall, differences have emerged. The ungirdled vines exhibit a tri-modal distribution with peaks around 1.0 mg, 5.0 mg and 35 mg. The 1.0 mg and 5.0 mg peaks are of a similar height, but the 35 mg peak represents the largest proportion of berries. This clone has the lowest proportion of “shot” berries and the highest proportion of “hens” among the three clones studied. Berry mass distribution for girdled vines from Antav 84 indicates a single peak around 125 mg. Differences in mean berry mass between the ungirdled sample (43.58 mg) and the girdled sample (116.08 mg) are significant at $p < 0.001$ (*Table 3.2*).

Interclonal Variation

The mean mass and CV for each harvest date of ovaries/berries from ungirdled and girdled vines for the three Chardonnay clones are shown in *Table 3.2*. Significant differences between clones were determined by REML and are indicated by the letters that follow the mean mass values (LSD at $p < 0.05$). Significant differences between ungirdled and girdled sample pairs were determined by Student t-tests and significance levels are indicated in the table.

The mean ovary mass for the ungirdled sample of each clone was significantly different at day 15. I10V1 (2.76 mg) was the lightest, Antav 84 (3.27 mg) of intermediate weight, and Antav 13 (3.75 mg) the heaviest. Among the girdled vines, only Antav 13 (4.33 mg) proved to have statistically larger ovaries than the other two clones (Antav 84 was 3.70 mg; I10V1 was 3.88 mg). At day 43, ovary mass for the ungirdled sample from I10V1 (30.09 mg) was significantly less than Antav 13 (43.06 mg) and Antav 84 (43.58 mg). In the girdled sample, ovary mass for Antav 84 (116.08 mg) was significantly greater than both I10V1 (97.14 mg) and Antav 13 (99.34 mg).

No trend among CVs was evident at day 15: CVs for ungirdled and girdled samples from all clones were within the range of 36% to 46%. However, by day 43, the CVs had changed remarkably. All ungirdled samples exhibited increased variation, with CVs in the range 120% to 170%. I10V1 was the highest at 169.95%. In contrast, CVs from girdled samples had increased only marginally, and were in the vicinity of 56% to 64%.

3.4.2 Berry Age Classes

Two ungirdled and two girdled bunches were harvested at 15 days after first capfall from each of the three clones – I10V1, Antav 13 and Antav 84. Four age class of ovaries are represented in the sample: 1-4 days, 5-7 days, 8-11 days, 12-15 days. The frequency distribution of ovary mass for each age class is plotted in **Figure 3.3**. Points indicate ovary mass class intervals of 0.5 mg.

An identical sample was harvested from the same vines at 43 days after first capfall from each of the three clones. The four age classes of berries represented in this sample were 29-32 days, 33-35 days, 36-39 days, and 40-43 days. The frequency distribution of berry mass for each age class is plotted in **Figure 3.4**. Points indicate berry mass class intervals of 20 mg.

The mean mass (mg) and CV (%) for all age class of ovaries/berries from ungirdled and girdled vines for the three Chardonnay clones is presented in **Table 3.3**. Each age class and girdling treatment is the mean of two bunches. Significant differences between age classes were determined by REML (LSD at $p < 0.05$). Significant differences between ungirdled and girdled sample pairs were determined by Student t-tests (significance levels “*” = $p < 0.05$, “**” = $p < 0.01$, “***” = $p < 0.001$, “ns” = not significant).

Clone I10V1

Ovary mass distributions for the ungirdled and girdled samples from I10V1 indicate separate peaks in each of the four age classes (**Figure 3.3**). The number of ovaries in the 1-4 day age

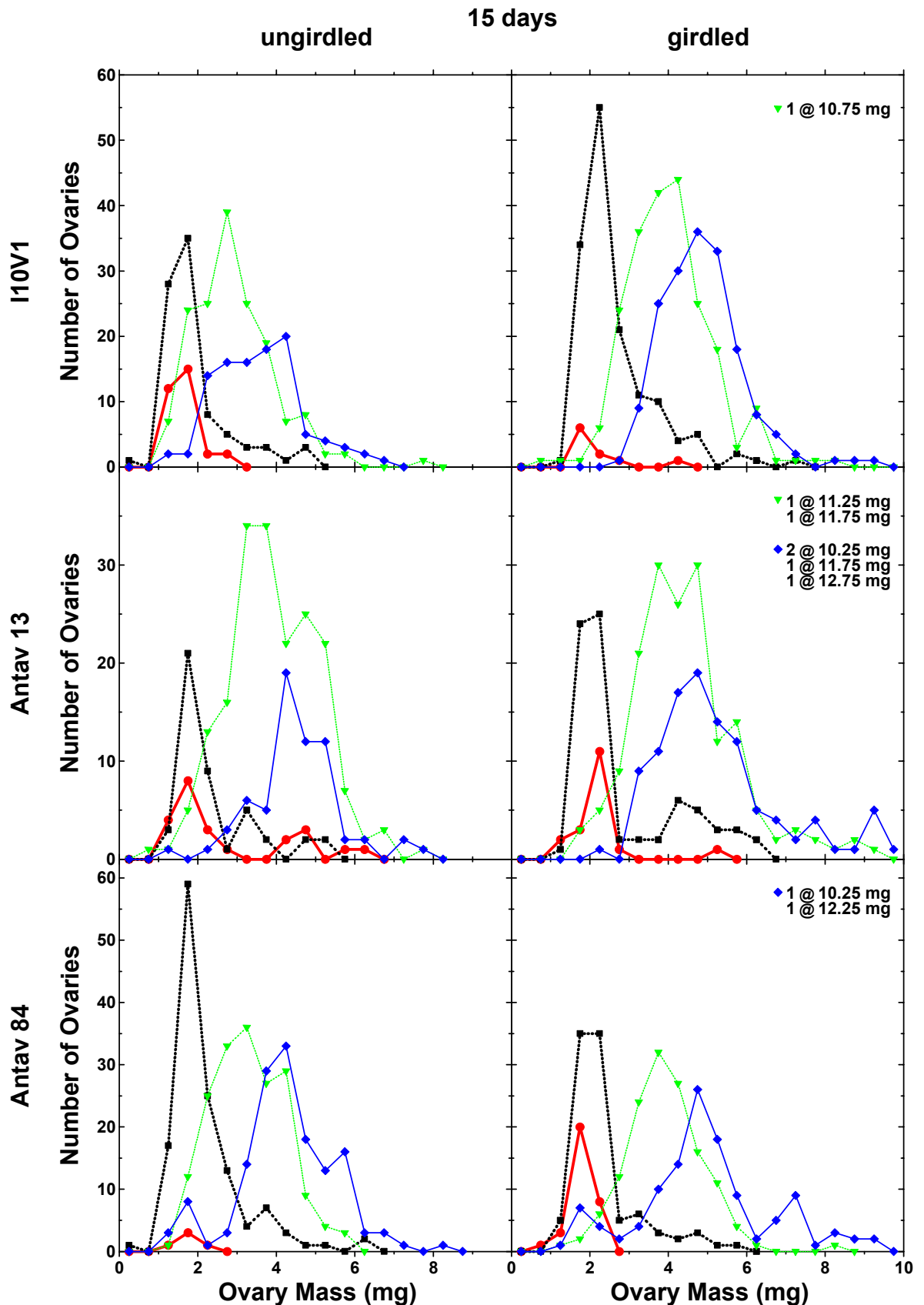


Figure 3.3 Frequency distribution of ovary mass. Two bunches were harvested at 15 days after first capfall from each of the three clones – I10V1, Antav 13 and Antav 84. Bunches from ungirdled vines are positioned on the LHS. Bunches from girdled vines are positioned on the RHS. Age class of ovaries at harvest is indicated by the following symbols: ● (1-4 days), ■ (5-7 days), ▼ (8-11 days), ◆ (12-15 days). Points indicate ovary mass class intervals of 0.5 mg. Data points outside of the x-axis range are indicated on three graphs.

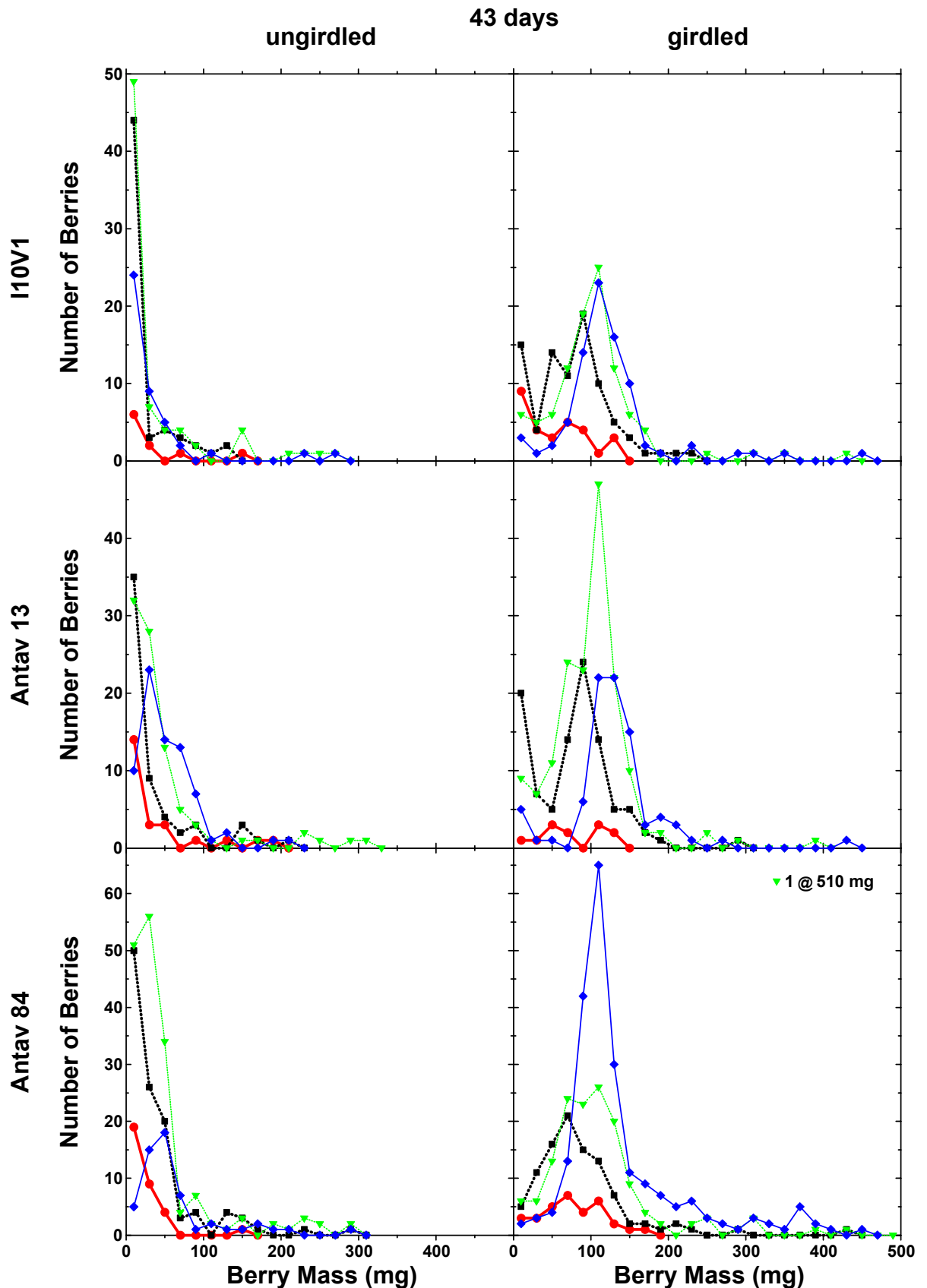


Figure 3.4 Frequency distribution of berry mass. Two bunches were harvested at 43 days after first capfall from each of the three clones – I10V1, Antav 13 and Antav 84. Bunches from ungirdled vines are positioned on the LHS. Bunches from girdled vines are positioned on the RHS. Age class of berries at harvest is indicated by the following symbols: ● (29-32 days), ■ (33-35 days), ▼ (36-39 days), ◆ (40-43 days). Points indicate berry mass class intervals of 20 mg. Data points outside of the x-axis range are indicated on one graph.

Table 3.3 Variation in ovary and berry mass with age. The mean mass (mg) and coefficient of variation (%) for each age class of ovaries/berries from ungyrdled and gyrdled vines for the three Chardonnay clones – I10V1, Antav 13, and Antav 84. Bunches were harvested at 15 days after first capfall (age classes 1-4, 5-7, 8-11 and 12-15) and at 43 days after first capfall (age classes 29-32, 33-35, 36-39 and 40-43). Each age class and gyrdling treatment is the mean of two bunches. Significant differences between age classes were determined by REML and are indicated by the letters that follow the mean mass values (LSD at $p < 0.05$). Significant differences between ungyrdled and gyrdled sample pairs were determined by Student t-tests and significance levels are indicated by the following symbols: “*” = $p < 0.05$, “**” = $p < 0.01$, “***” = $p < 0.001$, “ns” = not significant.

I10V1				
ovary/berry age class	ungyrdled		gyrdled	
	mean mass (mg)	CV (%)	mean mass (mg)	CV (%)
1-4	1.65 ^a	23.80	2.12 ^a *	42.68
5-7	1.93 ^a	43.91	2.62 ^b ***	37.50
8-11	2.92 ^b	35.64	4.05 ^c ***	28.70
12-15	3.56 ^c	30.29	4.86 ^d ***	20.93
29-32	29.56 ^a	157.28	56.33 ^a ns	75.41
33-35	20.54 ^a	161.42	76.99 ^a ***	63.13
36-39	36.38 ^a	167.76	104.44 ^b ***	59.26
40-43	32.48 ^a	164.58	123.32 ^b ***	53.18
Antav 13				
ovary/berry age class	ungyrdled		gyrdled	
	mean mass (mg)	CV (%)	mean mass (mg)	CV (%)
1-4	2.75 ^a	57.26	2.22 ^a ns	35.85
5-7	2.39 ^a	42.19	2.81 ^a ns	48.28
8-11	3.94 ^b	28.93	4.51 ^b ***	34.40
12-15	4.48 ^c	24.61	5.44 ^c ***	35.09
29-32	34.46 ^{ab}	154.54	75.75 ^a *	53.27
33-35	30.71 ^a	156.53	76.04 ^a ***	67.80
36-39	46.39 ^{ab}	132.09	99.18 ^b ***	50.42
40-43	51.76 ^b	74.44	129.85 ^c ***	44.51
Antav 84				
ovary/berry age class	ungyrdled		gyrdled	
	mean mass (mg)	CV (%)	mean mass (mg)	CV (%)
1-4	1.69 ^a	23.41	1.81 ^a ns	16.68
5-7	2.19 ^a	43.47	2.37 ^b ns	37.39
8-11	3.31 ^b	27.63	3.89 ^c ***	25.53
12-15	4.26 ^c	28.45	5.04 ^d ***	36.91
29-32	22.23 ^a	131.15	76.67 ^a ***	50.52
33-35	37.34 ^{ab}	128.52	87.16 ^a ***	69.36
36-39	45.52 ^b	122.40	112.75 ^b ***	67.63
40-43	63.29 ^c	85.89	137.08 ^c ***	56.02

class is lower for girdled bunches. In contrast, the number of ovaries in the 5-7 day and 12-15 day categories is higher for girdled bunches. The frequency distribution peaks correspond to the means in **Table 3.3**. The first two age classes are not significantly different from each other – 1-4 days (1.65 mg) and 5-7 days (1.93 mg). However, significant increases in mean ovary mass are observed at 8-11 days (2.92 mg) and 12-15 days (3.56 mg). Individual peaks are also discernible in the girdled sample. Each consecutive age class exhibits a significant increase in ovary mass – 1-4 days (2.12 mg), 5-7 days (2.62 mg), 8-11 days (4.05 mg), and 12-15 days (4.86 mg). All girdled samples are significantly heavier than their ungirdled counterparts. CVs range from 24% to 44% for ungirdled vines, and from 21% to 43% for girdled vines. In most cases the value is lower for girdled vines, but the differences are minor.

At 43 days after first capfall, the frequency distribution of ungirdled vines from I10V1 is complex (**Figure 3.4**). A large proportion of berries from all age classes is confined to the lowest mass category. The sample did not exhibit significant differences in berry mass between the age classes – 29-32 days (29.56 mg), 33-35 days (20.54 mg), 36-39 days (36.38 mg), and 40-43 days (32.48 mg). Peaks are discernible in the girdled treatment that is comprised of two significantly different groups. Group one included the younger berries – 29-32 days (56.33 mg) and 33-35 days (76.99 mg). Group two included the older berries – 36-39 days (104.44 mg), and 40-43 days (123.32 mg). Excluding the 29-32 day sample, all girdled berries are significantly heavier than their ungirdled counterparts. CVs range from 157% to 168% for ungirdled vines, and from 53% to 75% for girdled vines. The difference is 2.1-fold or greater, and is significant.

Clone Antav 13

Ovary mass distributions for ungirdled and girdled bunches of Antav 13 harvested at day 15 are similar at every age class (**Figure 3.4**). The ungirdled sample means (**Table 3.3**) in the first two age classes are not significantly different from each other – 1-4 days (2.75 mg) and 5-7 days (2.39 mg). However, significant increases in mean ovary mass are observed at 8-11 days (3.94 mg) and 12-15 days (4.48 mg). The girdled sample also displays individual peaks in the frequency distribution. As with the ungirdled sample, the first two age classes are not significantly different from each other – 1-4 days (2.22 mg) and 5-7 days (2.81 mg) – but the latter two are – 8-11 days (4.51 mg) and 12-15 days (5.44 mg). Only the oldest two girdled samples are significantly heavier than their ungirdled counterparts. CVs range from 25% to 57% for girdled vines, and from 34% to 48% for girdled vines. In most instances, the value is higher for girdled vines, but the differences are minor.

The frequency distribution of ungirdled vines from Antav 13 at 43 days is skewed

towards the lower range of berry mass (**Figure 3.4**), though to a lesser extent than I10V1. A significant difference in berry mass exists between age classes at 33-35 days (30.71 mg) and 40-43 days (51.76 mg), but the values at 29-32 days (34.46 mg) and 36-39 days (46.39 mg) are intermediate between these two. Girdling normalises the frequency distribution of berry mass, and increases the number of berries in the 36-39 day age class. The two youngest classes are not significantly different from each other – 29-32 days (75.75 mg), 33-35 days (76.04 mg) (**Table 3.3**). However, a significant increase in mean berry mass is observed at 36-39 days (99.18 mg) and 40-43 days (129.85 mg). All girdled berries are significantly heavier than their ungirdled counterparts. CVs for ungirdled vines range from 74% to 157%, and from 45% to 68% for girdled vines. Berries from the oldest ungirdled age class exhibit a noticeable decrease in variation. The difference between ungirdled and girdled vines is typically 1.7-fold or greater, and is significant.

Clone Antav 84

The frequency distribution of ovary mass for ungirdled and girdled vines at 15 days for Antav 84 is shown in **Figure 3.3**. Both distributions are similar, but the number of ovaries in the 1-4 days category is higher in the girdled sample, whereas the number of ovaries in the 5-7 days category is lower. The difference between ovary mass of ungirdled samples at 1-4 days (1.69 mg) and 5-7 days (2.19 mg) is not significant (**Table 3.2**). However, the difference does become significant at 8-11 days (3.31 mg) and at 12-15 days (4.26 mg). For girdled vines, mean ovary mass increases significantly between consecutive age classes – 1-4 days (1.81 mg), 5-7 days (2.37 mg), 8-11 days (3.89 mg), and 12-15 days (5.04 mg). Only the latter two age classes exhibit a significant increase in berry mass over their ungirdled counterparts. CVs from ungirdled vines range from 23% to 43%, and from girdled vines from 17% to 37%. The values for girdled vines are predominantly lower, but the difference is minor.

Figure 3.4 shows the frequency distribution of berry mass for girdled and ungirdled vines at 43 days for Antav 84. The ungirdled vines are skewed toward the lower range of berry mass, but less so than for I10V1. Girdling normalises this distribution and shifts it significantly to the right for all age classes. The number of berries in the 40-43 day age class increases in response to girdling, whereas the number allocated to the lowest mass class is reduced. Three age classes show significant increases in berry mass – 29-32 days (22.23 mg), 36-39 days (45.50 mg), and 40-43 days (63.29 mg). Berry mass at 33-35 days (37.34 mg) is intermediate between the first and third age class. The girdled bunches also fall into three significantly different groups. Berries at 29-32 days (76.67 mg) and 33-35 days (87.16 mg) are statistically inseparable, but significant differences exist at 36-39 days (112.75 mg) and

40-43 days (137.08 mg). All age classes exhibit a significant mass increase over their ungirdled counterparts. CVs from ungirdled vines range from 86% to 131%, and from girdled vines from 51% to 69%. The 40-43 ungirdled age class exhibits a substantial decline in variation relative to the other ungirdled age classes. A minimum 1.5-fold difference exists between the ungirdled and girdled vines. This represents a significant reduction in variation.

3.4.3 Variation between Bunches

Clone I10V1

Frequency distributions of individual ovaries in each age class for I10V1 at 15 days after first capfall are shown in **Figure 3.5**. Two bunches were harvested from ungirdled vines and two more from girdled vines. Each bunch is displayed in a separate graph with individual ovaries identified as single points. Four separate age classes are identified on the y-axis: 1-4 days, 5-7 days, 8-11 days, 12-15 days. Ovary mass classes are divided into intervals of 0.2 g. The vertical, broken lines indicate groups of ovaries within the 3 predominant mass ranges: 1.4-1.8 mg, 2.8-3.2 mg, 4.8-5.2 mg. These mass ranges are chosen to represent “shot” berries, “chicks” and “hens”, respectively.

Figure 3.6 displays the frequency distribution of individual berries in each age class for I10V1 at 43 days after first capfall. Two bunches were harvested from ungirdled vines and two more from girdled vines. Each bunch is displayed separately. Individual berries are identified as single points on the graphs. Four separate age classes are identified on the y-axis: 29-32 days, 33-35 days, 36-39 days, 40-43 days. Berry mass classes are divided into equal intervals on a log scale. The broken lines indicate groups of berries within the 2 predominant mass ranges: 11-15 mg, 57-81 mg. These mass ranges are chosen to represent “chicks” and “hens”, respectively. “Shot” berries at 1 mg or less are still evident within the ungirdled bunches, but are lacking among the girdled bunches.

The mean mass (mg) and CV (%) for each age class of ovaries/berries from ungirdled and girdled vines for the Chardonnay clone I10V1 are indicated in **Table 3.4**. Two bunches were harvested at 15 days after capfall (age classes 1-4, 5-7, 8-11 and 12-15) and two more at 43 days after capfall (age classes 29-32, 33-35, 36-39 and 40-43). Data for each bunch are presented separately. Significant differences between bunch pairs were determined by Student t-tests and significance levels are indicated by the following symbols: “*” = $p < 0.05$, “**” = $p < 0.01$, “***” = $p < 0.001$, “ns” = not significant, “na” = not applicable (insufficient sample numbers).

An obvious feature of the distributions is the inequality of ovary/berry numbers

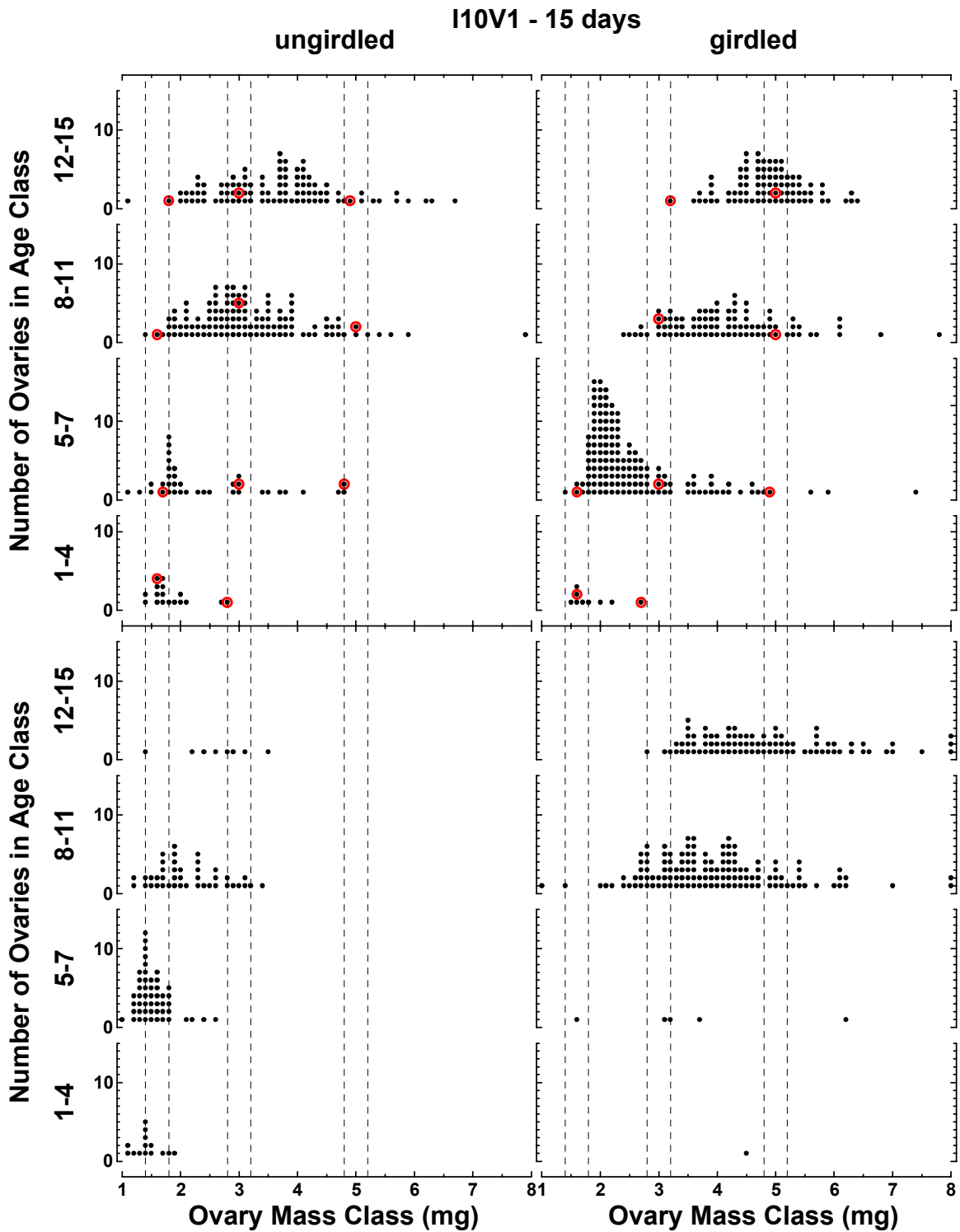


Figure 3.5 Frequency distribution of ovaries in age classes (I10V1). Duplicate bunches were harvested at 15 days after first capfall. Bunches from ungirdled vines are positioned on the LHS. Bunches from girdled vines are positioned on the RHS, bunch 1 at the top and bunch 2 below. Individual ovaries are identified as solid circles (●). Four separate age classes are identified on the y-axis: 1-4 days, 5-7 days, 8-11 days, 12-15 days. Ovary mass classes are divided into intervals of 0.2 g. The broken lines indicate groups of ovaries within the 3 predominant mass ranges: 1.4-1.8 mg, 2.8-3.2 mg, 4.8-5.2 mg. These mass ranges are chosen to represent “shot” berries, “chicks” and “hens”, respectively. Ovaries used in CLSM measurements are indicated with an open circle (○).

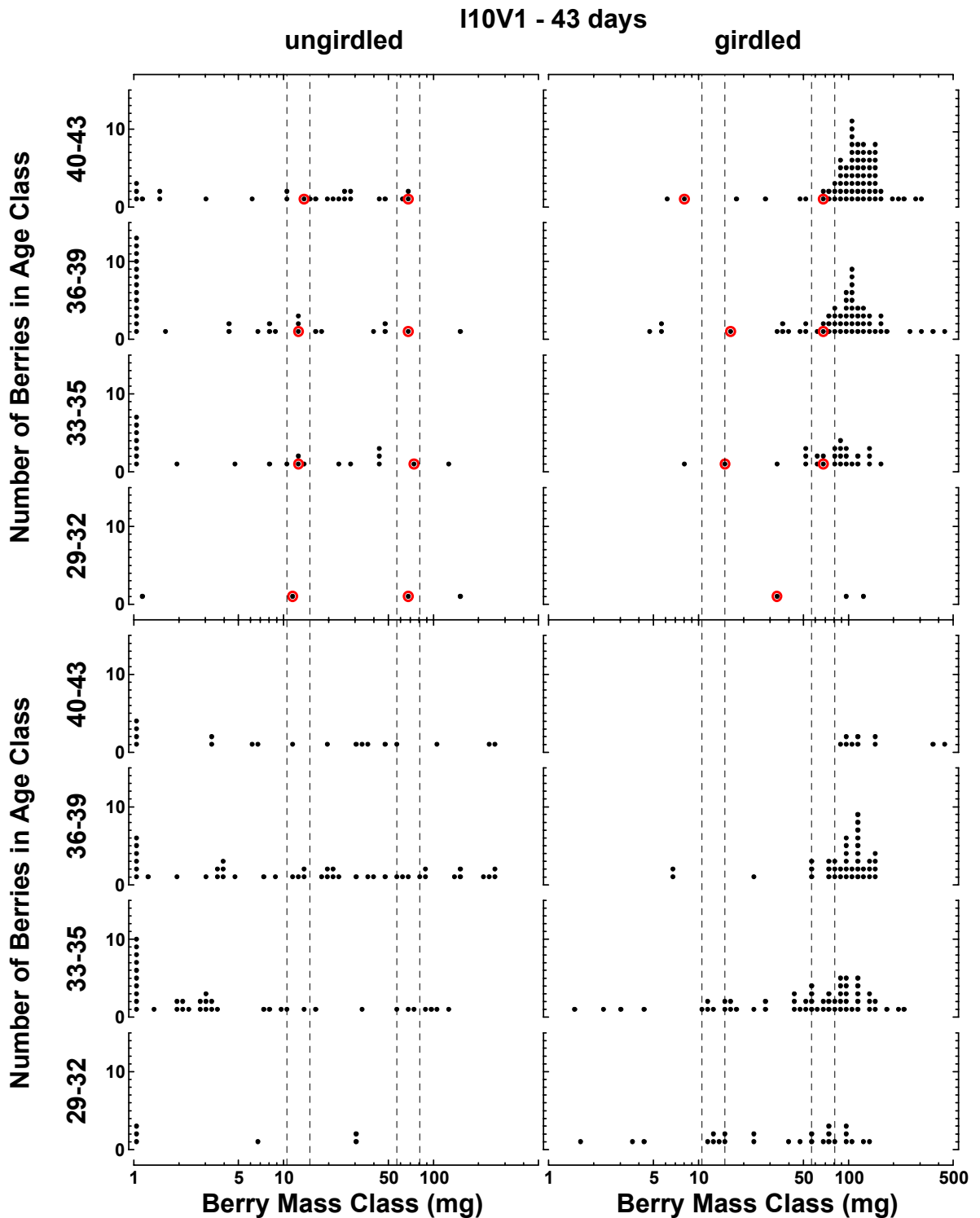


Figure 3.6 Frequency distribution of berries in age classes (I10V1). Duplicate bunches were harvested at 43 days after first capfall. Bunches from ungirdled vines are positioned on the LHS. Bunches from girdled vines are positioned on the RHS, bunch 1 at the top and bunch 2 below. Individual berries are identified as solid circles (●). Four separate age classes are identified on the y-axis: 29-32 days, 33-35 days, 36-39 days, 40-43 days. Berry mass classes are divided into equal intervals on a log scale. The broken lines indicate groups of berries within the 2 predominant mass ranges: 10-10.2 mg, 52-77 mg. These mass ranges are chosen to represent “chicks” and “hens”, respectively. “Shot” berries at 1 mg or less are still evident within the ungirdled bunches, but are lacking among the girdled bunches. Berries used in CLSM measurements are indicated with an open circle (○).

Table 3.4 Variation in ovary and berry mass between bunches (I10V1). The mean mass (mg) and coefficient of variation (%) for each age class of ovaries/berries from ungirdled and girdled vines for the Chardonnay clone I10V1. Two bunches were harvested at 15 days after first capfall (age classes 1-4, 5-7, 8-11 and 12-15) and two more at 43 days after first capfall (age classes 29-32, 33-35, 36-39 and 40-43). Data for each bunch are presented separately. The number of ovaries/berries in each age class is recorded in parentheses. Significant differences between bunch pairs were determined by Student t-tests and significance levels are indicated by the following symbols: “*” = $p < 0.05$, “***” = $p < 0.01$, “****” = $p < 0.001$, “ns” = not significant, “na” = not applicable (insufficient sample numbers).

I10V1				
age class (bunch)	ungirdled		girdled	
	mean mass (mg)	CV (%)	mean mass (mg)	CV (%)
1-4				
bunch 1	1.83** (17)	22.40	1.86 ^{na} (9)	21.26
bunch 2	1.43 (14)	16.40	4.46 (1)	na
5-7				
bunch 1	2.48*** (37)	40.57	2.59** (140)	36.37
bunch 2	1.52 (50)	22.06	3.54 (5)	48.07
8-11				
bunch 1	3.20*** (117)	32.06	4.16 ^{ns} (87)	23.77
bunch 2	2.13 (42)	26.62	3.97 (128)	31.82
12-15				
bunch 1	3.64** (95)	29.42	4.86 ^{ns} (83)	13.23
bunch 2	2.61 (8)	24.54	4.85 (87)	26.36
29-32				
bunch 1	56.69 ^{ns} (4)	118.11	86.09 ^{ns} (3)	55.52
bunch 2	11.47 (6)	128.79	52.89 (26)	78.40
33-35				
bunch 1	21.16 ^{ns} (21)	144.20	84.34 ^{ns} (27)	44.23
bunch 2	20.19 (38)	172.91	73.57 (58)	72.04
36-39				
bunch 1	16.05* (30)	195.06	108.36 ^{ns} (59)	68.96
bunch 2	50.25 (44)	143.21	98.66 (40)	36.03
40-43				
bunch 1	21.49 ^{ns} (25)	96.25	116.42** (73)	43.43
bunch 2	47.75 (18)	162.65	173.75 (10)	71.72

between age classes and bunches. The major difference between ungirdled bunches occurs at 12-15 days (n=95 vs n=8). The major difference between girdled bunches occurs at 5-7 days (n=140 vs n=5). The youngest age class at each harvest generally contains the least ovaries/berries.

Significant differences in ovary and berry mass between pairs of ungirdled bunches occur within the following age classes: 1-4 days (1.83 mg vs 1.43 mg), 5-7 days (2.48 mg vs 1.52 mg), 8-11 days (3.20 mg vs 2.13 mg), 12-15 days (3.64 mg vs 2.61 mg), 36-39 days (16.05 mg vs 50.25 mg). For the three remaining age classes, differences in berry mass were not significant: 29-32 days (56.69 mg vs 11.47 mg), 33-35 days (21.16 mg vs 20.19 mg), 40-43 days (21.49 mg vs 47.75 mg). CVs differ between bunch pairs by an average of 1.4 fold. There does not appear to be any trend associated with a particular vine. CVs increase by an average of 4.7-fold between the 15 day and the 43 day harvest.

Girdled bunch pairs also presented a range of significant and non-significant differences in ovary and berry mass. Significant differences are exhibited within two age classes: 5-7 days (2.59 mg vs 3.54 mg), 40-43 days (116.42 mg vs 173.75 mg). Differences are not significant throughout the intermediate age classes: 8-11 days (4.16 mg vs 3.97 mg), 12-15 days (4.86 mg vs 4.85 mg), 29-32 days (86.09 mg vs 52 89 mg), 33-35 days (84.34 mg vs 73.57 mg), 36-39 days (108.36 mg vs 98.66 mg). Insufficient sample numbers prevent an analysis of significance at 1-4 days (1.86 mg vs 4.46 mg). CVs differ between bunch pairs by an average of 1.5-fold. No trend is associated with any particular vine. CVs increase by an average of 1.8-fold between the 15 day and the 43 day harvest. Mean CVs for ungirdled vines at day 43 are 2.4-fold greater than their girdled counterparts.

Clone Antav 13

A similar series of frequency distributions was plotted for the Chardonnay clone Antav 13. **Figure 3.7** indicates the mass of individual ovaries distributed according to age class, girdling treatment and bunch replicate at 15 days after first capfall. Each bunch is displayed separately and individual ovaries identified by points on the graphs. As before, the broken lines are used to indicate the mass ranges of “shot” berries, “chicks” and “hens”.

Figure 3.8 indicates the mass of individual berries distributed according to age class, girdling treatment and bunch replicate at 43 days after first capfall. Bunches are displayed separately and individual berries identified by points on the graph. The broken lines indicate the mass ranges of “chicks” and “hens”. “Shot” berries at 1 mg or less are still evident within the ungirdled bunches, but are infrequent among the girdled bunches.

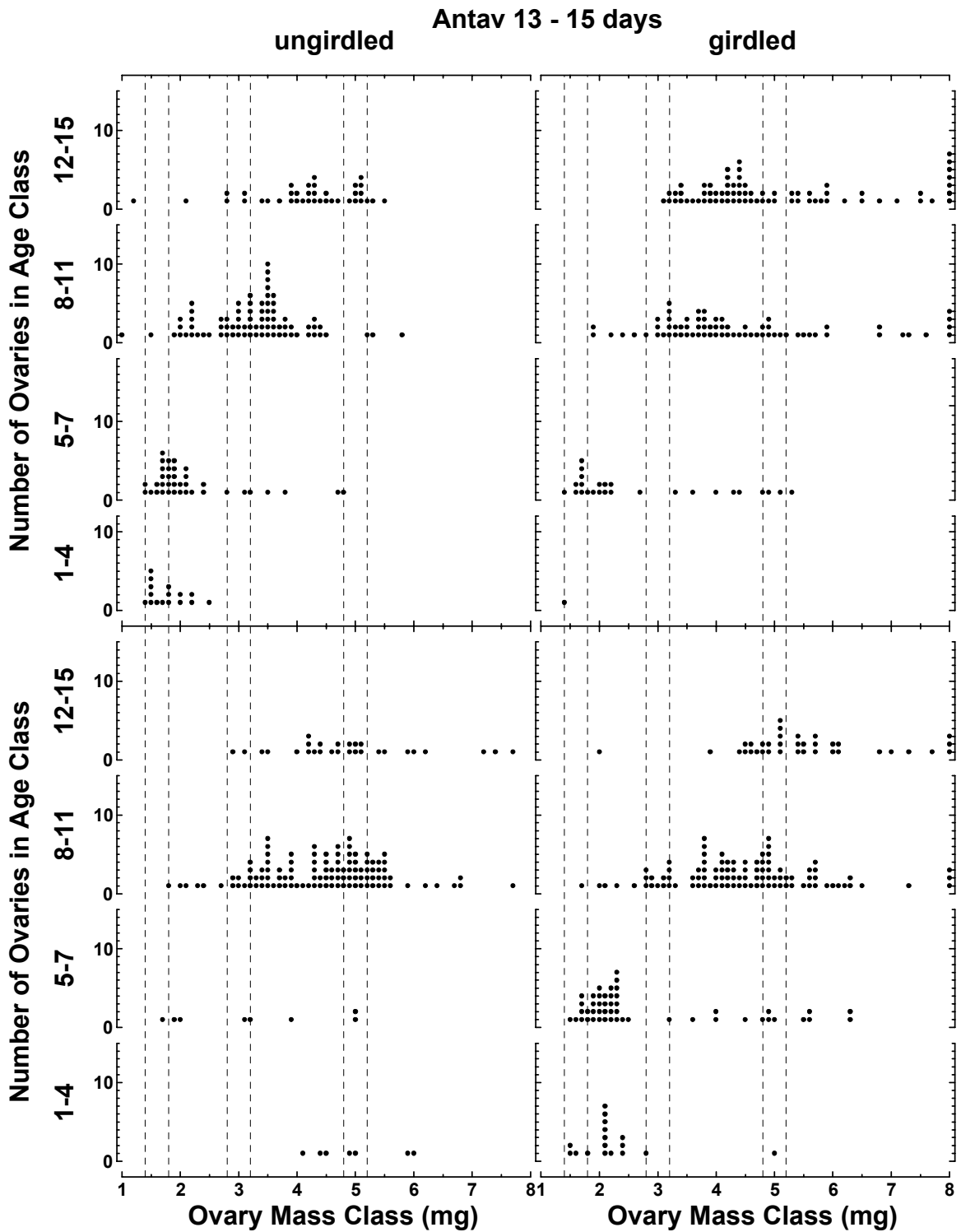


Figure 3.7 Frequency distribution of ovaries in age classes (Antav 13). Duplicate bunches were harvested at 15 days after first capfall. Bunches from ungirdled vines are positioned on the LHS. Bunches from girdled vines are positioned on the RHS, bunch 1 at the top and bunch 2 below. Individual ovaries are identified as solid circles (●). Four separate age classes are identified on the y-axis: 1-4 days, 5-7 days, 8-11 days, 12-15 days. Ovary mass classes are divided into intervals of 0.2 g. The broken lines indicate groups of ovaries within the 3 predominant mass ranges: 1.4-1.8 mg, 2.8-3.2 mg, 4.8-5.2 mg. These mass ranges are chosen to represent “shot” berries, “chicks” and “hens”, respectively.

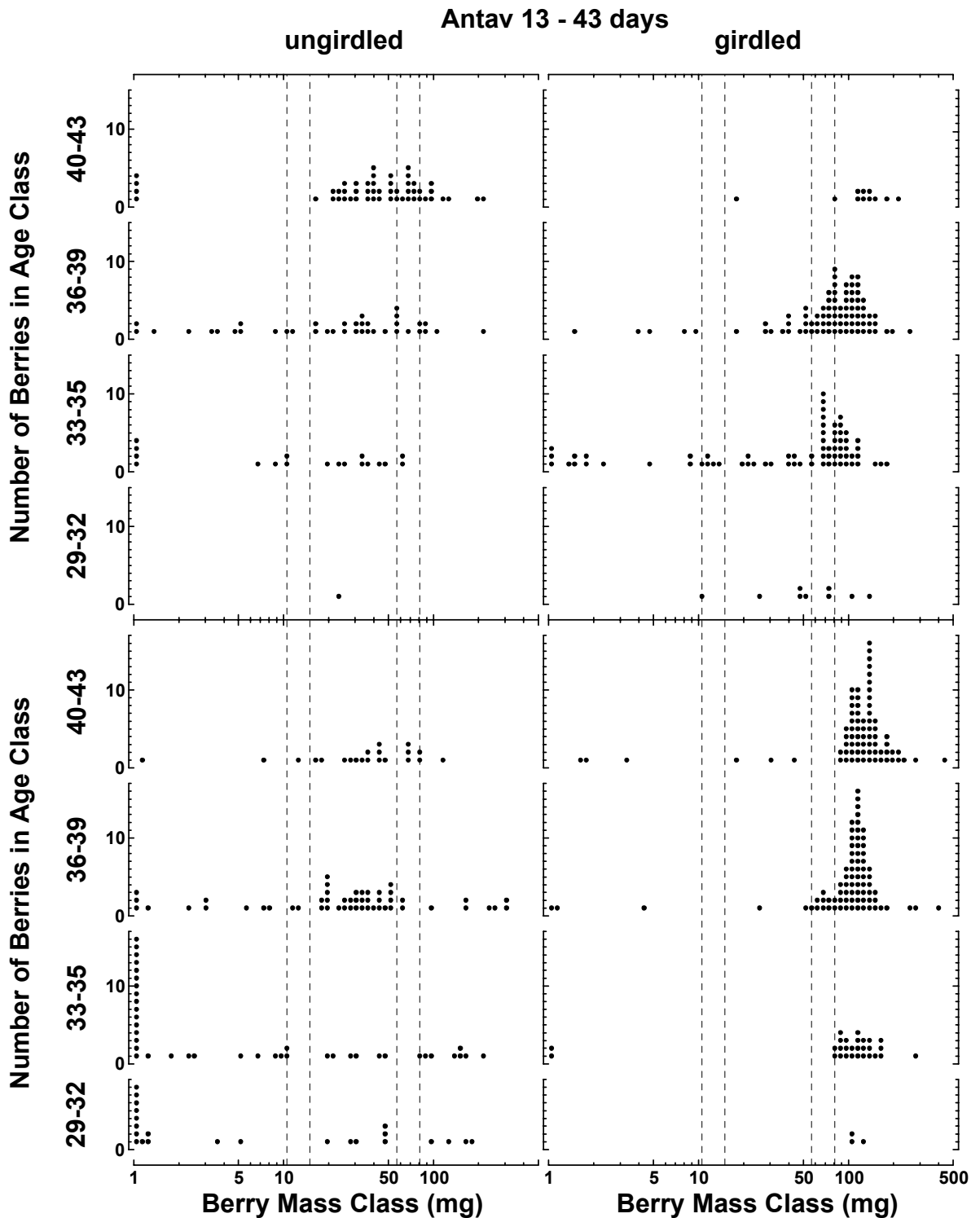


Figure 3.8 Frequency distribution of berries in age classes (Antav 13). Duplicate bunches were harvested at 43 days after first capfall. Bunches from ungirdled vines are positioned on the LHS. Bunches from girdled vines are positioned on the RHS, bunch 1 at the top and bunch 2 below. Individual berries are identified as solid circles (●). Four separate age classes are identified on the y-axis: 29-32 days, 33-35 days, 36-39 days, 40-43 days. Berry mass classes are divided into equal intervals on a log scale. The broken lines indicate groups of berries within the 2 predominant mass ranges: 10-10.2 mg, 52-77 mg. These mass ranges are chosen to represent “chicks” and “hens”, respectively. “Shot” berries at 1 mg or less are still evident within the ungirdled bunches, but are lacking among the girdled bunches.

Table 3.5 Variation in ovary and berry mass between bunches (Antav 13). The mean mass (mg) and coefficient of variation (%) for each age class of ovaries/berries from ungriddled and griddled vines for the Chardonnay clone Antav 13. Two bunches were harvested at 15 days after first capfall (age classes 1-4, 5-7, 8-11 and 12-15) and two more at 43 days after first capfall (age classes 29-32, 33-35, 36-39 and 40-43). Data for each bunch are presented separately. The number of ovaries/berries in each age class is recorded in parentheses. Significant differences between bunch pairs were determined by Student t-tests and significance levels are indicated by the following symbols: “*” = $p < 0.05$, “**” = $p < 0.01$, “***” = $p < 0.001$, “ns” = not significant, “na” = not applicable (insufficient sample numbers).

Antav 13				
age class (bunch)	ungirdled		girdled	
	mean mass (mg)	CV (%)	mean mass (mg)	CV (%)
1-4				
bunch 1	1.78 ^{***} (16)	18.48	1.35 ^{na} (1)	na
bunch 2	4.98 (7)	14.98	2.27 (17)	34.76
5-7				
bunch 1	2.20 ^{**} (37)	37.90	2.75 ^{ns} (26)	47.21
bunch 2	3.23 (8)	41.34	2.84 (49)	49.23
8-11				
bunch 1	3.26 ^{***} (78)	26.05	4.46 ^{ns} (70)	38.51
bunch 2	4.43 (108)	24.19	4.54 (98)	31.43
12-15				
bunch 1	4.16 ^{**} (38)	21.97	5.35 ^{ns} (74)	39.12
bunch 2	4.92 (28)	24.38	5.62 (36)	26.14
29-32				
bunch 1	22.60 ^{na} (1)	na	63.18 ^{ns} (9)	60.96
bunch 2	34.98 (23)	155.51	113.45 (3)	11.71
33-35				
bunch 1	23.84 ^{ns} (18)	88.68	60.74 ^{***} (70)	71.04
bunch 2	33.80 (40)	166.08	114.31 (28)	45.17
36-39				
bunch 1	38.39 ^{ns} (38)	108.95	86.85 ^{***} (83)	49.86
bunch 2	52.35 (51)	138.13	112.30 (78)	47.63
40-43				
bunch 1	55.36 ^{ns} (51)	75.26	128.90 ^{ns} (11)	40.90
bunch 2	43.00 (21)	66.46	129.99 (74)	45.37

The mean mass (mg) and CV (%) for each age class of ovaries/berries from ungirdled and girdled vines for the Chardonnay clone Antav 13 are indicated in **Table 3.5**. Data for each bunch are presented separately. Significant differences between bunch pairs were determined by Student t-tests and significance levels are indicated.

The distributions reveal inequalities in ovary and berry numbers between age classes and bunches. The major difference between ungirdled bunches occurs at 5-7 days (n=37 vs n=8). Differences between girdled bunches occur at 1-4 days (n=140 vs n=5) and at 40-43 days (n=11 vs n=74). The youngest age class at both the 15 day and the 43 day harvest generally contains the least ovaries/berries.

Significant differences in ovary and berry mass occur between pairs of ungirdled bunches within the first four age classes: 1-4 days (1.78 mg vs 4.98 mg), 5-7 days (2.20 mg vs 3.23 mg), 8-11 days (3.26 mg vs 4.43 mg), and 12-15 days (4.16 mg vs 4.92 mg). Differences in berry mass were not significant within the last three age classes: 33-35 days (23.84 mg vs 33.80 mg), 36-39 days (38.39 mg vs 52.35 mg), and 40-43 days (55.36 mg vs 43.00 mg). Insufficient berry numbers do not allow a significance value to be determined at 29-32 days (22.60 mg vs 34.98 mg). CVs differ between bunch pairs by an average of 1.2-fold. CVs increase by an average of 4.1-fold between the 15 day and the 43 day harvest.

Girdled bunch pairs also presented a range of significant and non-significant differences in ovary and berry mass. Significant differences are exhibited within two age classes: 33-35 days (60.74 mg vs 114.31 mg), 36-39 days (86.85 mg vs 112.30 mg). Differences are not significant at 5-7 days (2.75 mg vs 2.84 mg), 8-11 days (4.46 mg vs 4.45 mg), 12-15 days (5.35 mg vs 5.62 mg), 29-32 days (63.18 mg vs 114.31 mg), and 40-43 days (128.90 mg vs 129.99 mg). Insufficient sample numbers prevent an analysis of significance at 1-4 days (1.35 mg vs 2.27 mg). CVs differ between bunch pairs by an average of 1.7-fold. No trend is associated with any particular vine. Mean CVs increase marginally (1.1-fold) between the 15 day and the 43 day harvest. CVs for ungirdled vines at day 43 are on average 2.5-fold greater than their girdled counterparts.

Clone Antav 84

Figure 3.9 shows the frequency distribution and age of individual ovaries within a bunch from the clone Antav 84 at 15 days after first capfall. Two bunches were harvested from ungirdled vines and two more from girdled vines. Four age classes are identified on the y-axis: 1-4 days, 5-7 days, 8-11 days, 12-15 days. Ovary mass classes are divided into intervals of 0.2 g. The broken lines indicate groups of ovaries within the 3 predominant mass ranges: “shot” berries (1.4-1.8 mg), “chicks” (2.8-3.2 mg) and “hens” (4.8-5.2 mg).

Figure 3.10 displays the same frequency distributions at 43 days after first capfall. The four age classes on the y-axis are at 29-32 days, 33-35 days, 36-39 days, and 40-43 days. Berry mass classes are divided into equal intervals on a log scale. The broken lines indicate groups of berries within the 2 predominant mass ranges: “chicks” (11-15 mg) and “hens” (57-81 mg). Although “shot” berries at 1 mg or less are still evident within the ungirdled bunches, they are lacking among the girdled bunches.

Table 3.6 lists the mean mass (mg), number, and CV (%) for each age class of ovaries/berries from ungirdled and girdled vines of the Chardonnay clone Antav 84. Data for each bunch are presented separately. Significant differences between bunch pairs were determined by Student t-tests and significance levels are indicated.

Ungirdled bunches differ markedly in ovary/berry number at 40-43 days (n=12 vs n=43). Differences between girdled bunches occur at 1-4 days (n=30 vs n=2), 29-32 days (n=30 vs n=2), and 40-43 days (n=48 vs n=170). The youngest age class at both the 15 day and the 43 day harvest generally contains the least ovaries/berries.

Significant differences in ovary and berry mass occur between pairs of ungirdled bunches within the following two age classes: 8-11 days (2.96 mg vs 3.49 mg), 12-15 days (3.98 mg vs 4.69 mg). Differences in berry mass were not significant for the five remaining age classes: 1-4 days (1.52 mg vs 1.95 mg), 5-7 days (2.27 mg vs 2.15 mg), 29-32 days (23.72 mg vs 20.83 mg), 33-35 days (33.52 mg vs 42.90 mg), 36-39 days (41.36 mg vs 47.89 mg), 40-43 days (50.84 mg vs 66.76 mg). Mean CVs differ between bunch pairs by 1.2-fold. CVs increase by an average of 3.5-fold between the 15 day and the 43 day harvest.

Girdled bunch pairs also present a range of significant and non-significant differences in ovary and berry mass. Significant differences are exhibited within four age classes: 8-11 days (3.47 mg vs 4.21 mg), 12-15 days (4.04 mg vs 6.24 mg), 33-35 days (104.72 mg vs 73.99 mg), 36-39 days (135.95 mg vs 97.72 mg). Differences are not significant within the remaining four age classes: 1-4 days (1.81 mg vs 1.71 mg), 5-7 days (2.53 mg vs 2.25 mg), 29-32 days (74.00 mg vs 116.69 mg), 40-43 days (136.87 mg vs 137.14 mg). CVs differ between bunch pairs by an average of 1.2-fold. No trend is associated with any particular vine. CVs increase by an average of 2.2-fold between the 15 day and the 43 day harvest. Mean CVs for ungirdled vines at day 43 are 1.9-fold greater than their girdled counterparts.

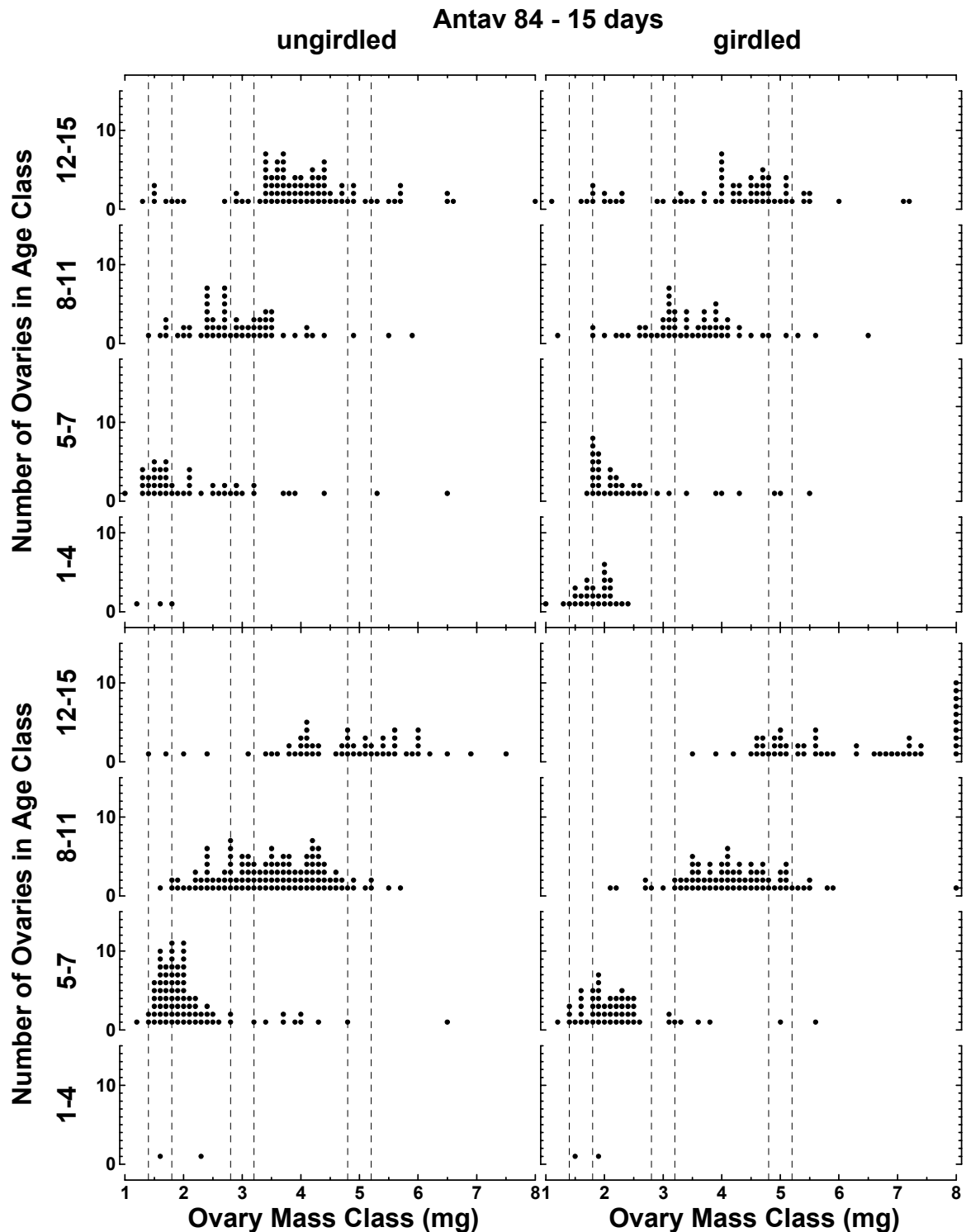


Figure 3.9 Frequency distribution of ovaries in age classes (Antav 84). Duplicate bunches were harvested at 15 days after first capfall. Bunches from ungirdled vines are positioned on the LHS. Bunches from girdled vines are positioned on the RHS, bunch 1 at the top and bunch 2 below. Individual ovaries are identified as solid circles (●). Four separate age classes are identified on the y-axis: 1-4 days, 5-7 days, 8-11 days, 12-15 days. Ovary mass classes are divided into intervals of 0.2 g. The broken lines indicate groups of ovaries within the 3 predominant mass ranges: 1.4-1.8 mg, 2.8-3.2 mg, 4.8-5.2 mg. These mass ranges are chosen to represent “shot” berries, “chicks” and “hens”, respectively.

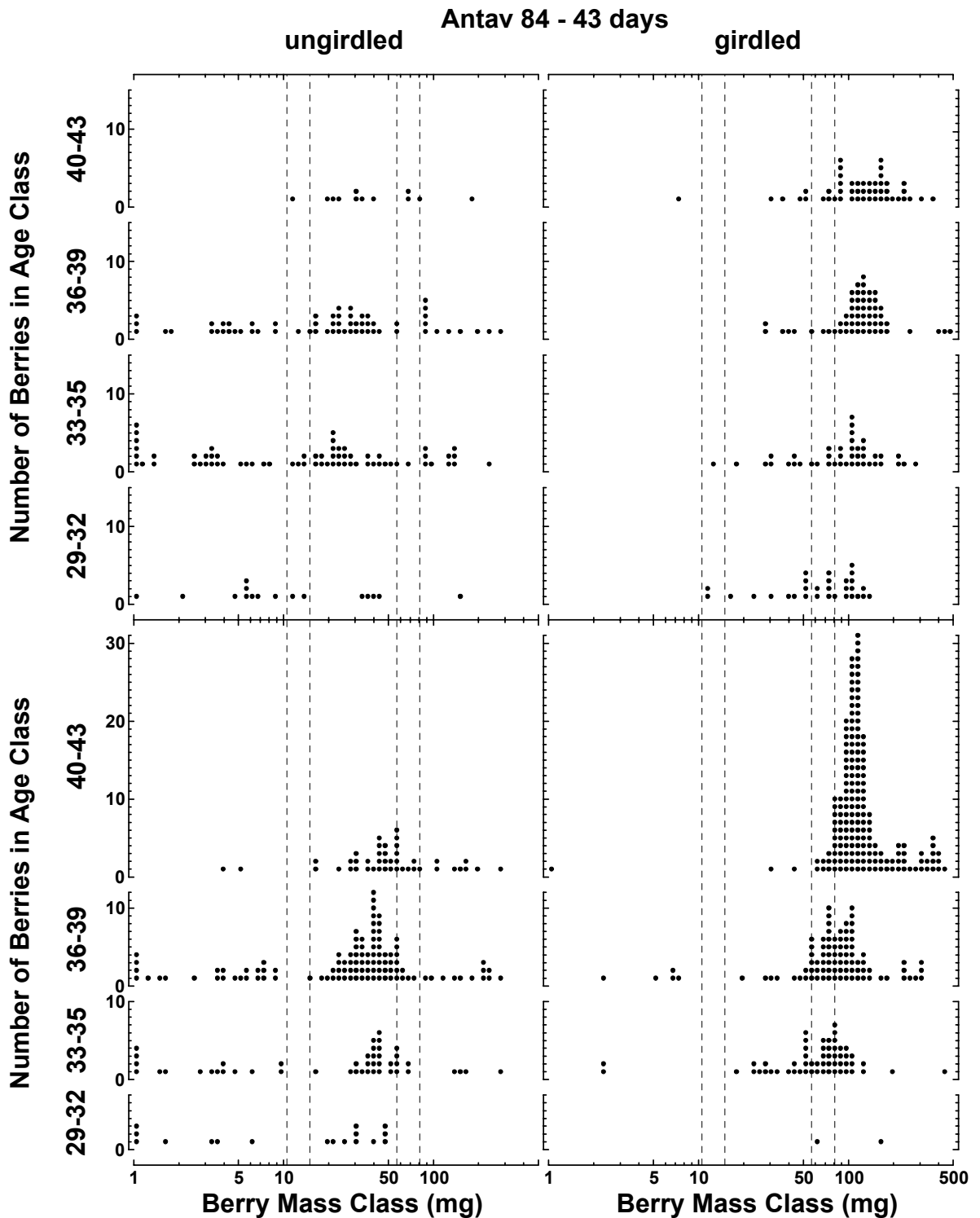


Figure 3.10 Frequency distribution of berries in age classes (Antav 84). Duplicate bunches were harvested at 43 days after first capfall. Bunches from ungirdled vines are positioned on the LHS. Bunches from girdled vines are positioned on the RHS, bunch 1 at the top and bunch 2 below. Individual berries are identified as solid circles (●). Four separate age classes are identified on the y-axis: 29-32 days, 33-35 days, 36-39 days, 40-43 days. Berry mass classes are divided into equal intervals on a log scale. The broken lines indicate groups of berries within the 2 predominant mass ranges: 10-10.2 mg, 52-77 mg. These mass ranges are chosen to represent “chicks” and “hens”, respectively. “Shot” berries at 1 mg or less are still evident within the ungirdled bunches, but are lacking among the girdled bunches.

Table 3.6 Variation in ovary and berry mass between bunches (Antav 84). The mean mass (mg) and coefficient of variation (%) for each age class of ovaries/berries from ungirdled and girdled vines for the Chardonnay clone Antav 84. Two bunches were harvested at 15 days after first capfall (age classes 1-4, 5-7, 8-11 and 12-15) and two more at 43 days after first capfall (age classes 29-32, 33-35, 36-39 and 40-43). Data for each bunch are presented separately. The number of ovaries/berries in each age class is recorded in parentheses. Significant differences between bunch pairs were determined by Student t-tests and significance levels are indicated by the following symbols: “*” = $p < 0.05$, “**” = $p < 0.01$, “***” = $p < 0.001$, “ns” = not significant, “na” = not applicable (insufficient sample numbers).

Antav 84				
age class (bunch)	ungirdled		girdled	
	mean mass (mg)	CV (%)	mean mass (mg)	CV (%)
1-4				
bunch 1	1.52 ^{ns} (3)	20.49	1.81 ^{ns} (30)	16.94
bunch 2	1.95 (2)	23.63	1.71 (2)	13.69
5-7				
bunch 1	2.27 ^{ns} (48)	49.25	2.53 ^{ns} (40)	38.66
bunch 2	2.15 (85)	39.57	2.25 (56)	35.59
8-11				
bunch 1	2.96 ^{***} (61)	29.70	3.47 ^{***} (60)	26.77
bunch 2	3.49 (118)	25.25	4.21 (77)	21.89
12-15				
bunch 1	3.98 ^{***} (89)	28.88	4.04 ^{***} (66)	31.75
bunch 2	4.69 (57)	25.32	6.24 (55)	27.81
29-32				
bunch 1	23.72 ^{ns} (16)	161.40	74.00 ^{ns} (30)	48.71
bunch 2	20.83 (17)	86.16	116.69 (2)	63.03
33-35				
bunch 1	33.52 ^{ns} (67)	133.92	104.72* (42)	56.65
bunch 2	42.90 (46)	121.62	73.99 (56)	78.91
36-39				
bunch 1	41.36 ^{ns} (61)	136.07	135.95** (57)	62.91
bunch 2	47.89 (107)	115.92	97.72 (88)	67.36
40-43				
bunch 1	50.84 ^{ns} (12)	91.52	136.87 ^{ns} (48)	53.49
bunch 2	66.76 (43)	84.40	137.14 (170)	56.87

3.4.4 Ovary and Berry Growth Rates

Figure 3.11 shows ovary growth rates at 15 days after first capfall for each of the three Chardonnay clones – I10V1, Antav 13, Antav 84. Data for ungirdled and girdled bunches are plotted separately. Mean ovary mass (\pm standard error) was calculated for ovaries within each age class: 1-4 days, 5-7 days, 8-11 days, 12-15 days. Absolute growth rate (AGR) and relative growth rate (RGR) are plotted for the 3 time periods between the midpoint of each age class (2.5 days, 6days, 9.5 days, 13 days).

Figure 3.12 shows berry growth rates at 43 days after first capfall for each of the three Chardonnay clones – I10V1, Antav 13, Antav 84. Data for ungirdled and girdled bunches are plotted separately. Mean berry mass (\pm standard error) was calculated for each age class: 29-32 days, 33-35 days, 36-39 days, 40-43 days. AGR and RGR are plotted for the 3 time periods between the midpoint of each age class (30.5 days, 34 days, 37.5 days, 41.5 days).

A clonal comparison of mean ovary/berry mass at each age class from ungirdled and girdled vines for the three Chardonnay clones is displayed in **Table 3.7**. Each age class and girdling treatment is the mean of two bunches. Significant differences between clones within each age class were determined by REML and are indicated by the letters that follow the mean mass values (LSD at $p < 0.05$). Note that the mean ovary/berry mass values have been rearranged from **Table 3.3**.

Ovary Growth (1-15 days)

Ovary development during the first 15 days after capfall follows a similar course for all three of the Chardonnay clones (**Figure 3.11**). Interclonal differences in mean ovary mass are significant at all four age classes among the ungirdled bunches (**Table 3.7**). Antav 13 is consistently heavier than Antav 84 and I10V1. Among the girdled bunches, interclonal differences are not significant at 1-4 days, but become significant at 5-7 days, 8-11 days, and 12-15 days. Antav13 is again heavier than I10V1 and Antav 84.

Clonal differences in AGR are more noticeable among the ungirdled vines. Antav 13 ovaries exhibit the greatest fluctuation in AGR, with an initial negative rate (-0.105, 0.443, 0.156 mg/day). Antav 84 ovaries exhibit the least fluctuation in AGR (0.144, 0.320, 0.271 mg/day). I10V1 is intermediate (0.080, 0.283, 0.184 mg/day). The maximum AGR for all three clones occurs during the middle growth period between 6 and 9.5 days.

Girdled ovaries of all clones exhibit positive AGRs. The values are higher than their ungirdled counterparts during all three growth periods. The values for I10V1 are consistently lower than the other clones (0.144, 0.408, 0.231 mg/day). Antav 13 has the highest AGR during growth periods one and two (0.171, 0.485, 0.267 mg./day). Antav 84 has the highest

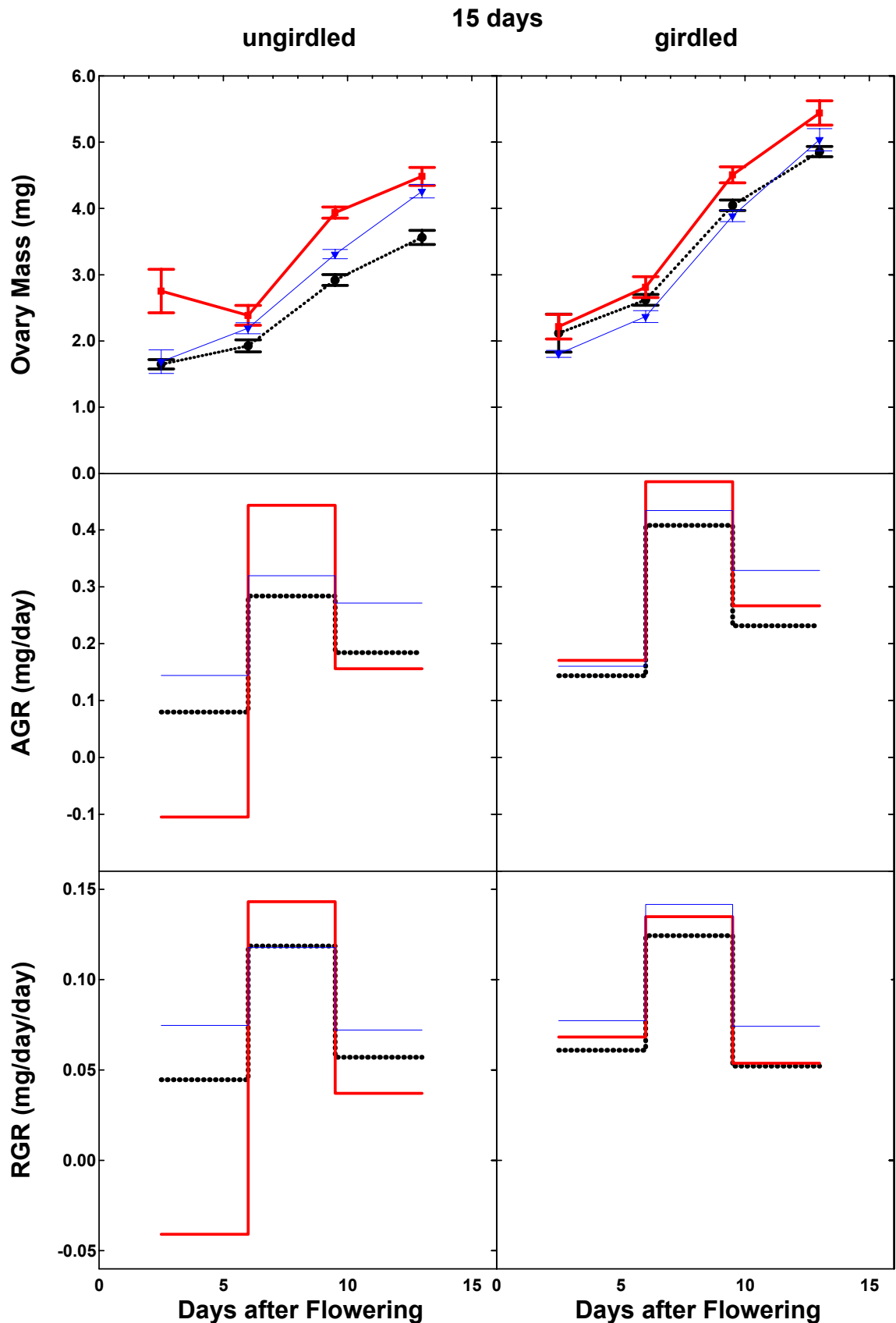


Figure 3.11 Ovary growth rates. Two bunches were harvested at 15 days after first capfall from each of the three clones – I10V1 (● ····), Antav 13 (■ —), Antav 84 (▼ —). Plots of ungirdled vines are positioned on the LHS. Plots of girdled vines are positioned on the RHS. Mean ovary mass (\pm standard error) was calculated for ovaries within each age class: 1-4 days, 5-7 days, 8-11 days, 12-15 days. Absolute growth rate (AGR) and relative growth rate (RGR) are plotted for the 3 time periods between the midpoints of each age class.

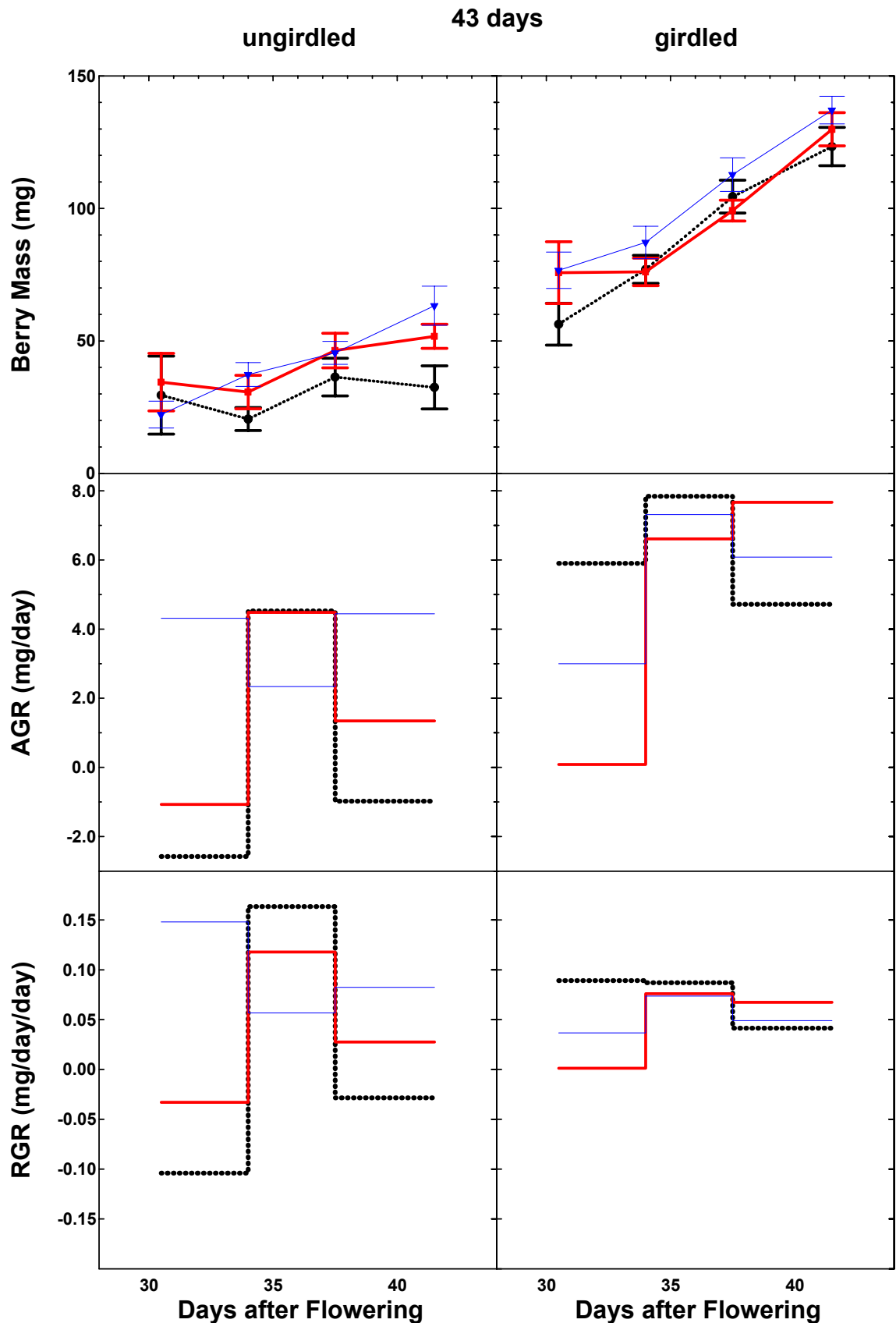


Figure 3.12 Berry growth rates. Two bunches were harvested at 43 days after first capfall from each of the three clones – I10V1 (● ····), Antav 13 (■ —), Antav 84 (▼ —). Plots of ungirdled vines are positioned on the LHS. Plots of girdled vines are positioned on the RHS. Mean berry mass (\pm standard error) was calculated for berries within each age class: 29-32 days, 33-35 days, 36-39 days, 40-43 days. Absolute growth rate (AGR) and relative growth rate (RGR) are plotted for the 3 time periods between the midpoints of each age class.

Table 3.7 Clonal variation in ovary and berry mass. Clonal comparison of mean ovary/berry mass at each age class from ungirdled and girdled vines for the three Chardonnay clones – I10V1, Antav 13, and Antav 84. Bunches were harvested at 15 days after first capfall (age classes 1-4, 5-7, 8-1 and 12-15) and at 43 days after first capfall (age classes 29-32, 33-35, 36-39 and 40-43). Each age class and girdling treatment is the mean of two bunches. Significant differences between clones within each age class were determined by REML and are indicated by the letters that follow the mean mass values (LSD at $p < 0.05$). Note that the mean ovary/berry mass values have been rearranged from **Table 3.3**.

ovary/berry age class	clone	ungirdled mean mass (mg)	girdled mean mass (mg)
1-4	I10V1	1.65 ^a	2.12 ^a
	Antav 13	2.75 ^b	2.22 ^a
	Antav 84	1.69 ^a	1.81 ^a
5-7	I10V1	1.93 ^a	2.62 ^{ab}
	Antav 13	2.39 ^b	2.81 ^b
	Antav 84	2.19 ^{ab}	2.37 ^a
8-11	I10V1	2.92 ^a	4.05 ^a
	Antav 13	3.94 ^c	4.51 ^b
	Antav 84	3.31 ^b	3.89 ^a
12-15	I10V1	3.56 ^a	4.86 ^a
	Antav 13	4.48 ^b	5.44 ^b
	Antav 84	4.26 ^b	5.04 ^a
29-32	I10V1	29.56 ^a	56.33 ^a
	Antav 13	34.46 ^a	75.75 ^a
	Antav 84	22.23 ^a	76.67 ^a
33-35	I10V1	20.54 ^a	76.99 ^a
	Antav 13	30.71 ^a	76.04 ^a
	Antav 84	37.34 ^a	87.16 ^a
36-39	I10V1	36.38 ^a	104.44 ^a
	Antav 13	46.39 ^a	99.18 ^a
	Antav 84	45.52 ^a	112.75 ^a
40-43	I10V1	32.48 ^a	123.32 ^a
	Antav 13	51.76 ^b	129.85 ^a
	Antav 84	63.29 ^b	137.08 ^a

AGR during growth period three (0.160, 0.434, 0.329 mg/day). Maximum AGR for all three clones occurs during the middle growth period.

RGR is a more suitable measure of comparative growth since it is independent of mean ovary size. Antav 13 is again the most variable of the ungirdled vines, and the only clone to exhibit a negative RGR (-0.041, 0.143, 0.037 mg/day/day). Antav 84 is the least variable (0.075, 0.118, 0.072 mg/day/day), and I10V1 is intermediate (0.045, 0.119, 0.057 mg/day/day). All three clones achieve their maximum RGR during the middle growth period.

Girdling affects the RGR of each clone differently. I10V1 is virtually identical to its ungirdled counterpart (0.061, 0.124, 0.052 mg/day/day). Antav 13 shows a marked increase during the first growth period, but little change thereafter (0.068, 0.135, 0.054 mg/day/day). Antav 84 is stable during the initial and final growth periods, but increases as a result of girdling during the middle phase (0.077, 0.142, 0.074 mg/day/day). The RGR of Antav 84 > Antav 13 > I10V1 for all three growth periods. All three clones achieve their maximum RGR during the middle growth period.

Berry Growth (29-43 days)

Berry development between days 29 and 43 is more variable among the ungirdled bunches for all three Chardonnay clones. Interclonal differences in berry mass only become significant at 41.5 day – I10V1 (32.48 mg) is less than both Antav 13 (51.76 mg) and Antav 84 (63.29 mg). No significant interclonal differences in berry mass exist among the girdled vines at any age class, but Antav 84 is consistently heavier than the other clones.

AGR among the ungirdled vines is particularly variable. The fluctuations are greatest for I10V1, which exhibits negative growth during the first and last period (-2.58, 4.53, -0.976 mg/day). Antav 13 also indicates negative growth during the first period (-1.07, 4.48, 1.34 mg/day). Although I10V1 and Antav 13 attain their AGR maxima during the middle growth period, Antav 84 declines to a minimum at this time (4.32, 2.34, 4.44 mg/day).

Girdling results in positive AGRs for all clones. Antav 13 is the most variable, exhibiting a continuous increase (0.084, 6.61, 7.67 mg/day). Antav 84 shows an initial decrease during the first growth period, followed by subsequent increases (3.00, 7.31, 6.08 mg/day). The most dramatic increase in AGR in response to girdling occurs in I10V1 (5.90, 7.84, 4.72 mg/day).

A similar RGR range exists for the 43 day and the 15 day sample. A comparison of clonal RGRs among the ungirdled bunches at 43 days indicates that I10V1 is the most variable across the three growth periods, with two negative values (-0.104, 0.163, -0.028 mg/day/day). Antav 84 is the least variable, with a minimum during the middle growth period

(0.148, 0.057, 0.082 mg/day/day). I10V1 is intermediate, with a negative first growth period (-0.033, 0.118, 0.027 mg/day/day).

Girdling has a significant impact on the RGR of all three Chardonnay clones. Variation between growth periods for all clones is reduced in comparison to their ungirdled counterparts. Variation between clones is also reduced. The RGR for I10V1 shows a continuous decline (0.089, 0.087, 0.042 mg/day/day). Both Antav 13 (0.001, 0.076, 0.067 mg/day/day) and Antav 84 (0.037, 0.074, 0.049 mg/day/day) achieve their maximum RGR during the middle growth period.

3.4.5 The Relationship between Ovary/Berry Mass and Ovule/Seed Mass

Ovary Mass versus Ovule Mass (days 1-15)

The relationship between ovary mass and ovule mass for the Chardonnay clone I10V1 is shown in **Figure 3.13**. Each graph represents a separate bunch that was harvested at 15 days after first capfall. Two bunches were sampled from ungirdled vines and two from girdled vines. Different symbols are used to represent each of the four ovary age classes present within the sample (1-4 days, 5-7 days, 8-11 days, and 12-15 days). Linear regressions are fitted to the data.

The linear relationships between ovary and ovule mass appear consistent between bunches and girdling treatment during the first two weeks of ovary development. The regression coefficients range from 5.27 to 9.08, the y-intercepts from 1.06 to 2.70, and the coefficients of determination from 0.33 to 0.61.

The linear regressions were compared using an analysis of covariance (Zar 1974). Significant differences between the slopes ($F_{0.05(1),3,235} = 3.5354$, $p < 0.025$) and elevations ($F_{0.05(1),3,235} = 12.5629$, $p < 0.0005$) were identified. Student-Newman-Keuls (SNK) multiple range tests were undertaken to determine which slope and elevation was different from the others, but a Type II error (not rejecting the null hypothesis when it is in fact false) prevented an unambiguous determination.

Berry Mass versus Seed Mass (days 29-43)

The log-log relationship between berry mass and seed mass for the Chardonnay clone I10V1 is shown in **Figure 3.14**. Each graph represents a separate bunch that was harvested at 43 days after first capfall. Two bunches were sampled from ungirdled vines and two from girdled vines. Different symbols are used to represent each of the four berry age classes present within the sample (29-32 days, 33-35 days, 36-39 days, and 40-43 days). Linear

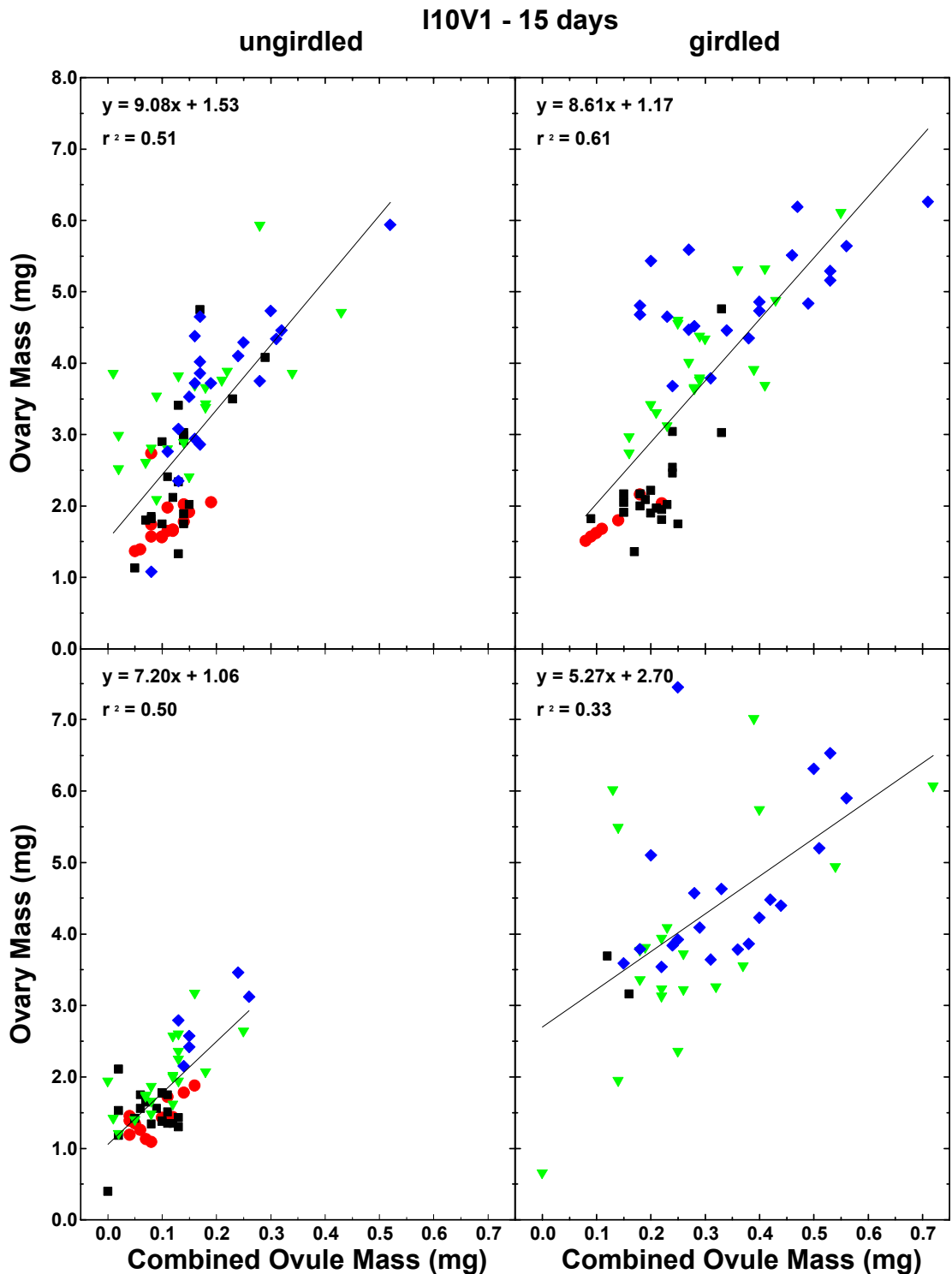


Figure 3.13 The relationship between ovary mass and ovule mass (I10V1). Duplicate bunches were harvested at 15 days after first capfall. Bunches from ungirdled vines are positioned on the LHS. Bunches from girdled vines are positioned on the RHS, bunch 1 at the top and bunch 2 below. Age class of ovaries at harvest is indicated by the following symbols: ● (1-4 days), ■ (5-7 days), ▼ (8-11 days), ◆ (12-15 days). Twenty ovaries were randomly selected from each age class (where available). The ovules from each ovary were removed and weighed collectively. The solid lines represent the linear relationships between ovary and ovule mass during the first two weeks of ovary development. Regression equations and coefficients of determination (r^2) are indicated the graphs.

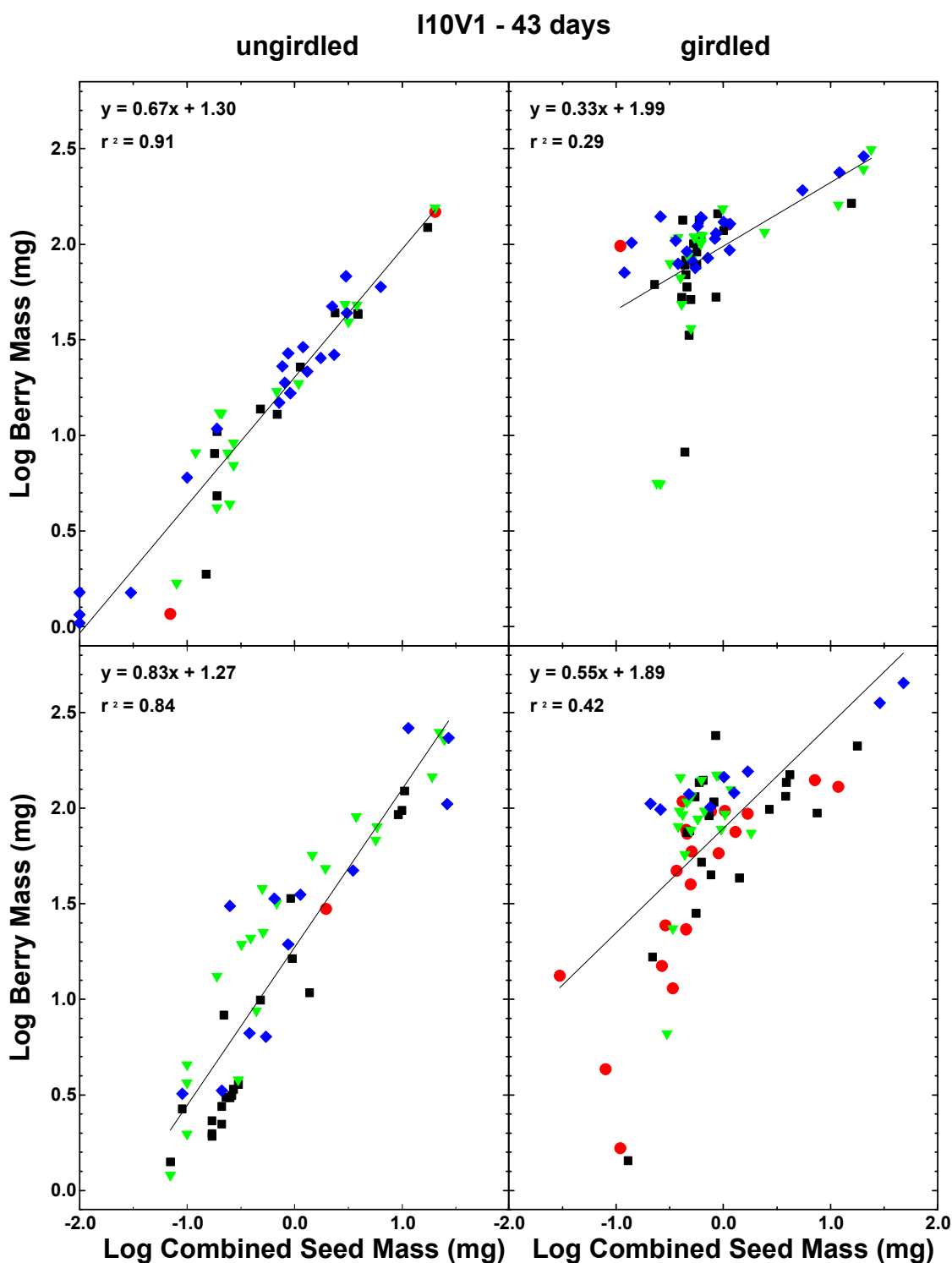


Figure 3.14 The log-log relationship between berry mass and seed mass (I10V1). Duplicate bunches were harvested at 43 days after first capfall. Bunches from ungirdled vines are positioned on the LHS. Bunches from girdled vines are positioned on the RHS, bunch 1 at the top and bunch 2 below. Age class of berries at harvest is indicated by the following symbols: ● (29-32 days), ■ (33-35 days), ▼ (36-39 days), ◆ (40-43 days). Twenty berries were randomly selected from each age class (where available). The seeds from each berry were removed and weighed collectively. The solid lines represent the linear relationships between berry and seed mass plotted on a log-log scale during weeks five and six of berry development. Regression equations and coefficients of determination (r^2) are indicated on the graphs.

regressions were fitted to the data.

The linear relationships between log berry mass and log seed mass differ between girdling treatments during weeks five and six of berry development. Girdled bunches exhibit reduced slopes (0.33, 0.55) and increased elevations (1.99, 1.89) in comparison to their ungirdled counterparts (slopes = 0.67, 0.83; y-intercepts = 1.30, 1.27). Coefficients of determination are also significantly lower for girdled bunches (0.49, 0.42) in comparison to ungirdled bunches (0.91, 0.84).

An analysis of covariance (Zar 1974) revealed significant differences between the slopes ($F_{0.05(1),3,223} = 11.6088$, $p < 0.0005$) and elevations ($F_{0.05(1),3,223} = 98.4440$, $p < 0.0005$). Student-Newman-Keuls (SNK) multiple range tests were undertaken to identify which slope and elevation was different from the others, but a Type II error again prevented an unambiguous determination.

3.5 Discussion

The objective of Chapter 3 was to identify the extent of variation present during the early developmental stages of berry growth. Experiments were designed to test the hypothesis that variation in berry size was already significant during the early postflowering period.

Berry mass of ungirdled vines had exhibited clonal differences within 15 days after the first capfall. Varying degrees of *coulure* and *millerandage* were apparent among all three Chardonnay clones. These differences were more obvious among the ungirdled vines, but they were initiated at different times for different clones. Bunch-to-bunch differences in berry mass among ungirdled vines are significant at 15 days. An analysis of berry growth rates indicates that clonal differences between ungirdled vines also originated in the early phases of berry development. In the developing grape berry, the inter-relationship between ovary and seed growth affects the rate and duration of cell division (Coombe 1973, Ebadi *et al.* 1996a). The dependence of ovary growth on seed growth is described by a series of regression analyses. Linear relationships exist between ovary and ovule mass during the first two weeks of berry development. During weeks 5 and 6 of berry development, linear relationships exist between log berry mass and log seed mass. Given a continuum of levels of seed development (Ebadi *et al.* 1996b), the greatest variation in berry size should be associated with those factors that maximise variation in the developing seeds within berries on a bunch.

The girdling treatment permits an assessment of the role of organic nutrition in the seed/pericarp interaction (Weaver and McCune 1959a, Caspari *et al.* 1998). All clones responded to girdling by an increase in berry mass. I10V1 was most responsive, displaying the greatest proportional increase in berry mass at both 15 and 43 days after first capfall. The

Table 3.8 Variation in ovary and berry mass. Coefficients of variation (CVs) in ovary and berry mass for each harvest date from ungirdled and girdled vines for the three Chardonnay clones – I10V1, Antav 13, and Antav 84. Bunches were harvested at 15 days and at 43 days after first capfall. Each age class and girdling treatment is the mean of two bunches. This table is a rearrangement of the data presented in *Table 3.2*.

clone	ungirdled CV (%)		girdled CV (%)	
	15 days	43 days	15 days	43 days
I10V1	43	170	36	63
Antav 13	36	120	44	56
Antav 84	40	120	46	64
mean	39	137	42	61

earliest detected increase in berry mass as a result of girdling also occurred in I10V1 (1-4 days). This same increase was not significant among other clones until several days later (8-11 days). Bunch-to-bunch differences in berry mass were less significant among girdled vines. It would appear that differences in berry number between bunches may be a factor in the lack of significance among these relationships. Girdling had no effect on the slope of the regressions between ovary and ovule mass during early berry development. However, the slope of the regressions between log berry mass and log seed mass was reduced by girdling during the later phase. Coombe (1959), working with Chardonnay in the Napa Valley, California, found that girdling increased the proportion of fewer-seeded berries in a bunch but did not greatly increase berry weight. The current results do not indicate a difference in the retention of seedless berries, but they imply that berry mass per unit seed mass is enhanced for berries at the lower end of the mass scale.

The coefficient of variation (CV) is a dimensionless value that quantifies the sample variability relative to the sample mean. It enables a comparison of variation among samples despite inequalities among sample means and, as such, is independent of the mean. The results suggest that differences in mean berry mass and variation do not parallel one another.

Variation among ungirdled vines (*Table 3.8*) was low during the early stages of berry development (1-15 days after first capfall), but CVs increased over three-fold during the later stages (29-43 days after first capfall). Among the three Chardonnay clones, I10V1 showed a higher level of variation in the ungirdled state. Bunch-to-bunch variation was similar within a particular age class. Absolute growth rates tended to be lower among ungirdled vines, but relative growth rates were more variable. Both of these factors are indicative of a limited carbohydrate supply to the berries that may hasten their entry into the lag phase but delay the onset of ripening (Ollat and Gaudillere 1998).

Variation (CV) among girdled vines was similar to that of ungirdled vines at 15 days,

but at 43 days was only ~50% higher. These values are relatively consistent across all age classes and clones. Bunch-to-bunch variation within an age class was minor. Typically, absolute growth rates were higher among girdled vines and relative growth rates were less variable. As a result of the increased carbohydrate supply, these berries are more likely to experience a shortened lag phase in comparison to the ungirdled berries.

In the present study, the CV presents the clearest indication that girdling reduces variation in berry mass during the later stages of berry development. This reduction is likely to be the result of increased organic nutrition to the bunch that counteracts the variation that arises from differences in hormonal stimulus to growth by the developing seed (Ebadi *et al.* 1996b, Chaudhury *et al.* 2001). The antagonistic impacts of girdling and seed development are both significant in the early postflowering period of berry development.

CHAPTER 4 – CONFOCAL MEASUREMENT OF 3D CELL SIZE AND SHAPE

4.1 Summary

Parenchyma cells from the inner mesocarp of a grape berry (*Vitis vinifera* L. cv. Chardonnay) were visualised in three-dimensions within a whole mount of cleared, stained tissue using confocal laser scanning microscopy and digital image reconstruction. The whole berry was fixed, bisected longitudinally, cleared in methyl salicylate, stained with safranin O and mounted in methyl salicylate. Optical slices were collected at 1.0 μm intervals to a depth of 150 μm . Neighbouring z-series were joined postcollection to double the field of view. Transmission electron microscopy was used to assess the accuracy of fluorescent measurements of cell wall thickness. Attenuation at depth of the fluorescent signal from cell walls was quantified and corrected. Axial distortion due to refractive index mismatch between the immersion and mounting media was calibrated using yellow-green fluorescent microspheres, and corrected. Digital image reconstructions of wall-enclosed spaces enabled cells to be rendered as geometric solids of measurable surface area and volume. Percentages of the tissue occupied by cell walls and cells were calculated. Cell volumes within the inner mesocarp tissue of a single grape berry exhibited a fifteen-fold range, with polysigmoidal distribution and groupings around specific size classes. Variability in cell shape was indicated by the range in surface area to volume ratios, from 0.084 to 0.217 μm^{-1} . Structural detail at the internal surface of the cell wall was apparent. The technique is applicable to a wide range of morphometric analyses in plant cell biology, particularly developmental studies, and reveals details of cell size and shape that were previously unattainable.

4.2 Introduction

The anatomical characteristics of a tissue are a function of cell number and their shape, size and positioning in space. Parenchyma is the principal ground tissue in plant organs and parenchyma cells retain their physiological plasticity due to the presence of a complete protoplast, and an ability to resume meristematic activity (Esau 1977). Elucidation of the relative positioning, shape and size of plant parenchyma cells *in situ* has hitherto been achieved by indirect methods involving microscopic analyses of thin, serial sections followed by stereological analysis (Underwood 1970, Considine 1978, 1981, Weibel 1979, 1980, Møller *et al.* 1990, Cruz-Orive 1997) or three-dimensional (3D) reconstruction of physical

slices (Lewis 1926, Matzke 1948, Williams 1968, Korn and Spalding 1973, Korn 1974, Bron *et al.* 1990). While appropriate for tissues composed of isodiametric cells, stereological methods underestimate mean cell sizes (Considine and Knox 1981) and do not allow accurate determinations of intra-tissue variation (Parsons *et al.* 1989). Although 3D reconstruction of serial sections has yielded invaluable insights into the organisation of cells in specific tissues (e.g. Williams 1970), the methodology clearly has limitations due to artefacts introduced during the preparation of tissue slices and the subsequent tedious reconstruction. Cell maceration and cytometry have been applied to the problem, but these destructive procedures do not allow visualisation of cells in their original tissue and therefore lack the precision required to distinguish among cells from various tissue regions in the plant (Brown and Rickless 1949, Jackson and Coombe 1966a, 1966b, Harris *et al.* 1968).

It is desirable that methods be adopted for investigating cells within tissues in which physical sectioning is not required. The recent development of confocal laser scanning microscopy (CLSM) allows this possibility. Whole mounts of cleared, stained tissue in combination with optical sectioning by CLSM and digital 3D image reconstruction offers an alternative to conventional techniques.

CLSM combines laser light illumination, fluorescence microscopy and computer imaging. Under ideal circumstances it has sharp depth discrimination and produces horizontal optical slices of tissues in the plane of focus (Pawley 1995). The detector pinhole is confocal with the illuminated spot on the sample and rejects light reflected from objects that are not in the focal plane (Figure 4.1) (Dixon *et al.* 1991). As with most modern fluorescence

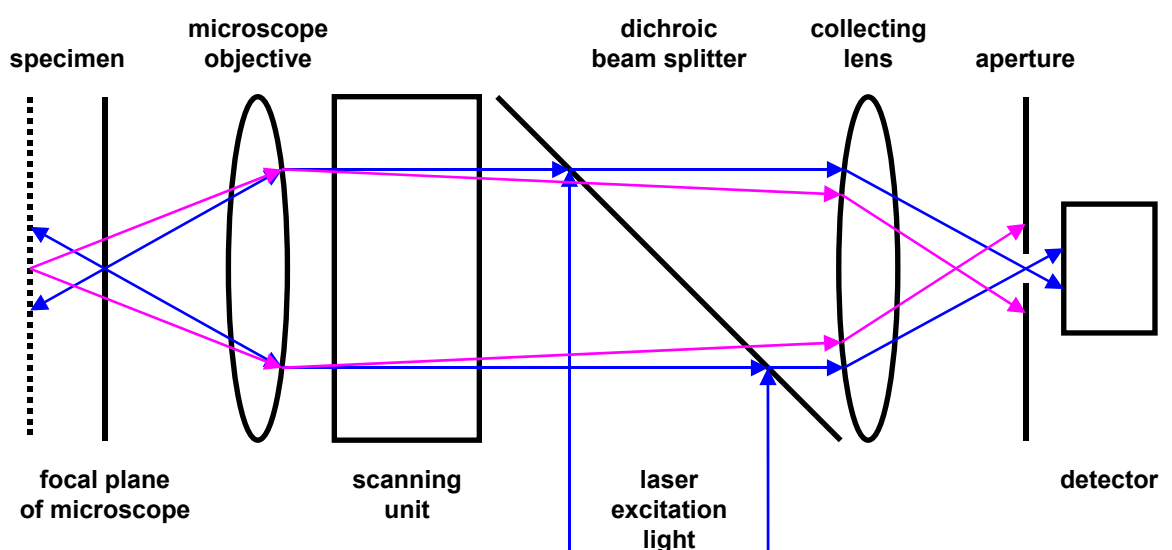


Figure 4.1 Ray paths in a confocal laser scanning microscope (CLSM). In the CLSM, light from sections of the specimen located out of focus (pink lines) will largely fall outside the aperture and is thus strongly attenuated. This property makes optical sectioning possible (Carlsson *et al.* 1985).

microscopes, the shorter wavelength light used for excitation is reflected onto the specimen through the objective that acts as a condenser (epi-fluorescence). The longer wavelength fluorescent emission is transmitted through to the ocular. The dichromatic mirror preferentially reflects shorter wavelengths while preferentially transmitting longer wavelengths. Excitation filters and emission filters used in conjunction with the dichromatic mirror enable wavelengths to be selected with precision (Rost 1994). In the CLSM, the source of illumination is a single beam laser that scans the specimen, fluorescence is measured by a photomultiplier, and the image compiled into a video frame by a charge-coupled device (CCD). The resultant images are digitised and stored as a vertical image stack, or z-series. Digital 3D image reconstruction enables the z-series to be visualised as a geometric structure (Carlsson *et al.* 1985, Yu *et al.* 1994). Applications of CLSM to the study of plant microstructure include 3D reconstruction of guard cells in *Commelina* leaves (White *et al.* 1996), the measurement of cell wall thickness in spring barley (*Hordeum vulgare*) and maize (*Zea mays*) (Travis *et al.* 1997), and *in vivo* observation of sieve tubes in fava bean leaves (Knoblauch and van Bel 1998).

This **third experiment** describe a further development for the detailed study of plant cell morphology and organisation using as object the parenchyma cells of the inner mesocarp of the grape berry that develop from the undifferentiated ovary wall after flowering (Pratt 1971, Srinivasan and Mullins 1981, Gerrath 1991). The combination of traditional clearing procedures with confocal microscopy enabled entire parenchyma cells (wall-enclosed spaces) to be visualised and measured *in situ*. The technique was tested successfully on a number of berries of different ages. The images and measurements presented in this paper pertain to a collection of parenchyma cells from a single tissue block within one young grape berry (cv. Chardonnay, 26 days after flowering, 5 mm diameter).

4.3 Experimental Procedures

4.3.1 Tissue Preparation

Grape berries were sampled from a 1984 planting of own-rooted *Vitis vinifera* L. cv. Chardonnay vines (clone I10V1) growing on Scott-Henry trellis in the Adelaide Hills, 26 days after flowering had commenced. Medial diameters of berries ranged from 1.31 to 5.25 mm and weights from 1.20 to 70.5 mg. The tissue of interest in this study is the parenchymatous inner mesocarp of the grape berry consisting of about 10 layers of large, highly vacuolated cells. At this developmental stage, cell division and cell expansion would be occurring concurrently within the mesocarp (Considine and Knox 1979a). Berries were

fixed in FPA₅₀ [formalin:propionic acid:50% ethanol 1:1:18] and stored in 70% ethanol. Individual berries were bisected longitudinally using a razor blade fragment under a dissecting microscope and stored in 70% ethanol at 4°C. The half-berries were used in two ways: first, for testing of stains using thin, embedded sections; secondly, for confocal microscopy without further cutting.

Berry halves were dehydrated through an alcohol series [methoxy-ethanol, ethanol, propanol, butanol], infiltrated with GMA [butanol-GMA, GMA], embedded in GMA in gelatin capsules and oven-cured at 65°C according to Feder and O'Brien (1968). Sections 2 µm thick were cut with a glass knife on a Reichert-Jung rotary microtome and air-dried onto a glass slide. Sections from small, medium and large half-berries were checked for autofluorescence and treated with one of the following stains: acridine orange (0.2% aq. for 1 min), Calcofluor White M2R (0.01% aq. for 1 min), Congo red (0.01% aq. for 1 min), Evans blue (0.005% aq. for 1 min), safranin O (0.5% aq. for 1 min), magdala red (0.1% aq. for 1 min), pontamine sky blue (0.05% aq. for 1 min), aniline blue (1.0% schedule for 5 min), periodic acid-Schiff's (1.0% schedule), Ponceau S (0.1% aq. for 2 min), trypan blue (0.01% aq. for 2 min), coriphosphine O (0.1% aq. for 2 min), euchrysin 2GNX (0.01% aq. for 2 min), FITC (0.01% aq. for 2 min), resorcin blue (0.1% aq. for 2 min), aniline blue fluorochrome (0.01% aq. for 30 min). Stained sections were visualised under a Zeiss Axiophot fluorescent microscope using a mercury vapour lamp with appropriate filter combinations.

Although background autofluorescence was observed in developing berries, it was too irregular to consistently define the cellular structure of all tissues (personal observation). During early stages of berry development, background autofluorescence (Goodwin 1953, Krause and Weis 1991) and formaldehyde induced fluorescence (Clark 1981, Rost 1992) may even become potential problems. Counterstaining can be used to eliminate their influence (de la Landa and Waterson 1968, Negishi *et al.* 1981, Schmued *et al.* 1982, Cowen *et al.* 1985).

Clearing of half-berries was explored after it was found that untreated tissue was too opaque to allow sufficient penetration of laser light. Mounting the tissue in a medium of higher RI increases optical penetration. The RI of parenchyma cells approximates that of water [RI ~ 1.33]. Several highly refractive immersion media were tested in this study: glycerol [RI ~ 1.47], xylene [RI ~ 1.50], methyl benzoate [RI ~ 1.52], and methyl salicylate [RI ~ 1.54] (O'Brien and McCully 1981). The efficacies of more destructive clearing techniques were also tested: mounting the tissue directly in 80% lactic acid at 50-60°C (Simpson 1929) and the use of specialised mixtures (Herr 1971, 1982). From these tests methyl salicylate was selected.

The following protocol was adopted: berry halves were dehydrated under vacuum through an ethanol series [70%, 85%, 95%, 100% twice] for 30 min per stage then cleared in methyl salicylate for 30 min under vacuum and stored overnight in a sealed glass container at 4°C. The next day they were stained with 0.5% safranin O in methyl salicylate for 15 min, rinsed in methyl salicylate and mounted, cut face down, on a 0.14 mm glass coverslip in a well constructed of a ring of silicone rubber (Dow Corning) filled with methyl salicylate (**Figure 4.2**). The further work described hereunder consisted of examination of the visualised tissue zone, illustrated in **Figure 4.2**, of a young Chardonnay grape berry, 26 days after flowering, 5 mm in diameter.

4.3.2 Confocal Laser Scanning Microscopy (CLSM)

Confocal images of the cell walls were collected using a BioRad MRC-1000 confocal system attached to a Nikon Diaphot-300 inverted microscope. The objective lens was a Nikon 60x oil

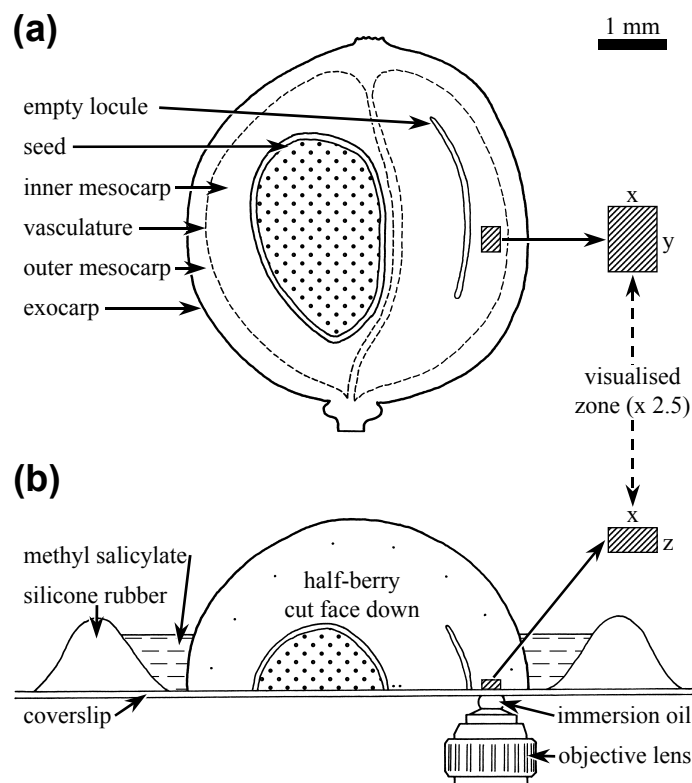


Figure 4.2 Grape berry tissues. Diagram of young grape berry showing location of tissues and zone viewed by CLSM (berry and zone to scale). (a) Longitudinally cut surface of the berry. (b) Section of stained and cleared half-berry positioned cut face down on coverslip in a well constructed of silicone rubber filled with methyl salicylate. The dimensions of the visualised zone are $x = 289 \mu\text{m}$, $y = 385 \mu\text{m}$, $z = 150 \mu\text{m}$.

immersion plan apochromat with a numerical aperture of 1.4 and a working distance of 170 μ m. A krypton/argon laser was used to excite the specimen at 488/10 nm and emission was collected at 522/35 nm with the confocal aperture closed down to 1.5 mm. A sequence of 151 x-y optical slices was collected, each with a 1.0 μ m separation on the z-axis. Each image was averaged over 4 scans using a Kalman filtering process. Images from a 289 x 193 μ m field-of-view (768 x 512 pixels) were captured as computer files. Fluorescent intensity was digitally coded using 256 levels of grey, with 0 representing the lowest intensity (black) and 255 the highest (white). Two neighbouring z-series were combined into a single z-series postcollection thus doubling the volume of tissue examined and increasing the number of cells included in the analysis. The combined field-of-view was 289 x 385 μ m (384 x 512 pixels). This combined z-series was the subject of the following experiment.

4.3.3 Transmission Electron Microscopy (TEM) of Cell Walls

Cell wall thickness was verified using TEM. A Chardonnay berry, 5.25 mm in diameter and weighing 70.5 mg, was selected from the sample that had been collected 26 days after flowering, fixed and stored as described previously. Berry sections were postfixed in 2% osmium tetroxide for 90 minutes, dehydrated through an acetone series [70%, 90%, 95%, 100% each 3 x 20 minutes, 100% 1 x 60 minutes], infiltrated with an araldite embedding resin [50% acetone/50% resin 1 x 8 hours, 100% resin 3 x 8 hours], embedded in fresh resin and polymerised under vacuum at 70°C (Mollenhauer 1964). Sections 70 nm thick were cut with a diamond knife on a Reichert Ultracut S ultramicrotome, stained with 5% uranyl acetate in 70% ethanol and Reynolds' lead citrate, and mounted on an aluminium grid. The sections were visualised under a Philips CM100 TEM and cell wall thickness was estimated from a stratified random sample.

4.3.4 Calibration of Intensity Attenuation with Depth

Signal attenuation is a function of absorption and scattering of both excitation and emission light (Rigaut and Vassy 1991, Guilak 1994). In the present study, the collected fluorescent signal represented cell walls, whereas the unstained cell interior appeared black. Lessening of the fluorescent signal deriving from the cell walls could result in an overestimation of the true size of the cell.

Signal attenuation was quantified by plotting the number of black pixels in each optical slice of the combined image stack with an intensity below a predetermined binary threshold (100) against slice depth using NIH Image analysis software (Version 1.61 U.S. National Institute of Health 1996). Attenuation was statistically proven to be linearly related to depth

so an intensity threshold correction factor was sought to minimise its impact on cell size calculations. Intensity thresholds for both slices 1 and 151 were recalculated to yield a regression line of zero slope. This intensity threshold range was used to derive an incremental threshold adjustment and new intensity thresholds for each optical slice in the entire z-series were applied prior to the correction for axial distortion.

4.3.5 Calibration of Axial Distortion

Some degree of axial distortion in the z-axis of the z-series was anticipated on the basis of the RI mismatch between the lens immersion medium (oil RI = 1.5124 @ 22.5°C) and the specimen mounting medium (methyl salicylate RI = 1.5358 @ 22.5°C) (Carlsson 1991, Hell *et al.* 1993). This was calibrated with nominal 10 µm yellow-green fluorescent microspheres (Molecular Probes/Triton Technologies) composed of a polystyrene envelope containing a fluorescent dye. A droplet of the diluted microsphere suspension was air-dried on a 0.14 mm glass coverslip then mounted between two coverslips in 100% methyl salicylate. Since polystyrene is soluble in methyl salicylate, the fluorescent dye leached into the methyl salicylate, causing it to fluoresce, while the microsphere itself became non-fluorescent but retained its spherical shape. Confocal, non-saturated, vertical sections of 10 microspheres were collected using the same filter set as the berry images. The x and z diameters of the spheres were determined as the distance between the edges of the spheres located at 50% of the greyscale intensity threshold between the centre of the microsphere and the adjacent background. A correction factor was calculated using the ratio of x to z diameter of microspheres. This factor of 4.5% was incorporated into the confocal z-series prior to digital 3D image reconstruction.

4.3.6 Three-Dimensional (3D) Reconstruction

To visualise the confocal data, ImageVolumes (Version 2.0 Minnesota Datametrics Corporation 1994) software run on a Silicon Graphics Indigo 2 computer under the Irix 5.3 operating system was used.

Cell walls and cells were reconstructed from the z-series using two-dimensional binary overlays of the cell walls and wall-enclosed spaces. These overlays were integrated in the axial dimension by the Marching Cubes algorithm (Lorenson and Cline 1987), a surface-based technique used to render 3D images from voxel data by forming isointensity contours of the object surface. The resolution of the reconstruction was twice the unit pixel size in x-y (1.504 µm) and equal to the distance between the optical slices in z (1.0445 µm). Image rendering, smoothing and lighting techniques allowed individual cells to be viewed as

geometric solids. Cells were reconstructed only if they were fully enclosed within a continuous cell wall (i.e. only entire cells were considered, partial cells were ignored).

Cell surface area and volume were measured with a distance field analysis software package (Dfield Version 2.0 Minnesota Datametrics Corporation 1994) which calculated 3D scalar quantities whose values described the Euclidean distance from any given point in space at Cartesian coordinates (x,y,z) to the closest surface of the 3D model.

4.4 Results

4.4.1 Staining and Mounting the Tissue Block

Fluorescence, either autofluorescence or stain induced, was a prerequisite to imaging cell walls under CLSM. Autofluorescence of berry cell walls was heterogeneous therefore staining was needed to induce even fluorescence for cell wall imaging under CLSM. Of the 16 stains tested, the majority gave poor or incomplete fluorescence of cell walls. However, safranin O was satisfactory, indicating adequate binding, useful wavelengths of excitation and emission, and absence of photobleaching problems. Safranin O was adopted for the remainder of the study. Calcofluor White M2R provided excellent staining in thin, glycol methacrylate (GMA) embedded sections but proved less specific to cell walls in cleared tissues. While GMA-mounted tissue was useful for classical sectioning techniques, it was unsatisfactory for embedding large, stained blocks of tissue prior to CLSM because of loss of stain specificity after embedding.

Excessive shrivelling of parenchyma cells resulted from the application of destructive clearing fluids, but the immersion of tissue in media of high refractive index (RI) produced acceptably cleared, whole mounts. Of the media tested, methyl salicylate proved the most successful: tissue distortion appeared to be minimal and the entire berry half was transparent under bright-field illumination. The adopted mounting procedure is shown in **Figure 4.2**.

4.4.2 Visualising Cell Walls

The tissue was imaged to a depth of 150 μm with the CSLM. The 151 optical slices that comprised the confocal z-series indicated the high degree of resolution attainable. Some loss of detail was caused by joining the two neighbouring z-series into a single z-series because the overall pixel number for each slice was reduced four-fold. Nevertheless, parenchyma cell walls were clearly visible in the consecutive optical slices, 1.0 μm apart, shown in **Figure 4.3**. Membranous structures visible within certain cells indicated possible plasmolysis. Despite this, cell walls remained intact and no intercellular spaces were apparent.

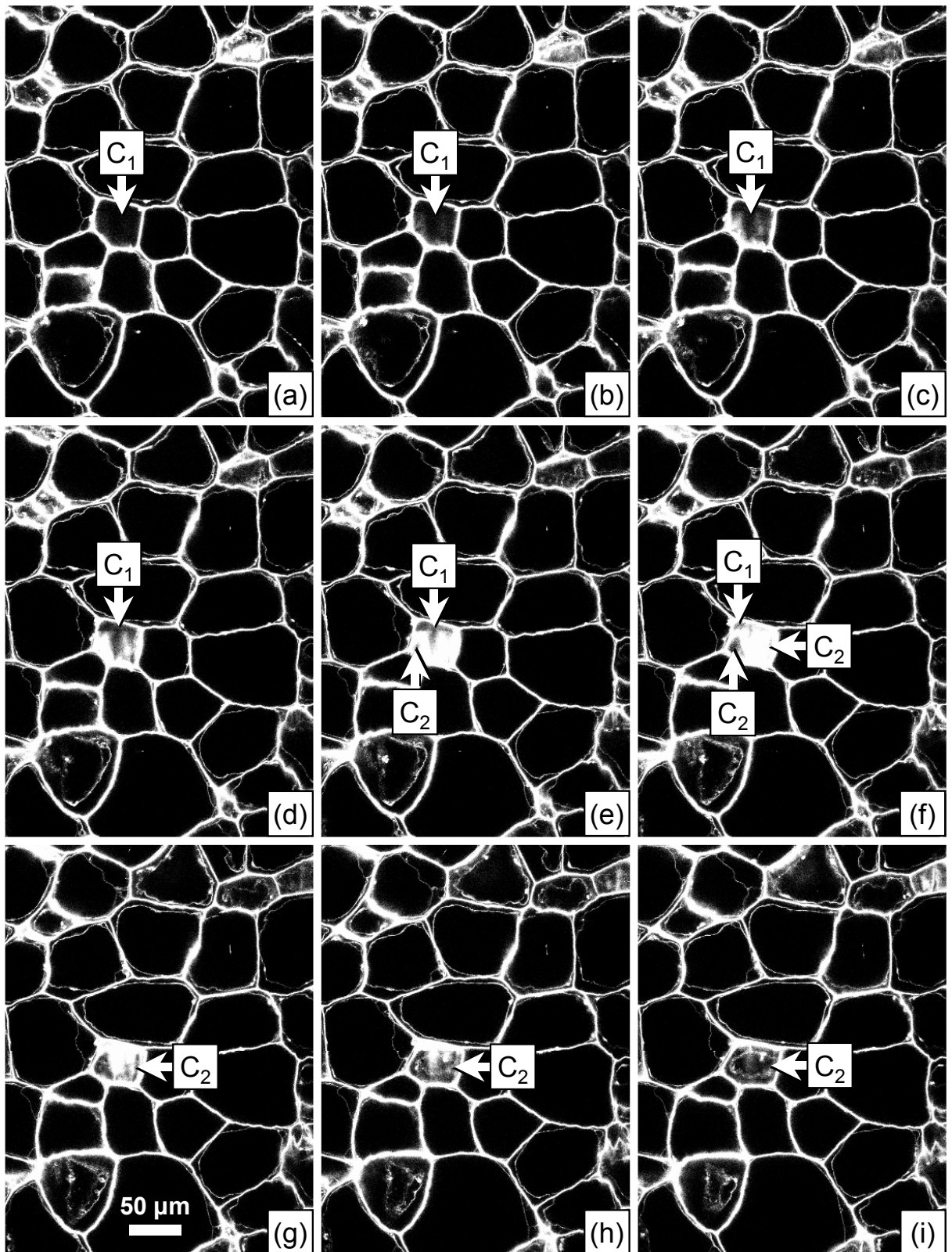


Figure 4.3 Optical slices of parenchyma cells. (a) to (i) represent consecutive optical slices, 1.0 μm apart, through a block of parenchyma tissue of the inner mesocarp of a Chardonnay berry collected 26 days after flowering. Fluorescent cell walls are white and the non-fluorescent wall-enclosed spaces are black. Cell C_1 begins to close in slice C and disappears fully in slice (g). Cell C_2 begins to appear in slice (e). Only C_2 is visible in slices (g) to (i). Plasma membranes are visible within some cells indicating possible plasmolysis due to the fixation process.

4.4.3 Comparison of Cell Wall Thickness (TEM vs CLSM)

The mean thickness of parenchyma cell walls obtained using TEM was 194 nm (std dev. = 50.4 nm, $n = 15$). This was an order of magnitude lower than the mean cell wall thickness of 4.15 μm (std dev. = 2.52 μm , $n = 15$) estimated from a stratified random sample within the confocal series. The discrepancy resulted from excessive fluorescent emission within a single confocal slice. The further the cell wall plane deviated from parallel to the optical z-axis, the greater its apparent thickness. Where cell walls were parallel, thickness decreased to a minimum of one pixel, 0.752 μm . In cell walls closer to the perpendicular x-y axis, thickness reached a maximum of 12.0 μm . Differences in cell wall thickness between TEM and CLSM were corrected by applying a rank 3 x 3 filter to erode cell walls by one pixel width in each optical slice.

4.4.4 Correcting the Confocal Z-Series for Signal Attenuation and Axial Distortion

Analysis of the z-series indicated the need to correct for signal attenuation. The number of pixels per optical slice with a greyscale intensity threshold less than 100 increased significantly with depth, as indicated by the original regression line ($r^2 = 0.839$) in **Figure 4.4**. This slope would cause an increase in the wall-enclosed area of 20% at 150 μm depth. A

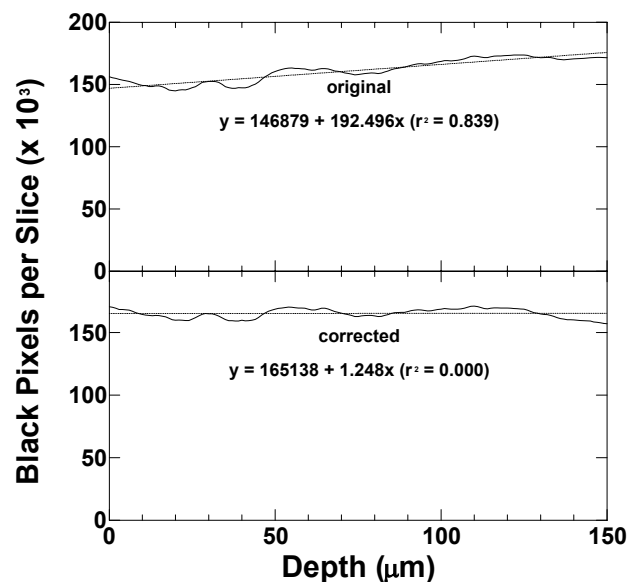


Figure 4.4 Signal attenuation. Attenuation of the fluorescent signal with depth quantified after binary intensity thresholding by plotting the number of black pixels per optical slice for the entire z-series. The original curve has a fixed binary intensity threshold of 100. The wall-enclosed area, measured as the number of black pixels per optical slice, increases significantly with depth ($r^2 = 0.839$). The corrected curve has a decremental binary intensity threshold starting at 210 for slice 1 and decreasing sequentially to 42 for slice 151. The wall-enclosed area does not change with depth ($r^2 = 0.000$).

20% increase in unit area equated to a 30% increase in unit volume and represented a serious potential for overestimating individual cell size. To minimise this error, attenuation of the fluorescent signal was corrected by modifying the intensity threshold. A starting threshold of 210 at slice 1, decreasing sequentially to 42 at slice 151, provided the best empirical solution. The corrected data displayed no fluorescence attenuation with depth, as indicated by the regression line ($r^2 = 0.000$) in **Figure 4.4**.

A visual demonstration of this result is shown in **Figure 4.5** that depicts a y-z vertical section through the z-series (a) before thresholding the image, and (b) after thresholding and correcting for fluorescence attenuation. Despite the more obvious pixelation in the binary image, **Figure 4.5(b)** is superior to **Figure 4.5(a)** in its representation of cell walls with a consistent thickness, independent of the depth of confocal imaging.

To check the extent of axial distortion within the confocal z-series, due to RI mismatch, the dimensions of fluorescent microspheres were measured. A confocal vertical section through a microsphere is shown in **Figure 4.6** detailing the position of the five intensity threshold measurements taken to establish the top, bottom and sides of the microsphere. The mean x/z ratio was 1.0445 (std dev. = 0.0205, n = 10), suggesting an axial compression of 4.45%. A multiplication factor of 1.0445 was applied to the z-series, changing the z-step from a nominal 1.0 μm to 1.0445 μm . As a consequence, the maximum image depth was expanded to 156.7 μm .

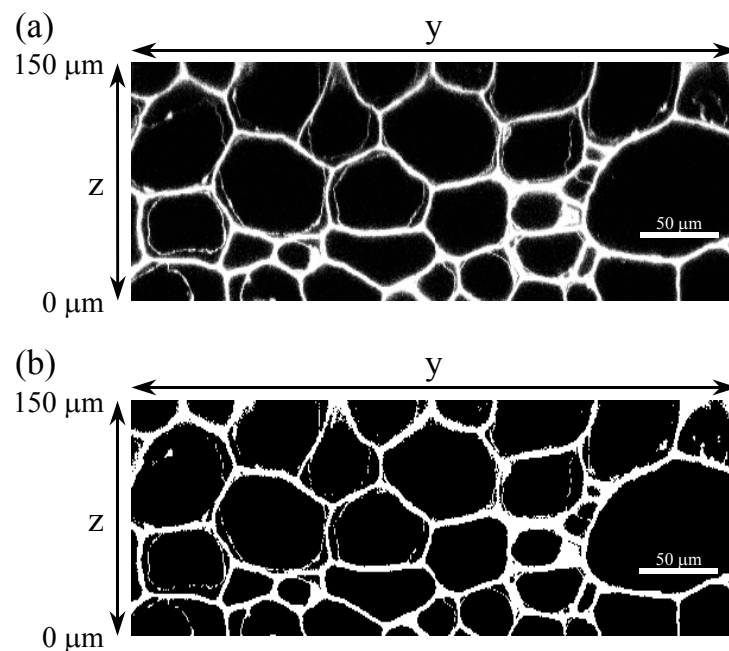


Figure 4.5 Attenuation correction. (a) Original y-z vertical section through the collected z-series showing decrease in cell wall fluorescence with depth. (b) Attenuation-corrected binary image of above y-z vertical section showing no discernible weakening of cell wall fluorescence with tissue depth.

4.4.5 Reconstructed Three-Dimensional (3D) Models of Cells and Cell Walls

Two-dimensional binary overlays of cell walls and wall-enclosed spaces from single optical slices were integrated to form 3D images. The 3D reconstructions in **Figure 4.7** of (a) cell walls and (b) 29 individual cells occupied 16% and 44%, respectively, of the total volume of the tissue block. The size range for individual cells extended more than 15-fold, from $24700 \mu\text{m}^3$ to $386000 \mu\text{m}^3$ (mean = $131000 \mu\text{m}^3$, std dev. = $108000 \mu\text{m}^3$, $n = 29$). The population dynamics of the cells were represented graphically by plotting cell volume in ascending order (**Figure 4.8**). Groupings of cells around specific size classes were evident. Six distinct plateaux suggest the maximum size for a cell in that particular size class – $40000 \mu\text{m}^3$, $79000 \mu\text{m}^3$, $136000 \mu\text{m}^3$, $208000 \mu\text{m}^3$, $321000 \mu\text{m}^3$, and $386000 \mu\text{m}^3$. Note the decreasing interval between successive pairs of size class maxima. Variability in cell shape was indicated by the range in surface area to volume ratios, from 0.084 to $0.217 \mu\text{m}^{-1}$.

Structural detail greater than $1.5 \mu\text{m}$ was apparent at the internal surface of the cell wall. Surface contours exhibited protuberances and invaginations that appeared to relate to the structure and location of internal membranes.

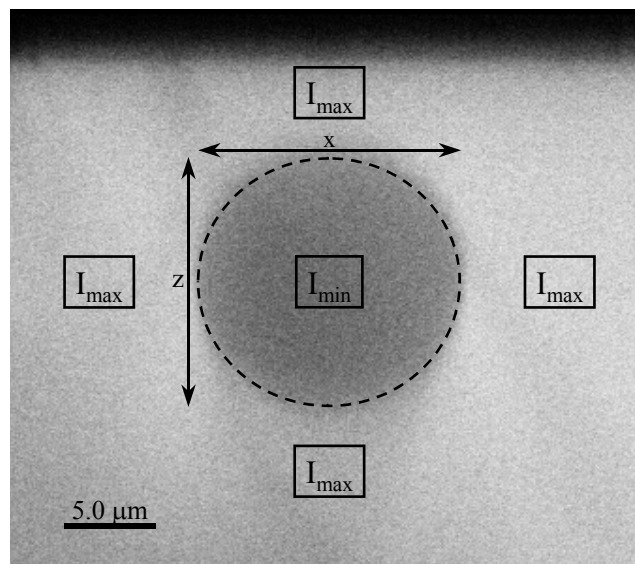


Figure 4.6 Fluorescent microsphere. A vertical confocal section through a fluorescent microsphere detailing the position of the five fluorescence intensity measurements (4 maxima and 1 minimum) taken to establish the edges of the microsphere. The ratio of x and z diameters were used to calculate axial distortion due to refractive index mismatch between the lens immersion medium and the specimen mounting medium.

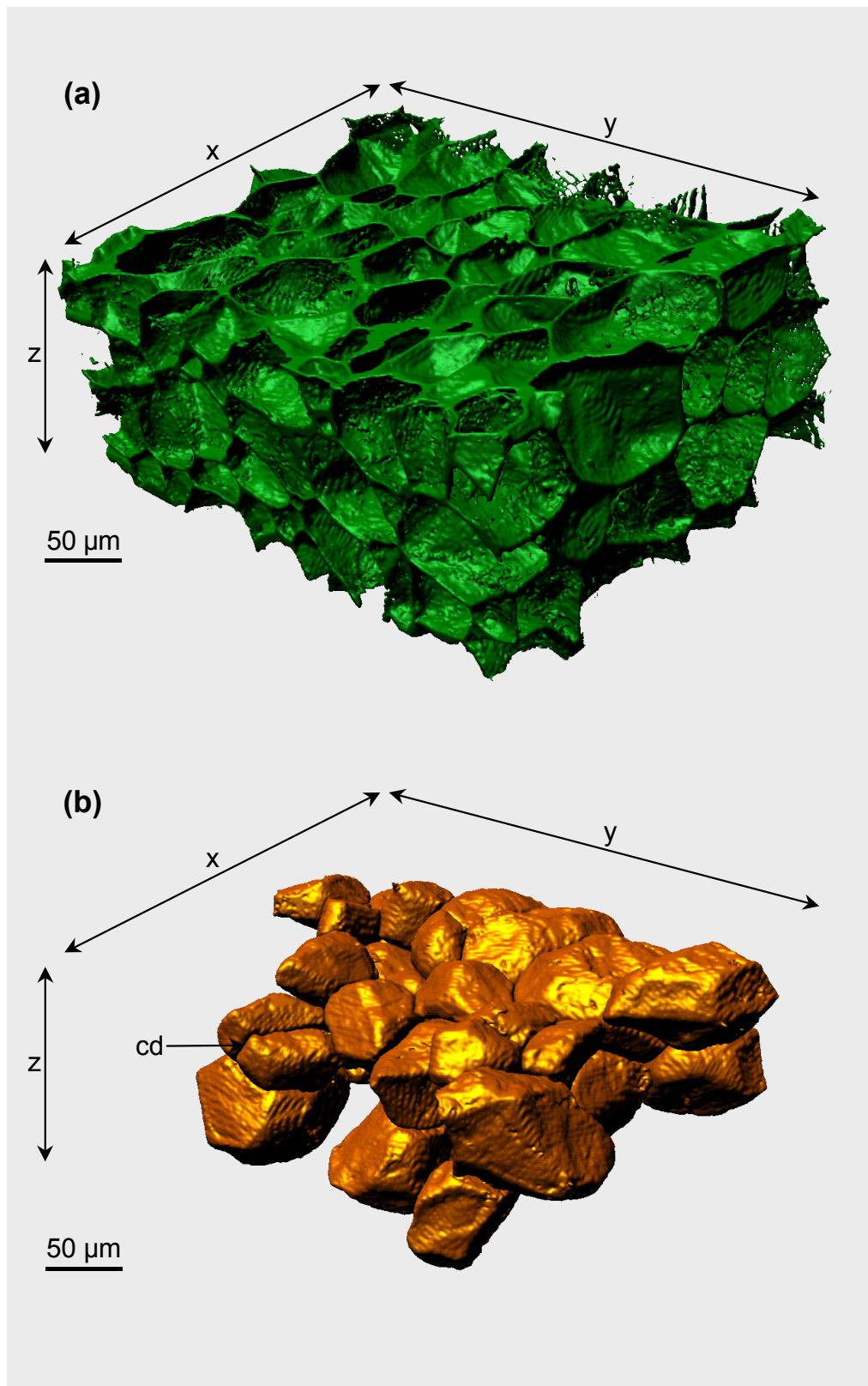


Figure 4.7 Parenchyma cell reconstructions. Digital 3D reconstruction of (a) cell walls and (b) 29 individual cells indicate the variety of shapes and sizes found among parenchyma cells in the inner mesocarp tissue of a Chardonnay berry harvested 26 days after flowering. Only entire cells are included, partial cells are excluded. A recent cell division is indicated at “cd”.

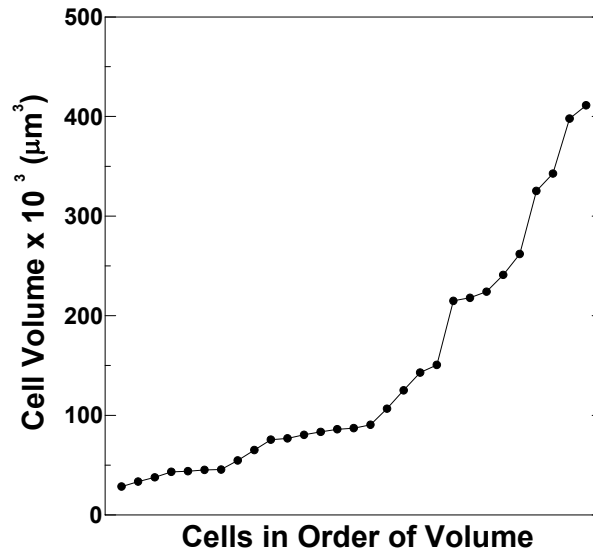


Figure 4.8 Parenchyma cell volumes. Cell volumes of all 29 reconstructed parenchyma cells in **Figure 4.7(b)** from the inner mesocarp tissue of a Chardonnay berry harvested 26 days after flowering, grouped in ascending order. The curve suggests 6 distinct plateaux around particular size classes.

4.5 Discussion

In order to improve understanding of the relationship between cell division, cell expansion and final berry anatomy, development of a confocal technique for non-destructive 3D reconstruction of the parenchyma was pursued. As a prerequisite for such studies, suitable methods of tissue preparation, mounting, staining and clearing to render cell walls fluorescent and distinct from wall-enclosed spaces under the confocal microscope were investigated. Calibration of potential errors in measurement was investigated prior to digital reconstruction of 3D images. The volume of individual, whole parenchyma cells within a block of grape berry mesocarp tissue could be measured *in situ* to a precision of $2 \mu\text{m}^3$.

4.5.1 Comments on Techniques Used

Judicious, minimal cutting of the organ enabled the berry to maintain the integrity of its tissues, thus reducing the likelihood of cell distortion. This aspect of the project was necessary if individual cells were to be viewed *in situ*.

The selection of stains for complete fluorescence of cell walls was crucial. Many of the accepted cell wall stains proved inadequate in their specificity, frequently staining additional structures within the cell. This problem was accentuated in cleared tissues where the clearing solvents gradually extracted the stain from the tissue back into solution. Safranin O is a basic,

metachromatic dye of the quinone-imine group, widely used in plant and animal microtechnique for bright-field and fluorescence microscopy (Rost 1995). It fluoresces under a wide range of excitation wavelengths (violet-blue) and is resistant to photobleaching making it suitable for many confocal applications.

Clearing with media of high refractive indices greatly increased the transparency of the tissue, enabling laser penetration to significant depth. Methyl salicylate proved the most suitable of all the mounting media tested: it was non-fluorescent, produced the greatest increase in tissue transparency and was able to dissolve safranin O (Hering and Nicholson 1964).

The working distance of the objective lens (170 μm) proved to be the main limiting factor to the depth of tissue penetration in this experimental system. Although optical penetration was consistently high throughout the entire tissue, a high numerical aperture lens (1.4) was required to resolve cell walls running horizontal to the optical plane. This trade-off between working distance and numerical aperture in optical systems is unavoidable (Pawley 1995). Larger volumes of tissue can be studied by aligning and combining adjacent z-series (Oldmixon and Carlsson 1993): this increases the x and y dimensions of the scanned region, but z remains unchanged.

Confocal slices were deliberately over-saturated to ensure that all cell walls were adequately visualised to a thickness of at least one pixel. It was anticipated that cell wall thickness in the confocal slices would be greater than the TEM measurements. An over-estimation in the associated calculation of cell wall volume and a corresponding under-estimation in the calculation of cell volume were therefore unavoidable.

Since the attenuation of fluorescence signal with depth was linear, a correction factor was derived from simple linear models. In the absence of this correction factor estimations of unit volume at 150 μm depth could be up to 30% too high.

The use of fluorescent microspheres to derive a single empirical correction factor for axial distortion obviated the need for complex theoretical estimates involving geometric ray tracing models that often yield conflicting results (Visser and Oud 1994, White *et al.* 1996). This was only an approximation to what is theoretically a nonmonotonic function (Török *et al.* 1997). The fact that the microsphere's polystyrene outer coating was permeable to methyl salicylate was an added bonus since it circumvented any complications that may have arisen due to the unknown RI of the microsphere contents.

4.5.2 Shapes and Sizes of Parenchyma Cells

Contemporary 3D reconstruction techniques in plant biology are infrequent (White *et al.*

1996, Travis *et al.* 1997, Knoblauch and van Bel 1998) although many of the stereological principles were established by botanists earlier this century. The group of 29 cells visualised here, or each cell individually, can be viewed on screen from all angles. Measurements can be made of volume, surface area, surface morphology, and the number of surface planes.

Quantitative confocal microscopy has typically visualised single fluorescent structures in a non-fluorescent matrix (Becker *et al.* 1991, Rigaut and Vassy 1991, Yu *et al.* 1994). The present paper takes a contrary perspective by measuring multiple non-fluorescent structures contained within a complex fluorescent matrix.

Intercellular spaces were not detected at the given level of resolution, hence the volume of the network of fluorescent cell wall material was measured and calculated as 16% of the total volume of the tissue block in **Figure 4.7(a)**. The difference between the total volume of the tissue block and the cell wall volume would be expected to equal the cell volume (84%), but that raises the difficulty of specifying such a space since, as shown in **Figure 4.7(b)**, no measurements were made of cells unless they were completely enclosed by cell walls (i.e. only entire cells were considered, partial cells were ignored). Entire cells occupied 44% of the total tissue volume. Therefore, the remaining 40% was composed of partial cells.

Note that the cells in **Figure 4.7(b)** are incomplete since their enveloping fluorescent walls are absent. The complementary network of cell walls is shown in **Figure 4.7(a)**. The allocation of space to cell or cell wall is determined by the intensity of fluorescence at each pixel. Hence the boundary surfaces in **Figure 4.7(b)** are presumably mirror images of the inside surfaces of the walls; their authenticity depends on the assumption that all cell wall material is stained completely and fluoresces above the intensity threshold. Fluorescence of membranes and other non-wall material, evident in some optical slices, did not interfere with delineation of cell walls since most of the membrane fluorescence was below the intensity threshold used.

The mean size found for grape mesocarp cells at this stage of development compares favourably with published sources (Harris *et al.* 1968, Coombe 1976, Considine and Knox 1981) but the range and variability have not previously been described. The indication of a succession of size classes deserves further study. Such classes might represent developmental cohorts of cells, where the smaller cells have arisen as mitotic divisions of the larger cells. The decreasing interval between successive cohorts suggests asynchronous divisions of different sized cells. Future analyses of parenchyma cell sizes from postflowering grape berries might identify morphological sources of variation in berry size during early development.

A study of the shape of individual cells could be developed from these results. Cell

shape in space-filling tissues is described by the planes of contact (facets) with neighbouring cells. In homogeneous, space-filling tissues, the mean number of facets per cell is said to approach 14. This is true of plant cells, soap bubbles and compressed metal grains (Williams 1968). The orthic tetrakaidecahedron, a geometrically perfect 14-sided polyhedron with 8 hexagonal and 6 quadrilateral faces, was proposed as the archetypal shape for parenchyma cells (Kelvin 1887, Thompson 1942, Matzke 1948, Korn and Spalding 1973, Korn 1974), but this form is rarely achieved in nature due to the occurrence of varying cell sizes within a developing tissue (Matzke and Duffy 1956). Where both small and large cells are present in the same tissue, it is obligatory for the larger cells to have more facets than the smaller cells. The relevance of mean number of facets per cell as a quantitative descriptor of cell size is questionable, given that cell contacts are not always flat, planar surfaces. It is less precise than the absolute measurements of cell volume, surface area and shape obtained in the present study.

Structural details greater than 1.5 μm are apparent at the internal surface of the cell wall. The regular, large undulations are typical of integrated serial sections. The interconnected patterns of protuberances and invaginations appear to be associated with the structure and position of internal cellular membranes. The more irregular, solitary structures may indicate the presence of primary pit fields.

The technique described in this paper for measuring and visualising plant parenchyma cells in 3D using whole mounts of cleared, stained tissue in conjunction with CLSM and digital 3D reconstruction is applicable to a wide range of morphometric analyses in plant cell biology. Its major advantages over traditional serial sectioning are in the precision and accuracy of the measurements obtained in comparison to stereological methods without the tedium and potential for error. It could be a valuable complement to molecular genetics for elucidating factors critical to the development of plant form and function.

CHAPTER 5 – BERRY SIZE AND CELL SIZE IN CHARDONNAY

5.1 Summary

This chapter describes an experiment that sought to resolve the relationship between fruit size and cell size in a developing grape berry. The hypothesis was that variation in cell size occurs early in the postflowering period of berry development and that this variation was responsible for the subsequent macroscopic size differences observed between berries. Individual Chardonnay berries on ungirdled and girdled vines were assessed on four occasions throughout the flowering period. Individual flowers that had opened during the intervening time period were tagged. One bunch from each vine was harvested at 15 days after first capfall (age classes 1-4, 5-7, 8-11, 12-15 days), the other at 43 days (age classes 29-32, 33-35, 36-39, 40-43). Subsamples of “shot”, “chick”, and “hen” ovaries were selected from each age class of the day 15 population. Subsamples of “chick”, and “hen” berries were selected from each age class of the day 43 population. Volumes of parenchyma cells from the inner mesocarp of each ovary and berry were measured using the CLSM technique developed in the previous chapter. Only 10 cells were measured for each combination of treatments (where available).

At day 15, mean cell volume for the “hens” was consistently greater than that of “shot” or “chick” ovaries for both girdling treatments. CVs were lower for “shot” ovaries than for “chicks” or “hens”, regardless of girdling treatment, but differences were minor. By day 43, the differences in mean cell volume between “chicks” and “hens” were well established. “Hens” were several-fold larger than “chicks”, indicating different amounts of cell expansion. This observation was common to berries from ungirdled and girdled vines. Significant differences in cell volume between ungirdled and girdled berry pairs would suggest that girdling had increased the cell volume of “chicks”. The effect of girdling on “hens” was less predictable. No trend among CVs was evident. Girdling may have resulted in a minor reduction of variation. Between day 15 and day 43, cell volumes for both “chicks” and “hens” continued to increase, although this increase was proportionally greater for the “hens”. This size increase was not accompanied by an increase in variation. The impact of time on variation was not significant. CVs from samples at day 15 and day 43 were consistently high within a girdling treatment. Berries from girdled vines displayed ~50% more variation in comparison to ovaries from ungirdled vines. The lowest level of variation was associated with

cells from “shot” ovaries, for both girdling treatments.

This study indicates that cell division and cell enlargement occur in all three berry types, but these processes are partially restricted in “chicks”, and severely restricted in “shot” berries. Preliminary observations suggest that the increase in cell volume proceeds in a stepwise manner, which might be coordinated across different berry types and ages. Further investigations would be required to confirm this finding.

5.2 Introduction

The objective of the **fourth experiment** was to resolve the relationship between fruit size and cell size in a developing grape berry. The hypothesis was that variation in cell size occurs early in the postflowering period of berry development and that this variation was responsible for the subsequent macroscopic size differences observed between berries.

The study should enhance our understanding of the morphological and physiological basis of variation in developing fruit by determining when variation in cell number and cell size is manifest within a given pericarp tissue. This information could promote new hypotheses on the relative roles of cell division and cell expansion in the determination of berry size, berry composition and berry-to-berry variation. The techniques provide a much needed analytical approach for quantitative research in plant morphology.

5.3 Experimental Procedures

5.3.1 Biological Materials

The Chardonnay ovaries and berries used in this experiment were a subset of the material collected for Chapter 3 (see 3.3.1). The experimental site consisted of a 1984 planting of own-rooted Chardonnay vines (clone I10V1) on Scott-Henry trellis at Lenswood, South Australia (34°55'S, 138°49'E). Ten vines were selected and inflorescence numbers were counted on each vine. The four vines with the most similar inflorescence numbers to the overall mean were identified. Three similar shoots from each of these vines were selected and tagged, their length and node number were recorded, and the progress of flowering closely monitored. From these three shoots, two basal inflorescences that began flowering at the same time were selected and their potential flowers counted. Opened flowers (E-L stage 19) were tagged at 4 days after the first flower had opened by marking their pedicels with water-resistant acrylic ink (Opaque Magic Color, Royal Sovereign, UK) using a technical pen (Isograph, Rotring, Germany). On the same day, two of the vines were trunk girdled with a 5 mm wide incision to the depth of the cambium severing the phloem vessels at 30 cm above

ground level (Coombe and Dry 1992). Thereafter, bunches were checked at 3-4 day intervals. Individual flowers that had opened within this interval were also tagged (E-L stage 19).

One of the two tagged bunches per vine was removed after 2 weeks (15 day sample) when 100% of the flowers had opened (E-L stage 26). By this time, many of the flowers would have undergone nucellus and integument growth in the seed, and cell division in the pericarp would be well advanced (Barritt 1970, Ebadi *et al.* 1996b). The other bunch was sampled 4 weeks later (43 day sample) (E-L stage 30) after embryo formation and cell division in the pericarp would have finished (Barritt 1970, Ebadi *et al.* 1996b). Bunches were stored in plastic bags on ice until returning to the lab. Berries were removed from each bunch, sorted by flowering date, counted, fixed in FPA₅₀ for one week, and stored in 70% ethanol in the refrigerator until ready for analysis.

Ovaries from the 15 day sample comprised four age classes – 1-4 days, 5-7 days, 8-11 days, 12-15 days. Frequency distributions (**Figure 3.5**) indicated “hen”, “chick”, and “shot” types were present among the ovaries sampled from both girdled and ungirdled bunches. One ovary of each type (3x) was selected from each age class (4x) and each girdling treatment (2x), where available. Berries from the 43 day sample comprised four additional age classes – 29-32 days, 33-35 days, 36-39 days, 40-43 days. Frequency distributions (**Figure 3.6**) revealed “chicks” and “hens” among bunches of both girdling treatments. “Shot” berries were lacking among girdled bunches. One “chick” and one “hen” (2x) were selected from each age class (4x) and each girdling treatment (2x), where available.

5.3.2 Calculating Berry Volume

The grape berry is essentially a prolate spheroid of volume:

$$V = \frac{4}{3} \pi ab^2 \quad \text{Equation 5.1}$$

where, a and b are the major and minor radii, respectively. The volume of a tissue region within the berry can be estimated from a longitudinal section through the berry using the equation:

$$V_r = \frac{4}{3} \pi (a_r - a_{r-1}) (b_r - b_{r-1})^2 \quad \text{Equation 5.2}$$

where, the subscript "r" denotes the region in question, and "r-1" denotes the previous concentric tissue region (**Figure 5.1**).

It was not possible to repeat this procedure for all tissue regions, but since the inner mesocarp represents some 64% of total berry volume at harvest (Harris *et al.* 1968), it was reasonable that the study should focus on the mesocarp parenchyma. A random sample of mesocarp cells was selected from each berry, their shapes reconstructed, and their volumes

measured (see 5.3.3 and 5.3.4). Mean cell volume for each region is given by the average of these cells.

5.3.3 Confocal Laser Scanning Microscopy (CLSM)

The CLSM protocol was developed in Chapter 4. Whole berries were fixed, bisected longitudinally, cleared in methyl salicylate, stained with safranin O and mounted in methyl salicylate. Optical slices were collected at 1.0 μm intervals to the maximum tissue depth possible ($\leq 150 \mu\text{m}$). Attenuation at depth of the fluorescent signal from cell walls was quantified and corrected. Axial distortion due to refractive index mismatch between the immersion and mounting media was calibrated using yellow-green fluorescent microspheres, and corrected.

5.3.4 Calculating Cell Volume

Image processing for the cell volume calculations was undertaken in Scion Image for Windows (Version 4.0.2 Scion Corporation 2000). The digital images of inner mesocarp cell walls from larger berries were sufficiently distinct from the non-fluorescent, wall-enclosed spaces to be detected by intensity thresholding (see 4.4.5). A binary overlay of the wall-

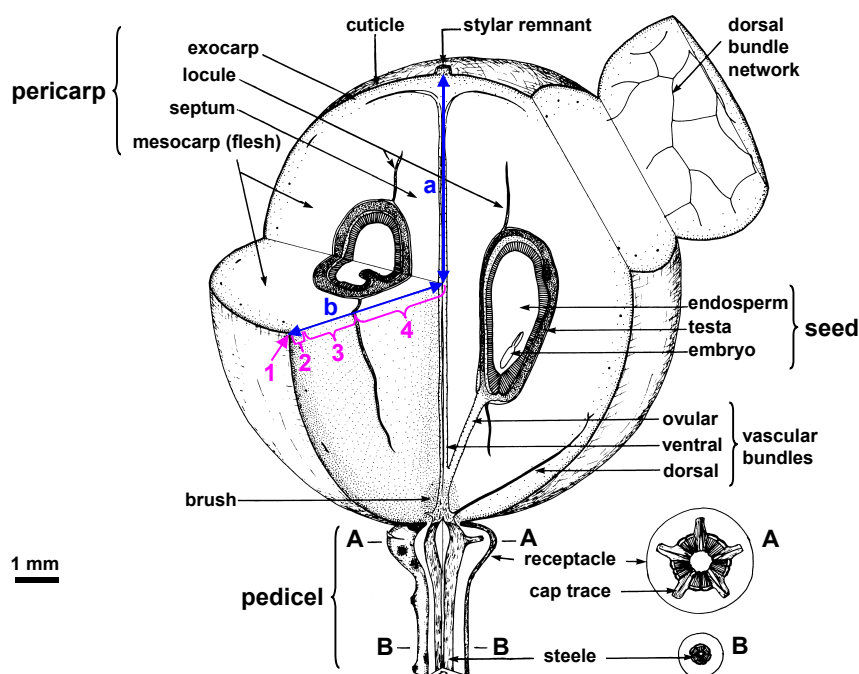


Figure 5.1 Tissues in a mature grape berry. Three-dimensional diagram of a grape berry at maturity (Coombe 1987a). The berry is composed of four concentric tissue regions. The major and minor radii are a and b , respectively. Numbers 1, 2, 3 and 4 denote the regions occupied by the septum, inner mesocarp, outer mesocarp and hypodermis, respectively. Magnification is insufficient to clearly show the inner and outer epidermal tissues, but they also contribute to fruit size, though to a lesser extent.

enclosed space was created, dilated (rank 3 x 3 filter), and measured (in pixels). The procedure was repeated for each optical slice in which the particular cell was observed. The areas were converted to μm^2 , multiplied by the width of the optical section and a correction factor to compensate for axial distortion (see 4.3.5), and summed across all optical slices. The formula is:

$$V = \left(\sum_{s=1}^i A \cdot p \cdot w \cdot d \right) \quad \text{Equation 5.4}$$

where, V = cell volume (μm^3)
 A = area of binary overlay (pixels)
 p = pixel size (μm^2)
 w = width of optical section (1 μm)
 d = correction factor for axial distortion (1.0445)
 i = number of optical slices occupied by cell

Inner mesocarp cells of smaller berries tended to have higher concentrations of phenolic compounds making intensity thresholding of cell walls problematic. These cell walls were digitally traced along the middle lamella with a drawing tablet (Intuos, Wacom Technology Corporation, USA). A binary overlay of the traced area was created and measured (in pixels). Since the tracing was only a single pixel wide and approximated the actual width of the cell walls as determined by TEM (4.4.3), no dilation of the overlay was required. The rest of the protocol followed that described for larger berries (above). Ten cells volumes were measured from each berry, although on some occasions this was not possible because insufficient whole cells were contained within the image stack. In total, the volumes were calculated for 321 individual parenchyma cells from the inner mesocarp tissues of developing grape berries.

5.3.3 Statistical Techniques

Individual cell volumes were plotted in ascending order at 15 days and at 43 days for each age class and girdling treatment. Significant differences in mean cell volume for each ovary/berry type, age class, and girdling treatment were checked using Genstat 5 Statistical Package (Genstat 5 Committee, 1987a). Significant differences between ovary/berry cell volumes within an age class were determined by REML (LSD at $p < 0.05$). Significant differences between girdling treatment pairs were determined by Student t-tests. The CVs associated with each mean were calculated using Equation 1.8. These were compared to determine if variation has decreased, remained static, or increased during the postflowering sample period. A process of elimination was used to identify the developmental stage at which variation began.

5.4 Results

5.4.1 Ovary Cell Volumes (1-15 days)

Inner mesocarp cell volumes of Chardonnay ovaries from an ungyrdled bunch harvested at 15 days after first capfall are shown in **Figure 5.2**. The age classes are plotted separately: 1-4 days, 5-7 days, 8-11 days, 12-15 days. Three ovary types from each age class were analysed (where available): “shot”, “chick”, and “hen”.

Inner mesocarp cell volumes of Chardonnay ovaries from a girdled bunch harvested at 15 days after first capfall are shown in **Figure 5.3**. The layout is the same as the previous figure where the four age classes are plotted separately and the three ovary types (where available) are uniquely identified.

Note that the cell volumes in **Figures 5.2** and **5.3** are plotted in ascending order creating a stepwise effect as cell volume increases (Gray *et al.* 1999, refer to **Figure 4.8**). The reason for this was to compare the successive size classes of cells between “shot”, “chick”, and “hen” ovaries and berries. It was postulated in Chapter 4 that these size classes might represent developmental cohorts of cells, where the smaller cells could have arisen as mitotic divisions of the larger cells.

Inner mesocarp cell volumes of ovaries from the ungyrdled bunch a(i) and the girdled bunch b(i) harvested at 15 days after first capfall are shown in **Table 5.1**. Mean cell volume has been calculated for three ovary types (“shot”, “chick” and “hen”) in four age classes (1-4 days, 5-7 days, 8-11 days, and 11-15 days). Variation in cell volume within each age class and ovary type is indicated by the CV (%). Significant differences between ovary types were determined by REML (LSD at $p < 0.05$). Significant differences between ungyrdled and girdled sample pairs were determined by Student t-tests and significance levels are indicated.

In the ungyrdled bunch, the graphs of ovary cell volume from days 1 to 15 are consistent (**Figure 5.2**). “Shot”, “chick” and “hen” ovaries display similar patterns of cell volume increase despite differences in berry age. Within any particular age class, the three curves that represent each ovary type display similarities in shape, but differ in their slope. Typically, the order of slopes is “shot” < “chick” < “hen”, although an exception occurs at 8-11 days when “shot” and “chick” are reversed. Using the model of a stepwise increase in cell volume (see 4.5.2), these graphs indicate that a similar principle might be in operation. Even the timing of stepwise increases in cell volume would appear to be coordinated, although the data are limited.

Significant differences in mean cell volume (**Table 5.1(a)**) were exhibited at 5-7 days between “shot” ovaries ($10845 \mu\text{m}^3$) and “hens” ($20220 \mu\text{m}^3$). At 12-15 days, mean cell

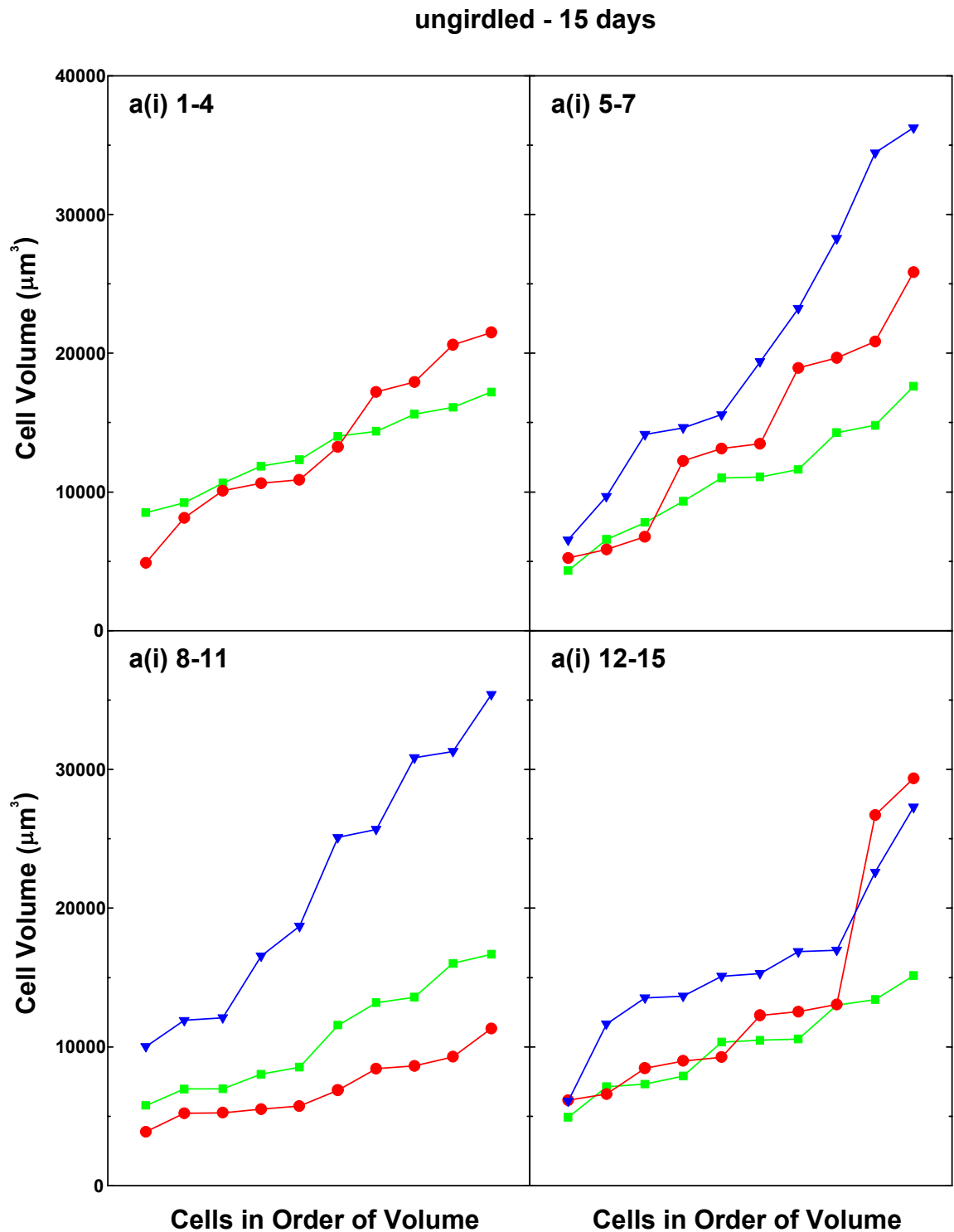


Figure 5.2 Chardonnay cell volumes (ungirdled, 1-15 days). Inner mesocarp cell volumes of ovaries from ungerdled bunch a(i) harvested at 15 days after first capfall. The numbers following the bunch identity indicate the age classes from within which the ovaries were sampled: 1-4 days, 5-7 days, 8-11 days, 12-15 days. Three ovaries from each age class were analysed (where available) – one “shot” ovary (■), one “chick” (●) and one “hen” (▼).

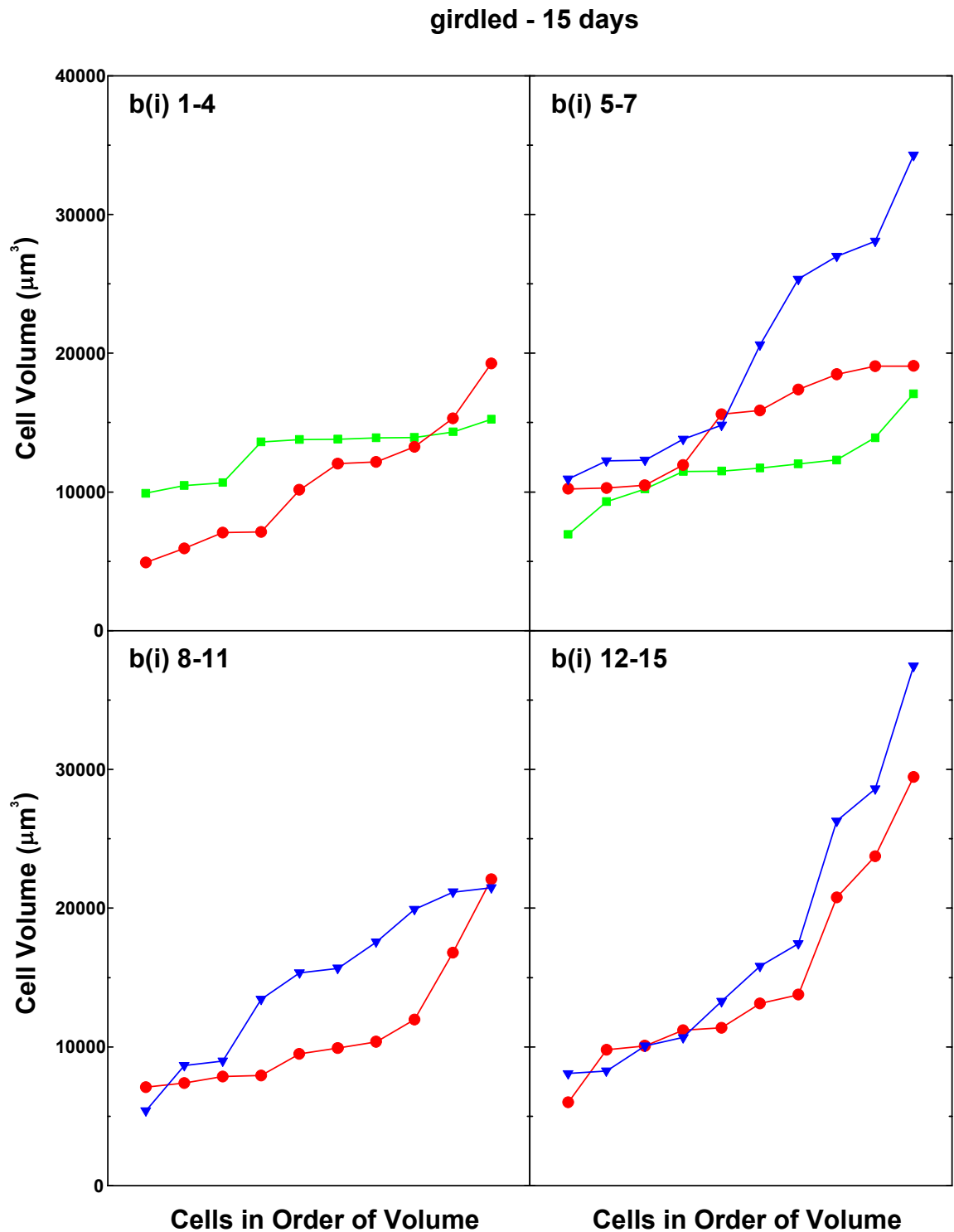


Figure 5.3 Chardonnay cell volumes (girdled, 1-15 days). Inner mesocarp cell volumes of ovaries from girdled bunch b(i) harvested at 15 days after first capfall. The numbers following the bunch identity indicate the age classes from within which the ovaries were sampled: 1-4 days, 5-7 days, 8-11 days, 12-15 days. Three ovaries from each age class were analysed (where available) – one “shot” ovary (■), one “chick” (●) and one “hen” (▼).

Table 5.1 Variation in cell volume (1-15 days). Inner mesocarp cell volumes of ovaries from ungirdled bunch a(i) and girdled bunch b(i) harvested at 15 days after first capfall. Mean cell volume has been calculated for three ovary types (“shot”, “chick” and “hen”) in four age classes (1-4 days, 5-7 days, 8-11 days, and 11-15 days). Variation in cell volume within each age class and ovary type is indicated by the coefficient of variation (CV%). Significant differences between ovary types were determined by REML and are indicated by the letters that follow the mean cell volume values (LSD at $p < 0.05$). Significant differences between ungirdled and girdled sample pairs were determined by Student t-tests and significance levels are indicated by the following symbols: “*” = $p < 0.05$, “**” = $p < 0.01$, “***” = $p < 0.001$, “ns” = not significant, “na” = not applicable (insufficient sample numbers). Note that **(a)** is a comparison of ovary types within an age class, whereas **(b)** is a comparison of ovary types between age classes (by rearrangement).

(a)					
ovary		ungirdled		girdled	
age class	type	cell volume (μm^3)	CV (%)	cell volume (μm^3)	CV (%)
1-4	shot	12988 ^a	22.76	12966 ^{a ns}	14.42
	chick	13514 ^a	41.11	10720 ^{a ns}	42.58
	hen	na	na	na	na
5-7	shot	10845 ^a	37.18	11651 ^{a ns}	23.05
	chick	14203 ^{ab}	49.38	14847 ^{a ns}	25.26
	hen	20220 ^b	50.04	19947 ^{b ns}	41.38
8-11	shot	10734 ^a	37.14	na	na
	chick	7017 ^a	33.04	11095 ^{a *}	43.36
	hen	21761 ^b	41.95	14765 ^{a *}	37.86
12-15	shot	10023 ^a	32.14	na	na
	chick	13342 ^a	60.84	14935 ^{a ns}	49.06
	hen	15905 ^a	36.44	17596 ^{a ns}	56.67

(b)

ovary		ungirdled		girdled	
type	age class	cell volume (μm^3)	CV (%)	cell volume (μm^3)	CV (%)
shot	1-4	12988 ^a	22.76	12966 ^{a ns}	14.42
	5-7	10845 ^a	37.18	11651 ^{a ns}	23.05
	8-11	10734 ^a	37.14	na	na
	12-15	10023 ^a	32.14	na	na
chick	1-4	13514 ^b	41.11	10720 ^{a ns}	42.58
	5-7	14203 ^b	49.38	14847 ^{a ns}	25.26
	8-11	7017 ^a	33.04	11095 ^{a *}	43.36
	12-15	13342 ^b	60.84	14935 ^{a ns}	49.06
hen	1-4	na	na	na	na
	5-7	20220 ^a	50.04	19947 ^{a ns}	41.38
	8-11	21761 ^a	41.95	14765 ^{a *}	37.86
	12-15	15905 ^a	36.44	17596 ^{a ns}	56.67

volumes of “shot” ovaries ($10734 \mu\text{m}^3$) and “chicks” ($7017 \mu\text{m}^3$) were significantly less than “hens” ($21761 \mu\text{m}^3$). Typically, the order of mean cell volume was “shot” < “chick” < “hen”, but there was once again an exception at 8-11 days, when “shot” and “chick” were reversed. Across all age classes (**Table 5.1(b)**), only the “chicks” differed in mean cell volume with the value at 8-11 days ($7017 \mu\text{m}^3$) being significantly less than the other three times: $13514 \mu\text{m}^3$ (1-4 days), $14203 \mu\text{m}^3$ (5-7 days) and $13342 \mu\text{m}^3$ (12-15 days).

The girdled bunch also displayed consistent patterns of cell volume increase across the four age classes (**Figure 5.3**). Once again, there were similarities in curve shape for all three ovary types and the stepwise increases in cell volume would appear to be coordinated within an age class. Despite similarities in curve shape, differences in slope were evident. The order of slopes was “shot” < “chick” < “hen”.

Significant differences in mean cell volume were only observed at days 5-7 when the “shot” ($11651 \mu\text{m}^3$) and “chick” ($14847 \mu\text{m}^3$) values were less than the “hens” ($19947 \mu\text{m}^3$) (**Table 5.1(a)**). Typically, the order of mean cell volume was “shot” < “chick” < “hen”, but there is once again an exception at 1-4 days, when “shot” and “chick” were reversed. Unfortunately, no “shot” ovaries were present in the 8-11 day and 12-15 day sample. No significant difference in mean cell volume were evident between the “shot”, “chick” and “hen” ovaries during their first two weeks of postflowering development (**Table 5.1(b)**). Significant differences between ungirdled and girdled pairs of ovary cell volumes were identified between “chicks” at 8-11 days (ungirdled $7017 \mu\text{m}^3$, girdled $11096 \mu\text{m}^3$) and “hens” at 8-11 days (ungirdled $21761 \mu\text{m}^3$, girdled $14765 \mu\text{m}^3$).

CVs for age classes and girdling treatments do not indicate any particular trend (**Table 5.1(a)**), but it would appear that CVs for “shot” ovaries are lower than their “chick” and “hen” counterparts (**Table 5.1(b)**).

5.4.2 Berry Cell Volumes (29-43 days)

Inner mesocarp cell volumes of Chardonnay berries from an ungirdled bunch harvested at 43 days after first capfall are shown in **Figure 5.4**. The age classes are plotted separately: 29-32 days, 33-35 days, 36-39 days, 40-43 days. Two berry types from each age class were analysed (where available): “chick” and “hen”.

Inner mesocarp cell volumes of Chardonnay berries from a girdled bunch harvested at 43 days after first capfall are shown in **Figure 5.5**. The layout is the same as the previous figure where the four age classes are plotted separately and the two berry types (where available) are uniquely identified. As described previously, the cell volumes in **Figures 5.4** and **5.5** were plotted in ascending order to create a stepwise effect as cell volume increased.

Inner mesocarp cell volumes of berries from the ungyrdled bunch c(i) and the gyrdled bunch d(i) harvested at 43 days after first capfall are shown in **Table 5.2**. Mean cell volume has been calculated for two berry types (“chick” and “hen”) in four age classes (29-32 days, 33-35 days, 36-39 days, and 40-43 days). Variation in cell volume within each age class and berry type is indicated by the CV (%). Significant differences between berry types were determined by REML (LSD at $p < 0.05$). Significant differences between ungyrdled and gyrdled sample pairs were determined by Student t-tests and significance levels are indicated.

In the ungyrdled bunch, the graphs of berry cell volume from days 29 to 43 appear consistent (**Figure 5.4**). “Chick” and “hen” berries display similar patterns of cell volume increase despite differences in berry age. The two curves that represent each berry type at a particular age are similar in shape, but differ in slope (“chick” < “hen”). The timing of stepwise increases in cell volume also appears as though it may be coordinated.

Significant differences in mean cell volume (**Table 5.2(a)**) were exhibited between “chicks” and “hens” at 29-32 days ($35475 \mu\text{m}^3$, $258555 \mu\text{m}^3$) and at 33-35 days ($60894 \mu\text{m}^3$, $283055 \mu\text{m}^3$). Cells of “chicks” were frequently several-fold smaller than “hens”. Across all age classes (**Table 5.2(b)**), only the “chicks” differed in mean cell volume with the value at 36-39 days ($29590 \mu\text{m}^3$) being significantly less than the value at 40-43 days ($68751 \mu\text{m}^3$). The other two values were intermediate: $35475 \mu\text{m}^3$ (29-32 days) and $60894 \mu\text{m}^3$ (33-35 days). Note that the mean cell volumes at 43 days are often an order of magnitude greater than those sampled four weeks earlier, suggesting that a large amount of cell expansion has occurred in the meantime.

The gyrdled bunch also displayed consistent patterns of cell volume increase across the four age classes (**Figure 5.5**). Once again, there were similarities in curve shape for both berry types and the stepwise increases in cell volume would appear to be coordinated within any particular age class. Despite these similarities in curve shape, significant differences in slope were evident (exception at 33-35 days). The order of slopes was “chicks” \ll “hens”.

Significant differences in mean cell volume between “chicks” and “hens” were observed at every age class where a comparison could be made: 33-35 days ($99219 \mu\text{m}^3$ vs $162853 \mu\text{m}^3$), 36-39 days ($95269 \mu\text{m}^3$ vs $379917 \mu\text{m}^3$), and 40-43 days ($29886 \mu\text{m}^3$ vs $373002 \mu\text{m}^3$) (**Table 5.2(a)**). “Chicks” differed significantly between age classes during weeks five and six of postflowering berry development: 40-43 days ($29886 \mu\text{m}^3$) < 36-39 days ($95269 \mu\text{m}^3$) = 33-35 days ($99219 \mu\text{m}^3$) < 29-32 days ($164044 \mu\text{m}^3$) (**Table 5.2(b)**). Every statistical comparison of mean cell volume that was made between ungyrdled and gyrdled berry pairs indicated a significant difference (**Table 5.2(a)**).

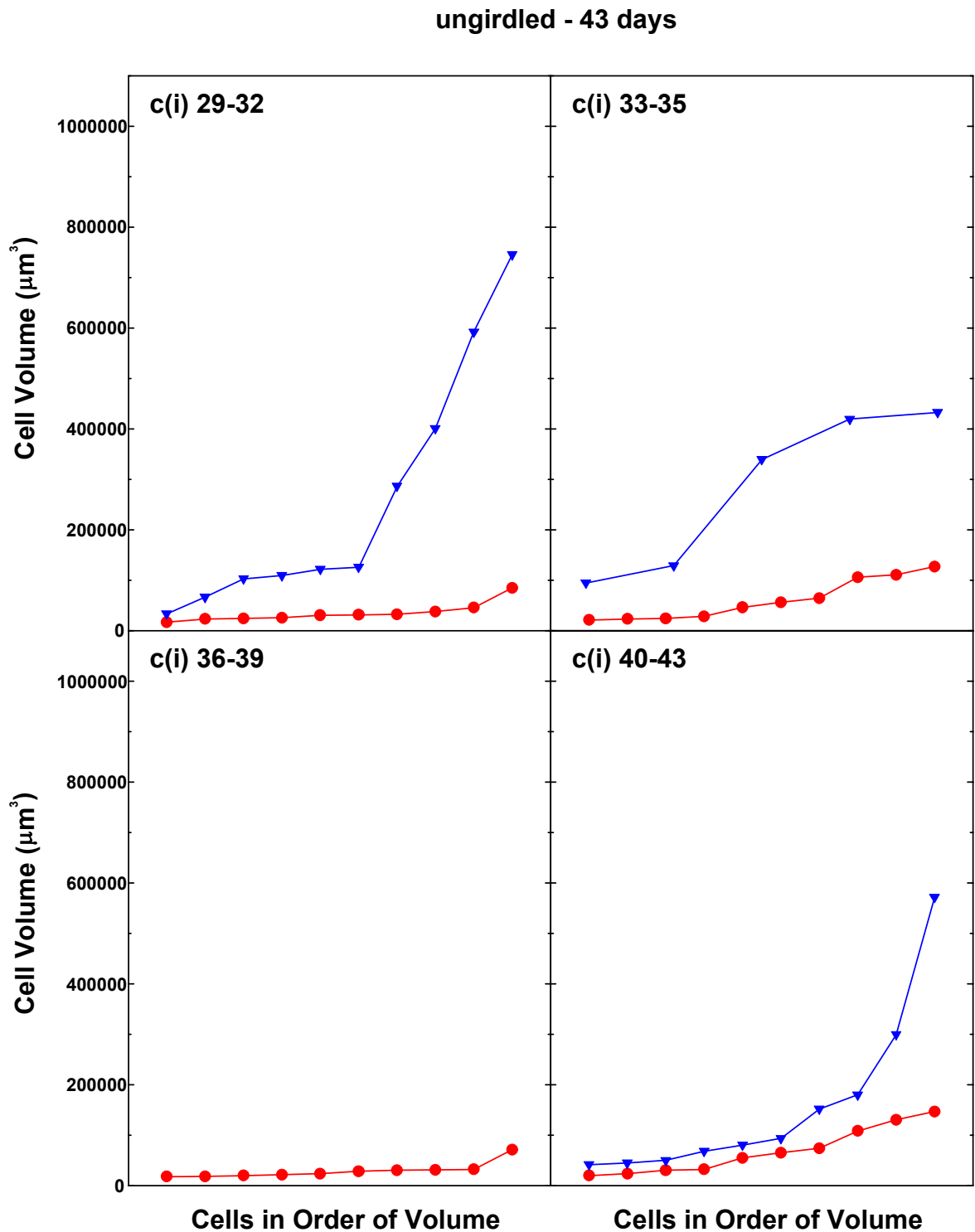


Figure 5.4 Chardonnay cell volumes (ungirdled, 29-43 days). Inner mesocarp cell volumes of berries from ungirdled bunch c(i) harvested at 43 days after first capfall. The numbers following the bunch identity indicate the age classes from within which the berries were sampled: 29-32 days, 33-35 days, 36-39 days, 40-43 days. Two berries from each age class were analysed (where available) – one “chick” (●) and one “hen” (▼).

girdled - 43 days

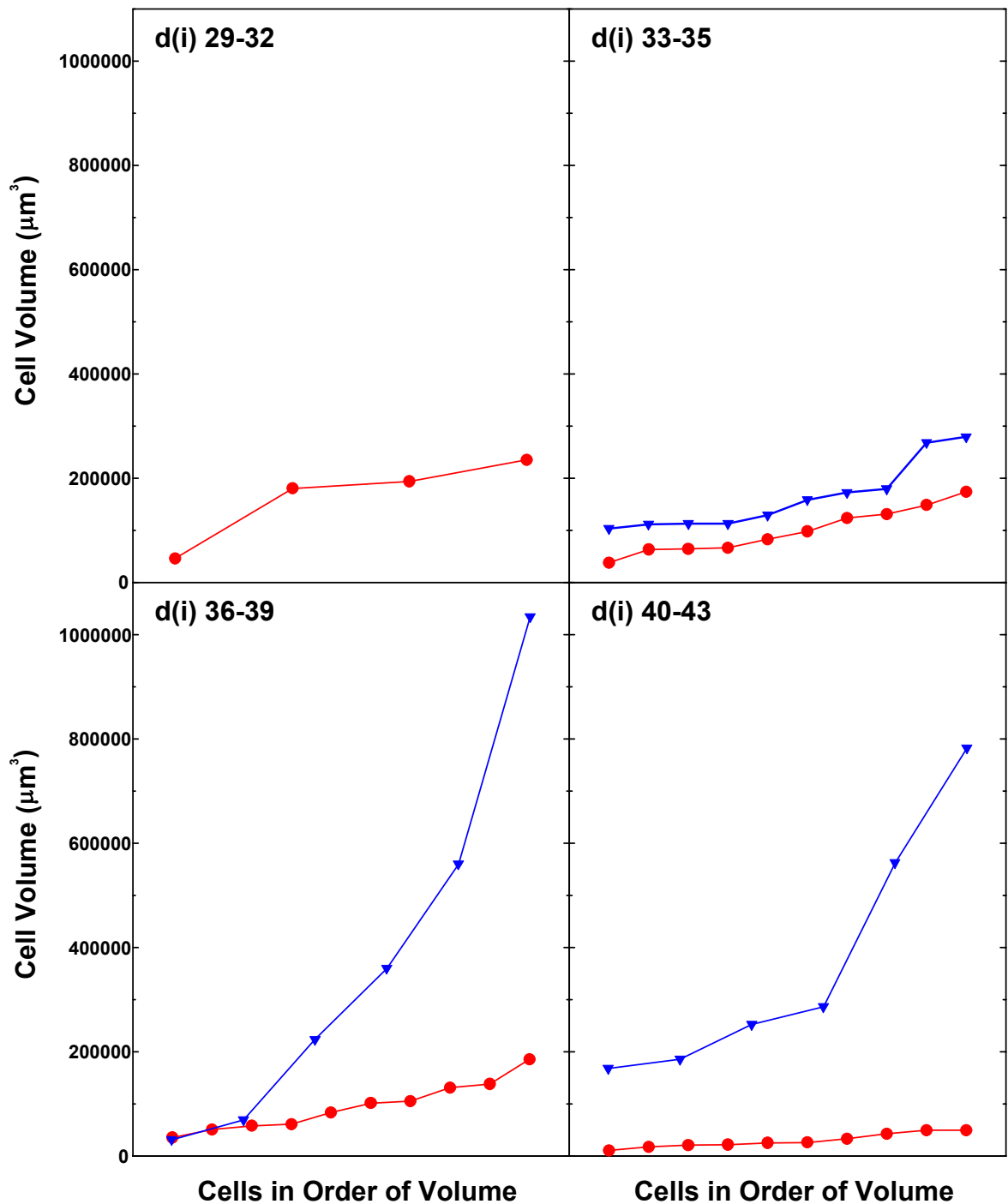


Figure 5.5 Chardonnay cell volumes (girdled, 29-43 days). Inner mesocarp cell volumes of berries from girdled bunch d(i) harvested at 43 days after first capfall. The numbers following the bunch identity indicate the age classes from within which the berries were sampled: 29-32 days, 33-35 days, 36-39 days, 40-43 days. Two berries from each age class were analysed (where available) – one “chick” (●) and one “hen” (▼).

Table 5.2 Variation in cell volume (ungirdled, 29-43 days). Inner mesocarp cell volumes of berries from ungirdled bunch c(i) and girdled bunch d(i) harvested at 43 days after first capfall. Mean cell volume has been calculated for two berry types (“chick” and “hen”) in four age classes (29-32 days, 33-35 days, 36-39 days, and 40-43 days). Variation in cell volume within each age class and berry type is indicated by the coefficient of variation (CV%). Significant differences between berry types were determined by REML and are indicated by the letters that follow the mean cell volume values (LSD at $p < 0.05$). Significant differences between ungirdled and girdled sample pairs were determined by Student *t*-tests and significance levels are indicated by the following symbols: “*” = $p < 0.05$, “**” = $p < 0.01$, “***” = $p < 0.001$, “ns” = not significant, “na” = not applicable (insufficient sample numbers). Note that **(a)** is a comparison of ovary types within an age class, whereas **(b)** is a comparison of ovary types between age classes (by rearrangement).

(a)					
berry		ungirdled		girdled	
age class	type	cell volume (μm^3)	CV (%)	cell volume (μm^3)	CV (%)
29-32	chick	35475 ^a	53.83	164044 ^{na ***}	49.99
	hen	258555 ^b	94.71	na	na
33-35	chick	60894 ^a	65.90	99219 ^{a *}	44.00
	hen	283055 ^b	56.80	162853 ^{b *}	39.56
36-39	chick	29590	52.54	95269 ^{a ***}	49.05
	hen	na	na	379917 ^{b na}	98.72
40-43	chick	68751 ^a	66.61	29886 ^{a *}	45.05
	hen	158270 ^a	104.78	373002 ^{b *}	65.96

(b)					
berry		ungirdled		girdled	
type	age class	cell volume (μm^3)	CV (%)	cell volume (μm^3)	CV (%)
chick	29-32	35475 ^{ab}	53.83	164044 ^{c ***}	49.99
	33-35	60894 ^{bc}	65.90	99219 ^{b *}	44.00
	36-39	29590 ^a	52.54	95269 ^{b ***}	49.05
	40-43	68751 ^c	66.61	29886 ^{a *}	45.05
hen	29-32	258555 ^a	94.71	na	na
	33-35	283055 ^a	56.80	162853 ^{a *}	39.56
	36-39	na	na	379917 ^{a na}	98.72
	40-43	158270 ^a	104.78	373002 ^{a *}	65.96

Table 5.3 Variation in ovary/berry cell volume and with harvest date. Mean cell volume and coefficient variation (%) for each harvest date of ovaries/berries from ungyrdled and girdled vines for the Chardonnay clone I10V1. Bunches were harvested at 15 days and at 43 days after first capfall. Each value is the mean of 40 ovaries/berries (where available). Significant differences between “shot”, “chick” and “hen” types were determined by REML and are indicated by the letters that follow the mean mass values (LSD at $p < 0.05$). Significant differences between ungyrdled and girdled sample pairs were determined by Student t-tests and significance levels are indicated by the following symbols: “*” = $p < 0.05$, “**” = $p < 0.01$, “***” = $p < 0.001$, “ns” = not significant, “na” = not applicable (insufficient sample numbers).

harvest date (ovary/berry type)	ungirdled		girdled	
	cell volume (μm^3)	CV (%)	cell volume (μm^3)	CV (%)
15 days				
shot	11148 ^a	32.46	12308 ^{a ns}	19.10
chick	12019 ^a	54.93	12899 ^{a ns}	42.37
hen	19295 ^b	44.71	17436 ^{b ns}	46.71
43 days				
chick	48678 ^a	73.36	85291 ^{a **}	69.83
hen	223341 ^b	89.70	279365 ^{b ns}	88.80

CVs for age classes and berry type do not indicate any particular trend (*Table 5.2(a), (b)*). Although girdling would appear to reduce variation in all instances, its impact is only minor.

Table 5.3 summarises the data on variation in mean cell volume at each harvest date and girdling treatment for all ovary and berry types. For ungyrdled vines, the cell volume of “shot” (11148 μm^3) and “chick” (12019 μm^3) ovaries at day 15 were significantly less than those of the “hens” (19295 μm^3). The same pattern held for girdled vines: “shot” (12308 μm^3) = “chick” (12899 μm^3) < “hen” (19295 μm^3). There were no significant pairwise differences between ungyrdled and girdled ovaries. By 43 days after capfall, cell volumes had increased for both “chicks” and “hens”, but proportionally more for the “hens”. The mean cell volumes of “chicks” and “hens” differed significantly for both ungyrdled (48678 μm^3 vs 223341 μm^3) and girdled (85291 μm^3 vs 279365 μm^3) vines. The only significant pairwise difference between ungyrdled and girdled cell volumes was between “chicks” at day 43 (ungirdled 48678 μm^3 , girdled 85291 μm^3).

CVs tended to be less at day 15 than at day 43 for all treatments. “Shot” ovaries, in particular, displayed lower CVs than either “chicks” or “hens” in the day 15 sample. The impact of girdling on the variation in cell volume is minimal.

5.5 Discussion

The objective of this chapter was to provide information to compare the relationship between fruit size (Ch. 3) and cell size (Ch.5) in a developing grape berry. The hypothesis was that variation in cell size occurs early in the postflowering period of berry development and that this variation was responsible for the subsequent macroscopic size differences observed between berries.

Few significant differences were apparent in mean cell volume in the day 15 sample. The differences were not linked to age class, but were associated with ovary type. Cell volume for the “hens” was consistently greater than that of “shot” or “chick” ovaries for both girdling treatments. CVs were lower for “shot” ovaries than for “chicks” or “hens” regardless of girdling treatment, but differences were minor.

By day 43, the differences in cell volume between “chicks” and “hens” were well established. “Hens” were several-fold larger than “chicks”, indicating different amounts of cell expansion. This scenario was common to berries from both ungirdled and girdled vines. Significant differences in cell volume between ungirdled and girdled berry pairs would suggest that girdling had increased the cell volume of “chicks”. The effect of girdling on “hens” was less predictable. No trend among CVs was evident but girdling may have resulted in a minor reduction of variation.

A comparison of the day 15 and day 43 samples indicated that cell volumes for both “chicks” and “hens” continued to increase, although this increase was proportionally greater for the “hens”. This size increase brought a concomitant increase in variation, irrespective of the girdling treatment.

Variation in mean cell volume associated with each ovary and berry type is summarised in **Table 5.4**. The impact of time on variation was not significant. CVs from samples at day 15 and day 43 were consistently high within a girdling treatment. Ovaries from ungirdled vines displayed less variation in comparison to berries from girdled vines. The lowest level of variation was associated with cells from “shot” ovaries, for both girdling treatments.

It is interesting to compare the degree of berry response in overall growth measurements due to time and girdling with the concurrent changes in variability. There is little guide to this aspect from the literature and as a first guess one might expect the degree of variation to remain the same (refer to hypothesis above). The results in these chapters suggest a different story. As illustration, **Table 5.5** shows a simplified comparison of the geometric changes in mean berry mass and mean cell volume to changes in associated coefficients of variation for the same Chardonnay berries between days 15 and 43. On ungirdled vines both berry mass and cell volume increase by about the same degree (10 to 12-

Table 5.4 Variation in cell volume throughout development. Coefficient variation (%) for each harvest date of ovaries/berries from ungirdled and girdled vines for the Chardonnay clone I10V1. Bunches were harvested at 15 days and at 43 days after first capfall. Each value is the mean of 40 ovaries/berries (where available). This is a rearrangement of data from *Table 5.3*.

ovary/berry	ungirdled CV(%)		girdled CV(%)	
	15 days	43 days	15 days	43 days
shot	32	19	-	-
chicks	55	42	73	70
hens	45	47	90	89
mean	44	36	82	80

fold). Mass is associated with the largest increase in CV (4x), but cell volume the smallest (1x). This is a clear indication of the operation of different metabolic controls of these two facets of berry growth. Thus, the hypothesis presented in the first paragraph of the Discussion is not supported. Variation in cell size remains relatively constant during early postflowering development, but variation in berry mass increases regardless.

Differences in cell number and cell volume are the root cause of variability between grapes at harvest. The developmental nature of variability was best described by Coombe (1976), when he suggested that the number and volume of cells at ripeness would be influenced by the number and volume at flowering and the rate and duration of cell division thereafter (Coombe 1976). The relationship between cell size, cell number and berry size in the grape has formed the basis of a number of scientific investigations, involving a variety of techniques. Although conventional microscopy is favoured by many researchers (Considine 1978,1981, Fougère-Rifot *et al.* 1995, 1997, Chloet *et al.* 1998), some novel methods have been employed to count and measure cells. Harris *et al.* (1968) measured cell number and cell size in Sultana (Thompson Seedless) by macerating berries and counting cells on a

Table 5.5 Geometric changes in size and variation of berry mass and cell volume. Changes in mean berry mass and mean cell volume between Chardonnay berries from ungirdled and girdled vines sampled at 15 day and 43 days after first capfall. The differences between the two harvest times are represented as approximate geometric increases from the base value at 15 days.

category	berry mass increase		cell volume increase	
	ungirdled	girdled	ungirdled	girdled
size	10x	25x	12x	15x
CV(%)	4x	2x	1x	1x

haemocytometer slide. Ojeda *et al.* (1999) indirectly determined the rate of cell division and cell enlargement in Shiraz berries by extracting and quantifying their DNA at different stages of development.

Comparison of “shot”, “chick”, and “hen” berries are scarce in the literature. In part this may be due to a lack of adequate terminology to describe these different berry types. Although “shot” and “chick” berries are both the result of *millerandage*, their development differs. Some authors differentiate between them as “small shot” and “medium shot”, but this could lead to confusion (Fougère-Rifot *et al.* 1995, Chloet *et al.* 1998). In comparison to normal berries, “chicks” develop more slowly, and they may enter veraison late, or not at all (Chloet *et al.* 1998). “Shot” berries fail to grow and enlarge at all, and remain seedless (Fougère-Rifot *et al.* 1995).

The relationship between seed development and cell size in grapes was investigated by Shiozaki *et al.* (1997). They found that the duration of cell division and the rate of cell enlargement were greater for seedless berries of Delaware in comparison to seeded berries. However, the findings of their work were inconclusive because seedlessness was induced artificially by the application of exogenous gibberellin that is known to impact on developmental processes at a cellular level (Stuart *et al.* 1977, Groot *et al.* 1987, Rebers *et al.* 1999, Yamaguchi and Kamiya 2000).

The present study indicates that cell division and cell enlargement does occur in all three berry types, but these processes are partially restricted in “chicks”, and severely restricted in “shot” berries. Preliminary observations suggest that the increase in cell volume proceeds in a stepwise manner (see 4.5.2). This might be coordinated across different berry types (“shot”, “chick” and “hen”) and ages. However, the data are limited and further investigations would be needed to confirm this finding.

The techniques used to measure cell volume are not subject to the usual limitations associated with two-dimensional microscopy, and the improvements in precision and accuracy have been established (Gray *et al.* 1999). Future development of this technique could enable precise analysis of cell division in the grape berry. Since volume of a particular berry tissue (V_r) can be estimated from Equation 5.2, and mean cell volume in a tissue region can be measured directly, and assuming there are no intercellular spaces (Nakagawa and Nanjo 1966), the mean cell number in a particular berry tissue is given by the simple ratio:

$$\text{mean cell number}_r = \frac{V_r}{\text{mean cell volume}_r} \pm \text{SE} \quad \text{Equation 5.3}$$

(refer to 5.3.2 for definitions). This procedure would be repeated for each of the concentric tissue regions. The total number of cells in the berry would be given by the sum of the

number of cells in each of those regions.

CHAPTER 6 – GENERAL DISCUSSION

6.1 Summary

This study set out to test three hypotheses that were believed to be linked to the causes of variation in grape berry size and composition:

- (i) relative levels of variation in size and composition remain constant throughout the postflowering period of berry development;
- (ii) variation in berry size is already significant in the early postflowering period of berry development;
- (iii) variation in cell size occurs in the early postflowering period of berry development and is responsible for the subsequent macroscopic size differences observed between berries.

Hypothesis (i) was disproved. Variation in berry size (mass, volume, surface area) was high throughout most of the growing period, but declined significantly as the Shiraz berries shrivelled late in the ripening stage. Conversely, variation in berry composition (flavonoid concentration, amount) was initially high, declined at softening, then increased towards ripening. Changes in physical and chemical characteristics of the berry were not paralleled by changes in variation. Berry softening and berry shrivel are pivotal events in the course of berry development where metabolic processes are in a state of flux. The reductions in variation associated with these events indicate that berry softening and berry shrivel may also be points of synchronisation, where developmental processes converge and the berries become more homogeneous (Coombe 1984). Note that a point of synchronisation for one aspect of development (e.g. berry mass at harvest) may be quite different from another (e.g. flavonoids at softening). High levels of variation in the early postflowering period suggest that variation must have been initiated at an earlier time. This places considerable importance on the impact that preflowering events may have on cell division in the floral primordia at budburst (Coombe 1973, Srinivasan and Mullins 1976, Considine and Knox 1979b).

Hypothesis (ii) was proven. Variation in berry size (mass) had already reached significant levels within the first 4 days after flower capfall. This was observed for all three Chardonnay clones examined despite their known historical differences in yield performance. Trunk girdling had no effect on variation during the first two weeks of berry growth, despite significant increases in berry mass. However, girdling markedly reduced variation during weeks 5 and 6. This reduction is likely to result from the antagonistic impacts of girdling and seed development where the increased organic nutrition arising from the girdle counteracts

the variation in hormonal stimulus to growth by the developing seed (Coombe 1959, Ebadi 1996b, Swain *et al.* 1997, Chaudhury 2001).

Hypothesis (iii) was disproved. While it was shown that variation in cell size (volume) remained relatively constant during the early postflowering period, variation in berry size (mass) continued to increase. The implication is that variation in cell size and variation in berry size are not as closely linked as was first thought. One explanation is that cell number (division) could be more important than cell size (expansion) throughout the entire period of early postflowering berry development. Earlier work was inconclusive as to which aspect was more important. It has been demonstrated that both processes occur during the first 3-4 weeks after flowering (Harris *et al.* 1968, Considine and Knox 1979a, Hardie *et al.* 1996). After 4 weeks, cell division is usually complete and the remaining growth of the berry is due to cell expansion alone. Several proponents suggested that cell volume was a better determinant of final berry size (Nakagawa and Nanjo 1965, 1966, Harris *et al.* 1968), while others opted for cell number (Considine and Knox 1979b, 1981). Asynchronous cell division was also perceived as a cause of variation (MacArthur and Butler 1938, Korn and Spalding 1973, Coombe 1976, Considine and Knox 1981). It was anticipated that the present investigation might resolve this issue. While it appears that cell divisions are synchronised in Chardonnay berries despite different developmental potential (“shot”, “chick”, “hen”), the data are limited and further investigations would be required to verify this finding.

This thesis has attempted to document a number of characteristics of berry growth (size and composition) and the variation (CV) associated with those characteristics. When CVs increased between one developmental stage and the next, this signified a loss of synchronisation (asynchronisation) among the berries (eg deformability at softening). Conversely, when CVs decreased between developmental stages, this signified a gain of synchronisation (resynchronisation) among the berries (eg malvidin, quercetin, catechin at softening; mass, volume, surface area at harvest). A similar analysis of CVs for other components of berry growth (sugars, acids, flavour compounds, secondary metabolites, amino acids, ions, etc.) might enable the concept of synchronisation to be expanded and identify additional points of developmental synchrony (homogeneity) or asynchrony (heterogeneity).

Several results through Chapters 2, 3 and 5 reinforce the general conclusion that averages of the measurements of the population tell nothing about the variation within that population. Calculation of variance permits this, but requires that all individuals be measured. This is rarely done.

Aspects of variation in winegrape yield and juice composition have been widely

explored in the literature (Strickland *et al.* 1932, Amerine and Roessler 1958b, Rankine *et al.* 1962, Naylor 2001). Studies that analyse variation at the berry level are less common (Coombe 1984, Coombe and Iland 1987, Trought and Tannock 1994). Studies that attempt to define variation at the cellular level are scarce (Harris *et al.* 1968, Considine and Knox 1979a, Fougère-Rifot *et al.* 1995, Shiozaki *et al.* 1997, Chloet *et al.* 1998). This would appear to be the first recorded study using 3D digital microscopy to analyse variation in cell volume and fruit size.

6.2 Future Directions

Preliminary measurements of cell volume on a relatively small sample size indicate the possibility that cell divisions in the first 2 weeks of berry development might be synchronised in Chardonnay, across different berry types and ages. This observation should be confirmed with a larger sample population. The technique is not exclusive to grape berries. It could be applied equally well to a model plant like *Arabidopsis thaliana*, where the genome has been mapped, and might enable researchers to determine the molecular basis of synchronous and asynchronous development.

Further development of the technique should be directed towards resolving the interplay between cell division versus cell expansion. This work has set new standards of precision and accuracy in the 3D measurement of cell volume *in situ*. This precision could be readily transferred to the analysis of cell number. Once both of these parameters have been measured it should be possible to separate their variance components at any specified time during the course of berry development. Rates and durations of cell division and expansion could be measured for different tissues (including the developing ovule). A better understanding of these processes should ultimately lead to a reduction in the incidence of viticultural problems such as *coulure* and *millerandage*, and annual fluctuations in the quantity and quality of the Australian winegrape crop could perhaps be predicted and their impact minimised.

With respect to the question of the effect of berry variability on wine quality potential, Coombe and Iland (personal communication) are promoting the view that any variation in composition between berries is negative to a maximum possible quality potential of a batch of grapes. Variation between units needs to be measured.

Although variation is apparent throughout berry development, its origins are the result of events that occur prior to Stage I of berry growth. The possibility of reducing variation during the postflowering period is limited to techniques like girdling that minimise the formation of “shot” and “chick” berries. Events that could potentially modify cell division between budburst and flowering (e.g. changes in light, temperature, irrigation and nutrition)

may have a greater impact on berry variability than was previously envisioned.

BIBLIOGRAPHY

- Abbott, N.A., Coombe, B.G. and Williams, P.J.** (1991) The contribution of hydrolyzed flavor precursors to quality differences in Shiraz juice and wines: An investigation by sensory descriptive analysis. *Am. J. Enol. Vitic.* **42**, 167-174.
- Abbott, N.A., Coombe, B.G., Sefton, M.A. and Williams, P.J.** (1990) The secondary metabolites of Shiraz grapes as an index of table wine quality. *In* Williams, P.J., Davidson, D.M. and Lee, T.H. (eds.) Proceedings of the seventh Australian wine industry technical conference. South Australia: Winetitles. pp. 117-120.
- Allen, M.S. and Lacey, M.J.** (1992) Methoxypyrazine grape flavour components: influence of grape cultivar. *In* Stockley, C.S., Johnstone, R.S., Leske, P.A. and Lee, T.H. (eds.) Proceedings of the eighth Australian wine industry technical conference. South Australia: Winetitles, pp. 195.
- Amerine, M.A.** (1956) Maturation of wine grapes. *Wines and Vines* **37**, 27-32.
- Amerine, M.A. and Roessler, E.B.** (1958a) Field testing of grape maturity. *Hilgardia* **28**, 93-114.
- Amerine, M.A. and Roessler, E.B.** (1958b) Methods of determining field maturity of grapes. *Am. J. Enol. Vitic.* **9**, 37-40.
- Amerine, M.A. and Roessler, E.B.** (1976) *Wines: their sensory evaluation*. San Francisco: W.H. Freeman and Co..
- Anon.** (1994a) *Viticulture Australia — 1993-94*. Australian Bureau of Statistics, Cat. No. 7310.0.
- Anon.** (1994b) *Wine production, Australia and States — 1993-94*. Australian Bureau of Statistics, Cat. No. 8366.0
- Asenstorfer, R.E.** (2001) Isolation, structures and properties of anthocyanins and wine pigments. Ph.D. Thesis, The University of Adelaide, Australia.
- Baker, G.A., Amerine, M.A. and Roessler, E.B.** (1965) Characteristics of sequential measurements on grape juice and must. *Am. J. Enol. Vitic.* **16**, 21-28.
- Barritt, B.H.** (1970) Ovule development in seeded and seedless grapes. *Vitis* **9**, 7-14.
- Bearder, J.R.** (1980) Plant Hormones and Other Growth Substances — Their Background, Structures and Occurrence. Chapter 1. *In* MacMillan, J. (ed.). *Hormonal Regulation of Development. I. Molecular Aspects of Plant Hormones*. Encyclopedia of Plant Physiology. Vol. 9. Berlin: Springer-Verlag.
- Becker, D.L., Dekkers, J.H., Navarrette, R., Green, C.R. and Cook, J.E.** (1991) Enhancing the laser scanning confocal microscopic visualisation of lucifer yellow filled cells in whole-mounted tissue. *Scanning Microsc.* **5**, 619-624.
- Bernard, A.C.** (1977) Observations histologiques sur les baies de *Vitis vinifera* au cours de leur croissance. Extrait de la France Viticole des numéros de 5, 6, 7.
- Bethke, P.C., Gilroy, S. and Jones, R.L.** (1995) Calcium and Plant Hormone Action. Chapter D5. *In* Davies, P.J. (ed.) *Plant Hormones: Physiology, Biochemistry and Molecular Biology*. Dordrecht: Kluwer Academic Publishers.
- Biale, J.B.** (1964) Growth, maturation, and senescence in fruits. *Science* **146**, 880-888.
- Blackmann, V.H.** (1919) The compound interest law and plant growth. *Ann. Bot.* **33**, 353-360.
- Bollard, E.G.** (1970) The Physiology and Nutrition of Developing Fruits. Chapter 14. *In* Hulme, A.C. (ed.) *The Biochemistry of Fruits and their Products*, Vol. 1. London: Academic.
- Boulton, R.** (1980a) The general relationship between potassium, sodium and pH in grape juice and wine. *Am. J. Enol. Vitic.* **31**, 182-186.
- Boulton, R.** (1980b) The relationship between total acidity, titratable acidity and pH in grape tissue. *Vitis* **19**, 113-120.

- Bron, Cph., Gremillet, Ph., Launay, D., Jourlin, M., Gautschi, H.P., Bächli, Th. and Schüpbach, J.** (1990) Three-dimensional electron microscopy of entire cells. *J. Microsc.* **157**, 115-126.
- Brown, R. and Rickless, P.** (1949) A new method for the study of cell division and cell extension with some preliminary observations on the effect of temperature and of nutrients. *Proc. Roy. Soc. B.* **136**, 110-125.
- Bryant, J.A.** (1976) The Cell Cycle. *In* Bryant, J.A. (ed.) *Molecular Aspects of Gene Expression in Plants*. London: Academic Press.
- Carlsson, K.** (1991) The influence of specimen refractive index, detector signal integration, and non-uniform scan speed on the imaging properties in confocal microscopy. *J. Microsc.* **163**, 167-178.
- Carlsson, K., Danielsson, P.E., Lenz, R., Liljeborg, A., Majlöf, L. and Åslund, N.** (1985) Three-dimensional microscopy using a confocal laser scanning microscope. *Opt. Lett.* **10**, 53-55.
- Caspari, H.W., Lang, A. and Alspach, P.** (1998) Effects of girdling and leaf removal on fruit set and vegetative growth in grape. *Am. J. Enol. Vitic.* **49**, 359-366.
- Chaudhury, A.M., Koltunow, A., Payne, T., Luo, M., Tucker, M.R., Dennis, E.S. and Peacock, W.J.** (2001) Control of early seed development. *Annu. Rev. Cell Dev. Biol.* **17**, 677-699.
- Cirami, R.M., Cameron, I.J. and Hedberg, P.R.** (1992) Special Cultural Methods for Tablegrapes. Chapter 12. *In* Coombe, B.G. and Dry, P.R. (eds.) *Viticulture*. Vol. 2. Practices. Adelaide: Winetitles.
- Clark, G.** (ed.) (1981) *Staining Procedures*. (4th ed.) London: Williams and Wilkins.
- Cholet, C., Fougère-Rifot, M. and Bouard, J.** (1998) Particularités cellulaires des baies millerandées de taille moyenne de *Vitis vinifera* L. var. Merlot. *J. Int. Sci. Vigne Vin* **32**, 193-201.
- Considine, J.A.** (1969) Aspects of the hormonal physiology of fruit development in *Vitis vinifera* L. M.Ag.Sc. Thesis, University of Adelaide.
- Considine, J.A.** (1978) Stereology of the dermal system of fruit. *J. Microsc.* **113**, 61-68.
- Considine, J.A.** (1981) Stereological analysis of the dermal system of the fruit of the grape *Vitis vinifera* L. *Aust. J. Bot.* **29**, 463-474.
- Considine, J.A.** (1983) Concepts and practice of use of plant growth regulating chemicals in viticulture. *In* Nickell, L.G. (ed.) *Use of Plant Growth Regulators in Agriculture*. Boca Raton: CRC Press. pp. 89-183.
- Considine, J.A. and Knox, R.B.** (1979a) Development and histochemistry of the cells, cell walls, and cuticle of the dermal system of the fruit of the grape, *Vitis vinifera*. *Protoplasma* **99**, 347-365.
- Considine, J.A. and Knox, R.B.** (1979b) Development and histochemistry of the pistil of the grape, *Vitis vinifera*. *Ann. Bot.* **43**, 11-22.
- Considine, J.A. and Knox, R.B.** (1981) Tissue origins, cell lineages and patterns of cell division in the developing dermal system of the fruit of *Vitis vinifera* L. *Planta* **151**, 403-412.
- Coombe, B.G.** (1959) Fruit set and development in seeded grape varieties as affected by defoliation, topping, girdling, and other treatments. *Am. J. Enol. Vitic.* **10**, 85-100.
- Coombe, B.G.** (1960) Relationship of growth and development to changes in sugars, auxins, and gibberellins in fruit of seeded and seedless varieties of *Vitis vinifera*. *Plant Physiol.* **35**, 241-250.
- Coombe, B.G.** (1962) The effect of removing leaves, flowers and shoot tips on fruit set in *Vitis vinifera* L. *J. Hort. Sci.* **37**, 1-15.
- Coombe, B.G.** (1973) The regulation of set and development of the grape berry. *Acta Hort.* **34**, 261-273.
- Coombe, B.G.** (1975) Development and maturation of the grape berry. *Aust Grapegr. Winemaker* **136**, 60,66.

- Coombe, B.G.** (1976) The development of fleshy fruits. *Ann. Rev. Plant Physiol.* **27**, 207-228.
- Coombe, B.G.** (1980) Development of the grape berry. I Effects of time of flowering and competition. *Aust. J. Agric. Res.* **31**, 125-131.
- Coombe, B.G.** (1984) The inception of ripening in the grape berry. *Quad. Vitic. Enol. Univ. Torino* **8**, 87-99.
- Coombe, B.G.** (1987a) Distribution of solutes within the developing grape berry in relation to its morphology. *Am. J. Enol. Vitic.* **38**, 120-127.
- Coombe, B.G.** (1987b) Influence of temperature on composition and quality of grapes. *Acta Hort.* **206**, 23-36.
- Coombe, B.G.** (1989a) Fruit setting, development and ripening. *Acta Hort.* **240**, 209-216.
- Coombe, B.G.** (1989b) The grape berry as a sink. *Acta Hort.* **239**, 149-158.
- Coombe, B.G.** (1992) Research on the development and ripening of the grape berry. *Am. J. Enol. Vitic.* **43**, 101-110.
- Coombe, B.G.** (1995) Adoption of a system of identifying grapevine growth stages. *Aust. J. Grape Wine Res.* **2**, 104-110.
- Coombe, B.G. and Bishop, G.R.** (1980) Development of the grape berry. II. Changes in diameter and deformability during veraison. *Aust. J. agric. Res.* **31**, 499-509.
- Coombe, B.G. and Dry, P.R.** (eds.) (1992) *Viticulture. Vol. 2. Practices.* Adelaide: Winetitles.
- Coombe, B.G. and Hale, C.R.** (1973) The hormone content of ripening grape berries and the effects of growth substance treatments. *Plant Physiol.* **51**, 629-634.
- Coombe, B.G. and Iland, P.** (1987) Grape berry development. *In* Lee, T. (ed.) *Proceedings of the sixth Australian wine industry technical conference.* Adelaide: Australian Industrial Publishers. pp. 50-54.
- Coombe, B.G. and McCarthy, M.G.** (2000) Dynamics of grape berry growth and physiology of ripening. *Aust. J. Grape Wine Res.* **6**, 131-135.
- Coombe, B.G. and Matile, P.** (1980) Solute accumulation by grape pericarp cells. I. Sugar uptake by skin segments. *Biochem. Physiol. Pflanzen* **175**, 369-381.
- Cormier, F., Crevier, H. and Do, C.B.** (1990) Effects of sucrose concentration on the accumulation of anthocyanins in grape (*Vitis vinifera*) cell suspension. *Can. J. Bot.* **68**, 1822-1825.
- Cowen, T., Haven, A.J. and Burnstock, G.** (1985) Pontamine sky blue: a counterstain for background autofluorescence in fluorescence and immunofluorescence histochemistry. *Histochem.* **82**, 205-208.
- Crane, J.C.** (1969) The role of hormones in fruit set and development. *HortSci.* **4**, 108-111.
- Crippen, D.D., Jr. and Morrison, J.C.** (1986a) The effects of sun exposure on the compositional development of Cabernet Sauvignon berries. *Am. J. Enol. Vitic.* **37**, 235-242.
- Crippen, D.D., Jr. and Morrison, J.C.** (1986b) The effects of sun exposure on the phenolic content of Cabernet Sauvignon berries during development. *Am. J. Enol. Vitic.* **37**, 243-247.
- Cruz-Orive, L.M.** (1997) Stereology of single objects. *J. Microsc.* **186**, 93-107.
- Darné, G.** (1993) Nouvelles hypothèses sur la synthèse des anthocyanes dans les baies et dans les feuilles de vigne. *Vitis* **32**, 77-85.
- Davies, C., Boss, P.K. and Robinson, S.P.** (1997) Treatment of grape berries, a nonclimacteric fruit with a synthetic auxin, retards ripening and alters the expression of developmentally regulated genes. *Plant Physiol.* **115**, 1155-1161.
- Davies, P.J.** (ed.) (1995a) *Plant Hormones: Physiology, Biochemistry and Molecular Biology.* Dordrecht: Kluwer Academic Publishers.
- Davies, P.J.** (1995b) The Plant Hormones: Their Nature, Occurrence and Functions. Chapter A1. *In* Davies, P.J. (ed.) *Plant Hormones: Physiology, Biochemistry and Molecular Biology.* Dordrecht: Kluwer Academic Publishers.

- de la Landa, I.S. and Waterson, J.G.** (1968) Modification of autofluorescence in the formaldehyde-treated rabbit ear artery by Evans blue. *J. Histochem. and Cytochem.* **16**, 281-282.
- Dfield** (1994) Version 2.0. Minnesota Datametrics Corporation, USA.
- Dixon, A.E., Damaskinos, S. and Atkinson, M.R.** (1991) A scanning confocal microscope for transmission and reflection imaging. *Nature* **351**, 551-553.
- Do, C.B. and Cormier, F.** (1990) Accumulation of anthocyanins enhanced by a high osmotic potential in grape (*Vitis vinifera* L.) cell suspensions. *Plant Cell Reports* **9**, 143-146.
- Dunn, G.M. and Martin, S.R.** (2000) Do temperature conditions at budburst affect flower number in *Vitis vinifera* L. cv. Cabernet Sauvignon? *Aust. J. Grape Wine Res.* **6**, 116-124.
- Du Plessis, C.S.** (1984) Optimum maturity and quality parameters in grapes: a review. *S. Afr. J. Enol. Vitic.* **5**, 35-42.
- Du Plessis, C.S. and Van Rooyen, P.C.** (1982) Grape maturity and wine quality. *S. Afr. J. Enol. Vitic.* **3**, 41-45.
- Ebadi, A., Coombe, B.G. and May, P.** (1995a) Fruit-set on small Chardonnay and Shiraz vines grown under varying temperature regimes between budburst and flowering. *Aust. J. Grape Wine Res.* **1**, 3-10.
- Ebadi, A., May, P., Sedgley, M. and Coombe, B.G.** (1995b) Effect of low temperature near flowering time on ovule development and pollen tube growth in the grapevine (*Vitis vinifera* L.), cvs Chardonnay and Shiraz. *Aust. J. Grape Wine Res.* **1**, 11-18.
- Ebadi, A., May, P. and Coombe, B.G.** (1996a) Effect of short-term temperature and shading on fruit-set, seed and berry development in model vines on *V. vinifera*, cvs Chardonnay and Shiraz. *Aust. J. Grape Wine Res.* **2**, 2-9.
- Ebadi, A., Sedgley, M., May, P. and Coombe, B.G.** (1996b) Seed development and abortion in *Vitis vinifera* L., cv. Chardonnay. *Int. J. Plant Sci.* **157**, 703-712.
- Esau, K.** (1977) *Anatomy of Seed Plants*. New York: John Wiley and Sons.
- Eschenbruch, R., Smart, R.E., Fisher, B.M. and Whittles, J.G.** (1987) Influence of yield manipulation on the terpene content of juices and wines of Müller Thurgau. *In* Lee, T. (ed.) *Proceedings of the sixth Australian wine industry technical conference*. Adelaide: Australian Industrial Publishers. pp. 89-93.
- Etiévant, P.** (1991) Wine. Chapter 10. *In* Maarse, H. (ed.) *Volatile Compounds in Foods and Beverages*. New York: Marcel Dekker Inc..
- Evans, M.L.** (1984) Functions of Hormones at the Cellular Level of Organization. Chapter 2. *In* Scott, T.K. (ed.) *Hormonal Regulation of Development. II. The Functions of Hormones from the Level of the Cell to the Whole Plant*. *Encyclopedia of Plant Physiology*. Vol. 10. Berlin: Springer-Verlag.
- Ewart, A.J.W and Brien, C.J.** (1986) Sensory evaluation, an art or a science? *Aust. Grapegr. Winemaker.* **268**, 45-46.
- Falco, M.R. and de Vries, J.X.** (1964) Isolation of hyperoside from the flowers of *Acacia melanoxylon*. *Naturwiss.* **51**, 462-463.
- Feder, N. and O'Brien, T.P.** (1968) Plant microtechnique: some principles and new methods. *Am. J. Bot.* **55**, 123-142.
- Fernández-López, J.A., Hidalgo, V., Almela, L. and López Roca, J.M.** (1992) Quantitative changes in anthocyanin pigments of *Vitis vinifera* cv Monastrell during maturation. *J. Sci. Food Agric.* **58**, 153-155.
- Ford, C.M. and Høj, P.B.** (1998) Multiple glucosyltransferase activities in the grapevine *Vitis vinifera* L. *Aust. J. Grape Wine Res.* **4**, 48-58.
- Fougère-Rifot, M., Benharbit el Alami, N., Brun, O. and Bouard, J.** (1993) Relations entre le développement défectueux des ovaires et l'involution des ovules chez *Vitis vinifera* L. var. Chardonnay. *J. Int. Sci. Vigne Vin* **27**, 99-112.

- Fougère-Rifot, M., Park, H.S. and Bouard, J.** (1995) Données nouvelles sur l'hypoderme et la pulpe des baies normales et des baies millerandées d'une variété de *Vitis vinifera* L., le Merlot noir. *Vitis* **34**, 1-7.
- Fougère-Rifot, M., Park, H.S. and Bouard, J.** (1997) Ontogenèse du péricarpe de la baie de *Vitis vinifera* L. var Merlot de la fécondation à la maturité. *J. Int. Sci. Vigne Vin* **31**, 109-118.
- Francis, D. and Sorrell, D.A.** (2001) The interface between the cell cycle and plant growth regulators: a mini review. *Plant Growth Regulation* **33**, 1-12.
- Francis, I.L.** (1994) The role of glycosidically-bound volatile compounds in white wine flavour. Ph.D. Thesis. University of Adelaide, Australia.
- Frear, D.S.** (1976) Pesticide conjugates-glycosides. *In* Kaufman, D.D. (ed.) American Chemical Symposium Series **29**, 35-54.
- Freeman, B.M.** (1983) Effects of irrigation and pruning of Shiraz grapevines on subsequent red wine pigments. *Am. J. Enol. Vitic.* **34**, 23-26.
- Genstat 5 Committee.** (1987a) Genstat 5 Reference manual. Oxford: Clarendon Press.
- Genstat 5 Committee.** (1987b) Genstat 5 Reference manual. Variance Component Estimation. Chapter 13. Oxford: Clarendon Press.
- Gerrath, J.M.** (1991) Developmental morphology and anatomy of grape flowers. *Hortic. Rev.* **13**, 315-337.
- Gholami, M. and Coombe, B.G.** (1995) Occurrence of anthocyanin pigments in berries of the white cultivar Muscat Gordo Blanco (*Vitis vinifera* L.). *Aust. J. Grape Wine Res.* **1**, 67-70.
- Gholami, M., Hayasaka, Y., Coombe, B.G., Jackson, J.F., Robinson, S.P. and Williams, P.J.** (1995) Biosynthesis of flavour compounds in Muscat Gordo Blanco grape berries. *Aust. J. Grape Wine Res.* **1**, 19-24.
- Goodwin, R.H.** (1953) Fluorescent substances in plants. *Ann. Rev. Plant Physiol.* **4**, 283-304.
- Grams/32** (1996) Spectral Notebase 4.01a. Galactic Industries Corporation, USA.
- Gray, J.D., Gibson, R.J., Coombe, B.G., Giles, L.C. and Hancock, T.W.** (1994) Assessment of winegrape quality in the vineyard — a preliminary, commercial survey. *Aust. N.Z. Wine Ind. J.* **9**, 253-261.
- Gray, J.D., Gibson, R.J., Coombe, B.G., Iland, P.G. and Pattison, S.J.** (1997) Assessment of winegrape value in the vineyard — survey of cv. Shiraz from South Australian vineyards 1992. *Aust. J. Grape Wine Res.* **3**, 109-117.
- Gray, J.D., Kolesik, P., Coombe, B.G. and Høj, P.B.** (1999) Confocal measurement of the three-dimensional size and shape of plant parenchyma cells in a developing fruit tissue. *Plant J* **19**, 229-236.
- Groot, S.P.C., Bruinsma, J. and Karsen, C.M.** (1987) The role of endogenous gibberellin in seed and fruit development of tomato: studies with a gibberellin-deficient mutant. *Physiol. Plant.* **71**, 184-190.
- Guilak, F.** (1994) Volume and surface area measurement of viable chondrocytes *in situ* using geometric modelling of serial confocal sections. *J. Microsc.* **173**, 245-256.
- Gustafson, F.G.** (1936) Inducement of fruit development by growth-promoting chemicals. *Proc. natn. Acad. Sci., U.S.A.* **22**, 628-636.
- Gutiérrez-Granda, M. and Morrison, J.C.** (1992) Solute distribution and malic enzyme activity in developing grape berries. *Am. J. Enol. Vitic.* **43**, 323-328.
- Hale, C.R.** (1968) Growth and senescence of the grape berry. *Aust. J. Agric. Res.* **19**, 939-945.
- Hale, C.R.** (1977) Relation between potassium and the malate and tartrate contents of grape berries. *Vitis* **16**, 9-19.
- Hale, C.R. and Coombe, B.G.** (1974) Abscisic acid: an affect on the onset of ripening of grapes (*Vitis vinifera* L.). *In* Mechanisms of Regulation of Plant Growth. Bull. 12, Royal Society of New Zealand. pp. 831-836.

- Hamilton, R.P. and Coombe, B.G.** (1992) Harvesting of Winegrapes. Chapter 13. In Coombe, B.G. and Dry, P.R. (eds.) *Viticulture*. Vol. 2. Practices. Adelaide: Winetitles.
- Hardie, W.J.** (1992) Aspects of the development of the grape pericarp in relation to its biological function and secondary metabolism. Ph.D. Thesis. Monash University, Australia.
- Hardie, W.J. and Aggenbach, S.J.** (1996) Effects of site, season and viticultural practices on grape seed development. *Aust. J. Grape Wine Res.* **2**, 21-24.
- Hardie, W.J., O'Brien, T.P. and Jaudzems, V.G.** (1996) Morphology, anatomy and development of the pericarp after anthesis in grape, *Vitis vinifera* L. *Aust. J. Grape Wine Res.* **2**, 97-142.
- Harris, J.M., Kriedemann, P.E. and Possingham, J.V.** (1968) Anatomical aspects of grape berry development. *Vitis* **7**, 106-119.
- Hassall, K.A.** (1990) *The Biochemistry and Uses of Pesticides: Structure, Metabolism, Mode of Action and Uses in Crop Protection*. (2nd ed.) New York. pp. 536.
- Hawker, J.S.** (1969a) Changes in the activities of enzymes associated with sugar metabolism during the development of grape berries. *Phytochem.* **8**, 9-17.
- Hawker, J.S.** (1969b) Changes in the activities of malic enzyme, malate dehydrogenase, phosphopyruvate carboxylase and pyruvate decarboxylase during the development of a non-climacteric fruit (the grape). *Phytochem.* **8**, 19-23.
- Hell, S., Reiner, G., Cremer, C. and Stelzer, E.H.K.** (1993) Aberrations in confocal fluorescence microscopy induced by mismatches in refractive index. *J. Microsc.* **169**, 391-405.
- Hering, T.F. and Nicholson, P.B.** (1964) A clearing technique for the examination of fungi in plant tissue. *Nature* **201**, 942-943.
- Herr, J.M., Jr.** (1971) A new clearing-squash technique for the study of ovule development in angiosperms. *Am. J. Bot.* **58**, 785-790.
- Herr, J.M., Jr.** (1982) An analysis of methods for permanently mounting ovules cleared in four-and-a-half type clearing fluids. *Stain Tech.* **57**, 161-169.
- Houghtaling, H.B.** (1935) A developmental analysis of size and shape in tomato fruits. *Bull. Torrey Bot. Club* **62**, 243-253.
- Huglin, P.** (1986) *Biologie et Écologie de la Vigne*. Paris: Payot Lausanne.
- Hulme, A.C.** (ed.) (1970) *The Biochemistry of Fruits and their Products*, Vol. 1. London: Academic.
- Hulme, A.C.** (ed.) (1971) *The Biochemistry of Fruits and their Products*, Vol. 2. London: Academic.
- Hunt, R.** (1982) *Plant Growth Curves: The Functional Approach to Plant Growth Analysis*. London: Edward Arnold.
- Huxley, J.S. and Teissier, G.** (1936) Terminology of relative growth. *Nature* **137**, 780-781.
- Iland, P., Ewart, A. and Sitters, J.** (1993) *Techniques for Chemical Analysis and Stability Tests of Grape Juice and Wine*. Adelaide: Kitchener Press.
- Iland, P.G.** (1984) Studies on the composition of pulp and skin of ripening grape berries. M.Ag.Sc. Thesis. University of Adelaide, Australia.
- Iland, P.G.** (1987) Interpretation of acidity parameters in grapes and wine. *Aust. Grapegr. Winemaker* **280**, 81-85.
- Iland, P.G. and Coombe, B.G.** (1988) Malate, tartrate, potassium and sodium in flesh and skin of Shiraz grapes during ripening: concentration and compartmentation. *Am. J. Enol. Vitic.* **39**, 71-76.
- ImageVolumes.** (1994) Version 2.0. Minnesota Datametrics Corporation, St. Paul, Minnesota.
- Jackson, D.I. and Coombe, B.G.** (1966a) Gibberellin-like substances in the developing apricot fruit. *Science* **154**, 277-278.

- Jackson, D.I. and Coombe, B.G.** (1966b) The growth of apricot fruit. I. Morphological changes during development and the effects of various tree factors. *Aust. J. Agric. Res.* **17**, 465-477.
- Jaquinet, A., Domahidy, M. and Aerny, J.** (1982) Le Chasselas millerandé – evolution quantitative et qualitative au cours de la maturation. *Revue suisse Vitic. Arboric. Hortic.* **14**, 163-168.
- Kasimatis, A.N. and Vilas, E.P.** (1985) Sampling for degrees Brix in vineyard plots. *Am. J. Enol. Vitic.* **36**, 207-213.
- Kasimatis, A.N., Vilas, E.P., Jr., Swanson, F.H. and Baranek, P.P.** (1975) A study of the variability of 'Thompson Seedless' berries for soluble solids and weight. *Am. J. Enol. Vitic.* **25**, 37-42.
- Kelvin, Lord.** (1887) On the division of space with minimum partitional area. *Phil. Mag.* **24**, 503-514.
- Kennedy, J.A., Troup, G.J., Pilbrow, J.R., Hutton, D.R., Hewitt, D., Hunter, C.R., Ristic, R., Iland, P.G. and Jones, G.P.** (2000) Development of seed polyphenols in berries from *Vitis vinifera* L. cv. Shiraz. *Aust. J. Grape Wine Res.* **6**, 244-254.
- Kleczkowski, K. and Schell, J.** (1995) Phytohormone conjugates: nature and function. *Crit. Rev. Plant Sci.* **14**, 283-298.
- Kliwer, W.M.** (1964) Influence of environment on metabolism of organic acids and carbohydrates in *Vitis vinifera*. I. Temperature. *Plant Physiol.* **39**, 869-880.
- Kliwer, W.M.** (1965a) Changes in concentration of glucose, fructose, and total soluble solids in flowers and berries of *Vitis vinifera*. *Am. J. Enol. Vitic.* **16**, 101-110.
- Kliwer, W.M.** (1965b) Changes in the concentration of malates, tartrates, and total free acids in flowers and berries of *Vitis vinifera*. *Am. J. Enol. Vitic.* **16**, 92-100.
- Kliwer, W.M.** (1965c) The sugars of grapevines. II. Identification and seasonal changes in the concentration of several trace sugars in *Vitis vinifera*. *Am. J. Enol. Vitic.* **16**, 168-178.
- Kliwer, W.M.** (1971) Effect of day temperature and light intensity on concentration of malic and tartaric acid in *Vitis vinifera* L. grapes. *J. Amer. Soc. Hort. Sci.* **96**, 372-377.
- Kliwer, W.M.** (1981) Grapevine physiology. How does a grapevine make sugar? Leaflet 21231, Div. Agric. Sci., University of California.
- Knoblauch, M. and van Bel, A.J.E.** (1998) Sieve tubes in action. *Plant Cell* **10**, 35-50.
- Koblet, W.** (1966) Fruchtansatz bei Reben in Abhängigkeit von Triebbehandlung und Klimafaktoren. Thèse E.T.H. Zürich.
- Korn, R.W.** (1974) The three-dimensional shape of plant cells and its relationship to pattern of tissue growth. *New Phytol.* **73**, 927-935.
- Korn, R.W. and Spalding, R.M.** (1973) The geometry of plant epidermal cells. *New Phytol.* **72**, 1357-1365.
- Krause, G.H. and Weis, E.** (1991) Chlorophyll fluorescence and photosynthesis: the basics. *Annu. Rev. Plant Physiol. Plant Mol. Biol.* **42**, 313-349.
- Lambry, M.** (1817) Exposé d'un moyen mis en pratique pour empêcher la vigne de couler et hâter la maturité du raisin. 2d. ed. Paris, Imprimerie Labrairie Madame Huzard. *In* Winkler, A.J. 1974. *General Viticulture*. (2nd ed.) Berkeley: University of California Press.
- Lavee, S. and Nir, G.** (1986) Grape. *In* Monselise, S.P. (ed.) *Handbook of Fruit Set and Development*. Boca Rouge: C.R.C. Press.
- Ledbetter, C.A. and Ramming, D.W.** (1989) Seedlessness in grapes. *Hort. Rev.* **11**, 159-184.
- Ledbetter, C.A. and Shonnard, C.B.** (1990) Improved seed development and germination of stenospermic grapes by plant growth regulators. *J. Hort. Sci.* **65**, 269-274.
- Ledbetter, C.A. and Shonnard, C.B.** (1991) Berry and seed characteristics associated with stenospermy in vinifera grapes. *J. Hort. Sci.* **66**, 247-252.
- Letham, D.S.** (1973) Cytokinins from *Zea mays*. *Phytochemistry* **12**, 2445-2455.

- Lewis, F.T.** (1926) The effect of cell division on the shape and size of hexagonal cells. *Anat. Rec.* **33**, 331-355.
- Lorensen, W.E. and Cline, H.E.** (1987) Marching cubes: a high resolution 3D surface construction algorithm. *Comp. Graphics* **21**, 163-169.
- Lorenz, D.H., Eichhorn, K.W., Bleiholder, H., Klose, R., Meier, U. and Weber, E.** 1994. Phänologische Entwicklungsstadien der Weinrebe (*Vitis vinifera* L. ssp. *vinifera*) – Codierung und Beschreibung nach der erweiterten BBCH-Skala. *Die Weinwissenschaft* **49**, 66-70.
- MacArthur, J.W. and Butler, L.** (1938) Size inheritance and geometric growth processes in the tomato fruit. *Genetics* **23**, 253-268.
- MacMillan, J. and Takahashi, N.** (1968) Proposed procedure for the allocation of trivial names to the gibberellins. *Nature* **217**, 170-171.
- Marais, J.** (1983) Terpenes in the aroma of grapes and wines: a review. *S. Afr. J. Enol. Vitic.* **36**, 230-239.
- Matthews, M.A. and Anderson, M.M.** (1988) Fruit ripening in *Vitis vinifera* L.: Responses to seasonal water deficits. *Am. J. Enol. Vitic.* **39**, 313-320.
- Matthysse, A.G. and Scott, T.K.** (1984) Functions of Hormones at the Whole Plant Level of Organisation. Chapter 6. In Scott, T.K. (ed.) *Hormonal Regulation of Development. II. The Functions of Hormones from the Level of the Cell to the Whole Plant.* Encyclopedia of Plant Physiology. Vol. 10. Berlin: Springer-Verlag.
- Matzke, E.B.** (1948) The three-dimensional shape of epidermal cells of the apical meristem of *Anacharis densa* (Elodea) *Am. J. Bot.* **35**, 323-332.
- Matzke, E.B. and Duffy, R.M.** (1956) Progressive three-dimensional shape changes of dividing cells within the apical meristem of *Anacharis densa*. *Am. J. Bot.* **43**, 205-225.
- May, P.** (1970) Physiological and horticultural aspects of flowering and fruit set. *Proc. 18th International Horticultural Congress*, Vol. 4. pp. 211-221.
- May, P.** (1972) Forecasting the grape crop. *Aust. Wine, Brew. Spirit Rev.* **90**, 46,48.
- May, P.** (1987) The grapevine as a perennial, plastic and productive plant. In Lee, T. (ed.) *Proceedings of the sixth Australian wine industry technical conference.* Adelaide: Australian Industrial Publishers. pp. 40-49.
- McCarthy, M.G.** (1986) Influence of irrigation, crop thinning, and canopy manipulation on composition and aroma of Riesling grapes. M.Ag.Sc. Thesis. University of Adelaide, Australia.
- McCarthy, M.G.** (1997) The effect of transient water deficit on berry development of cv. Shiraz (*Vitis vinifera* L.). *Aust. J. Grape Wine Res.* **3**, 102-108.
- McCarthy, M.G. and Coombe, B.G.** (1985) Water status and wine grape quality. *Acta Hortic.* **171**, 447-456.
- McCarthy, M.G. and Coombe, B.G.** (1999) Is weight loss in ripening grape berries cv Shiraz caused by impeded phloem transport? *Aust. J. Grape Wine Res.* **5**, 10-16.
- Merin, U., Rosenthal, I. and Lavi, U.** (1983) A chemical method for the assessment of grapes according to their seed content. *Vitis* **22**, 306-310.
- Mollenhauer, H.H.** (1964) Plastic embedding mixtures for use in electron microscopy. *Stain Tech.* **39**, 111-114.
- Møller, A., Strange, P. and Gundersen, J.G.** (1990) Efficient estimation of cell volume using the nucleator and the disector. *J. Microsc.* **159**, 61-71.
- Monselise, S.P.** (ed.) (1986) *Handbook of Fruit Set and Development.* Boca Rouge: C.R.C. Press.
- Motomura, Y.** (1990a) ¹⁴C-assimilate partitioning in grapevine shoots: effects of shoot pinching, girdling of shoot, and leaf-halving on assimilates partitioning from leaves into clusters. *Am. J. Enol. Vitic.* **44**, 1-7.
- Motomura, Y.** (1990b) Distribution of ¹⁴C-assimilates from individual leaves on clusters in grape shoots. *Am. J. Enol. Vitic.* **41**, 306-312.

- Müller-Thurgau, H.** (1898) Abhängigkeit der Ausbildung der Traubenbeeren und einiger anderer Früchte von der Entwicklung der Samen. *Landw. Jahr. Schweiz*, **12**, 135-203.
In Pratt, C. 1971. Reproductive anatomy in cultivated grapes — a review. *Am. J. Enol. Vitic.* **22**, 92-109.
- Mullins, M.G., Bouquet, A. and Williams, L.E.** (1992) *Biology of the Grapevine*. Cambridge: Cambridge University Press.
- Nakagawa, S. and Nanjo, Y.** (1965) A morphological study of Delaware grape berries. *J. Jap. Soc. Hort. Sci.* **34**, 85-95.
- Nakagawa, S. and Nanjo, Y.** (1966) Comparative morphology of the grape berry in three cultivars. *J. Jap. Soc. Hort. Sci.* **35**, 117-126.
- Naylor, A.P.** (2001) The effects of row orientation, trellis type, shoot and bunch position on the variability of Sauvignon Blanc (*Vitis vinifera* L.) juice composition. M.App.Sc. Thesis, Lincoln University, New Zealand.
- Naylor, A.W.** (1984) Functions of Hormones at the Organ Level of Organization. Chapter 5. *In Scott, T.K. (ed.) Hormonal Regulation of Development. II. The Functions of Hormones from the Level of the Cell to the Whole Plant. Encyclopedia of Plant Physiology. Vol. 10.* Berlin: Springer-Verlag.
- Negishi, K., Drujan, B.D. and Laufer, M.** (1981) Counterstaining of fluorescent retinal preparations: cell densities in different layers. *Neuroscience* **6**, 2047-2051.
- Nelson, K.E., Baker, G.A., Winkler, A.J., Amerine, M.A., Richardson, H.B. and Jones F.R.** (1963) Chemical and sensory variability in table grapes. *Hilgardia* **34**, 1-42.
- NIH Image.** (1996) Version 1.61. U.S. National Institutes of Health.
- Niketić-Aleksić, G.K. and Hrazdina, G.** (1972) Quantitative analysis of the anthocyanin content in grape juices and wines. *Lebensm.-Wiss. u. Technol.* **5**, 163-165.
- Nitsch, J.P.** (1952) Plant hormones in the development of fruits. *Q. Rev. Biol.* **27**, 33-57.
- Nitsch, J.P.** (1970) Hormonal Factors in Growth and Development. Chapter 15. *In Hulme, A.C. (ed.) The Biochemistry of Fruits and their Products, Vol. 1.* London: Academic.
- Noble, A.C., Arnold, R.A., Buechsenstein, J., Leach, E.J., Schmidt, J.O. and Stern, P.M.** (1987) Modification of a standardised system of wine aroma terminology. *Am. J. Enol. Vitic.* **38**, 143-146.
- Noble, A.C., Arnold, R.A., Masuda, B.M., Pecore, S.D., Schmidt, J.O. and Stern, P.M.** (1984) Progress towards a standardised system of wine aroma terminology. *Am. J. Enol. Vitic.* **35**, 107-109.
- Nursten, H.E.** (1970) Volatile Compounds: the Aroma of Fruits. Chapter 10. *In Hulme, A.C. (ed.) The Biochemistry of Fruits and their Products, Vol. 1.* London: Academic.
- O'Brien, T.P. and McCully, M.E.** (1981) *The Study of Plant Structure: Principles and Selected Methods*. Melbourne: Termarcaphi.
- Ojeda, H., Deloire, A., Carbonneau, A., Ageorges, A. and Romieu, C.** (1999) Berry development of grapevines: Relations between the growth of berries and their DNA content indicate cell multiplication and enlargement. *Vitis* **38**, 145-150.
- Oldmixon, E.H. and Carlsson, K.** (1993) Methods for large data volumes from confocal scanning laser microscopy of lung. *J. Microsc.* **170**, 221-228.
- Ollat, N. and Gaudillere, J.P.** (1998) The effect of limiting leaf area during stage I of berry growth on development and composition of berries of *Vitis vinifera* L. cv. Cabernet Sauvignon. *Am. J. Enol. Vitic.* **49**, 251-258.
- Olmo, H.P.** (1934) Empty-seededness in varieties of *Vitis vinifera*. *Proc. Am. Soc. Hort. Sci.* **32**, 376-380.
- Olmo, H.P.** (1946) Correlations between seed and berry development in some seeded varieties of *Vitis vinifera*. *Proc. Am. Soc. Hort. Sci.* **48**, 291-297.
- Oszmianski, J., Romeyer, F.M., Sapis, J.C. and Macheix, J.J.** (1986) Grape seed phenolics: extraction as affected by some conditions occurring during wine processing. *Am. J. Enol. Vitic.* **37**, 7-12.

- Park, S.K., Morrison, J.C., Adams, D.O. and Noble, A.C.** (1991) Distribution of free and glycosidally bound monoterpenes in the skin and mesocarp of Muscat of Alexandria grapes during development. *J. Agric. Food Chem.* **39**, 514-518.
- Parsons, D.F., Cole, R.W. and Kimelberg, H.K.** (1989) Shape, size, and distribution of cell structures by 3D graphics reconstruction and stereology. *Cell Biophys.* **14**, 27-42.
- Pawley, J.B.** (ed.) (1995) *Handbook of Biological Confocal Microscopy*. (2nd ed.) New York: Plenum Press.
- Perl, M., Lavi, U. and Spiegel-Roy, P.** (1985) A possible tool for detecting seed traces in grape berries. *J. So. Afr. Soc. Enol. Vitic.* **5**, 1-7.
- Petrie, P.R., Trought, M.C.T. and Howell, G.S.** (2000) Fruit composition and ripening of Pinot Noir (*Vitis vinifera* L.) in relation to leaf area. *Aust. J. Grape Wine Res.* **6**, 46-51.
- Peynaud, E. and Ribéreau-Gayon, P.** (1971) The Grape. Chapter 4. *In* Hulme, A.C. (ed.) *The Biochemistry of Fruits and their Products*, Vol. 2. London: Academic.
- Pirie, A. and Mullins, M.G.** (1977) Interrelationships of sugars, anthocyanins, total phenols and dry weight in the skin of grape berries during ripening. *Am. J. Enol. Vitic.* **28**, 204-209.
- Pirie, A.J.G.** (1977) Phenolics accumulation in red wine grapes. Ph.D. Thesis, University of Sydney, Australia.
- Possner, D. and Kliwer, W.M.** (1985) The localisation of acids, sugars, potassium and calcium in developing grape berries. *Vitis* **24**, 229-240.
- Power, F.B. and Chesnut, V.K.** (1921) The occurrence of methyl anthranilate in grape juice. *Am. Chem. Soc. J.* **43**, 1741-1742.
- Pratt, C.** (1971) Reproductive anatomy in cultivated grapes — a review. *Am. J. Enol. Vitic.* **22**, 92-109.
- Pratt, H.K. and Reid, M.S.** (1974) Chinese gooseberry: seasonal patterns in fruit growth and maturation, ripening, respiration and the role of ethylene. *J. Sci. Food Agric.* **25**, 747-757.
- Price, S.** (1994) Sun exposure and flavonols in grapes. Ph.D. Thesis. Oregon State University.
- Rankine, B.** (1990) *Tasting and Enjoying Wine*. Australia: Winetitles.
- Rankine, B.C., Cellier, K.M. and Boehm, E.W.** (1962) Studies on grape variability and field sampling. *Am. J. Enol. Vitic.* **13**, 58-72.
- Rapp, A.** (1988) Wine Aroma Substances from Gas Chromatographic Analysis. *In* Linskens, H.F. and Jackson, J.F. (eds.) *Wine Analysis*. Berlin: Springer-Verlag.
- Ravaz, L.** (1903) La brunissure de la vigne. *Annales Ecole Nat. Agric. Montpellier*. *In* Huglin, Pierre 1986. *Biologie et Écologie de la Vigne*. France: Payot Lausanne.
- Rebers, M., Kaneta, T., Kawaide, H., Yamaguchi, S., Yang, Y.Y., Imai, R. Sekimoto, H. and Kamiya, Y.** (1999) Regulation of gibberellin biosynthesis genes during flower and early fruit development of tomato. *Plant J.* **17**, 208-212.
- Reid, M.S.** (1995) Ethylene in Plant Growth, Development, and Senescence. Chapter G2. *In* Davies, P.J. (ed.) *Plant Hormones: Physiology, Biochemistry and Molecular Biology*. Dordrecht: Kluwer Academic Publishers.
- Ribéreau-Gayon, G.** (1966) Etude du métabolisme des glucides, des acides organique et des acides aminés chez *Vitis vinifera* L. Thèse Sciences Physiques, Paris.
- Ricardo da Silva, J.M., Rigaud, J., Cheynier, V., Cheminat, A. and Moutounet, M.** (1991) Procyanidin dimers and trimers from grape seeds. *Phytochem.* **30**, 1259-1264.
- Rigaut, J.P. and Vassy, J.** (1991) High resolution three-dimensional images from confocal scanning laser microscopy. Quantitative study and mathematical correction of the effects due to bleaching and fluorescence attenuation in depth. *Anal. Quant. Cytol. Histo.* **13**, 223-232.
- Rivière, J.-L. and Cabanne, F.** (1987) Animal and plant cytochrome P-450 systems. *Biochimie* **69**, 743-752.
- Robinson, D.L.** (1987) Estimation and use of variance components. *The Statistician* **36**, 3-14.

- Rock, C.D. and Quatrano, R.S.** (1995) Chapter G10. *In* Davies, P.J. (ed.) Plant Hormones: Physiology, Biochemistry and Molecular Biology. Dordrecht: Kluwer Academic Publishers
- Roessler, E.B. and Amerine, M.A.** (1958) Studies on grape sampling. *Am. J. Enol. Vitic.* **9**, 139-145.
- Roessler, E.B. and Amerine, M.A.** (1963) Further studies on field sampling of wine grapes. *Am. J. Enol. Vitic.* **14**, 144-147.
- Rogiers, S.Y., Smith, J.A., White, R., Keller, M., Holzapfel, B.P. and Virgona, J.M.** (2001) Vascular function in berries of *Vitis vinifera* (L) cv. Shiraz. *Aust J. Grape Wine Res.* **7**, 47-51.
- Rost, F.W.D.** (1992) Fluorescence Microscopy. Vol. 1. Cambridge: Cambridge University Press.
- Rost, F.W.D.** (1994) Throwing light on living tissue. *Today's Life Science* **6**, 32-36.
- Rost, F.W.D.** (1995) Fluorescence Microscopy. Vol. 2. Cambridge: Cambridge University Press.
- Ruffner, H.P.** (1982a) Metabolism of tartaric and malic acids in *Vitis*: a review — part A. *Vitis* **21**, 247-259.
- Ruffner, H.P.** (1982b) Metabolism of tartaric and malic acids in *Vitis*: a review — part B. *Vitis* **21**, 346-358.
- Salisbury, F.B. and Ross, C.W.** (1992) Plant Physiology. (4th ed.) California: Wadsworth Inc..
- Schmued, L.C., Swanson, L.W. and Sawchenko, P.E.** (1982) Some fluorescent counterstains for neuroanatomical studies. *J. Histochem. and Cytochem.* **30**, 123-128.
- Schreier, P.** (1979) Flavour composition of wines: a review. *CRC Crit. Rev. Food Sci. Nutr.* **12**, 59-111.
- Schreier, P.** (1982) Volatile constituents in different grape species. *In* Webb, A.D. (ed.) University of California, Davis. Grape and Wine Centennial: Symposium Proceedings. pp. 317-321.
- Scion Image for Windows.** (2000) Version 4.0.2. Scion Corporation, Frederick, Maryland.
- Sembdner, G., Gross, D., Liebisch, H.-W. and Schneider, G.** (1980) Chapter 4. *In* MacMillan, J. (ed.) Hormonal Regulation of Development. I. Molecular Aspects of Plant Hormones. Encyclopedia of Plant Physiology. Vol. 9. Berlin: Springer-Verlag.
- Seo, M. and Koshiba, T.** (2002) Complex regulation of ABA biosynthesis in plants. *Trends Plant Sci.* **7**, 41-48.
- Sepúlveda, G. and Kliever, W.M.** (1986) Effect of high temperature on grapevines (*Vitis vinifera* L.). II. Distribution of soluble sugars. *Am. J. Enol. Vitic.* **37**, 20-25.
- Shiozaki, S., Miyagawa, T., Ogata, T., Horiuchi, S. and Kawase, K.** (1997) Differences in cell proliferation and enlargement between seeded and seedless grape berries induced parthenocarpically by gibberellin. *J. Hort. Sci.* **72**, 705-712.
- Simpson, J.L.S.** (1929) A short method of clearing plant tissues for anatomical studies. *Stain Tech.* **4**, 131-132.
- Singleton, V.L.** (1966) The total phenolic content of grape berries during the maturation of several varieties. *Am. J. Enol. Vitic.* **17**, 126-134.
- Singleton, V.L. and Trousdale, E.K.** (1992) Anthocyanin-tannin interactions explaining differences in polymeric phenols between white and red wines. *Am. J. Enol. Vitic.* **43**, 63-70.
- Singleton, V.L., Ough, C.S. and Nelson, K.E.** (1966) Density separations of wine grape berries and ripeness distribution. *Am. J. Enol. Vitic.* **17**, 95-105.
- Sinnott, E.W.** (1939) A developmental analysis of the relation between cell size and fruit size in cucurbits. *Am. J. Bot.* **26**, 179-189.
- Sinnott, E.W.** (1945) The relation of growth to size in cucurbit fruits. *Am. J. Bot.* **32**, 439-446.

- Sinnott, E.W.** (1958) The genetic basis of organic form. *Ann. N.Y. Acad. Sci.* **71**, 1223-1233.
- Smart, R.E.** (1974) Photosynthesis by grapevine canopies. *J. Appl. Ecol.* **11**, 997-1006.
- Somers, T.C. and Evans, M.E.** (1977) Spectral evaluation of young red wines: anthocyanin equilibria, total phenolics, free and molecular SO₂, "chemical age". *J. Sci. Food Agric.* **28**, 279-287.
- Somers, T.C. and Vérette, E.** (1988) Phenolic Composition of Natural Wine Types. In Linskens, H.F. and Jackson, J.F. (eds.) *Wine Analysis*. Berlin: Springer-Verlag.
- Sommer, K.J., Islam, M.T. and Clingeleffer, P.R.** (2000) Light and temperature effects on shoot fruitfulness in *Vitis vinifera* L. cv. Sultana: influence of trellis type and grafting. *Aust. J. Grape Wine Res.* **6**, 99-108.
- Srinivasan, C. and Mullins, M.G.** (1976) Reproductive anatomy of the grape-vine (*Vitis vinifera* L.): origin and development of the anlage and its derivatives. *Ann. Bot.* **38**, 1079-1084.
- Srinivasan, C. and Mullins, M.G.** (1981) Physiology of flowering in the grapevine — a review. *Am. J. Enol. Vitic.* **32**, 47-63.
- Stahl, W.H.** (ed.) (1973) *Compilation of Odor and Taste Threshold Values Data*. American Society for Testing and Materials, Data Series, 48. Baltimore: McCormick and Co. Inc..
- Stahl-Biskup, E., Intert, F., Holthuijzen, J., Stengele, M. and Schultz, G.** (1993) Glycosidically bound volatiles — a review 1986-1991. *Flavour Fragr. J.* **8**, 61-80.
- Staudt, G.** (1986) Flowering, pollination and fertilization in *Vitis*. 4th International Symposium on Grape-Vine Breeding, Verona, 1985. *Vignevini* **13**, 265-267.
- Staudt, G.** (1999) Opening of flowers and time of anthesis in grapevines, *Vitis vinifera* L. *Vitis* **38**, 15-20.
- Staudt, G., Schneider, W. and Leidel, J.** (1986) Phases of berry growth in *Vitis vinifera*. *Ann Bot.* **58**, 789-800.
- Stout, A.B.** (1936) Seedlessness in grapes. New York State Agr. Expt. Sta., Geneva, Tech. Bull. **238**, 68.
- Strachan, S., Van Hilst, R., Wright, J. and Stanford, L.** (1994) Projections of wine grape production and winery intake to 1996-97. Australian Bureau of Agricultural and Resource Economics. Research Report 94.14, Canberra.
- Strickland, A.G., Forster, H.C. and Vasey, A.J.** (1932) A vine uniformity trial. *Vic. J. Agric.* **30**, 584-593.
- Stuart, D.A., Durnam, D.J. and Jones, R.L.** (1977) Cell elongation and cell division in elongating lettuce hypocotyl sections. *Planta*, **135**, 249-255.
- Swain, S.M., Reid, J.B. and Kamiya, Y.** (1997) Gibberellins are required for embryo growth and seed development in pea. *Plant J.* **12**, 1329-1338.
- Swanson, C.A. and El-Shishiny, E.D.H.** (1958) Translocation of sugars in the Concord grape. *Plant Physiol.* **33**, 33-37.
- Thompson, D'Arcy W.** (1942) *On Growth and Form*. (2nd ed.) Cambridge: Cambridge University Press.
- Török, P., Hewlett, S.J. and Varga, P.** (1997) The role of specimen-induced spherical aberration in confocal microscopy. *J. Microsc.* **188**, 158-172.
- Travis, A.J., Murison, S.D., Perry, P. and Chesson, A.** (1997) Measurement of cell wall volume using confocal microscopy and its application to studies of forage degradation. *Ann. Bot.* **80**, 1-11.
- Trought, M.C.T.** (1995) Some comments on variation in fruit composition in the vineyard. *Proceedings: Grape and Wine Symposium*, Lincoln University, NZ. pp. 19-21.
- Trought, M.C.T. and Tannock, S.J.C.** (1994) Berry variation within a bunch of grapes. Abstracts of NZ meetings, August 1994.
- Underwood, E.E.** (1970) *Quantitative Stereology*. Massachusetts: Addison-Wesley Publishing Co..

- Visser, T.D. and Oud, J.L.** (1994) Volume measurements in three-dimensional microscopy. *Scanning* **16**, 198-200.
- Weaver, R.J. and Johnson, J.O.** (1985) Relation of Hormones to Nutrient Mobilization and the Internal Environment of the Plant: The Supply of Mineral Nutrients and Photosynthate. Chapter 1. *In* Pharis, R.P. and Reid, D.M. (eds.) *Hormonal Regulation of Development. III. Role of Environmental Factors. Encyclopedia of Plant Physiology.* Vol. 11. Berlin: Springer-Verlag.
- Weaver, R.J. and McCune, S.B.** (1959a) Girdling: Its relation to carbohydrate nutrition and development of Thompson Seedless, Red Malaga, and Ribier grapes. *Hilgardia* **28**, 421-456.
- Weaver, R.J. and McCune, S.B.** (1959b) Effect of gibberellin on seedless *Vitis vinifera*. *Hilgardia* **29**, 247.
- Weaver, R.J. and Pool, R.M.** (1965) Relation of seededness and ripening to gibberellin-like activity in berries of *Vitis vinifera*. *Plant Physiol.* **40**, 770-776.
- Weibel, E.R.** (1979) *Stereological Methods. Vol. 1. Practical Methods for Biological Morphometry.* London: Academic Press.
- Weibel, E.R.** (1980) *Stereological Methods. Vol. 2. Theoretical Foundations.* London: Academic Press.
- White, N.S., Errington, R.J., Fricker, M.D. and Wood, J.L.** (1996) Aberration control in quantitative imaging of botanical specimens by multidimensional fluorescence microscopy. *J. Microsc.* **181**, 99-116.
- Whiting, G.C. and Coggins, R.A.** (1975) Estimation of the monomeric phenolics of ciders. *J. Sci. Fd Agric.* **26**, 1833-1838.
- Whiting, J.R.** (1992) Harvesting and Drying of Grapes. Chapter 14. *In* Coombe, B.G. and Dry, P.R. (eds.) *Viticulture. Vol. 2. Practices.* Adelaide: Winetitles.
- Williams, P.J.** (1993) Hydrolytic Flavor Release in Fruits and Wines Through Hydrolysis of Non-Volatile Precursors. *In* Acree, T.E. and Teranishi, R. (eds.) *Flavor Science: Sensible Principles and Techniques.* Washington DC: American Chemical Society.
- Williams, P.J., Cynkar, W., Francis, I.L., Gray, J.D., Iland, P.G. and Coombe, B.G.** (1995) Quantification of glycosides in grapes, juices, and wines through a determination of glycosyl glucose. *J. Agric. Food Chem.* **43**, 121-128.
- Williams, P.J., Strauss, C.R. and Wilson, B.** (1980) Hydroxylated linalool derivatives of volatile monoterpenes of Muscat grapes. *J. Agric. Food Chem.* **28**, 766-771.
- Williams, P.J., Strauss, C.R., Aryan, A.P. and Wilson, B.** (1987) Grape flavour — a review of some pre- and postharvest influences. *In* Lee, T. (ed.) *Proceedings of the sixth Australian wine industry technical conference.* Adelaide: Australian Industrial Publishers. pp. 111-116.
- Williams, R.E.** (1968) Space-filling polyhedron: its relation to aggregates of soap bubbles, plant cells, and metal crystallites. *Science* **161**, 276-277.
- Williams, R.F.** (1970) The genesis of form in flax and lupin as shown by scale drawings of the shoot apex. *Aust. J. Bot.* **18**, 167-173.
- Wilson, B., Strauss, C.R. and Williams, P.J.** (1986) The distribution of free and glycosidally-bound monoterpenes among skin, juice, and pulp fractions of some white grape varieties. *Am. J. Enol. Vitic.* **37**, 107-111.
- Winkler, A.J. and Williams, W.O.** (1936) Effect of seed development on the growth of grapes. *Proc. Am. Soc. Hort. Sci.* **33**, 430-434.
- Winkler, A.J., Cook, J.A., Kliewer, W.M. and Lider, L.A.** (1974) *General Viticulture.* (2nd ed.) Berkeley: University of California Press.
- Wolpert, J.A. and Howell, G.S.** (1984) Sampling Vidal Blanc grapes. II. Sampling for precise estimates of soluble solids and titratable acidity of juice. *Am. J. Enol. Vitic.* **35**, 242-246.
- Yamaguchi, S. and Kamiya, Y.** (2000) Gibberellin biosynthesis: its regulation by endogenous and environmental signals. *Plant Cell Physiol.* **41**, 251-257.

-
- Yang, S.F. and Hoffman, N.E.** (1984) Ethylene biosynthesis and its regulation in higher plants. *Ann. Rev. Plant Physiol.* **35**, 155-189.
- Yu, R.C., Abrams, D.C., Alaibac, M. and Chu, A.C.** (1994) Morphological and quantitative analyses of normal epidermal Langerhans cells using confocal scanning laser microscopy. *Brit. J. Dermat.* **131**, 843-848.
- Zar, J.H.** (1974) *Biostatistical Analysis*. New Jersey: Prentice-Hall Inc..
- Zeroni, M. and Hall, M.A.** (1980) Molecular Effects of Hormone Treatment on Tissue. Chapter 6. *In* MacMillan, J. (ed.) *Hormonal Regulation of Development. I. Molecular Aspects of Plant Hormones. Encyclopedia of Plant Physiology. Vol. 9.* Berlin: Springer-Verlag.
- Zucconi, F.** (1986) Peach. *In* Monselise, S.P. (ed.) *Handbook of Fruit Set and Development.* Boca Rouge: C.R.C. Press.

PUBLICATIONS

- Gray, J.D., Gibson, R.J., Coombe, B.G., Giles, L.C. and Hancock, T.W.** (1994) Assessment of winegrape quality in the vineyard — a preliminary, commercial survey. *Aust. N.Z. Wine Ind. J.* **9**, 253-261.
- Gray, J.D., Gibson, R.J., Coombe, B.G., Iland, P.G. and Pattison, S.J.** (1997) Assessment of winegrape value in the vineyard — survey of cv. Shiraz from South Australian vineyards 1992. *Aust. J. Grape Wine Res.* **3**, 109-117.
- Gray, J.D., Kolesik, P., Coombe, B.G. and Høj, P.B.** (1999) Confocal measurement of the three-dimensional size and shape of plant parenchyma cells in a developing fruit tissue. *Plant J.* **19**, 229-236.

Assessment of Winegrape Value in the Vineyard – A Preliminary, Commercial Survey

J.D. GRAY¹, R.J. GIBSON², B.G. COOMBE³, L.C. GILES⁴ and T.W. HANCOCK⁴

1. Research Fellow, National Teaching Company Scheme

2. Viticulturist, Penfolds Wine Group, Nuriootpa

3. Department of Horticulture, Viticulture and Oenology, Waite Campus, The University of Adelaide

4. Department of Plant Science, Waite Campus, The University of Adelaide

Abstract

In an attempt to improve the assessment of winegrape value before vinification, over one thousand individual vineyards were identified and scored, and records kept of specified vineyard characteristics during each growing season. Each harvest lot was vinified and kept separate for 2 to 3 months until the preliminary tasting when the initial allocations to product are made; from these classifications a Value Index (VI) was calculated using figures of margin as a percentage of net selling price for each wine product. Vineyard characteristics of four varieties during three years were analysed statistically by multiple regression techniques in an attempt to identify characteristics that are associated with winegrape value.

VI did not relate consistently to any one characteristic. Some were significant more than once, e.g. yield per vine, vine age, shoot growth preharvest, fruit exposure and berry skin thickness; but significant effects were infrequent and inconsistent and, in that sense, the exercise was inconclusive. Further investigations are warranted that apply improved vineyard assessment procedures, involving quantitative measurement wherever possible, and that concentrate efforts to reduce the proportion of unrecorded data.

Introduction

Until the mid 1980s the pricing of winegrapes related poorly to their real value; instead, prices were influenced by such factors as legislated minima designed to help cover costs of production (Coombe 1991). A combination of forces in 1985 led to a large change in winegrape pricing: (a) an increased demand generated by, among other things, a prior 'vine-pull' scheme and low wine stocks; and (b) a recognition of the merit of rewarding high quality grapes with higher prices, bringing the opportunity for better viticultural decisions by growers and, also, improvements in seller/buyer relations. It was realised that such trends would bring greater stability to the winegrape industry.

These events highlighted the longstanding problem of how to quantify the quality, and hence value, of winegrapes before vinification (Coombe 1987). The usual analyses of grape juice composition (°Brix, acidity and pH) gave only crude guides to winegrape value under Australian conditions. Quantification by the subjective assessment of juice aroma (Cootes *et al.* 1981, Cootes 1984, Jordan and Croser 1984) has provided useful results but is cumbersome and expensive; moreover, the technique remains the province of the buyer and not of both the seller and the buyer.

This paper reports another approach to winegrape assessment, initiated by the Penfolds Wine Group, now Southcorp Wines. Vineyards were assessed by scoring and measuring a range of characters based initially upon the score-sheet of Smart (Smart *et al.* 1981, Smart and Robinson 1991). These data were related statistically to VI which derived largely from the winemakers' subjective assessment of the value of the individual wines made from each vineyard lot. It was hoped that these exploratory analyses would identify characteristics that were associated with winegrape value and, ultimately, wine quality.

Materials and methods

Vineyard assessment began in 1982 but only the records from 1988, 1989 and 1990 are reported here. These latter vintages experienced different weather conditions: in 1988, some regions had strong winds, hail damage or heat stress; in 1989, crop loads varied although the crush was the largest on record; 1990 was regarded generally as a benign vintage with above-average yields. The survey covered practically all vineyard blocks with fruit contracted to the company (including those owned by the company) in six South Australian regions—Adelaide, Barossa, Clare, Eden Valley, Langhorne Creek and Lyndoch—and varying in area from 0.2 to 25 ha. Only four varieties were analysed for the present purposes—Shiraz, Cabernet Sauvignon, Chardonnay and Riesling—giving two black and two white varieties with 596, 253, 237 and 198 vineyard blocks, respectively.

The methods used for vineyard assessment began with the original scorecard system of Smart *et al.* (1981) and evolved to the system displayed in Table 1. Modifications leading to the current format included the addition of a preharvest assessment (1983), alterations to classes recorded (1984 and 1988), the inclusion of berry weight (1984), vine size (1988), fruit skin thickness (1988), bunch number (1988) and berry weight (1988), and the differential weighting of scores according to winegrape variety (1988). Historical and postharvest data were collated from grower surveys and company records (1991). As shown in Table 1, seventeen qualitative and ten quantitative variables were measured. An example of a qualitative variable is fruit skin thickness, which was classified as thin, medium or thick; a quantitative variable is area per vine, measured in square metres. Four timings were used—historical, veraison, preharvest and postharvest.

The response variable, winegrape value, was quantified by a method developed within the company, based on the whole-

Table 1. Description of the data set

Characteristics	Timing	Description	Classes/units
Qualitative explanatory variables (factors)			
Region	historical	Specifies locality of vineyard by separating into six broad regions	Adelaide, Barossa, Clare, Eden Valley, Langhorne Creek, Lyndoch <80%, 80–90%, 90–100%
Leaf condition – v	veraison	Estimate of proportion of functioning/healthy leaves as a proportion of the total number of leaves on the vine	<5%, 5–10%, 10–20%, 20–50%, >50%
Growing tips – v	veraison	Estimate of proportion of actively growing shoot tips as a proportion of the total number of shoot tips on the vine	none, 2–8 nodes, 8–12 nodes, >12 nodes <50 cm, 50–150 cm, >150 cm
Laterals	veraison	Estimate of the average number of nodes per lateral shoot	
Shoot length	veraison	Estimate of the average shoot length per vine	
Periderm development	veraison	Estimate of the average extent of periderm development on each shoot, in nodes	<2 nodes, 2–5 nodes, 5–10 nodes, 10–20 nodes
Fruit shading	veraison	Estimate of the proportion of bunches on each vine completely concealed within and shaded by the canopy as a proportion of the total number of bunches on the vine	<20%, 20–60%, >60%
Vine size	veraison	Estimate of relative vine size based on the <i>usual</i> vigour of a variety at a particular locality	small, small-medium, medium, medium-large, large 0–25%, 25–50%, >50%
Canopy shading	veraison	Estimate of the proportion of leaves completely concealed within the canopy as a proportion of the total number of leaves on the vine	low, average, high
Vine balance	veraison	Estimate of relative vine crop/functioning leaf area based on the <i>usual</i> vigour and productivity exhibited by a variety at a particular locality	
Leaf condition – p	preharvest	Estimate of proportion of functioning/healthy leaves as a proportion of the total number of leaves on the vine	<40%, 40–80%, 80–95%, 95–100%
Growing tips – p	preharvest	Estimate on proportion of actively growing shoot tips as a proportion of the total number of shoot tips on the vine	nil, 0–10%, 10–20%, >20%
Fruit exposure	preharvest	Estimate of the proportion of bunches on each vine totally exposed to the sun for 25% of the day as a proportion of the total number of bunches on the vine (reverse of fruit shading)	<40%, 40–60%, 60–80%, 80–100%
Fruit colour	preharvest	Estimate of the potential colour available for extraction by squeezing individual berries	low, medium, high
Fruit size	preharvest	Estimate of the average berry size given the <i>usual</i> range and variation for that particular variety	small, medium, large
Fruit flavour	preharvest	Sensory evaluation of the varietal fruit characteristics of randomly sampled berries	low, medium, intense
Fruit skin thickness	preharvest	Sensory appraisal of skin thickness given varietal range and variation	thin, medium, thick
Quantitative explanatory variables (variables)			
Area per vine	historical	Calculated from grower survey returns specifying planting density and vineyard area	m ² per vine
Vine age	historical	Mean vine age per block calculated from grower survey returns specifying planting date & density	years
Bunch number	veraison	Rapid estimate of bunch number averaged over three vines	unitless
Bunch weight	preharvest	Mean weight of 3 typical bunches selected from a stratified 20 bunch sample	grams
Berry weight	preharvest	Mean weight of 50 berries randomly stripped from the 3 bunch sample	grams
Baume	preharvest	Temperature-corrected hydrometer reading of fresh (unsettled) juice, water-pressed from stratified sample	°Be
pH	preharvest	Meter reading on 25 mL sample of fresh juice	unitless
Titratable acid	preharvest	Autotitration of 25 mL sample against 0.333 normal NaOH to endpoint of pH 8.4	g/L tartrate equivalents
Potassium	preharvest	Spectrophotometric analysis on 10 mL sample of fresh juice	mg/L
Yield per vine	postharvest	Calculated from grower survey returns specifying planting density, vineyard area and block yield together with company intake records	kg/vine
Value Index	postharvest	Value Index for a specific block which contributes to a range of products can be calculated using the formula: $\frac{\sum(\text{product value index}) \times (\text{product tonnes})}{\text{total tonnes}}$	unitless

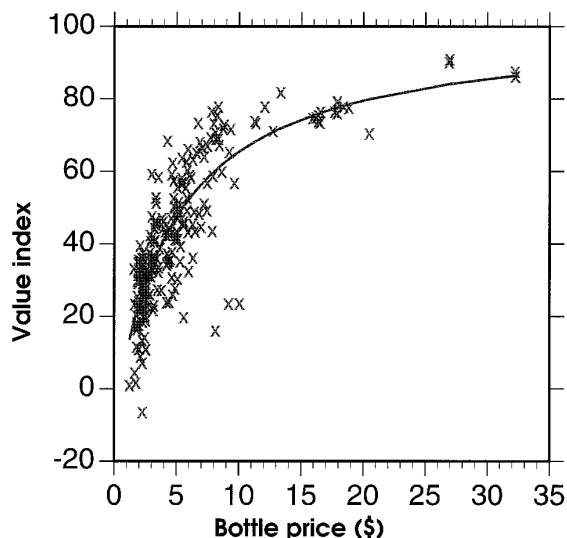


Figure 1. Scatter plot of VI against wholesale price per bottle for all products at 1 May 1990.

sale bottle price of their range of wines—the Value Index (VI). Margin as a percentage of net selling price was calculated for each product (VI_{product} ; see equation 1).

$$VI_{\text{product}} = \frac{M}{SP} \times \frac{100}{I} \tag{1}$$

where SP = net selling price
 CP = cost of production
 M = margin = SP - CP

e.g. for wine product A;

where SP = \$14.00
 CP = \$6.73
 M = \$7.27

$$\text{then } VI_{\text{product A}} = \frac{7.27}{14} \times \frac{100}{I} = 51.9$$

The graph of VI_{product} against wholesale bottle price for the total range of company products (Figure 1) shows a curved relationship. While the distribution of VI_{product} is approximately normal, that of bottle price is positively skewed.

The wine products from each vineyard block were allocated at the first classification tasting, and these were then weighted by proportion of the total fruit weight per block and summed to give VI_{block} (see equation 2).

$$VI_{\text{block}} = \sum_{i=1}^n (VI_i a_i) \tag{2}$$

where VI_i = value index for wine product i
 a_i = tonnes to wine i as a proportion of total vineyard tonnes
 n = number of wines produced from vineyard block

e.g. for block X, which contributes to products A, B and C;

Wine product	VI_i	a_i	$VI_i a_i$
A	51.9	0.70	36.3
B	35.9	0.17	6.1
C	90.8	0.13	11.8

$$VI_{\text{block X}} = 54.2$$

For the remainder of the paper, VI_{block} is referred to as VI.

Table 2. Summary of the significant simple linear regression analyses.

Variety/ year	Variable	y-intercept	Regression coefficient	Variance ratio
<i>Shiraz</i>				
1988	area per vine	32.3	1.46	7.56**
	vine age	39.3	0.16	15.90***
	yield per vine	48.8	-0.63	5.58*
1989	yield per vine	58.6	-1.58	17.89***
1990	area per vine	26.6	1.79	5.81*
	bunch number ^s	50.5	-0.21	12.54***
	bunch weight ^s	63.9	-0.16	11.76**
	berry weight ^s	64.1	-18.45	9.55**
	pH	121.2	-25.79	7.96**
	titratable acid	18.3	2.32	9.80**
	yield per vine	55.0	-1.88	43.39***
<i>Cabernet Sauvignon</i>				
1988	vine age	54.9	-0.52	9.89**
	berry weight ^s	70.1	-33.70	8.53**
	Baume ^s	81.4	-3.32	6.51*
	titratable acid ^s	32.2	1.31	5.20*
1989	vine age	33.4	0.46	16.89***
1990	vine age	24.2	0.65	24.65***
	bunch number	43.1	-0.15	6.24*
	berry weight ^s	84.9	-49.50	16.05***
	yield per vine	52.1	-2.33	12.98***
<i>Chardonnay</i>				
1988	Baume ^s	97.5	-5.47	18.89***
	titratable acid ^s	12.2	2.17	13.45***
1989	bunch weight	22.1	0.15	11.20**
	potassium ^s	21.0	11.24	5.97*
1990	area per vine	44.6	-1.88	11.22**
	titratable acid	36.1	-0.48	4.70*
<i>Riesling</i>				
1988	bunch number ^s	30.3	-0.11	8.44*
	bunch weight ^s	14.9	0.11	8.25*
1989	bunch number ^s	18.6	0.05	6.13*
1990	yield per vine	19.4	0.56	7.68**

^s Precluded from MBE since > 40% of potential data were not available.

Significance levels *** $\Rightarrow P < 0.001$
 ** $\Rightarrow P < 0.01$
 * $\Rightarrow P < 0.05$

Statistical analysis

For each of the twelve year-by-variety combinations, VI and up to 27 variables were tabulated (as shown in Table 1). Multiple linear regression (MLR) was used to study the data to establish which of these variables are associated with the observed variation in the response variable VI. Methods for identifying the best subset were considered since many of the explanatory variables are unlikely to contribute to the observed variation in VI. While the literature includes a number of alternative approaches, the procedure of backward elimination (Draper and Smith 1980) was applied, so that non-significant variables were successively eliminated until only variables explaining a significant portion of the variation in VI remained in the model.

Two important features of the data set needed to be recognized. First, there were many instances where portions of the data were not recorded for individual explanatory variables.

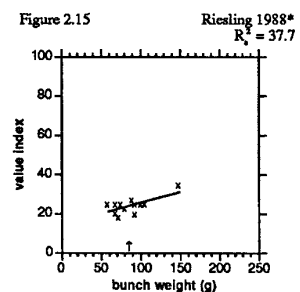
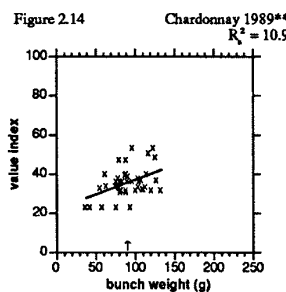
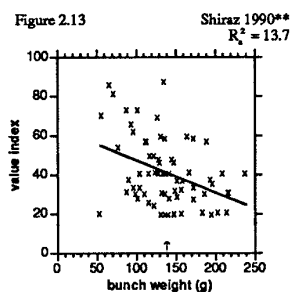
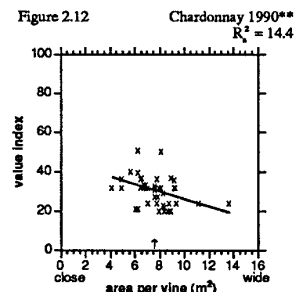
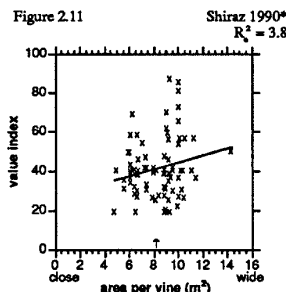
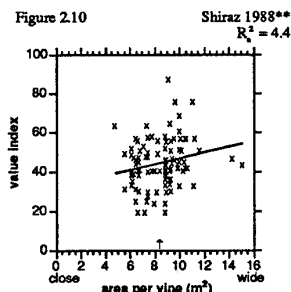
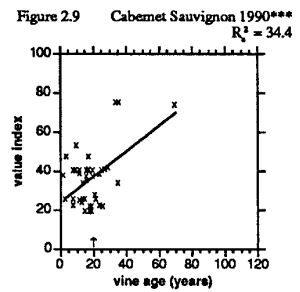
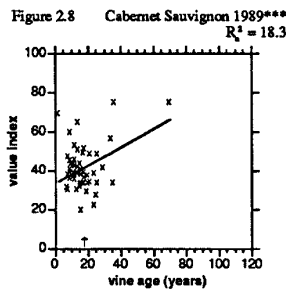
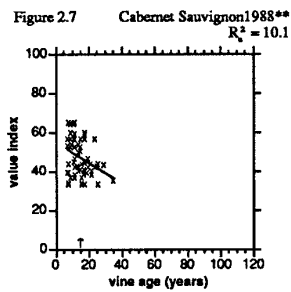
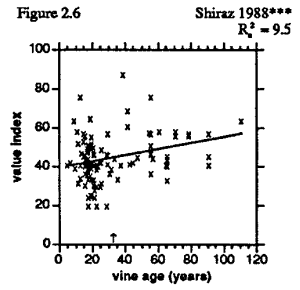
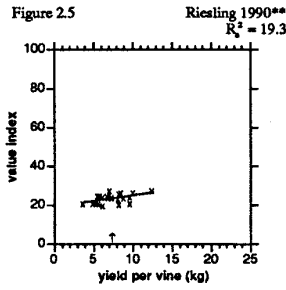
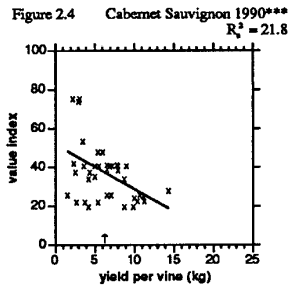
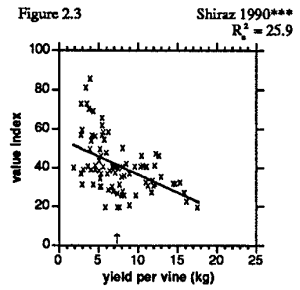
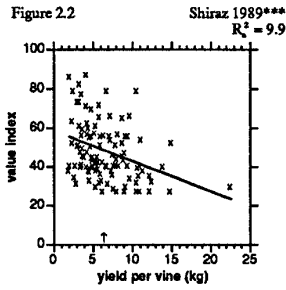
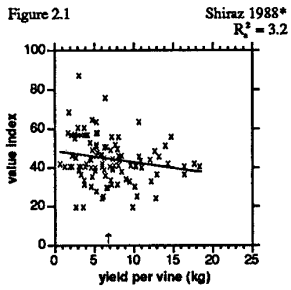


Figure 2. Scatter plots, regression lines, significance levels and adjusted R^2 values (R_a^2) of the simple linear regressions for significant quantitative variables, as in Table 2. The arrangement differs from Table 2; the graphs are grouped by variable rather than by variety and year. The arrow on the x-axis indicates the variable mean; significance levels are indicated by asterisks as in Table 2 footnote.

Figure 2.16 Shiraz 1990**
 $R^2 = 10.5$

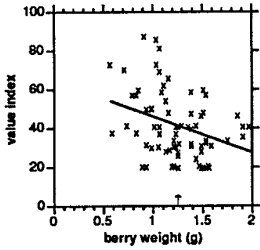


Figure 2.17 Cabernet Sauvignon 1988**
 $R^2 = 26.4$

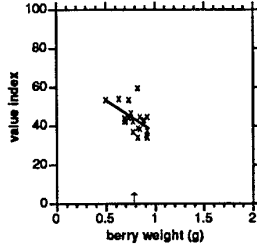


Figure 2.18 Cabernet Sauvignon 1990***
 $R^2 = 35.0$

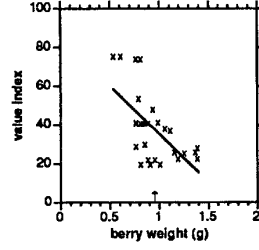


Figure 2.19 Shiraz 1990***
 $R^2 = 11.0$

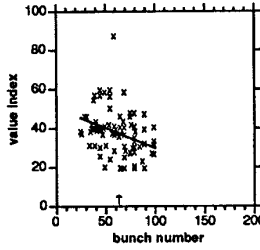


Figure 2.20 Cabernet Sauvignon 1990*
 $R^2 = 10.9$

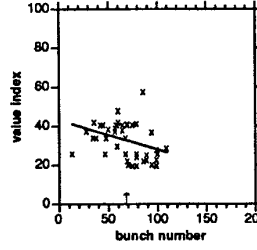


Figure 2.21 Riesling 1988*
 $R^2 = 30.4$

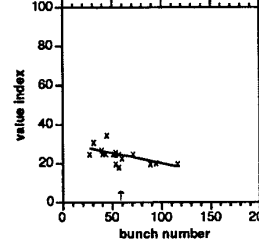


Figure 2.22 Riesling 1989*
 $R^2 = 10.9$

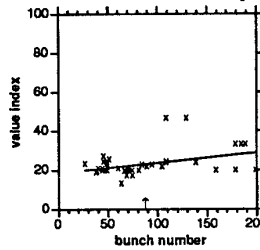


Figure 2.23 Cabernet Sauvignon 1988*
 $R^2 = 20.0$

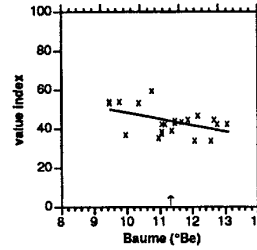


Figure 2.24 Chardonnay 1988***
 $R^2 = 36.6$

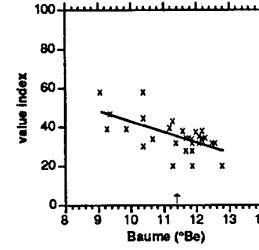


Figure 2.25 Shiraz 1990**
 $R^2 = 6.2$

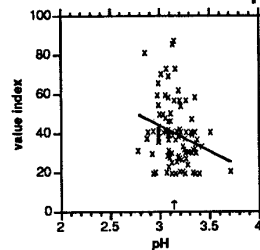


Figure 2.26 Chardonnay 1989*
 $R^2 = 35.6$

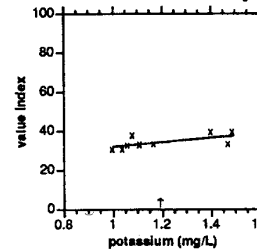


Figure 2.27 Shiraz 1990***
 $R^2 = 7.7$

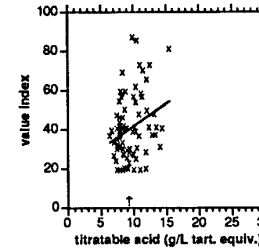


Figure 2.28 Cabernet Sauvignon 1988*
 $R^2 = 16.0$

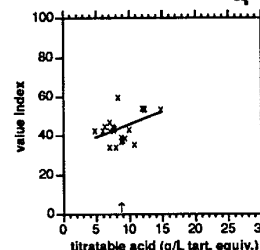


Figure 2.29 Chardonnay 1988***
 $R^2 = 28.7$

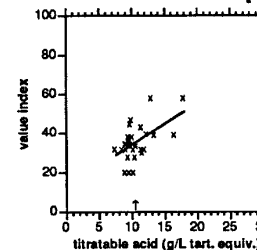


Figure 2.30 Chardonnay 1990*
 $R^2 = 4.8$

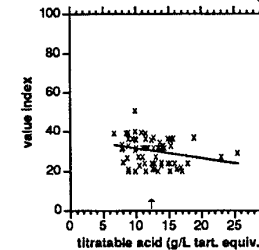


Table 3. Summary of the significant analyses of variance[†]

Variety	Year	Factor	Variance ratio 1	Variance ratio 2	Variance ratio 3	Variance ratio 4	
Shiraz	1988	region	4.43***				
		1989	region	4.47***			
	1989	leaf condition – v	3.48*	3.59*	1.68		
		leaf condition – p	2.20	3.57*	3.05	3.27*	
		fruit exposure	2.18	3.68*	0.40	4.41**	
		fruit skin thickness	2.18	4.96**	6.49**	3.75*	
		1990	region	4.53***			
			leaf condition – v	13.14***	18.14***	16.25***	
	1990	vine size	2.96*	2.58*	3.08*		
		leaf condition – p	9.49***	5.99***	4.45**	5.62**	
		fruit colour	1.64	5.48**	3.97*	3.64*	
		fruit size	6.42**	0.72	2.48	4.38*	
Cabernet Sauvignon		1988	region	13.46***			
		1989	leaf condition – v	11.38***	1.92	4.74*	
fruit exposure	0.94		1.02	3.14*	3.57*		
1990	fruit flavour	3.98*	7.33**	2.75	2.09		
	fruit skin thickness	6.41**	3.96*	2.07	3.04		
	leaf condition – v	26.22***	46.83***	11.96***			
	leaf condition – p	25.67***	10.33***	18.71***	10.66***		
	fruit colour	2.38	5.59**	4.36*	0.59		
	fruit skin thickness	11.69***	4.23*	3.45*	2.42		
Chardonnay	1988	region	9.53***				
		leaf condition – v	0.72	4.20*	3.79*		
		leaf condition – p	2.48	3.63*	4.23*	1.71	
	1989	growing tips – p	7.85***	4.12*	4.26*	3.18*	
		fruit colour	1.93	3.72*	7.76**	6.65**	
		fruit flavour	4.38*	2.37	4.04*	1.83	
	1989	growing tips – v	2.77*	2.77*	1.78		
		periderm development	1.86	6.18***	5.44**		
		growing tips – p	4.52*	1.45	0.12	3.21*	
	1990	fruit exposure	0.42	2.58	3.43*	5.93**	
		region	9.53***				
		growing tips – p	2.03	7.83**	4.31*	0.76	
		fruit exposure	2.40	4.00*	5.22**	2.58	
		fruit colour	2.72	5.03**	2.39	5.18**	
		fruit flavour	6.47**	6.01**	2.89	1.62	
	Riesling	1988	fruit skin thickness	9.42***	3.58*	0.99	7.14**
			region	2.87*			
		1990	region	8.73***			

[†] Separate analyses of variance based on different sample sizes

If one variance ratio ⇒ one measurement for each vineyard

If 3 or 4 variance ratios ⇒ 3 or 4 measurements for each vineyard, respectively [factors only retained if significant on at least two occasions]

Significance levels *** ⇒ P < 0.001
 ** ⇒ P < 0.01
 * ⇒ P < 0.05

The combined effect of this unrecorded data meant a diminished number of useable values in the response variable. As the number of degrees of freedom for the explanatory variables was comparatively large, it proved impractical to include all variables and apply MLR. Second, as mentioned above, the explanatory variables are either quantitative or qualitative. For brevity, 'the qualitative explanatory variables' are hereafter referred to as 'factors' and 'the quantitative explanatory variables' as 'variables'. If the data set included one or a few factors, these could have been included as dummy variables in the MLR, but given the large number of factors and the available degrees of freedom here, this was unmanageable.

In view of the above features of the data set, it was decided to apply a preliminary screening of the data to exclude all variables or factors that individually showed no association with VI. The remainder were included as the starting set for MLR with a view to establishing a final subset that best explained the variation in VI. Therefore, simple linear regression (SLR) was applied to all variables, while factors were subjected to an initial analysis of variance (AOV), with VI taken as the response variable in both cases. The models fitted were:

$$VI = \text{constant} + \text{regression coefficient} * \text{variable} + \text{residual variation}$$

Table 4. Probability values for the final subsets of modified backward eliminations (the lower the value, the more significant); those characteristics eliminated during the course of the analyses are identified with an E.

Characteristics	Shiraz			Cabernet Sauvignon			Chardonnay		
	1988	1989	1990	1988	1989	1990	1988	1989	1990
Region	<0.01	E	<0.01	<0.01	.	.	E	.	<0.01
Leaf condition – v	.	E	<0.01	E	.	†	E	.	.
Growing tips – v	<0.01	.
Periderm development	E	.
Vine size	.	.	E
Leaf condition – p	.	E	E	.	.	E	0.01	.	.
Growing tips – p	0.01	E	<0.01
Fruit exposure	.	E	.	.	E	.	.	<0.01	0.02
Fruit colour	.	.	E	.	.	E	E	.	E
Fruit size	.	.	E
Fruit flavour	0.01	.	E	.	E
Fruit skin thickness	.	<0.01	.	.	E	0.02	.	.	E
Area per vine	E	.	0.03	E
Vine age	<0.01	.	.	E	<0.01	E	.	.	.
Bunch number	<0.01	.	.	.
Bunch weight	<0.01	.
pH	.	.	E
Titratable acid	.	.	0.04	E
Yield per vine	E	<0.01	<0.01	.	.	E	.	.	.

† Problems with the refitting of factors

and

$$VI = \text{grand mean} + \text{effect of } i^{\text{th}} \text{ class of factor} + \text{residual variation}$$

where i is used to increment the classes of a factor for SLR and AOV, respectively. In cases where more than 40% of the potential data was unrecorded (due to lateness in sampling and staff constraints during vintage), the factor or variable was precluded from the starting set of the MLR (see Table 2 footnote). The term 'modified' backward elimination (MBE) was used to describe this statistical approach. The 'best subset' produced by the MBE can be described using the general model

$$VI = \sum_{i=1}^f \text{factor}_i + \sum_{j=1}^v \text{regression coefficient}_j * \text{variable}_j + \text{residual variation}$$

where there are f factors and v variables.

It is inevitable that correlations will occur both between and within variables and factors; hence the results should be interpreted with care. All analyses were completed using the Genstat 5 Statistical Package (Genstat 5 Committee, 1987).

Results

Simple linear regression analyses using variables

Significant SLR analyses are listed by variety and year in Table 2, along with their variance ratios and significance levels. Scatter plots, regression lines, significance levels and adjusted R^2 values for the significant regressions are shown in Figure 2, grouped by variables. In several instances, statistical significance is observed but the low adjusted R^2 indicates that the relationships are weak. In other cases, the slope of the line is influenced by one or more outliers. In a few cases, a strong linear relationship is apparent.

Recognizing the above limitations it can be noted that, with Shiraz, yield per vine was the only variable that was

significantly related to VI in each of the three years. The negative gradient was steepest in 1990 and flattest in 1988. Area per vine was positively associated with VI in 1988 and 1990, and again this was most pronounced in 1990. The remaining significant variables (vine age, bunch weight, berry weight, pH and titratable acidity) were only evident during a single vintage. With Cabernet Sauvignon, vine age was the only variable significantly related to VI in the three years; however the slope was negative in 1988, but positive in 1989 and 1990! The slope of berry weight was negative in 1988 and 1990, steeper in the latter. Four variables were significant in one of the three seasons—°Baume, titratable acid, bunch number and yield per vine.

With Chardonnay and Riesling, no variables were significant over the three seasons. For Chardonnay, titratable acidity was significant in two years, but trends were in opposite directions—positive in 1988 and negative in 1990; four variables (°Baume, bunch weight, potassium and area per vine) were correlated with VI in single seasons. For Riesling, bunch number was associated with VI in 1988 and 1989, but with opposite slopes; there was a significant relationship between bunch weight and VI in 1988, and between yield per vine and VI in 1990.

Analyses of variance using factors

Significant factors are presented in Table 3 together with their variance ratios and significance levels. Region was significant in the majority of instances. Five factors concerned with vegetative growth at veraison were not significant for any variety in any year viz., laterals per shoot, shoot length, canopy shading, vine balance and fruit shading. Of the significant factors, the most prevalent was leaf condition both at veraison and preharvest, especially in the black varieties. Others that were occasionally significant included vine size, periderm development and growing tips; the latter, preharvest, was the only factor that had a significant variance ratio in all three years. Among fruit characteristics, there were several

Table 5. Final subset of modified backward elimination with VI as response variable, including class means and regression coefficients of explanatory variables.

Character	Shiraz			Cab. Sauvignon			Chardonnay		
	88	89	90	88	89	90	88	89	90
Class means of factors									
<i>Region</i>									
Adelaide	39.1	.	17.6	42.8	22.4
Barossa	42.4	.	12.7	41.1	23.1
Clare	34.9	.	8.4	56.0	32.0
Eden Valley	48.8	.	0.7	59.0	26.4
Langhorne Ck	35.8	.	31.5	48.0	28.7
Lyndoch	32.6	.	22.8	64.8	15.1
<i>Leaf condition - v</i>									
<80%
80-90%	.	.	14.8
90-100%	.	.	4.2
<i>Growing tips - v</i>									
<5%	21.9
5-10%	16.9
10-20%	9.3
20-50%
>50%
<i>Leaf condition - p</i>									
<40%
40-80%
80-95%	4.7
95-100%	10.2
<i>Growing tips - p</i>									
nil	27.3
0-10%	25.7
10-20%	38.5
>20%
<i>Fruit exposure</i>									
<40%	5.2
40-60%	8.9
60-80%	4.1
80-100%	0.3
<i>Fruit flavour</i>									
low	32.1
medium	30.4
intense	39.3
<i>Fruit skin thickness</i>									
thin	.	78.8	.	.	.	50.1	.	.	.
medium	.	55.8	.	.	.	47.6	.	.	.
thick	.	57.3	.	.	.	55.9	.	.	.
Regression coefficients of variables									
area per vine	.	.	2.32
vine age	0.13	.	.	.	0.48
bunch number	-0.23	.	.	.
bunch weight	0.14	.
titratable acid	.	.	2.07
yield per vine	.	-1.46	-2.58
% variance explained	19.3	21.8	49.5	48.4	34.0	39.3	31.7	40.3	60.9

entries for fruit skin thickness, fruit colour, and fruit flavour, and a single entry for fruit size.

The lack of significance for some factors may have had more to do with the unequal distribution of observations over the possible classes than with the retention of the null hypothesis. In some cases, significance could have been due to chance alone given the large number of analyses completed.

Modified backward elimination

The final subsets of the MBE are given in Table 4. Characteristics found to be significant in the univariate analyses, but eliminated during the course of the MBE, are indicated. Riesling was excluded because of the paucity of significant entries and the small number of degrees of freedom. Table 5 provides the class means and regression coefficients of the significant terms. An example of the use of Table 5 is: VI of Shiraz in 1990 was influenced jointly by region, leaf condition at veraison, area per vine, titratable acid and yield per vine; area per vine and titratable acid were positively associated with VI, whereas yield per vine had a negative coefficient.

The proportions of variation in VI explained by the best subset of MBE were often low, ranging from 19 to 61%. Further, there was no pattern evident in the size of these percentages between years or varieties. Within each of the three varieties, no one factor or variable remained in the final subset for all three vintages and only a few were present for two of the three years—two for Shiraz (region, yield per vine), none for Cabernet Sauvignon, and two for Chardonnay (preharvest growing tips, fruit exposure). The class means for regions indicate the relative effect region had on VI where it was a significant factor; again, the range was large (from 1 to 65) and showed no consistent pattern among these six regions.

Discussion

The scatter plots in Figure 2, and the accompanying detail of Table 2, summarize a unique array of viticultural information. Interest not only derives from the relationships with winegrape value but also from their commercial character; they represent a historical record of the viticultural methods and vine performance over this large spread of conditions and regions sampled.

The significant negative regressions of VI against yield per vine, although inconsistent, suggest the commonly stated belief that high yielding vines produce wine of lesser quality, may have some basis. It is interesting that the four negative regression coefficients were for black grapes, while the only significant regression coefficient for a white grape (Riesling in 1990) was positive. These results do not disagree with the view held by many that high yield may lead to a lowered quality in black grapes but not in white grapes. Similar arguments may be advanced for the relationship between berry weight or bunch weight and VI.

The statistical methods used to cope with these data are appropriate. The form of multiple linear regression used (MBE) considers results from both the linear regressions using the quantitative explanatory variables (variables) and the analyses of variance using the qualitative explanatory variables (factors). Region was included most frequently in the best subset found by MBE. Of the remaining variables and factors, the measures that were significant twice in the MBE included preharvest growing tips, fruit exposure, fruit skin thickness, vine age and yield per vine. There were some other factors and variables that showed occasional significance, e.g. leaf condition at veraison and preharvest, growing tips at veraison, fruit flavour, titratable acidity, bunch number and weight, and area per vine.

The most obvious conclusion from the analyses is that significant effects were infrequent and inconsistent. This may mean that the approach is ineffective as a predictive tool for winemaking, or alternatively it may reflect the problems that can arise in a data set despite the best efforts of those responsible for its collection. Statistical interpretations of the work are hampered by using qualitative classifications rather than quantitative measurements, and by the cumulative effects of unrecorded data within a large data set. It is difficult to say whether more complete, quantitative measurements would have resulted in stronger associations with VI, or would have identified alternative indicators of winegrape value; this remains to be tested.

Two options exist for further investigation:

1. improving the set of explanatory variables; and
2. considering alternative response variables.

Option 1 is always important. Option 2 should be considered if option 1 fails to increase the explained variation in VI. No logical equivalent yet exists which incorporates the wine-makers', the company's and the market place's subjective judgements of winegrape value. Calculation of VI depends on a company's ability to maintain the separateness of block lots from vinification until the first classification tasting, and the accompanying accounting facility to calculate production costs and margins for each wine product.

Acknowledgements

The authors would like to acknowledge the data collection activities undertaken by Brian Pietsch, Peter Nash and Wendy Allan, the consultative advice provided by Dr Richard Smart, the completion of data analysis by Jason Goodyear, the co-operation of participating grapegrowers and winemakers, the resources and facilities made available through the Department of Horticulture, Viticulture and Oenology and the research funds jointly contributed by the Penfolds Wine Group and the Department of Industry,

Technology and Commerce under the National Teaching Company Scheme.

References

- Coombe, B.G. (1987) Viticultural research and technical development in Australia. In: T. Lee (ed.) Proceedings of the sixth Australian wine industry technical conference. Australian Industrial Publishers, Adelaide, South Australia. pp. 20–24.
- Coombe, B. (1991) From grape prices to vascular bundles. *Aust. NZ Wine Industry J.*, 6(1): 41–2.
- Cootes, R.L. (1984) Grape juice aroma and grape quality assessment used in vineyard classification. In: T.H. Lee and T.C. Somers (eds.) Advances in viticulture and oenology for economic gain: proceedings of the fifth Australian wine industry technical conference. The Australian Wine Research Institute, Glen Osmond, South Australia. pp. 275–92.
- Cootes, R.L., P.J. Wall and R.J. Nettelbeck (1981) Grape quality assessment. In: T.H. Lee (ed.) Grape quality: assessment from vineyard to juice preparation. The Australian Society for Viticulture and Oenology Inc., Glen Osmond, South Australia. pp. 39–56.
- Draper, N.R. and H. Smith (1980) Applied Regression Analysis. John Wiley and Sons, New York.
- Genstat 5 Committee. (1987) Genstat 5 Reference manual. Clarendon Press, Oxford.
- Jordan, A.D. and B.J. Croser (1984) Determination of grape maturity by aroma/flavour assessment. In: T.H. Lee and T.C. Somers (eds.) Advances in viticulture and oenology for economic gain: proceedings of the fifth Australian wine industry technical conference. The Australian Wine Research Institute, Glen Osmond, South Australia. pp. 261–74.
- Smart, R.E., J.B. Robinson and G.R. Due (1981) Manipulation of wine quality within the vineyard. In: Lee, T. (ed.) Grape quality: assessment from vineyard to juice preparation. The Australian Society for Viticulture and Oenology Inc., Glen Osmond, South Australia. pp. 19–26.
- Smart, R.E. and M.D. Robinson (1991) Sunlight into Wine: a handbook for winegrape canopy management. Winetitles, South Australia.

REFEREED PAPER:

Received 25 June 1993; accepted 25 May 1994

ADDRESS FOR CORRESPONDENCE: John Gray, Department of Horticulture, Viticulture and Oenology, Waite Campus, The University of Adelaide, Glen Osmond SA 5064.

Assessment of winegrape value in the vineyard—Survey of cv. Shiraz from South Australian vineyards in 1992

J.D. GRAY^{1,4}, R.J. GIBSON², B.G. COOMBE¹, P.G. ILAND¹ and S.J. PATTISON³

¹Department of Horticulture, Viticulture and Oenology, Waite Campus, The University of Adelaide, 5064

²Formerly Southcorp Wines Pty Ltd, Nuriootpa

³Formerly Department of Statistics, The University of Adelaide, 5005

⁴Corresponding author: Mr J.D. Gray, facsimile 61 8 8303 7116

Keywords: Winegrape value, scoresheet, variability

Abstract

In a previous survey of over one thousand individual vineyards (Gray et al. 1994), records of specified vineyard characteristics were compared during three years with assessments of potential value of the wines made at preliminary allocation to wine product ('Value Index' – 'VI'); significant relationships were infrequent and inconsistent. This paper reports the results from a more focused survey examining 148 cv. Shiraz vineyards in one year with an improved set of vineyard characteristics ('scoresheet'). Linear regression analyses showed small trends for lower 'VI' from vineyards with leafy, dense canopies, poor fruit exposure, lower anthocyanins, larger berries and higher yields. But the high variability of the data precludes reliance on these vineyard assessment methods, particularly as the assessments made at ripening were less successful than those made at harvest.

Abbreviations

AOV analysis of variance, **MLR** multiple linear regression; **SLR** simple linear regression, **'VI'** 'Value index'

Introduction

This report is an extension of the work begun in the 1980s by the participating commercial company, leading to a cooperative project with the University of Adelaide. The general approach followed the original concept developed by Smart et al. (1981) and the progress until 1990 was reported by Gray et al. (1994). The value of grapes for wine was assessed by the 'Value Index' calculated from classifications of young wines made under commercial conditions from separate harvest lots. These indices were compared statistically with many vineyard characteristics. Limited conclusions were drawn because only a few factors correlated with 'Value Index'; in addition, these correlations were inconsistent between years and regions. Several defects in the methods used in the original project were noted: (a) the large number of missing values in the data set, (b) the problems created when variables were qualitative rather than quantitative, and (c) the limited numbers of assessments made for some of the varieties. It was decided to test further the vineyard assessment system using a new set of vineyard characteristics collated into a 'scoresheet' and a single cultivar and year, namely Shiraz during vintage 1992. The objective was, as before, to seek vineyard measurements that correlate usefully with the quality of young wines at their first classification tasting.

Materials and methods

The scoresheet containing the variables used for vineyard assessment in the previous years (see Table 1 in Gray et al. 1994) was modified by eliminating qualitative variables (or substituting a quantitative scale), by eliminating those characteristics that were non-significant, by undertaking identical measurements at both veraison and harvest, and by introducing compositional measurements on harvested fruit. The range of variables are described in Table 1. 'Leaf size' was calculated according to Carbonneau (1976) and the variables of 'anthocyanins' and 'phenolics' according to Iland (1988). Some of the quantitative measurements were based upon subjective estimations made by the recorders in the field (e.g. the proportions of coloured berries, green leaves, active shoot tips and fruit exposure) in contrast to those made on the physical fruit samples at harvest. Attention was paid to the comprehensiveness of the recordings; however, measurements were not undertaken at veraison on Riverland vineyards due to poor timing of the sampling program in that region.

About one quarter (148) of the 629 pre-planned deliveries of Shiraz grapes to wineries belonging to the commercial partner for the 1992 South Australian vintage were randomly selected from among five regions; the number selected ranged from 16 to 46. The regions

Table 1. Description of the vineyard variables measured for the data set. Minima, maxima and means were calculated from the data of all regions.

Factor (region)^o				
Riverland, Central, Northern, Barossa, South Eastern				
Variables with (units)	min	mean	max	Description
<i>Vine variables at veraison:</i>				
Coloured berries (%)	2	84	100	coloured berries as proportion of total berries
Green leaves (%)	50	84	100	green, healthy leaves as proportion of total leaves
Growing tips (%)	0	2	40	actively growing shoot tips as proportion of total shoot tips
Mature periderm (node no.)	1	13	20	number of nodes/shoot where periderm is mature
Canopy density (m ² /m ³)	2.6	5.5	29.0	surface area/volume from cross section shape, size, length
Leaf size index (mm)	132	195	245	sum of lengths of 2nd and 4th lobes on leaf 5
Fruit exposure (%)	5	47	95	visible fruit as proportion of total fruit
<i>Vine variables at harvest:</i>				
Coloured berries (%)	90	100	100	coloured berries as proportion of total berries
Green leaves (%)	30	74	95	green, healthy leaves as proportion of total leaves
Growing tips (%)	0	0	3	actively growing shoot tips as proportion of total shoot tips
Mature periderm (node no.)	6	15	26	number of nodes/shoot where periderm is mature
Canopy density (m ² /m ³)	2.3	5.3	18.1	surface area/volume from cross section shape, size, length
Leaf size (mm)	145	197	260	sum of lengths of 2nd and 4th lobes on leaf 5
Fruit exposure (%)	5	52	100	visible fruit as proportion of total fruit
<i>Crop variables:</i>				
Bunch weight (g)	39	103	222	mean bunch weight (20 bunches [†] , c. 2 kg)
Berry weight (g)	0.46	0.98	2.13	mean berry weight (20 bunches [†] , c. 2 kg)
Baumé (°Bé)	7.9	12.2	19.7	temp.-corrected hydrometer reading on settled, clear juice ^{‡*}
pH	3.1	3.4	3.8	meter reading on 25 mL subsample of settled, fresh juice
Titrateable acid (g/L) [‡]	6.3	9.0	14.3	titration of 25 mL subsample of fresh, clarified juice ^o
Potassium (mg/L)	920	1565	3240	analysis on 10 mL subsample of fresh juice [^]
Anthocyanins/berry (mg)	0.32	1.36	2.48	ethanol extraction of subsample of frozen skins [†]
anthocyanins/g ^v (mg/g)	26	146	336	ethanol extraction of subsample of frozen skins [†]
Phenolics/berry (mg)	0.60	1.55	2.47	ethanol extraction of subsample of frozen skins [†]
Phenolics/g ^v (mg/g)	44	155	348	ethanol extraction of subsample of frozen skins ^{†x}
<i>Vineyard variables:</i>				
Vine age (years)	3	26	112	from grower survey returns and records
Yield/vine (kg/vine)	0.6	7.9	32.2	from grower survey returns, records and field studies
Yield/hectare (t/ha)	0.6	10.9	35.7	from grower survey returns, records and field studies
Surface area/vine (m ²)	2.5	7.5	14.7	from grower survey returns, records and field studies

^oLocality of vineyard based upon SA Phylloxera Board districts, but combining the three Murray River areas into a single unit, Riverland.

[†]Stratified sample.

[‡]tartaric acid equivalent.

^oAutotitration against 0.333 N NaOH to pH 8.4; [^]by spectrophotometry.

^vberry fresh mass.

^xtemp. = temperature.

followed the district boundaries specified by the South Australian Phylloxera Board, except that the three Murray River areas, Waikerie and Lower Murray, North Murray, and South Murray are combined as Riverland. The others are Northern, Barossa, Central, and South Eastern.

The unique identity of parcels of fruit was maintained from the vineyard through the winemaking process to the preliminary allocation to wine product (end-use). Blending options then allow the company to distribute the finished wines among its product range. Each of these products has a 'Value Index'

(VI_{Product}) based on its wholesale bottle price, and calculated as described in Gray et al. (1994):

$$VI_{\text{Product}} = \frac{SP - CP}{SP} \times \frac{100}{1}$$

where SP = net selling price, and CP = cost of production.

Wine from the sampled vineyards formed components of 49 separate bottled wine products in 1992. Corresponding to each sampled vineyard is another 'Value Index' (VI_{Vineyard}) computed from VI_{Product} for the

products to which wine from that vineyard was allocated, and calculated as described in Gray et al. (1994):

$$VI_{\text{vineyard}} = \frac{\sum[(VI_{\text{Product}}) \times (\text{tonnes to product})]}{\text{total vineyard tonnes}}$$

Some sample vineyards were allocated to a single product in 1992, while others were apportioned among as many as 11 different wine products. Hereafter, VI_{vineyard} is referred to simply as 'VI' in all ensuing analyses.

Three statistical procedures were used: one-way analysis of variance (AOV), simple linear regression (SLR) and multiple linear regression (MLR) using backward elimination. AOV was used to determine the significance of the difference between regional means for a single variable. SLR was used to test the significance of relationships between pairs of variables and the associated correlations were recorded in a correlation matrix. MLR was performed on three separate data sets: (a) all variables excluding the harvest group ('veraison MLR'); (b) all variables excluding the veraison group ('harvest MLR'); and (c) all variables together ('combined MLR'). Region was retained in the multiple regressions as a qualitative explanatory variable.

Two other statistical methods were explored in addition to those used, namely Boxplots (Ryan et al. 1985) and Tree-based models (Breiman et al. 1984). However, no advantage was apparent from these methods and their results are not included.

Results

The 1992 vintage in South Australia was characterised by dry, cool-to-mild growing conditions throughout the ripening period. Harvest was later than average in all regions and fruit quality was above-average. Mild outbreaks of powdery mildew were recorded in most regions and heavy rain towards harvest resulted in some berry splitting, with some crop losses in the Northern region. Shiraz yields were below-average in Central, Barossa and South Eastern regions, but above-average in Northern and Riverland regions (Deves 1992).

The 148 selected vineyard blocks, varying in size from 0.2 to 35.6 ha, covered a wide spectrum of vine-

yard types as is illustrated by the range of recorded measurements for each of the variables shown in Table 1; some spanned more than a ten-fold range, e.g. 'yield/hectare' (0.6–35.7 t/ha). The wide array of values for some factors indicates one of the problems of surveys of this type. For example, time of veraison should have been near '50% berries coloured' but the recorded values ranged from 2%–100%; also 'Baumé at harvest' ranged from 7.9°–19.7°Bé (i.e. 14°–35°Brix).

'VI' values for all Shiraz samples are presented in Figure 1 as distributions of 'VI' by region. Variation according to region is apparent. The assumption of homogeneity of variances for 'VI' was checked with Bartlett's Chi-square test, but was not met. The variance associated with 'VI' for Riverland vineyards was considerably lower than other regions. The mean 'VI' for Riverland vineyards (17.9) proved significantly lower than the grand mean encompassing all regions (31.5) using a Student-Newman-Keuls' multiple range test at $p < 0.05$. The ranking of means, in descending order, is—South Eastern (38.5) = Barossa (37.2) = Central (30.3) = Northern (29.0) > Riverland (17.9).

The relationships between 'VI' and the other variables are shown in Figure 2, for those relationships that were significant ($p < 0.05$). Note that none of the variables assessed at veraison were significant in these analyses. The regressions of 'green leaves at harvest', 'berry weight' and 'yield/hectare' against 'VI' were all negative, but 'nodes with mature periderm at harvest', 'canopy density', 'fruit exposure at harvest', 'anthocyanins/g berry mass' and 'phenolics/g berry mass' were positively correlated with 'VI'. Several of these relationships were shown to be significant for Shiraz in the previous study, but the slopes and intercepts could not then be determined because the measured variables were qualitative and therefore not amenable to regression analysis.

Regression equations are presented in Table 2 for each of the three MLR analyses. In 'veraison MLRs' and 'combined MLRs', intercepts of region regression lines with the 'VI' axis are, in descending order, South Eastern > Barossa > Northern > Central, an order which resembles the ranking established in the AOV of the regional distribution 'VIs' illustrated in Figure 1 (except that Riverland is not included due to the missing veraison measurements). The 'harvest MLRs' also show the equivalent intercept ranking, including Riverland. Overall, the MLR analyses indicated three variables that contributed significantly ($p < 0.05$): 'leaf size at veraison', 'fruit exposure at veraison' and 'fruit exposure at harvest'. These regression coefficients were positive, but neither of the veraison variables were significant in the SLR analyses. The two variables taken at veraison gave regressions which accounted for only 13.4% of the variance, a very low value. At harvest, 'fruit exposure' was the only significant term and the 'variance accounted for' was 27.9% of the total. 'Fruit exposure at harvest' was represented among the significant SLR analyses and its positive relationship to 'VI' is largely unchanged. In the 'combined MLR', 'leaf size at veraison' and 'fruit exposure at harvest' were the only significant variables ($p < 0.05$).

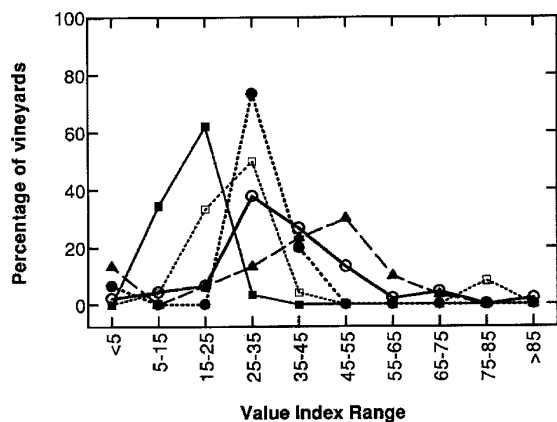


Figure 1. Percentages of Shiraz vineyards from each region falling within a defined 'VI' range. ■ Riverland, □ Central, ● Northern, ○ Barossa, ▲ South Eastern.

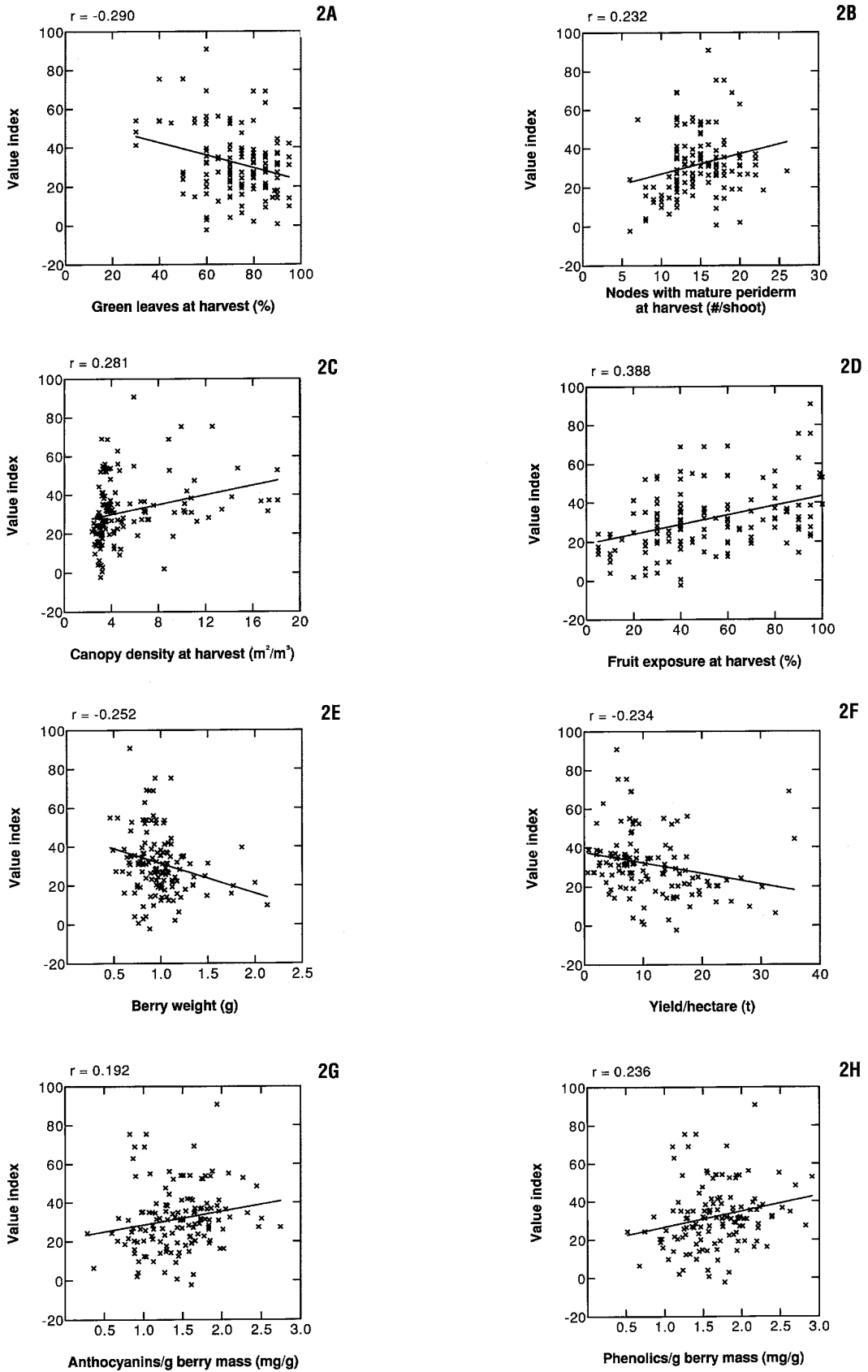


Figure 2. Significant correlations between 'VI' and the other variables ($p < 0.05$). The correlation coefficient r and the fitted straight line are shown.

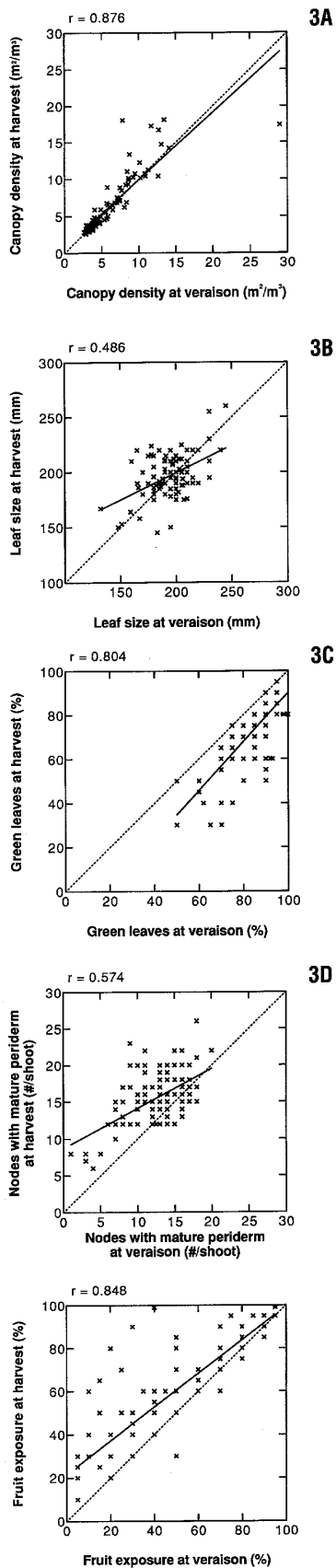


Figure 3. Significant correlations between variables measured at both veraison and harvest ($p < 0.05$). The correlation coefficient r , the fitted straight line and a line of unit slope are shown.

Table 2. Multiple linear regression (MLR) equations for 'VI' by region using (a) veraison variables only, (b) harvest variables only, and (c) all variables combined.

(a) Veraison MLRs by region

$$VI_{\text{Region}} = \text{Constant}_{\text{Region}} + 0.27(LS_{\text{Veraison}}) + 0.16(FE_{\text{Veraison}})$$

where

Constant _{Central}	= -33.9
Constant _{Northern}	= -33.3
Constant _{Barossa}	= -25.0
Constant _{South Eastern}	= -15.0

Variance accounted for = 13.4%

(b) Harvest MLRs by region

$$VI_{\text{Region}} = \text{Constant}_{\text{Region}} + 0.25(FE_{\text{Harvest}})$$

where

Constant _{Riverland}	= 11.8
Constant _{Central}	= 16.7
Constant _{Northern}	= 15.4
Constant _{Barossa}	= 21.1
Constant _{South Eastern}	= 29.3

Variance accounted for = 27.9%

(c) Combined MLRs by region

(variance accounted for)

$$VI_{\text{Region}} = \text{Constant}_{\text{Region}} + 0.26(LS_{\text{Veraison}}) + 0.29(FE_{\text{Harvest}})$$

where

Constant _{Central}	= -39.7
Constant _{Northern}	= -39.2
Constant _{Barossa}	= -31.2
Constant _{South Eastern}	= -9.6

Variance accounted for = 22.2%

LS= 'leaf size', FE = 'fruit exposure.

Each of these was represented in one or other of the 'veraison MLR' and 'harvest MLR'. The 'variance accounted for' in the 'combined MLR' was only 22.2%.

The SLRs conducted on the assessed variables indicated that there was a significant relationship between 15 pairs of them. For the significant correlations, the correlation coefficients were greater than 0.5. Five of the seven variables measured at both veraison and harvest were significantly and positively correlated with each other ($p < 0.05$). Figure 3 illustrates these relationships. The remaining ten significant relationships among the assessed variables ($p < 0.05$) are displayed in Figure 4.

Discussion

Relationships between assessed variables and VI

This comparison of young Shiraz wines in each of the five major South Australian winegrape regions (16 to 46 vineyards in each) shows an array of regional differences based on the commercial assessment of prospective wine value ('VI'). These differences were presented in two ways. Firstly, by distributions of mean 'VI' by region (Figure 1) using AOV and multiple range test to separate these individual means. Secondly, by the results of MLR shown in Table 2 where the regional differences are measured as intercepts on the 'VI' axis, being highest from South Eastern and lowest from Riverland. The results accord with general industry experience.

3E

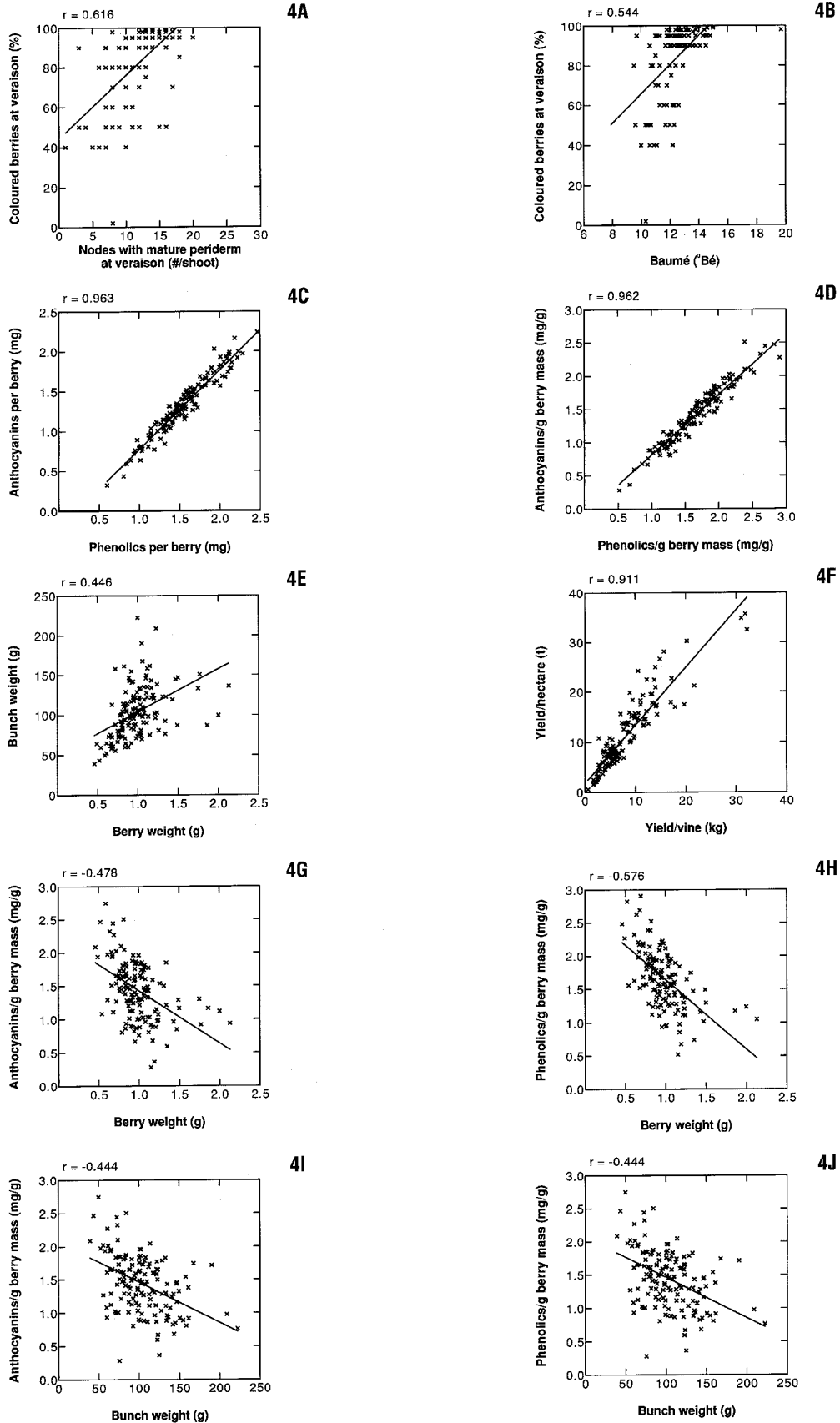


Figure 4. Significant correlations among assessed variables ($p < 0.05$). The correlation coefficient r and the fitted straight line are shown.

The significant relationships between 'VI' and measured variables (Figure 2) had both negative and positive slopes. Those with negative slopes showed that lower 'VI' was more likely with higher values of % green leaves, berry weight and vine yield. Of the five positive relationships, three were canopy-related—'nodes with mature periderm development at harvest', 'canopy density at harvest' and 'fruit exposure at harvest'—while two were related to the concentrations of anthocyanins and phenolics in the berry skin. As with regional differences, all of these results accord with industry perception (see Smart and Robinson 1991), but each shows large variation, indicated by the scatter of points around regression lines and the small correlation coefficients (all < 0.4). There are some surprise omissions from this list of significant relationships—e.g. 'Baumé at harvest' and 'leaf size at veraison' are missing. It is notable that all eight significant relationships were from measurements made at harvest, none at veraison.

The technique of backward elimination in MLR analysis involves successive elimination of factors that contribute least (i.e. lowest value of Student's *t*) to the 'variance accounted for' by the regression equation, eventually arriving at those characteristics giving the best and simplest result. In the present case the variables remaining were 'leaf size at veraison', 'fruit exposure at veraison' and 'fruit exposure at harvest'. Surprisingly only the latter of these three was significantly correlated with 'VI' in the SLR analyses.

Considered collectively, the results portray a picture of adverse trends against wine quality of leafy, dense canopies, poor fruit exposure, low anthocyanin levels, large berries and high yield. It is obvious that one major factor, environmentally the main factor, influencing all of these characteristics is the level of water supply.

Although this survey was useful to the participating company for improving their grape-sourcing strategies, it did not engender confidence in the method as a reliable technique to predict winegrape quality. The levels of 'variation accounted for' in 'VI' remained unacceptably low despite several changes to the methods—covering a more focused group of vineyards, reducing the proportion of missing data, and using quantitative rather than qualitative variables. There are several possibilities available for further testing: (a) seeking a different method for measuring the quality (potential value) of young wines, (b) redefining the way variables in the current list are measured and looking for new variables that might be related to 'VI', in particular by exploring different growth stages, and (c) improving sampling and measuring procedures by investigating the causes of variability in fruit quality, between and within vineyards.

Relationships among assessed variables

Tactically, vineyard assessments for predicting winegrape value are most useful if made as early as possible before harvest, e.g. at veraison. The survey showed that best correlations to 'VI' were with several variables measured at harvest, but few at veraison. To improve the chances of finding veraison variables that give useful correlations with 'VI' it is

worth exploring the relationships between those variables measured at these two stages. Of the seven such comparisons examined, five showed significant and positive correlations (Figure 3). The scatter plots show interesting differences in distribution of values. 'Canopy density' (Figure 3A) exhibited a curved relationship that changed little between veraison and harvest at lower densities, but did change at higher densities. 'Leaf size' (Figure 3B) was evenly distributed on both sides of the line of unit slope, indicating little change in distribution as the berries ripened. The distribution of the other three showed scatters that were above or below the line of unit slope—'% green leaves' (Figure 3C) was uniformly higher at veraison, while 'nodes with mature periderm' (Figure 3D), and '% fruit exposure' (Figure 3E) were higher at harvest. These three reflect senescence at nodes near and below bunches compared with their condition at veraison. The correlation coefficients exhibited in Figures 3A, 3C, and 3E (all > 0.8) indicate the relative strength of these linear relationships.

Of the remaining ten significant correlations shown between pairs of variables (Figure 4), the two involving variables at veraison are indicative of the logistical difficulties in sampling vineyards at a precise stage of berry development: 'coloured berries at veraison' correlates with both 'nodes with mature periderm at veraison' (Figure 4A) and 'Baumé' (Figure 4B). It would be worthwhile extending this study at veraison to other pre-harvest stages. The recent finding by McCarthy (1997) of low variability in the interval from flowering to 5.5°Bé (10°Brix) for Shiraz juice warrants exploration.

The two correlations between 'anthocyanins' and 'phenolics' on a 'per berry' basis (Figure 4C) and on a 'per gram berry mass' basis (Figure 4D) are self-evident. The linear relationship between 'bunch weight' and 'berry weight' (Figure 4E) is complicated by the number of berries per bunch which is not independent of berry size. This may explain the y-shaped scatter of points on the graph. The relationship between 'yield/hectare' and 'yield/vine' (Figure 4F) is dependent upon the number of vines per hectare. Both 'anthocyanins/g berry mass' (Figure 4G) and 'phenolics/g berry mass' (Figure 4H) are curvilinearly related to 'berry weight'. The role of berry size in influencing the concentration of both anthocyanins and phenolics has been emphasised by Coombe and Iland (1987) and Iland (1988). This relationship holds because of the geometric interdependence of berry surface area and berry volume (proportional to $x^{2/3}$). Since 'berry weight' and 'bunch weight' are not highly correlated, curvilinearity is not evident in the relationships between 'anthocyanins/g berry mass' and 'bunch weight' (Figure 4I) and 'phenolics/g berry mass' and 'bunch weight' (Figure 4J). The high correlation coefficients shown in the Figures 4C, 4D, and 4F (all > 0.9), indicate the coherence of these correlations.

Conclusions

Modifications to the scoresheet and focusing of the survey have not improved the poor degree of prediction of wine value from vineyard

measurements. Linear regression analyses showed small trends for lower 'VI' from vineyards with leafy, dense canopies, poor fruit exposure, lower anthocyanins, larger berries and higher yields. The general approach is laudable, but a combination of unidentified sources of variation reduces the chance of finding useful correlations. It is contended that the gaining of a better understanding of within-vineyard variability, particularly the site and developmental stage at which such variations originate, is a crucial first step.

Acknowledgments

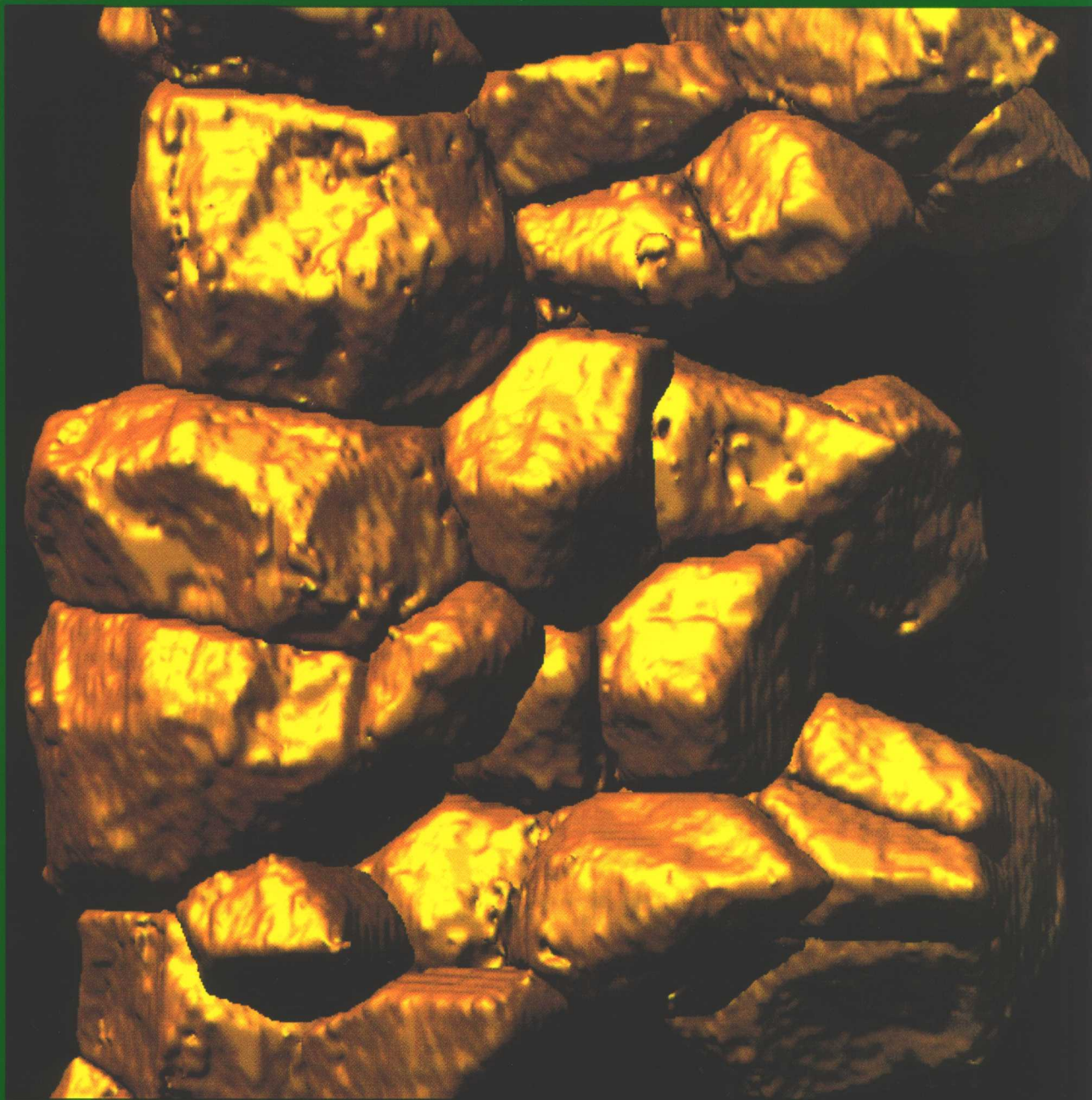
The authors acknowledge the data collection activities undertaken by technical staff of the Penfolds Wine Group (Ms W. Allan, Messrs A. Brock, P. Nash, A. Noack, Ms K. Strachan and Ms K. Williams), the assistance with sample preparation and analysis by Ms J. Iland and Ms A. Gray, the resources and facilities made available through the Department of Horticulture, Viticulture and Oenology of the University of Adelaide, the National Teaching Company Scheme for initiating the project, and the Penfolds Wine Group (now Southcorp Wines Pty Ltd) for its continued financial support.

References

- Breiman, L., Friedman, J.H., Olshen, R.A. and Stone, C.J. (1984) 'Classification and Regression Trees'. (Wadsworth International Group: Belmont, CA, USA)
- Carbonneau, A. (1976) Analyse de la croissance des feuilles du sarment de vigne: estimation de sa surface foliaire par échantillonnage. *Connaissance de la Vigne et du Vin* **10**, 141-159.
- Coombe, B.G. and Iland, P.G. (1987) Grape berry development. In: 'Proceedings 6th Australian Wine Industry Technical Conference, Adelaide'. (Australian Industrial Publisher: Adelaide) pp. 50-54.
- Deves, M. (1992) Cool, dry conditions characterise 1992 vintage. *The Australian & New Zealand Wine Industry Journal* **7**, 87-89.
- Gray, J.D., Gibson, R.J., Coombe, B.G., Giles, L.C. and Hancock, T.W. (1994) Assessment of winegrape value in the vineyard – a preliminary, commercial survey. *The Australian & New Zealand Wine Industry Journal* **9**, 253-261.
- Iland, P.G. (1988) Leaf removal effects on fruit composition. In: 'Proceedings 2nd International Symposium for Cool Climate Viticulture and Oenology'. (New Zealand Society for Viticulture and Oenology: Auckland, NZ) pp. 137-138.
- McCarthy, M.G. (1997) Effect of timing of water deficit on fruit development and composition of *Vitis vinifera* cv. Shiraz. Doctoral thesis, The University of Adelaide.
- Ryan, B.F., Joiner, B.L. and Ryan, T.A. (1985) 'Minitab Handbook. 2nd edition'. (PWS-Kent Publishing Co.: Boston)
- Smart, R.E., Robinson, J.B. and Due, G.R. (1981) Manipulation of wine quality within the vineyard. In: 'Grape quality: assessment from vineyard to juice preparation'. Ed. T.H. Lee (Australian Society for Viticulture and Oenology: Glen Osmond, South Australia) pp. 19-26.
- Smart, R.E. and Robinson, M. (1991) 'Sunlight into Wine: A Handbook for Winegrape Canopy Management'. (Winetitles: Adelaide)

Manuscript received: 20 October 1997

THE
plant JOURNAL



b

Blackwell
Science

Volume 19

Number 2

July 1999

TECHNICAL ADVANCE

Confocal measurement of the three-dimensional size and shape of plant parenchyma cells in a developing fruit tissue

John D. Gray^{1,*}, Peter Kolesik¹, Peter B. Høj^{1,2} and Bryan G. Coombe¹

¹Department of Horticulture, Viticulture and Oenology, Waite Campus, The University of Adelaide, Glen Osmond, SA 5064, Australia, and

²Australian Wine Research Institute, Glen Osmond, SA 5064, Australia

Summary

Parenchyma cells from the inner mesocarp of a grape berry (*Vitis vinifera* L. cv. Chardonnay) were visualised in three-dimensions within a whole mount of cleared, stained tissue using confocal laser scanning microscopy and digital image reconstruction. The whole berry was fixed, bisected longitudinally, cleared in methyl salicylate, stained with safranin O and mounted in methyl salicylate. Optical slices were collected at 1.0 µm intervals to a depth of 150 µm. Neighbouring z-series were joined post-collection to double the field-of-view. Attenuation at depth of the fluorescent signal from cell walls was quantified and corrected. Axial distortion due to refractive index mismatch between the immersion and mounting media was calibrated using yellow-green fluorescent microspheres and corrected. Transmission electron microscopy was used to correct fluorescent measurements of cell wall thickness. Digital image reconstructions of wall-enclosed spaces enabled cells to be rendered as geometric solids of measurable surface area and volume. Cell volumes within the inner mesocarp tissue of a single grape berry exhibited a 14-fold range, with polysigmoidal distribution and groupings around specific size classes. Cell shape was irregular and the planes of contact were rarely flat or simple. Variability in cell shape was indicated by the range in surface area to volume ratios, from 0.080 to 0.198 µm⁻¹. Structural detail at the internal surface of the cell wall was apparent. The technique is applicable to a

wide range of morphometric analyses in plant cell biology, particularly developmental studies, and reveals details of cell size and shape that were previously unattainable.

Introduction

Elucidation of the relative positioning, shape and size of plant parenchyma cells *in situ* has hitherto been achieved by indirect methods involving microscopic analyses of thin, serial sections followed by stereological analysis (Considine, 1978; Considine, 1981; Cruz-Orive, 1997; Møller *et al.*, 1990; Underwood, 1970; Weibel, 1979; Weibel, 1980) or three-dimensional (3D) reconstruction of physical slices (Bron *et al.*, 1990; Korn and Spalding, 1973; Korn, 1974; Lewis, 1926; Matzke, 1948; Williams, 1968). While appropriate for tissues composed of isodiametric cells, stereological methods underestimate mean cell sizes (Considine and Knox, 1981) and do not allow accurate determinations of intra-tissue variation (Parsons *et al.*, 1989). Although 3D reconstruction of serial sections has yielded invaluable insights into the organisation of cells in specific tissues (e.g. Williams, 1970), the methodology has limitations due to artefacts introduced during the preparation of tissue slices and the subsequent tedious reconstruction.

It is desirable that methods be adopted for investigating cells within tissues in which physical sectioning is not required. The recent development of confocal laser scanning microscopy (CLSM) allows this possibility. Whole mounts of cleared, stained tissue in combination with optical sectioning by CLSM and digital 3D image reconstruction offers an alternative to conventional techniques.

CLSM combines laser light illumination, fluorescence microscopy and computer imaging. Under ideal circumstances it has sharp depth discrimination and produces horizontal optical slices of tissues in the plane of focus (Pawley, 1995). The resultant images are digitised and stored as a vertical image stack, or z-series. Digital 3D image reconstruction enables the z-series to be visualised as a geometric structure (Carlsson *et al.*, 1985; Yu *et al.*, 1994). Applications of CLSM to the study of plant microstructure include 3D reconstruction of guard cells in *Commelina* leaves (White *et al.*, 1996), the measurement of cell wall thickness in spring barley and maize

Received 13 April 1999; accepted 28 May 1999.

*For correspondence: CSIRO Plant Industry, Horticulture Unit, Merbein Laboratory, Merbein, VIC 3505, Australia (fax +61 350513111; e-mail john.gray@pi.csiro.au).

Abbreviations: l, wavelength; 3D, three-dimensional; CLSM, confocal laser scanning microscopy; FPA₅₀, formalin:propionic acid:50% ethanol 1:1:18; GMA, glycol methacrylate; NA, numerical aperture; RI, refractive index; TEM, transmission electron microscopy.

(Travis *et al.*, 1997), and *in vivo* observation of sieve tubes in fava bean leaves (Knoblauch and van Bel, 1998).

In this study we describe a further development for the detailed study of plant cell morphology and organisation using the parenchyma cells of the inner mesocarp of the grape berry. The combination of traditional clearing procedures with confocal microscopy enabled entire parenchyma cells (wall-enclosed spaces) to be visualised and measured *in situ*. The technique was tested on a number of berries of different ages. The images and measurements presented in this paper pertain to a collection of parenchyma cells from a single tissue block within one young grape berry (cv. Chardonnay, 26 days after anthesis, 5 mm diameter).

Results

Staining and mounting the tissue block

Fluorescence, either autofluorescence or stain induced, is a prerequisite to imaging cell walls under CLSM. Autofluorescence of berry cell walls was heterogeneous, therefore staining was needed to induce even fluorescence. Of the 16 stains tested, the majority gave poor or incomplete fluorescence of cell walls. Safranin O was adopted because it exhibited adequate labelling, suitable wavelengths of excitation and emission, and resistance to photobleaching. Methyl salicylate proved the most successful clearing medium: tissue distortion appeared to be minimal and the entire berry half was transparent under bright-field illumination. The adopted mounting procedure is shown in Figure 1.

Visualising cell walls

The tissue was imaged to a depth of 150 µm with the CLSM. The 151 optical slices which comprised the confocal z-series indicated the high degree of resolution attainable. Parenchyma cell walls were clearly visible in the consecutive optical slices, 1.0 µm apart (Figure 2). Membranous structures visible within certain cells indicated possible plasmolysis. Despite this, cell walls remained intact and no intercellular spaces were apparent.

Correcting the confocal z-series for signal attenuation and axial distortion

Analysis of the z-series indicated the need to correct for signal attenuation. The number of black pixels per optical slice increased linearly with depth ($R^2 = 0.839$). This would cause an increase in the wall-enclosed area of 20% at 150 µm depth. A 20% increase in unit area would have led to a 30% increase in unit volume and represented a serious

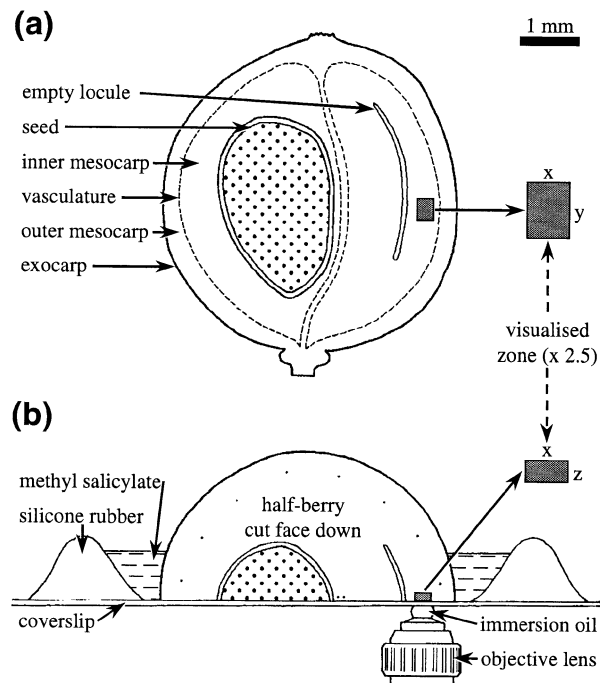


Figure 1. Diagram of young grape berry showing location of tissues and zone viewed by CLSM (berry and zone to scale).

(a) Longitudinally cut surface of the berry.

(b) Section of stained and cleared half-berry positioned cut face down on a coverslip in a well constructed of silicone rubber filled with methyl salicylate. The dimensions of the visualised zone are $x = 289 \mu\text{m}$, $y = 385 \mu\text{m}$, $z = 150 \mu\text{m}$.

potential for overestimating individual cell size. To minimise this error, attenuation of the fluorescent signal was corrected by sequentially increasing the intensity threshold. The corrected data displayed no fluorescence attenuation with depth, as indicated by regression analysis ($R^2 = 0.000$).

To check the extent of axial distortion within the confocal z-series, due to RI mismatch, the diameters of fluorescent microspheres were measured. The mean x/z ratio was 1.0445 (SD = 0.0205, $n = 10$), suggesting an axial compression of 4.45%. A multiplication factor of 1.0445 was applied to the z-series, changing the z-step from a nominal 1.0 µm to 1.0445 µm. As a consequence, the maximum image depth was expanded to 156.7 µm.

Comparison of cell wall thickness (TEM versus CLSM)

The mean thickness of parenchyma cell walls obtained using transmission electron microscopy (TEM) was 97 nm (SD = 25.2 nm, $n = 15$). The mean cell wall thickness estimated from a stratified random sample within the confocal series was 940 nm (SD = 170 nm, $n = 29$). This discrepancy (843 nm), caused by excessive fluorescent emission within single confocal slices, could

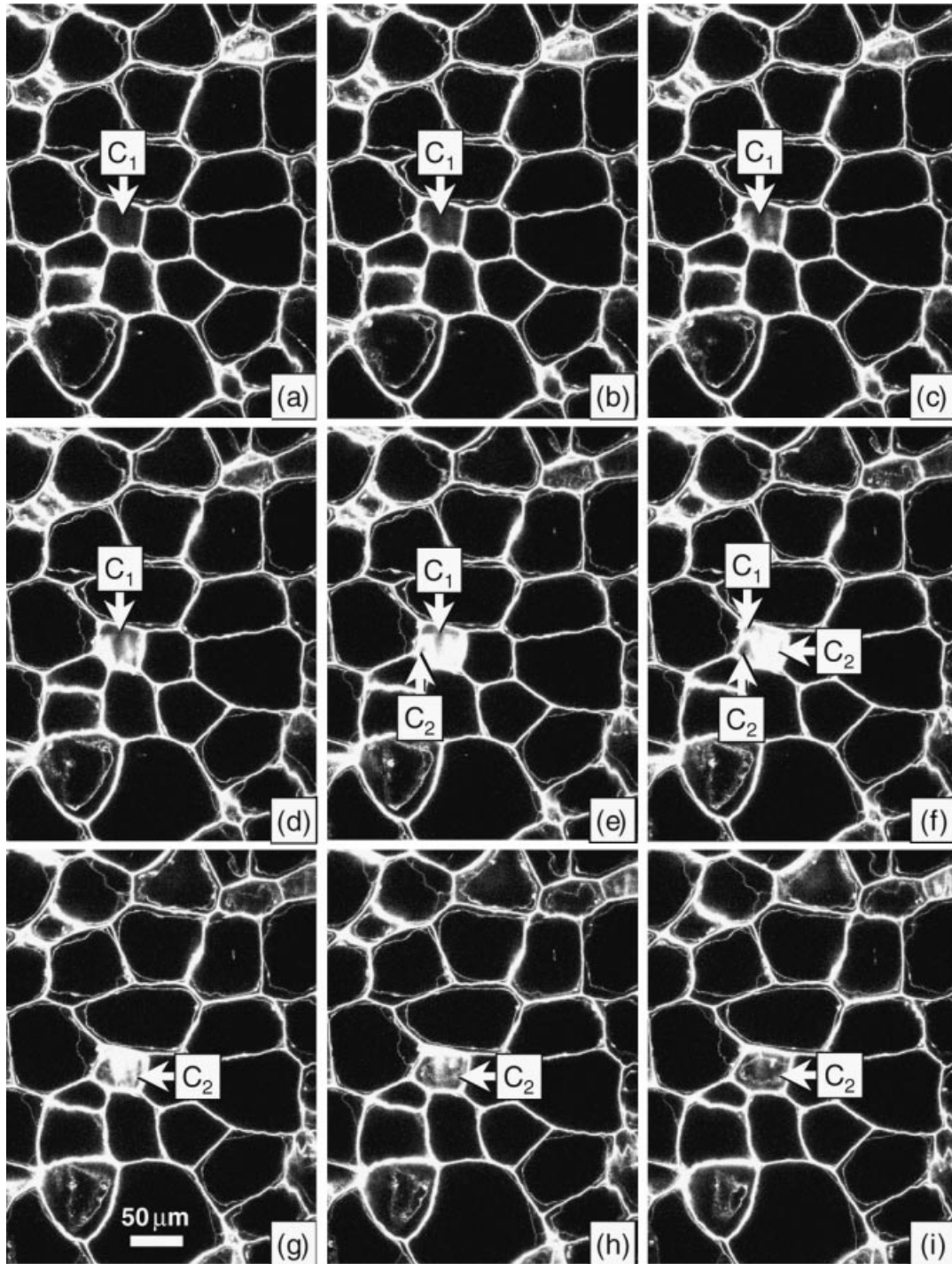


Figure 2. Optical slices of parenchyma cells.

(a–i) Consecutive optical slices, 1.0 μm apart, through a block of parenchyma tissue of the inner mesocarp of a Chardonnay berry collected 26 days after anthesis. Fluorescent cell walls are white and the non-fluorescent wall-enclosed spaces are black. Cell C₁ begins to close in slice (c) and disappears fully in slice (g). Cell C₂ begins to appear in slice (e). Only C₂ is visible in slices (g–i). Plasma membranes are visible within some cells indicating possible plasmolysis due to the fixation process.

have resulted in an underestimation of cell volume by as much as 15%. To approximate actual wall thickness

the cell wall signal was eroded by one pixel (752 nm) to 188 nm. Further erosion was not possible.

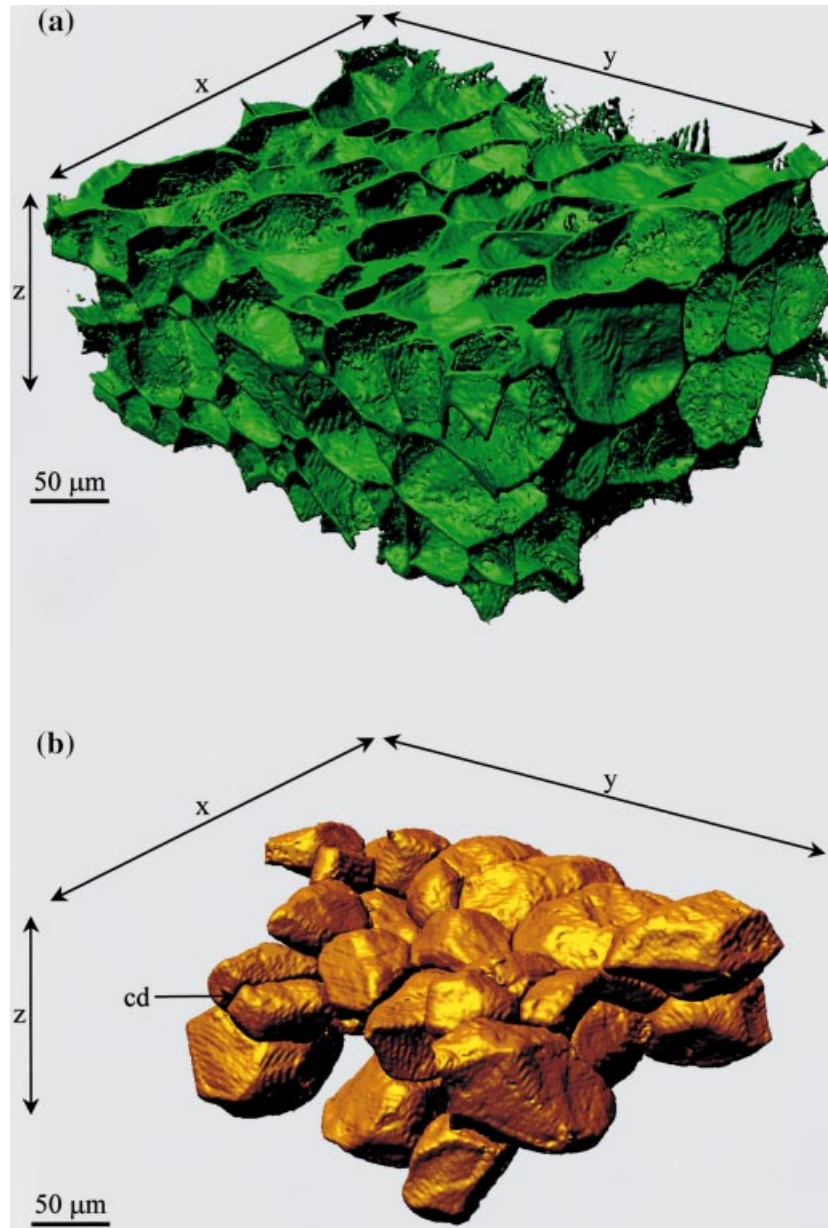
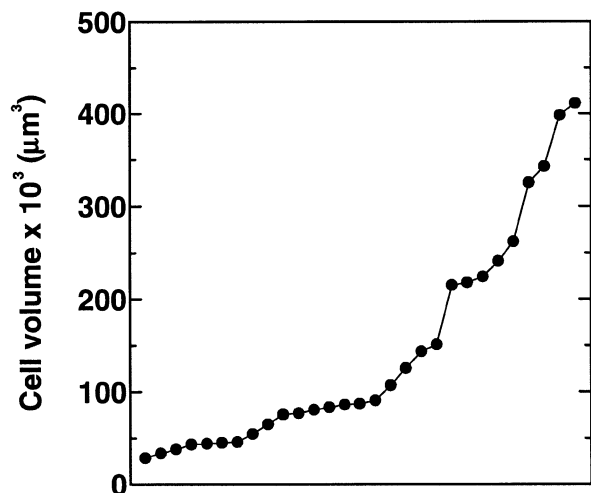


Figure 3. Parenchyma cell reconstructions. Digital 3D reconstruction of (a) cell walls prior to eroding and (b) 29 individual cells indicate the variety of shapes and sizes found among parenchyma cells in the inner mesocarp tissue of a Chardonnay berry harvested 26 days after flowering. Only entire cells are included, partial cells are excluded. A recent cell division is indicated at 'cd'.

Reconstructed three-dimensional (3D) models of cells and cell walls

Two-dimensional binary overlays of cell walls and wall-enclosed spaces from single optical slices were integrated to form 3D images. The 3D reconstructions of cell walls and 29 individual cells are shown in Figure 3. The size range for individual cells extended more than 14-fold, from $28\,400\ \mu\text{m}^3$ to $411\,000\ \mu\text{m}^3$ (mean = $143\,000\ \mu\text{m}^3$, SD = $115\,000\ \mu\text{m}^3$, $n=29$). The population dynamics of the cells were represented graphically by plotting cell volume in ascending order (Figure 4). Groupings of cells around specific size classes were

evident. Six distinct plateaux suggest that the maximum size for cells within a particular size class were $45\,000\ \mu\text{m}^3$, $90\,000\ \mu\text{m}^3$, $151\,000\ \mu\text{m}^3$, $224\,000\ \mu\text{m}^3$, $343\,000\ \mu\text{m}^3$, and $411\,000\ \mu\text{m}^3$. Note the decreasing interval between successive pairs of size class maxima. Cell shape was irregular and the planes of contact between cells were rarely flat or simple. Variability in cell shape was indicated by the range in surface area to volume ratios, from 0.080 to $0.198\ \mu\text{m}^{-1}$. Structural details greater than $1.5\ \mu\text{m}$ were apparent at the internal surface of the cell wall. The regular, large undulations were artefacts, typical of integrated serial sections. The interconnected patterns of protuberances and invaginations appeared to



Cells in ascending order of volume

Figure 4. Parenchyma cell volumes.

Cell volumes of all 29 reconstructed parenchyma cells in Figure 6(b) from the inner mesocarp tissue of a Chardonnay berry harvested 26 days after flowering, grouped in ascending order. The curve suggests six distinct plateaux around particular size classes.

be associated with the structure and position of internal cellular membranes. The more irregular, solitary protrusions may indicate the presence of primary pit fields.

Discussion

Techniques used

Judicious, minimal cutting of the organ enabled the berry to maintain the integrity of its tissues, thus reducing the likelihood of cell distortion. This aspect of the project enabled individual cells to be viewed *in situ*.

The working distance of the objective lens (170 μm) proved to be the main limiting factor to the depth of tissue penetration in this experimental system. Although optical penetration was consistently high throughout the entire tissue, a high numerical aperture lens (NA=1.4) was required to resolve cell walls running horizontal to the optical plane. This trade-off between working distance and numerical aperture in optical systems is unavoidable (Pawley, 1995). Larger volumes of tissue can be studied by aligning and combining adjacent z-series (Oldmixon and Carlsson, 1993): this increases the x and y dimensions of the scanned region, but z remains unchanged.

The use of fluorescent microspheres to derive a single empirical correction factor for axial distortion obviated the need for complex theoretical estimates involving geometric ray tracing models which often yield conflicting

results (Visser and Oud, 1994; White *et al.*, 1996). This correction was only an approximation to what is theoretically a non-monotonic function (Török *et al.*, 1997).

Cell wall thickness in confocal slices was greater than the estimates obtained using TEM. Confocal slices were deliberately over-saturated to ensure that all cell walls were visualised to a thickness of at least one pixel (0.752 μm). Attenuation of the fluorescent signal with depth caused cell walls to appear discontinuous on unsaturated slices. This was especially problematic for horizontal cell walls that emitted less fluorescence than their vertical counterparts. To avoid an under-estimation in the calculation of cell volume, each optical slice was corrected using a rank 3×3 filter which eroded the over-saturated cell walls by one pixel, thereby approaching the estimate of thickness obtained using TEM.

The 3D reconstruction software, ImageVolumes, was chosen on the grounds of the algorithm used, Marching Cubes, and its ability to visualise and measure structures imaged by CLSM. The merits of available 3D packages and algorithms are discussed in White (1995).

Shapes and sizes of parenchyma cells

Contemporary 3D reconstruction techniques in plant biology are infrequent (Knoblauch and van Bel, 1998; Travis *et al.*, 1997; White *et al.*, 1996) although many of the stereological principles were established by botanists earlier this century. The group of 29 cells visualised here, or each cell individually, can be viewed on screen from all angles. Measurements can be made of volume, surface area, surface morphology and the number of surface planes.

The final resolution of the reconstructed images is a function of the optical, digital and rendering resolution of the imaging system. Optical resolution is determined by the excitation wavelength ($\lambda=488\text{ nm}$) and the numerical aperture (NA=1.4) of the lens. It varies in the x-y (0.174 μm) and z ($\sim 0.5\mu\text{m}$) planes. Digital resolution is prescribed by the CCD in combination with lens magnification (0.376 $\mu\text{m pixel}^{-1}$) and post-collection modifications to the data (0.752 $\mu\text{m pixel}^{-1}$ after combining z-series). Rendering resolution in the x-y plane is twice the unit pixel size (1.504 μm), but rendering resolution in z-axis is the distance between the optical slices (1.0445 μm). Each voxel therefore represents 2.36 μm^3 . This number represents the precision of *in situ* volume measurements for individual, whole parenchyma cells within a block of grape berry mesocarp tissue.

The mean size found for grape mesocarp cells at this stage of development compares favourably with published sources (Considine and Knox, 1981; Coombe, 1976; Harris *et al.*, 1968) but the range and variability have not previously been described. The indication of a

succession of size classes deserves further study. Such classes might represent developmental cohorts of cells, where the smaller cells have arisen as mitotic divisions of the larger cells. The decreasing interval between successive cohorts suggests asynchronous divisions of different sized cells.

A study of the shape of individual cells could be developed from these results. Cell shape in space-filling tissues is described by the planes of contact (facets) with neighbouring cells. In homogeneous, space-filling tissues the mean number of facets per cell is said to approach 14. This is true of some plant cells, soap bubbles and compressed metal grains (Williams, 1968). The orthic tetrakaidecahedron, a geometrically perfect 14-sided polyhedron with eight hexagonal and six quadrilateral faces, was proposed as the archetypal shape for parenchyma cells (Kelvin, 1887; Korn and Spalding, 1973; Korn, 1974; Matzke, 1948; Thompson, 1942), but this form is rarely achieved in nature due to the occurrence of varying cell sizes within a developing tissue (Matzke and Duffy, 1956). Where both small and large cells are present in the same tissue it is obligatory for the larger cells to have more facets than the smaller cells. The relevance of mean number of facets per cell as a quantitative descriptor of cell size is questionable, given that cell contacts are not always flat, planar surfaces. It is less precise than the absolute measurements of cell volume, surface area and shape obtained in the present study.

The technique described in this paper for measuring and visualising plant parenchyma cells in 3D using whole mounts of cleared, stained tissue in conjunction with CLSM and digital 3D reconstruction is applicable to a wide range of morphometric analyses in plant cell biology. It could be a valuable complement to molecular genetics for elucidating factors critical to the development of plant form and function.

Experimental procedures

Tissue preparation

Grape berries were sampled from *Vitis vinifera* L. cv. Chardonnay vines, 26 days after anthesis had commenced. The tissue of interest in this study was the parenchymatous inner mesocarp of the grape berry consisting of about 10 layers of large, highly vacuolated cells. Berries were fixed in FPA₅₀ and stored in 70% ethanol. Individual berries were bisected longitudinally using a razor blade fragment. The half-berries were used in two ways: first, for testing of stains using thin, embedded sections; and second, for confocal microscopy without further cutting.

Berry halves were dehydrated through an alcohol series, infiltrated with GMA, embedded in GMA in gelatin capsules and oven-cured according to Feder and O'Brien (1968). Sections of 2 µm thickness were checked for autofluorescence and treated

with one of the following stains: acridine orange, aniline blue, aniline blue fluorochrome, Calcofluor White M2R, Congo red, coriphosphine O, euchrysin 2GNX, Evans blue, FITC, magdala red, periodic acid-Schiff's, Ponceau S, pontamine sky blue, resorcin blue, safranin O, trypan blue. Stained sections were visualised under a fluorescence microscope.

Clearing of half-berries was explored after it was found that untreated tissue was too opaque to allow sufficient penetration of laser light. Mounting the tissue in a medium of higher RI increases optical penetration. The RI of parenchyma cells approximates that of water (RI approximately 1.33) (O'Brien and McCully, 1981). Several highly refractive immersion media were tested in this study: glycerol (RI ~ 1.47), xylene (RI ~ 1.50), methyl benzoate (RI ~ 1.52), and methyl salicylate (RI ~ 1.54). More destructive clearing techniques were also tested: mounting the tissue directly in 80% lactic acid at 50–60°C (Simpson, 1929) and the use of specialised mixtures (Herr, 1971, 1982). Methyl salicylate was selected.

The following protocol was adopted: berry halves were dehydrated under vacuum through an ethanol series, cleared in methyl salicylate, stained with 0.5% safranin O in methyl salicylate and mounted, cut face down on a glass coverslip in a well constructed of a ring of silicone rubber filled with methyl salicylate (Figure 1). The further work consisted of examination of the visualised tissue zone, as illustrated in Figure 1.

Confocal laser scanning microscopy (CLSM)

Confocal images of the cell walls were collected using a BioRad MRC-1000 uv confocal system attached to a Nikon Diaphot-300 inverted microscope. The objective lens was a Nikon 60× oil immersion plan apochromat with a numerical aperture of 1.4 and a working distance of 170 µm. A krypton/argon laser was used to excite the specimen at 488/10 nm and emission was collected at 522/35 nm with the confocal aperture closed down to 1.5 mm. A sequence of 151 x–y optical slices was collected, each with a 1.0 µm separation on the z-axis. Images from a 289 × 193 µm field-of-view (768 × 512 pixels) were captured as computer files. Fluorescent intensity was digitally coded using 256 levels of grey, with 0 representing the lowest intensity (black) and 255 the highest (white). The cell wall intensity was deliberately over-saturated to compensate for reduced fluorescence in deeper parts of the tissue. Two neighbouring z-series were combined post-collection thus doubling the volume of tissue examined and increasing the number of cells included in the analysis. The combined field-of-view was 289 × 385 µm (384 × 512 pixels).

Calibration of intensity attenuation with depth

Signal attenuation is a function of absorption and scattering of both excitation and emission light (Guilak, 1994; Rigaut and Vassy, 1991). In the present study, the collected fluorescent signal represented cell walls, whereas the unstained cell interior appeared black. Lessening of the fluorescent signal deriving from the cell walls could result in an overestimation of the true size of the cell.

A binary threshold that qualitatively separated cell walls (white pixels) from cells (black pixels) was used to assess signal attenuation. The number of black pixels in each optical slice of the combined image stack was plotted against slice depth using NIH Image software (Version 1.61 U.S. National Institute of Health 1996). Attenuation increased linearly with depth so an intensity threshold correction factor was sought to minimise its impact on

cell size calculations. An incremental threshold adjustment which yielded a regression line of zero slope was used to recalculate intensity thresholds for each optical slice.

Calibration of axial distortion

Some degree of axial distortion in the z-axis was anticipated on the basis of the RI mismatch between the lens immersion medium (oil RI = 1.5124 at 22.5°C) and the specimen mounting medium (methyl salicylate RI = 1.5358 at 22.5°C) (Carlsson, 1991; Hell *et al.*, 1993). This was calibrated with nominal 10 µm yellow-green fluorescent microspheres composed of a polystyrene envelope containing a fluorescent dye. Confocal, non-saturated, vertical sections of 10 microspheres mounted in methyl salicylate were collected using the same filter set as the berry images. The x and z diameters of the spheres were determined as the distance between the edges of the spheres located at 50% of the greyscale intensity threshold between the centre of the microsphere and the adjacent background. A correction factor of 4.5% was calculated using the ratio of x to z diameter of microspheres.

Transmission electron microscopy (TEM) of cell walls

Cell wall thickness was verified using TEM. Berry tissue was post-fixed in 2% osmium tetroxide, dehydrated through an acetone series, infiltrated with an araldite embedding resin, embedded in fresh resin and polymerised under vacuum at 70°C (Mollenhauer, 1964). Sections of 70 nm thickness were cut on an ultramicrotome, stained with 5% uranyl acetate in 70% ethanol and Reynolds' lead citrate, and mounted on an aluminium grid. The sections were visualised under TEM and cell wall thickness was estimated from a stratified random sample. Differences in cell wall thickness between TEM and CLSM were corrected by applying a rank 3 × 3 filter to erode cell walls by one pixel in each optical slice.

Three-dimensional (3D) reconstruction

To visualise the confocal data, ImageVolumes (Version 3.0 Minnesota Datametrics Corporation 1994) software run on a Silicon Graphics Indigo 2 computer under the Irix 5.3 operating system was used. Cell walls and cells were reconstructed from the z-series using two-dimensional binary overlays of the cell walls and wall-enclosed spaces. These overlays were integrated in the axial dimension by the Marching Cubes algorithm (Lorenson and Cline, 1987), a surface-based technique used to render 3D images from voxel data by forming isointensity contours of the object surface. Image rendering, smoothing and lighting techniques allowed individual cells to be viewed as geometric solids. Cells were reconstructed only if they were fully enclosed within a continuous cell wall (i.e. only entire cells were considered, partial cells were ignored).

Cell surface area and volume were measured with a distance field analysis software package (Dfield Version 2.0 Minnesota Datametrics Corporation 1994) which calculated 3D scalar quantities whose values described the Euclidean distance from any given point in space at Cartesian co-ordinates (x,y,z) to the closest surface of the 3D model.

Acknowledgements

The Australian Research Council, the Grape and Wine Research and Development Corporation and Southcorp Wines Pty Ltd are

gratefully acknowledged for their financial support. We thank the following: Ian J. Gibbins and Grant Hennig from the Department of Anatomy and Histology, the Flinders University of South Australia, for access to the SGI Indigo 2 computer and 3D software; Marilyn Henderson from the Centre for Electron Microscopy and Microstructural Analysis, the University of Adelaide, for assistance with the TEM analysis; Prue Henschke from C.A. Henschke and Co., for providing the grape material; and Nick S. White from the Department of Plant Sciences, the University of Oxford, for commenting on a draft of the manuscript.

References

- Bron, Cph., Gremillet, Ph., Launay, D., Jourlin, M., Gautschi, H.P., Bächli, Th. and Schüpbach, J. (1990) Three-dimensional electron microscopy of entire cells. *J. Microsc.* **157**, 115–126.
- Carlsson, K. (1991) The influence of specimen refractive index, detector signal integration, and non-uniform scan speed on the imaging properties in confocal microscopy. *J. Microsc.* **163**, 167–178.
- Carlsson, K., Danielsson, P.E., Lenz, R., Liljeborg, A., Majlöf, L. and Åslund, N. (1985) Three-dimensional microscopy using a confocal laser scanning microscope. *Opt. Lett.* **10**, 53–55.
- Considine, J.A. (1978) Stereology of the dermal system of fruit. *J. Microsc.* **113**, 61–68.
- Considine, J.A. (1981) Stereological analysis of the dermal system of fruit of the grape *Vitis vinifera* L. *Aust. J. Bot.* **29**, 463–474.
- Considine, J.A. and Knox, R.B. (1981) Tissue origins, cell lineages and patterns of cell division in the developing dermal system of the fruit of *Vitis vinifera* L. *Planta*, **151**, 403–412.
- Coombe, B.G. (1976) The development of fleshy fruits. *Ann. Rev. Plant Physiol.* **27**, 207–228.
- Cruz-Orive, L.M. (1997) Stereology of single objects. *J. Microsc.* **186**, 93–107.
- Feder, N. and O'Brien, T.P. (1968) Plant microtechnique: some principles and new methods. *Am. J. Bot.* **55**, 123–142.
- Guilak, F. (1994) Volume and surface area measurement of viable chondrocytes *in situ* using geometric modelling of serial confocal sections. *J. Microsc.* **173**, 245–256.
- Harris, J.M., Kriedemann, P.E. and Possingham, J.V. (1968) Anatomical aspects of grape berry development. *Vitis*, **7**, 106–119.
- Hell, S., Reiner, G., Cremer, C. and Stelzer, E.H.K. (1993) Aberrations in confocal fluorescence microscopy induced by mismatches in refractive index. *J. Microsc.* **169**, 391–405.
- Herr, J.M., Jr (1971) A new clearing-squash technique for the study of ovule development in angiosperms. *Am. J. Bot.* **58**, 785–790.
- Herr, J.M., Jr (1982) An analysis of methods for permanently mounting ovules cleared in four-and-a-half type clearing fluids. *Stain Techn.* **57**, 161–169.
- Kelvin, Lord (1887) On the division of space with minimum partitioned area. *Phil. Mag.* **24**, 503–514.
- Knoblauch, M. and van Bel, A.J.E. (1998) Sieve tubes in action. *Plant Cell*, **10**, 35–50.
- Korn, R.W. (1974) The three-dimensional shape of plant cells and its relationship to pattern of tissue growth. *New Phytol.* **73**, 927–935.
- Korn, R.W. and Spalding, R.M. (1973) The geometry of plant epidermal cells. *New Phytol.* **72**, 1357–1365.
- Lewis, F.T. (1926) The effect of cell division on the shape and size of hexagonal cells. *Anat. Rec.* **33**, 331–355.
- Lorenson, W.E. and Cline, H.E. (1987) Marching cubes: a high

- resolution 3D surface construction algorithm. *Comp. Graphics*, **21**, 163–169.
- Matzke, E.B.** (1948) The three-dimensional shape of epidermal cells of the apical meristem of *Anacharis densa* (Elodea). *Am. J. Bot.* **35**, 323–332.
- Matzke, E.B. and Duffy, R.M.** (1956) Progressive three-dimensional shape changes of dividing cells within the apical meristem of *Anacharis densa*. *Am. J. Bot.* **43**, 205–225.
- Mollenhauer, H.H.** (1964) Plastic embedding mixtures for use in electron microscopy. *Stain Techn.* **39**, 111–114.
- Møller, A., Strange, P. and Gundersen, H.J.G.** (1990) Efficient estimation of cell, using the nucleator and the disector. *J. Microsc.* **159**, 61–71.
- O'Brien, T.P. and McCully, M.E.** (1981) *The Study of Plant Structure: Principles and Selected Methods*. Melbourne: Termarcarphi.
- Oldmixon, E.H. and Carlsson, K.** (1993) Methods for large data volumes from confocal scanning laser microscopy of lung. *J. Microsc.* **170**, 221–228.
- Parsons, D.F., Cole, R.W. and Kimelberg, H.K.** (1989) Shape, size, and distribution of cell structures by 3D graphics reconstruction and stereology. *Cell Biophys.* **14**, 27–42.
- Pawley, J.B., ed.** (1995) *Handbook of Biological Confocal Microscopy* 2nd edn. New York: Plenum Press.
- Rigaut, J.P. and Vassy, J.** (1991) High-resolution three-dimensional images from confocal scanning laser microscopy. Quantitative study and mathematical correction of the effects from bleaching and fluorescence attenuation in depth. *Anal. Quant. Cytol. Histol.* **13**, 223–232.
- Simpson, J.L.S.** (1929) A short method of clearing plant tissues for anatomical studies. *Stain Techn.* **4**, 131–132.
- Thompson, D'Arcy, W.** (1942) *On Growth and Form* 2nd edn. Cambridge: Cambridge University Press.
- Török, P., Hewlett, S.J. and Varga, P.** (1997) The role of specimen-induced spherical aberration in confocal microscopy. *J. Microsc.* **188**, 158–172.
- Travis, A.J., Murison, S.D., Perry, P. and Chesson, A.** (1997) Measurement of cell wall volume using confocal microscopy and its application to studies of forage degradation. *Ann. Bot.* **80**, 1–11.
- Underwood, E.E.** (1970) *Quantitative Stereology*. Massachusetts: Addison-Wesley Publishing Co.
- Visser, T.D. and Oud, J.L.** (1994) Volume measurements in three-dimensional microscopy. *Scanning*, **16**, 198–200.
- Weibel, E.R.** (1979) *Stereological Methods, Practical Methods for Biological Morphometry* Volume 1. London: Academic Press.
- Weibel, E.R.** (1980) *Stereological Methods, Theoretical Foundations* Volume 2. London: Academic Press.
- White, N.S.** (1995) Visualisation systems for multidimensional CLSM images. In *Handbook of Biological Confocal Microscopy* 2nd edn. (Pawley, J.B., ed.). New York: Plenum Press, pp. 211–254.
- White, N.S., Errington, R.J., Fricker, M.D. and Wood, J.L.** (1996) Aberration control in quantitative imaging of botanical specimens by multidimensional fluorescence microscopy. *J. Microsc.* **181**, 99–116.
- Williams, R.E.** (1968) Space-filling polyhedron: its relation to aggregates of soap bubbles, plant cells, and metal crystallites. *Science*, **161**, 276–277.
- Williams, R.F.** (1970) The genesis of form in flax and lupin as shown by scale drawings of the shoot apex. *Aust. J. Bot.* **18**, 167–173.
- Yu, R.C., Abrams, D.C., Alaibac, M. and Chu, A.C.** (1994) Morphological and quantitative analyses of normal epidermal Langerhans cells using confocal scanning laser microscopy. *Brit. J. Dermat.* **131**, 843–848.